AD_____

Award Number: DAMD17-98-1-8522

TITLE: Genes in FRA16D and FRA7G Mutated in Prostate Cancer

PRINCIPAL INVESTIGATOR: David I. Smith, Ph.D.

CONTRACTING ORGANIZATION: Mayo Foundation
Rochester, Minnesota 55905

REPORT DATE: November 2000

TYPE OF REPORT: Final

PREPARED FOR: U.S. Army Medical Research and Materiel Command
Fort Detrick, Maryland 21702-5012

DISTRIBUTION STATEMENT: Approved for public release;
Distribution unlimited

The views, opinions and/or findings contained in this report are
those of the author(s) and should not be construed as an official
Department of the Army position, policy or decision unless so
designated by other documentation.

20010716 114

REPORT DOCUMENTATION PAGE

Form Approved
OMB No. 074-0188

Public reporting burden for this collection of information is estimated to average 1 hour per response, including the time for reviewing instructions, searching existing data sources, gathering and maintaining the data needed, and completing and reviewing this collection of information. Send comments regarding this burden estimate or any other aspect of this collection of information, including suggestions for reducing this burden to Washington Headquarters Services, Directorate for Information Operations and Reports, 1215 Jefferson Davis Highway, Suite 1204, Arlington, VA 22202-4302, and to the Office of Management and Budget, Paperwork Reduction Project (0704-0188), Washington, DC 20503

1. AGENCY USE ONLY (Leave blank)	2. REPORT DATE November 2000	3. REPORT TYPE AND DATES COVERED Final (1 Jun 98 - 31 Oct 00)

4. TITLE AND SUBTITLE Genes in FRA16D and FRA7G Mutated in Prostate Cancer	5. FUNDING NUMBERS DAMD17-98-1-8522

6. AUTHOR(S)
David I. Smith, Ph.D.

7. PERFORMING ORGANIZATION NAME(S) AND ADDRESS(ES) Mayo Foundation Rochester, Minnesota 55905 E-MAIL: smith.david@mayo.edu	8. PERFORMING ORGANIZATION REPORT NUMBER

9. SPONSORING / MONITORING AGENCY NAME(S) AND ADDRESS(ES) U.S. Army Medical Research and Materiel Command Fort Detrick, Maryland 21702-5012	10. SPONSORING / MONITORING AGENCY REPORT NUMBER

11. SUPPLEMENTARY NOTES
This report contains colored photos

12a. DISTRIBUTION / AVAILABILITY STATEMENT Approved for public release; Distribution unlimited	12b. DISTRIBUTION CODE

13. ABSTRACT (Maximum 200 Words)

The goal of this project was to characterize two common fragile site regions that had previously been shown to be frequently lost during the development of prostate cancer. FRA16D corresponds to the second most active common fragile site and is at chromosomal band 16q23.2. FRA7G is a much less active common fragile site at chromosomal band 7q32, but this region is frequently deleted in prostate tumors too. We have defined both fragile site regions and find that the region of instability surrounding FRA7G is approximately 300 Kb in size. The region of instability surrounding FRA16D is greater than 2 megabases. We have defined genes within these two regions and they include WWOX, caveolin-1, caveolin-2, and TESTIN. None of these genes were mutated in prostate tumors and none of those tested were found to act as genomic sensors. However, these genes are frequently not expressed in prostate tumors and may still play an important role in prostate tumor development.

14. SUBJECT TERMS Prostate Cancer			15. NUMBER OF PAGES 98
			16. PRICE CODE

17. SECURITY CLASSIFICATION OF REPORT Unclassified	18. SECURITY CLASSIFICATION OF THIS PAGE Unclassified	19. SECURITY CLASSIFICATION OF ABSTRACT Unclassified	20. LIMITATION OF ABSTRACT Unlimited

NSN 7540-01-280-5500

Standard Form 298 (Rev. 2-89)
Prescribed by ANSI Std. Z39-18
298-102

Table of Contents

Genes in FRA16D and FRA7G Mutated in Prostate Cancer

Introduction

Chromosomal fragile sites are regions that show non-random breakage when cells are exposed to specific chemical conditions. Common fragile sites are present in all individuals and the majority of them are inducible by the DNA polymerase inhibitor aphidicolin. FRA16D (16q23.2) and FRA7G (7q31.2) are two aphidicolin-inducible fragile sites derived from chromosomal regions frequently deleted during the development of prostate cancer. Common fragile sites appear to be frequently involved in chromosomal rearrangements (including deletions, translocations, and amplification) during cancer development. The overall goal of this project was to determine the role that these two fragile site regions and the genes contained within them play in the development of prostate cancer. The first specific aim of this project was to physically characterize these two regions to determine the precise size and structure of each fragile site region. The second specific aim was to isolate genes from within these chromosomal regions and then to determine if these genes were mutational targets in prostate cancer. The final specific aim was to test whether or not these genes are sensors of genomic damage. Through this work we hoped to determine whether the common fragile sites play an active role in prostate cancer development.

****

Task 1: To construct high resolution physical maps of the FRA16D and FRA7G fragile site regions and isolate contigs of overlapping cosmids for several hundred kilobases surrounding these two common fragile sites. We proposed to construct pulsed field gel maps of YAC clones covering these two regions. We also proposed to use FISH analysis to determine the size of structure of each of these fragile sites. Finally, we proposed to construct cosmid contigs spanning these two chromosomal regions.

Task 2: To isolate genes from the fragile site regions and test them for mutations in primary prostate cancer. We proposed to scan for homozygous deletions in purified prostate tumor tissue. We also proposed to isolate genes from within these two regions and to test these genes for mutations in prostate cancer cell lines and in primary tumors.

Task 3: To determine if the genes from the fragile site regions are tumor suppressors, "sensors" or merely passengers to the genomic instability within the common fragile site regions. To answer this question, we proposed to examine whether there were tumor suppressor genes in these common fragile sites regions. Genes within the regions would also be tested to determine if they could function as sensors of genomic damage.

Task #1

Characterization of FRA7G

To construct high resolution physical maps of the FRA16D and FRA7G fragile site regions and isolate contigs of overlapping cosmids for several hundred kilobases surrounding these two common fragile sites. We proposed to construct pulsed field gel maps of YAC clones covering these two regions. We also proposed to use FISH analysis to determine the size of structure of each of these fragile sites. Finally, we proposed to construct cosmid contigs spanning these two chromosomal regions.

We first isolated three yeast artificial chromosome (YAC) clones that hybridized across the FRA7G region in aphidicolin-induced cells from a chromosome 7-only somatic cell hybrid. These three YAC clones contained the marker D7S522, the most frequently deleted marker from this region in breast, prostate, and ovarian cancers. All this work is summarized in our 1998 *Genes, Chromosomes and Cancer* paper (Appendix Manuscript #1: Huang et al. Fish mapping of YAC clones at human chromosomal band 7q31.2. *Genes Chromosom Cancer* 1998; 21:152-159). We then went on to identify three P1 artificial chromosomes (PACs) and one bacterial artificial chromosome (BAC) which covered a 300 Kb region around FRA7G. We performed a FISH-based analysis with these four clones to determine how frequently each clone hybridized proximal, distal, or crossing to the region of aphidicolin-induced decondensation/breakage in the FRA7G region. The results of this analysis are summarized below.

Clones	N	%Prox	%Crossing	%Dist	%Prox-%Dist
v203B	20	10	10	80	-70
RG30H15	22	9.1	27.3	63.6	-54.5
v203C	31	25.8	32.3	41.9	-16.1
v193A	41	63.4	22	14.6	48.8

Note: N, the number scored of metaphase spreads with FRA7G expression. The %Prox, %Dist, and %Crossing refer to the percentage of the time that FISH signals were seen proximal, distal, or across the breaks of FRA7G in different cells, respectively.

Since one of the goals for this Specific Aim was to construct a high-resolution physical map for the two common fragile site regions, we used the three PAC clones and one BAC clone spanning FRA7G to construct a precise restriction map for this region. We used pulsed field gel analysis to construct these high-resolution maps. Subsequent to this analysis we found that the BAC clone from this region was completely sequenced in early 1999, and this enabled us to verify that our restriction map was indeed correct. In addition, right in the middle of the sequenced BAC clone was a human endogenous retroviral sequence (HERV-H). This provides further support that the fragile sites might be hot-spots for viral integrations. A complete map of the FRA7G region is shown in the figure on the following page.

A

TELOMERE ←   D7S522 D7S486   → CENTROMERE

921B4 (1540kb)   100kb

831B12 (1040kb)

746H5 (1160kb)

FRA7G

B

v203B(91kb)   10kb

RG30H15 (151kb)

v203C(148kb)

v193A(135kb)

C

RG30H15   5kb

T D D   D   Three MERs D   THE1   Long L1 D   spcDNA
HERV-H   D7S522   Long L1

One of our stated goals was to construct a contig of overlapping cosmids from this region. Since we already had the slightly larger PAC and BAC clones and the high-resolution restriction map based upon these clones, we decided that it was not necessary to construct a cosmid contig across the exact same region. All of the work on the PAC clones and the single BAC clone were published in *Oncogene*, also in 1998 (Appendix Manuscript #2: Huang et al. FRA7G extends over a broad region: coincidence of HERV-H and spcDNA and fragile sites. *Oncogene* 1998; 16:2311-9).

Characterization of FRA16D

The second common fragile site that we proposed to analyze was FRA16D (16q23.2). This fragile site is derived from a chromosomal region frequently deleted in prostate cancer (and also in breast and ovarian cancers and hepatocellular carcinomas). Chromosomal band 16q23.2 is also the site of a reciprocal translocation between chromosomes 14 and 16 that is observed in up to 25% of multiple myelomas. When we submitted our proposal to the Department of Defense, we had a single YAC clone which was identified by our collaborator, Dr. Thomas Glover. However, a more detailed analysis of this YAC clone revealed that it was chimeric, containing pieces from at least three different chromosomes (including a small amount from chromosome 16q23.2). In addition, there were no known markers that mapped to this YAC clone. Rather than work on this YAC, we scanned the available databases and chose markers from chromosomal band 16q23.2 which were integrated into both the physical and genetic maps for this region.

We initiated the construction of a contig of BAC clones from this region by taking the available markers from this region and isolating large insert BAC clones that spanned these markers. This was done by screening the Research Genetics BAC pools to identify the BAC clones. The advantage of this strategy is that these BAC clones are also the reagents being sequenced by the Human Genome Project, and thus over time we would have a contig of BACs with more of them being completely sequenced. We very

quickly identified clones that hybridized proximal to the region of aphidicolin-induced decondensation/ breakage in some metaphases and distal in others. Depending upon the ratio of hybridization signals detected proximal to those detected distal, we could also determine approximately where within the FRA16D region each BAC clone resided. However, it soon became abundantly clear that the region of aphidicolin-induced decondensation/breakage in this region was very large. Our efforts to thus construct a contig of overlapping BACs which encompassed the entire FRA16D region took considerably longer than originally anticipated. We had a team of three researchers working on this project for almost two years. Our goal was to identify BAC clones which always hybridized proximal to the region of aphidicolin-induced decondensation/breakage (out of a minimum of 20 metaphases with clear discernible FISH hybridization signals) and then to have a complete contig (without gaps) of BACs until we had identified a BAC that always hybridized distal to the region of breakage. We found that the full size of the FRA16D region was actually 1.5 megabases in size, making this the largest common fragile site characterized to date. While we were constructing the complete BAC contig, we also found that four of four cloned multiple myeloma breakpoints with breakpoints within chromosomal band 16q23.2 mapped within the FRA16D region. Thus, instability in the FRA16D region also played a role in the development of the consistent chromosomal translocation observed in up to 25% of multiple myelomas. We also found that the markers which showed the most consistent loss in solid tumors (including prostate, breast, and ovarian cancers and hepatocellular carcinomas) were also derived from within the FRA16D region. The following figure shows the complete BAC contig constructed across this region. Also included on this figure are the positions of the four multiple myeloma translocation breakpoints and several of the markers which show consistent loss in multiple solid tumors.

Marker	Heterozygosity	Product Size (bp)	Sequenced Region
D16S3144	.42	259	D16S3144
293S			293S
436S			436S
D16S2742		165	D16S2742
A-645S			A-645S
D16S504	.65	267	D16S504
303S			303S
A-653S			A-653S
D16S516	.73	170	D16S516
A-645T			A-645T
436T			436T
D16S2812			D16S2812
D16S2830		134	D16S2830
A-653T			A-653T
36T			36T
D16S2683		117	D16S2683
D16S3056	.73		D16S3056
D16S2728		254	D16S2728
216S			216S
D16S3028	.68	167	D16S3028
D16S3048	.77	233	D16S3048
303T			303T
36S			36S
245T/551S			551S
112T/215S			112T
216T			216T
D16S3324		137	D16S3324 (MM.1)
315S			315S
256T			256T
243S			243S
215T			215T
315T			315T
V12755		112	V12755
D16S3213		114	D16S3213 (STSG-10102)
435T			435T
546S			546S
112S			112S
551T			551T
258S			258S
256S			256S
41S			41S
258T			258T
435S			435S
546T			546T
120T			120T
124S			124S
AFMA336YG3			AFMA336
41T			41T
120S			120S
347S			347S
124T			124T
D16S684	.63	336	D16S684
87T/164S/356T			164S
34TT			34TT
87S			87S
330S			330S
324S			324S
179S			179S
324T/330S			324T
D16S518	.83	211	D16S518
26T			26T
503T			503T
356S			356S
179T			179T
247S/211T			247S
26S			26S
219T			219T
503S			503S
247T			247T
D16S2793		321	D16S2793
328CT			328CT
221S			221S
219S			219S
313S			313S
331S/393T			331S
328CS			328CS
D16S3101			
221T			221T
26TT/414S			26TT
393S			393S
D16S3125	.81	183	D16S3125
D16S3138	.86	223	D16S3138
331T			331T
313T			313T
414T			414T
315T			315T
287S			287S
336T			336T
277KS			277KS
375S			375S
D16S3037	.84	134	D16S3037
D16S782		237	D16S782
277KT			277KT

BAC clones (column headers): 277_K_1, 328_J_19, 376_H_19, 396_L_24, 287_B_8, 414_J_4, 313_F_8, 331_A_11, 393_P_22, 328_C_8, 493_L_10, 219_E_3, 271_M_16, 247_G_13, 603_D_19, 26_K_6, 179_M_14, 356_D_21, 164_M_23, 330_Q_6, 324_Q_20, 87_C_4, 347_F_19, 124_L_16, 120_B_7, 41_P_2, 646_G_23, 435_K_13, 268_D_2, 286_K_13, 661_G_11, 112_B_17, 316_P_3, 216_B_7, 249_B_4, 660_A_11, 216_C_20, 36_O_22, 463_A_16, 277_B_6, 303_G_6, A-469_A_2, A-646_H_11, 469_E_14, 293_D_2, 269_H_23, 484_H_3

BAC Size (kb): 139, 130, 134, 108, 139, 123, 138, 131, 120, 101, 101, 144, 134, 121, 142, 141, 144, 136, 143, 96

When we submitted this work for publication, we found that several other groups were also working on the physical characterization of this very interesting region; including the groups of Dr. Rob Richards (Adelaide, Australia) and Dr. Vivien Watson (now at University of California, San Francisco). These two groups published results which were very similar to ours. However, their characterization of the FRA16D region led them to believe that the size of this common fragile site was considerably smaller than our determination. Our paper on the characterization of this interesting region was recently published in *Genomics* (Appendix Manuscript #3: Krummel et al. The characterization of the common fragile site FRA16D & its involvement in multiple myeloma translocations. *Genomics* 2000; 69:37-46).

The sequencing of the human genome has now resulted in a preliminary draft sequence containing 90% of the sequence. Many of the BAC clones from our 1.5 megabase BAC contig have been completely sequenced. As a result it is no longer necessary to construct high resolution pulsed field gel maps of any chromosomal region, so we did not bother to characterize this region with pulsed field gel analysis. As a result of the draft sequence, it is now possible to more accurately examine the entire region in search of important landmarks (including genes, repetitive sequences, etc.). This analysis revealed that the FRA16D region does not contain any obvious sequences responsible for instability within this region, nor does it contain simple repetitive sequences (as has been observed at the cloned rare fragile sites).

Task #2

To isolate genes from the fragile site regions and test them for mutations in primary prostate cancer. We proposed to scan for homozygous deletions in purified prostate tumor tissue. We also proposed to isolate genes from within these two regions and to test these genes for mutations in prostate cancer cell lines and in primary tumors.

Genes in FRA7G

The analysis of the region of aphidicolin-induced breakage/decondensation in FRA7G revealed that this common fragile site was approximately 300 Kb in size. Telomeric of this region was the c-met proto-oncogene. We analyzed this gene for mutations in primary prostate tumors using denaturing high performance liquid chromatography (DHPLC). We did not detect any mutations in c-met in any of the prostate tumors examined. We also examined primary breast and ovarian tumors but did not observe mutations in any of these samples. We did detect some simple sequence polymorphisms but no apparent disease-associated mutations. Our work was summarized in a paper published in 1998 (Appendix Manuscript #4: Jenkins et al. A molecular cytogenetic analysis of 7q31 in prostate cancer. *Cancer Res*. 1998; 58:759-766).

We collaborated with the group of Dr. Robert Jenkins and performed a molecular cytogenetic analysis of 7q31 in prostate cancer. We studied 25 prostate specimens using fluorescence *in situ* hybridization (FISH) with DNA probes for the chromosome 7 centromere and 5 loci mapped to 7q31 (D7S523, D7S486, D7S522, D7S480 and D7S490). Six tumors had no apparent anomaly for any chromosome 7 probe. Nine tumors showed an apparent simple gain of an entire chromosome 7, whereas one tumor had an apparent simple loss of a whole chromosome 7. Four tumors had gain of the chromosome 7 centromere and additional overrepresentation of the 7q arm. One tumor had overrepresentation of 7q31 without any apparent anomaly of the chromosome 7 centromere, and one tumor had apparent loss of the chromosome 7 centromere with no apparent anomaly of the 7q arm. Three tumors had gain of the chromosome 7 centromere and loss of the 7q31 region. Gain of 7q31 was strongly correlated with tumor Gleason score. Our data indicate that the 7q-arm, particularly the 7q31 region, was genetically unstable

in prostate cancer, and some of the gene dosage differences observed may be due to fragility at FRA7G. All this work was summarized in our paper that also described searching prostate tumors for c-met alterations (Appendix Manuscript #4: Jenkins et al. A molecular cytogenetic analysis of 7q31 in prostate cancer. *Cancer Res.* 1998; 58:759-766).

In collaboration with Dr. Jenkins' group, we also analyzed primary prostate tumors to determine if we could detect any homozygous deletions in the FRA7G region. We constructed PCR primers at a 20 Kb spacing throughout the entire FRA7G region but were not able to identify any tumors with homozygous deletions.

There were two small genes that were localized in the FRA7G region by the group of Dr. Michael Lisanti. These genes are caveolin-1 and caveolin-2. These genes have been claimed to be tumor suppressors and Dr. Lisanti's group observed that the re-introduction of caveolin-1 into tumors lacking it resulted in growth inhibition. We performed an extensive DHPLC analysis of both these genes in our resource of prostate tumors (and in breast and ovarian tumors) but did not detect any mutations in these genes. Thus, these genes may play an important role in tumor development, but they are not Type 1 tumor suppressor genes.

Recently, the group of Dr. Carlo Croce described a new gene that mapped in the FRA7G region. This gene is called TESTIN and Dr. Croce's group described alterations in this gene and changes in TESTIN expression in cell lines derived from leukemias and lymphomas and in some solid tumors. We have not, however, had time to analyze this gene for alterations in primary prostate tumors. The figure below shows the entire FRA7G region and the genes that have been localized within the region to date.

R-51M22 (162)
HSA133269 (191)
HS_5141_B1_H09_T7A   RG030H15 (152)   RG253B13 (172)   RG013N12 (32)
RG011K01 (~166)   RG300C03 (150)
Contig 1 (46 kb)   Contig 2 (120 kb)
q31.2   q31.2

204l16 F40/R38
51m22F83/R85
AI807692F45/R42
1bS490/A965
2522F107/R354
D7S486 F0/R102
AA432162 F0/R245
51m22F27/R302
51m22F50/R41
030F5/R15
030F17/R16
R99779 7NS/7NA
D7S522
AI138665 F21/R31
CAV2E1 F50/R34
CAV2E2 F26/R25
AA150792 F33/R24
CAV2E3 F34/R33
CAV1E1 F15/R12
CAV1E2 F43/R11
CAV1E3 F20/R38
AF070648 7HS/7HA
253 F1205/R1585
253B13 FC/RB
253 F86053/R86613
AI034367 F56/R457
AA218763 F1/R348
D7S2460
AA405639 F8/R395
MetH

CEN ←   TESTIN   HERV8   CAV2   CAV1   24651   MET   CAPZA2   TEL →

A
B

FRA7G

50   100   150   200 kb

Genes in FRA16D

While we were working to construct the complete BAC contig across the entire FRA16D region, we also initiated a search for genes within that region. We were fortunate that many more BAC clones from this region were sequenced (especially in the last few months). The first gene that we identified from this region was a c-type lectin. Unfortunately, this gene has a very restricted range of tissue-specific expression and this gene is not produced in normal prostate epithelial cells (or in normal breast or ovarian epithelial cells either). This gene seemed like a poor candidate for an important gene involved in prostate tumor development.

The gene for the proto-oncogene c-maf was localized telomeric of the markers that showed the most frequent loss in prostate tumors. However, once we realized that the FRA16D region was the largest common fragile site region characterized to date, we were curious whether c-maf could be localized on the telomeric edge of the FRA16D region. This did not turn out to be the case. Indeed, we now know that c-maf is at least 500 Kb telomeric to the edge of the FRA16D region. This is important as we were curious about two things with respect to c-maf: (1) Could it play a role in prostate tumor development? and (2) What role does c-maf play in multiple myelomas with the t(14:16) translocation? Since c-maf was outside of the FRA16D region, we did not pursue a detailed analysis of this gene in our resource of primary prostate tumors. However, we did analyze the four multiple myeloma cell lines with translocations into the FRA16D region. This analysis revealed that c-maf was at least 500 Kb from the translocation breakpoints in all four cell lines. Thus, what role could this proto-oncogene play in multiple myeloma development? Was there another gene within the FRA16D region that played an important role in both prostate tumor and multiple myeloma development?

The groups of Manuel Aldaz (University of Texas) and Rob Richards recently reported on the isolation of a very large gene called WWOX (by Dr. Aldaz) and FOR (by Dr. Richards). This gene was found to span the entire FRA16D region. In many respects it appears very similar to FHIT as it is a large gene with relatively small exons whose genomic structure spans greater than 1 megabase across a very active common fragile site. The figure below shows the genomic structure of the WWOX gene across the FRA16D region. We have examined over 20 primary prostate tumor specimens for alterations in the WWOX gene but have not yet detected either any gross structural alterations or subtle point mutations (however, we have not completed the sequencing of all WWOX exons).
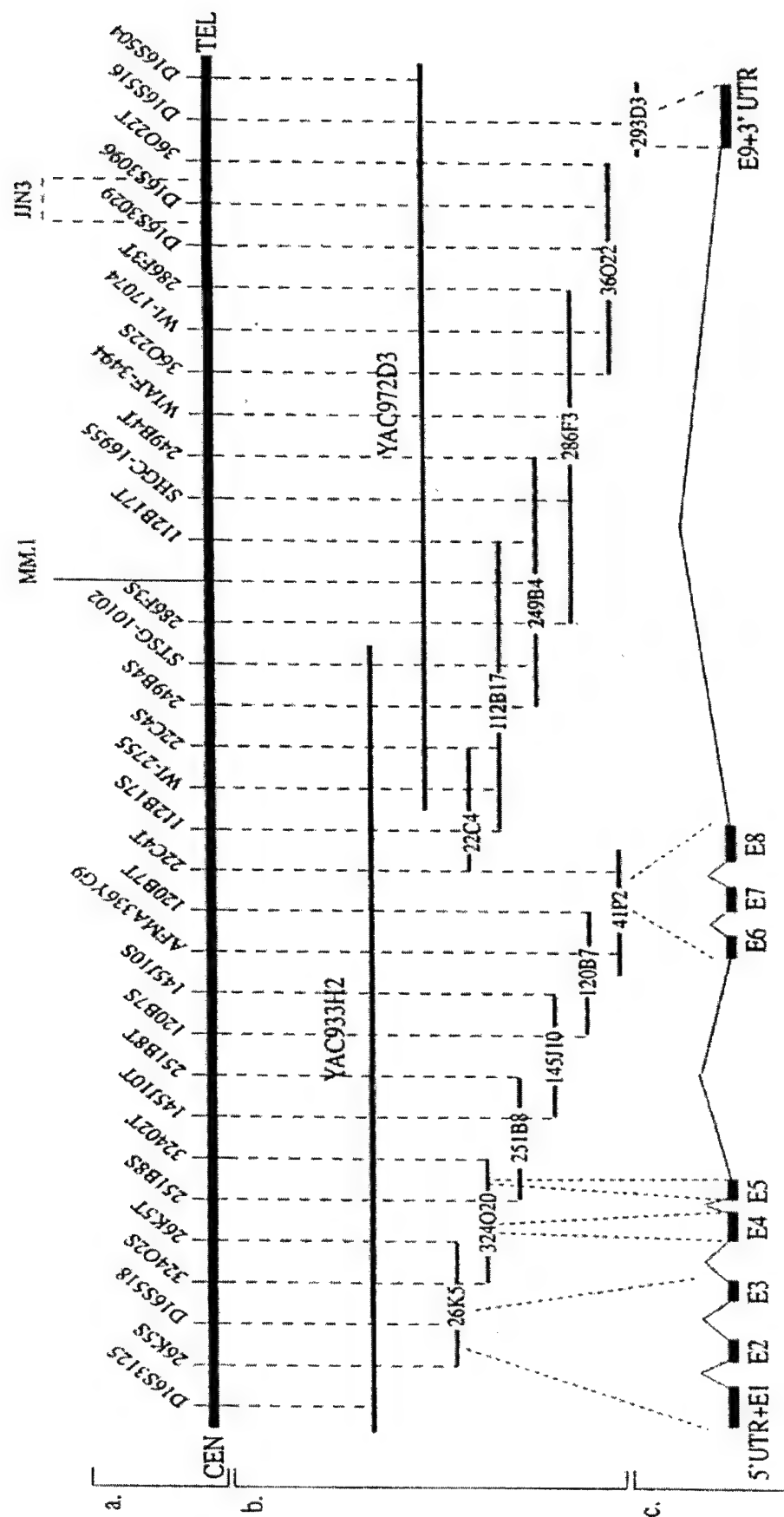
Although it was not a specific task of our original Prostate Proposal, we were interested in whether the FRA16D region and the WWOX gene that spans much of that region were evolutionarily conserved through evolution. Dr. Thomas Glover's group had demonstrated several years ago that the FRA3B region and the FHIT gene spanning it were conserved between man and mouse, and we wished to perform a similar analysis with the homologous mouse region and compare it to the genomic organization of the human FRA16D region. We isolated mouse BAC clones using primers designed from the human WWOX gene sequence. Using different WWOX exons we isolated several overlapping and several non-overlapping BAC clones from the mouse WWOX gene. When these BACs were used as FISH-based probes against aphidicolin-induced mouse spleen cells, we found that the mouse WWOX gene sits right on top of a mouse aphidicolin-sensitive fragile site region. However, the mouse band that contains the WWOX gene (which is on mouse chromosome 16) contains a less active common fragile site (as compared to mouse common fragile sites) than human chromosomal band 16q23.2 (FRA16D).

Task #3

To determine if the genes from the fragile site regions are tumor suppressors, "sensors" or merely passengers to the genomic instability within the common fragile site regions. To answer this question we proposed to examine whether there were tumor suppressor genes in these common fragile sites regions. Genes within the regions would also be tested to determine if they could function as sensors of genomic damage.

The first goal of this task was to determine if any of the genes identified from the FRA16D or FRA7G regions were in some way important to the development of prostate cancer. Each of the genes identified within or close to these two fragile regions was first tested for tumor-specific mutations (as described above under Task #2). While this analysis revealed that several of the genes (including caveolin-1, caveolin-2, and TESTIN) showed a loss of expression in different tumors (including prostate tumors), we detected no mutations in any of the genes analyzed (including the distal c-maf gene).

Our second goal was to test whether the genes in these two fragile regions could somehow be functioning as sensors of genomic damage. Our evidence to suggest this was based upon some preliminary assays with the FHIT gene (spanning FRA3B, the most active common fragile site) which suggested that agents affecting replication caused increases in FHIT expression. We analyzed several of the genes identified within these two regions. We did not test the two recently identified genes, TESTIN and WWOX, but worked instead with caveolin-1 and –2, c-maf, and the small c-type-lectin gene identified within the FRA16D region. We cultured cells with aphidicolin, distamycin A, or caffeine, and then measured the expression levels of these genes. Unfortunately, we saw no changes in the expression of any of the four genes tested, suggesting that the expression of these genes are not changed by chemicals which cause common fragile site expression.

Our original proposal stated that genes within the fragile site regions would either be tumor suppressors, sensors, or by process of elimination, merely passengers to the instability which occurs in these regions. There is no definitive evidence that any of the genes within the common fragile site regions are actually tumor suppressors. The FHIT gene has been suggested to be a tumor suppressor, but even in this much investigated gene there are some profound distinctions between alterations observed in this gene and alterations observed in the canonical tumor suppressor Rb. We found no evidence that the genes within FRA7G or FRA16D acted as "sensors" of genomic damage. However, it also appeared unlikely that the interesting genes from these regions are merely passengers of genomic instability. The caveolin-1 gene (from the FRA7G region) has been shown to not be expressed in many different tumor types and

suggested to be a tumor suppressor. A recent report from Michael Lisanti's group demonstrated that caveolin-1 expression is down-regulated in cells transformed by the human papilloma virus in a p53-dependent manner. In addition, replacement of caveolin-1 expression suppressed HPV-mediated cell transformation. Thus, caveolin-1 appears to play an important role at least in the development of cervical cancer (*Biochemistry* 2000; 39:13916-24).

We analyzed gene expression in primary ovarian tumors as part of our work in the Ovarian Cancer Program of the Mayo Clinic Cancer Center. When we analyzed the most consistently down-regulated genes from our preliminary analysis of 15 ovarian tumors, we found that many of these genes were derived from chromosomal bands known to contain common fragile sites. We analyzed the top 10 hit genes and found that 7 of these spanned a common fragile site. This analysis enabled us to quickly localize a number of previously uncloned common fragile sites. In addition, it demonstrated that many of the genes at other common fragile sites also show a frequent loss of expression in tumor cells. We submitted our competing renewal of this proposal based upon this observation. Our goal was to analyze a number of the genes derived from within the common fragile site regions for their expression in primary prostate tumors. We believe that the genes within the common fragile site regions are frequently inactivated during tumor development and that this inactivation does play an important role in cancer development. However, we still have not shown a definitive connection between the common fragile site regions, the genes contained within these regions, and cancer development.

KEY RESEARCH ACCOMPLISHMENTS
(1) Cloning of the FRA7G region.
(2) Cloning of the FRA16D region. Determination that this region spans over 1.5 megabases.
(3) Identification of multiple genes within the FRA7G region, including caveolin-1, caveolin-2, TESTIN, and the distal c-maf gene.
(4) Tested all the genes within FRA7G or FRA16D for mutations in primary prostate tumors. None detected.
(5) Determined that the genes within these regions were not "sensors" of genomic damage.
(6) Found that the genes within the common fragile site regions are frequently inactivated in many different solid tumors.
(7) Cloned a number of additional common fragile sites and have begun to characterize these regions and the genes contained within.

REPORTABLE OUTCOMES
Manuscripts/Papers since 1998
1. Wang X-Y, **Smith DI**, Frederick L, James CD. Analysis of EGF receptor amplicons reveals amplification of multiple expressed sequences. *Oncogene* 1998; 1:191-195.
2. Huang H, Qian C, Jenkins RB, **Smith DI**. FISH mapping of YAC clones at human chromosomal band 7q31.2: Identification of YACs spanning FRA7G within the common region of LOH in breast and prostate cancers. *Genes Chromosom. Cancer* 1998; 21:152-159.
3. Wang L, Darling J, Zhang J-S, Qian C-P, Hartmann L, Conover C, Jenkins R, **Smith DI**. Frequent homozygous deletions in the FRA3B region in tumor cell lines still leave the FHIT exons intact. *Oncogene* 1998; 16:635-642.
4. LeBeau MM, Drabkin H, Glover TW, Gemmill R, Rassool FV, McKeithan TW, **Smith DI**. A FHIT tumor suppressor gene? *Genes Chromosom. Cancer* 1998; 21:281-289.
5. Huang H, Qian J, Proffitt J, Wilber K, Jenkins R, **Smith DI**. FRA7G extends over a broad region: Coincidence of human endogenous retroviral sequences (HER-V) and small polydispersed circular DNAs (spcDNA) and fragile sites. *Oncogene* 1998; 16:2311-2319.
6. Jenkins RB, Qian J, Lee HK, Huang H, Hirasawa K, Bostwick DG, Proffitt J, Wilber K, Lieber MM, Liu W, **Smith DI**. Molecular cytogenetic analysis of 7q31 in prostate cancer. *Cancer Res.* 1998, 58:759-766.

7. Wang X-Y, Liu W, **Smith DI**, James CD. GBAS, a novel gene encoding a protein with tyrosine phosphorylation sites and a transmembrane domain, is co-amplified with EGFR. *Genomics* 1998; 49(3):448-51.

8. Liu W, **Smith DI**, Thibodeau S, James CD. Denaturing high performance liquid chromatography (DHPLC) used in the detection of germline and somatic mutations. *Nucl. Acids Res*. 1998; 26:1396-1400.

9. LeBeau MM, Rassool FV, Neilly ME, Espinosa III R, Glover TW, **Smith DI**, McKeithan TW. Replication of a common fragile site, FRA3B, occurs late in S phase and is delayed further upon induction: implications for the mechanism of fragile site induction. *Hum. Molec. Genet*. 1998; 7:755-761.

10. Willett CG, Wang MH, Emanuel RL, Graham SA, **Smith DI**, Shridhar V, Sugarbaker DJ, Sunday ME. Macrophage-stimulating protein and its receptor in non-small-cell lung tumors: induction of receptor tyrosine phosphorylation and cell migration. *Amer. J. Respir. Cell Mol. Biol*. 1998; 18:489-496.

11. Mai M, Yokomizo A, Tindall DJ, Qian C, Yang P, **Smith DI**, Liu W. Activation of silent alleles of p73 in lung cancer. *Cancer Res*. 1998; 58: 2347-2349.

12. Yokomizo A, Tindall DJ, Drabkin HA, Gemmill R, Franklin W, Yang P, Sugio K, **Smith DI**, Liu W. PTEN/MMAC1 mutations identified in small cell lung cancers, but not in non-small cell lung cancers. *Oncogene* 1998; 17:475-479.

13. Zhang J-S, Nelson M, McIver B, Hay ID, Goellner JR, Grant CS, Eberhardt NL, **Smith DI**. Differential loss of heterozygosity at 7q31.2 in follicular and papillary thyroid tumors. *Oncogene* 1998; 17:789-793.

14. Mai M, Huang H, Reed C, Qian C, Smith JS, Alderete B, Jenkins R, **Smith DI**, Liu W. Genomic organization and mutation analysis of p73 in oligodendrogliomas with chromosome 1p-arm deletions. *Genomics* 1998; 51:359-363.

15. Mai M, Qian C, Yokomizo A, Tindall DJ, Bostwick D, Polychronakos C, **Smith DI**, Liu W. Loss of imprinting and allele switching of p73 in renal cell carcinoma. *Oncogene* 1998; 17:1739-1741.

16. Eley G, Wang X-Y, Frederick L. **Smith DI**, and James CD. 3' end structure and rearrangements of EGFR in glioblastomas. *Genes Chromosom. Cancer* 1998; 23:248-254.

17. Yokomizo A, Tindall DJ, Hartmann L, Jenkins RB, **Smith DI**, Liu W. Mutation analysis of the putative tumor suppresor PTEN/MMAC1 in human ovarian cancer. *Int. J. Onc*. 1998, 13:101-105.

18. Zhang J-S, Nelson M, Wang L, Liu W, Qian C-P, Shridhar V, Urritia R, **Smith DI**. Identification and chromosomal localization of CTNNAL1, a novel leucine zipper protein homologous to α-catenin. Genomics 1998; 54:149-154.

19. *Gemmill* R, West JD, Boldog F, Sugita M, Robinson LJ, **Smith DI**, Li F, Drabkin HA. The hereditary renal cancer 3;8 translocation fuses FHIT to TRC8, a gene related to the hedgehog receptor, patched. *Proc. Natl. Acad. Sci. USA* 1998; 95:9572-9577.

20. Huang H, Reed CP, Mordi A, Lomberk G, Wang L, Shridhar V, Hartmann L, Jenkins R, **Smith DI**. Frequent deletions within FRA7G at 7q31.2 in invasive epithelial ovarian carcinomas. *Genes Chromosom. Cancer* 1999; 24:48-55.

21. Yokomizo A, Mia M, Tindall DJ, Cheng L, Bostwick DG, Naito S, **Smith DI**, Liu W. Over-expression of the wild type p73 gene in invasive bladder cancer. *Oncogene*. 1999; 18:1629-1633.

22. Yokomizo A, Mai M, Bostwick DG, Tindall DJ, Qian J, Cheng L, Jenkins RB, **Smith DI**, Liu W. Mutation and expression analysis of the p73 gene in prostate cancer. *Amer. J. Pathol*. 1999; 39: 94-100.

23. Mai M, Qian C, Yokomizo A, **Smith DI**, Liu W. Cloning of human conductin (axin), a gene mapping to chromosome 17q23-24. *Genomics* 1999; 55:341-344.

24. Wang L, Darling J, Zhang J-S, Liu W, **Smith DI**. Allele-specific late replication and fragility of the most active common fragile site, FRA3B. *Human Mol. Genet*. 1999; 8:431-437.

25. Shridhar V, Jett JR, **Smith DI**. Molecular advances in the biology of premalignant lesions of lung cancer. *Respiratory Care Matters*, 1999, 3:14-15.

26. Huang H, Reed CP, Zhang J-S, Shridhar V, Wang L, Bright R, **Smith DI**. Carboxypeptidase A3 (CPA3): A novel gene highly induced by histone decetylase inhibitors during differentiation of prostate epithelial cancer cells. *Cancer Res*. 1999, 59:2981-2988.

27. Shridhar V, Staub J, Huntley B, Cliby W, Jenkins R, Pass HI, Hartmann L, **Smith DI**. A novel region of deletion on chromosome 6q23.3 spanning less than 500 Kb in high grade invasive epithelial ovarian cancer. *Oncogene* 1999;18:3913-3918.

15

28. Schwartz DI, Lindor NM, Walsh-Vockley C, Roche PC, Mai M, **Smith DI**, Liu W, Couch F. p73 mutations are not associated with sporadic and familial breast cancer. *Breast Cancer Research and Treatment,* 1999, 58:25-29.

29. Kawakami M, Staub J, Cliby W, Hartmann L, **Smith DI**, Shridhar V. Involvement of H-cadherin (CDH13) on 16q in the region of frequent deletion in ovarian cancer. *Int. J. of Oncology,* 1999; 15:715-720.

30. Vockely J, Rogan PK, Anderson BD, Willard J, Seelan RS, **Smith DI**, Liu W. Exon skippping in isovaleric acidemia caused by point mutations in the IVD gene. *Amer. J. Hum. Genet.* 2000, 66:356-367.

31. Wang L, Darling J, Zhang J-S, Liu W, Qian J, Bostwick D, Hartmann L, Jenkins R, **Smith DI**. Loss of expression of the DRR-1 gene at chromosomal band 3p21.1 in renal cell carcinoma. *Genes, Chromosomes and Cancer.* 2000, 27: 1-10.

32. Liu W, Mai M, Yokomizo A, Qian C, Tindall DJ, **Smith DI**, Thibodeau SN. Differential expression and allelotyping of the p73 gene in neuroblastoma. *Int. J. Oncology,* 2000; 16:181-185.

33. Ren S, Smith MJ, Louro ID, Mckie-Bell P, Rosa Bani M, Wagner M, Zochodne B, Redden DT, Grizzle WE, Wang N-D, **Smith DI**, Herbst RA, Bardenheuer W, Opalka W, Schutte J, Trent JM, Ben-David Y, Ruppert JM. The p44 locus, encoding a subunit of the proteasome regulatory particle, is amplified during progression of cutaneous malignant melanoma. *Oncogene,* 2000, 19:1419-1427.

34. McIver B, Grebe SK, Wang L, Hay ID, Yokomizo A, Liu W, Goellner JR, Grant CS, **Smith DI**, Eberhardt NL. FHIT and tsg101 in thyroid tumors: aberrant transcripts reflect abnormal RNA processing events of uncertain pathogenetic or clinical significance. *Clin. Endocrinol.* 2000; 52:749-757.

35. Seelan RS, Qian C, Yokomizo A, Bostwick DG, **Smith DI**, Liu W. Structural organization of human acid ceramidase and expression in prostate cancer. *Genes, Chromosomes, Cancer,* 2000, 29:137-146.

36. Liu W, Dong X, Mai M, Seelan R, Taniguchi K, Krishnadath KK, Halling KC, Cunningham JM, Qian C, Christensen E, Roche PC, **Smith DI**, Thibodeau SN. Activation of β-catenin-Tcf signaling by mutated human conductin (AXIN2) in colorectal cancer with defective mismatch repair. *Nature Genetics,* 2000, 26:146-147.

37. Krummel KA, Roberts LR, Kawakami M, Glover TW, **Smith DI**. The characterization of the common fragile site FRA16D and its involvement in multiple myeloma translocations. *Genomics,* 2000, 69:37-46.

38. Irwin M, Marin MC, Phillips AC, Seelan RS, **Smith DI**, Liu W, Flores ER, Tsai KY, Jacks T, Vousden KH, Kaelin WG. Role of the p53 homologue p73 in E2F-1-induced apoptosis. *Nature* 2000, 407:645-648.

39. Thorland EC, Myers SL, Persing DH, Sarkar G, McGovern RM, Gostout BS, **Smith DI**. HPV16 integrations in cervical tumors frequently occur in common fragile sites. *Cancer Res.* 2000, 60:5916-5921.

40. Zhang J-S, Wang L, Huang H, Nelson M, **Smith DI**. Keratin 21 (K21), a novel acidic keratin, is highly induced by histone deactylase inhibitors during differentiation of pancreatic cancer cells. *Genes Chromosom. Cancer* 2000; in press.

Abstracts since 1998

1. **Smith DI**, Wang L, Huang H. Common fragile sites and cancer development. 1998 AACR meeting on Innovative approaches to the prevention, diagnosis and therapy of cancer. Innovative approaches to the prevention, diagnosis and therapy of cancer. Feb. 1998 in Maui, Hawaii.

2. Liu W, Yokomizo A, Cheong-Yong K, Frederick L, Qian C, Bostwick D, Jenkins R, Thibodeau S, **Smith DI**, Liu W. Denaturing HPLC identified PTEN mutations in glioblastomas but not in prostate cancers. Innovative approaches to the prevention, diagnosis and therapy of cancer. Feb. 1998 in Maui, Hawaii.

3. Qian J, Lee HK, Huang H, Hirasawa K, Bostwick DG, Proffitt J, Wilber K, Lieber MM, Liu W, **Smith DI**, Jenkins RB. A molecular cytogenetic analysis of 7q31 in prostate cancer. Amer. Assoc. Cancer **Res. 1998, 39:A875.**

4. **Smith DI**, Wang L, Qian J, James CD, Jenkins R, Huang H. Common fragile sites and cancer. Amer. Assoc. Cancer Res. 1998, 39:A3210.

5. Eley G, Wang X-Y, **Smith DI**, Frederick L, Hebrink D, James CD. Genomic characterization of EGFR rearrangements resulting in C-terminal protein truncations in glioblastomas. Amer. Assoc. Cancer Res. 1998, 39:A3211.

6. Wang X-Y, **Smith DI**, James CD. CAG, a novel gene encoding a protein with tyrosine phosphorylation sites and a transmembrane domain, is co-amplified with EGFR. Amer. Assoc. Cancer Res. 1998, 39:A3207.
7. McIver B, Hung A, Hay ID, **Smith** DI, Eberhardt NL. PTEN/MMAC1 mutations are common in follicular thyroid cancer. Amer. Assoc. Cancer Res. 1998; 39:A4205.
8. Vockley J, Anderson BD, Willard JM, Seelan RS, **Smith DI**, Liu W. Abnormal splicing of IVD RNA in isovaleric acidemia caused by amino acid altering point mutations in the IVD gene: a novel molecular mechanism for disease. Amer. J. Hum. Genet. 1998, 63:A65.
9. Gemmill R, West JD, Boldog F, Tanaka L, Robinson LJ, **Smith DI**, Li FP, Drabkin HA. The hereditary renal cell carcinoma 3;8 translocation fuses FHIT to a novel patched related gene, TRC8. Amer. J. Hum. Genet. 1998, 63:A201.
10. Wang L, Darling J, Zhang J-S, Liu W, **Smith DI**. Allele-specific late replication in the most active common fragile site, FRA3B. Amer. J. Hum. Genet. 1998, 63:A216.
11. Huang H, Reed CP, Qian J, Proffit J, Wilber K, Hartmann L, Liu W, Jenkins RB, **Smith DI**. Colocalization of the common fragile site, FRA7G, and the common region of deletion in prostate, breast and ovarian cancer. Amer. J. Hum. Genet. 1998, 63:A395.
12. James CD, Eley G, Wang X-Y, **Smith DI**. 3' end structure and rearrangements of EGFR in glioblastomas. Amer. J. Hum. Genet. 1998, 63:A399.
13. Kawakami M, Hartmann L, Huntley B, **Smith DI**, Shridhar V. Allele loss on 16q in high-grade invasive epithelial ovarian cancer. Amer. J. Hum. Genet. 1998, 63:A400.
14. Liu W, Mai M, Yokomizo A, Qian C, Tindall DJ, **Smith DI**, Thibodeau S. Loss of imprinting and haplotype association of the p73 gene in neuroblastoma. Amer. J. Hum. Genet. 1998, 63:A411.
15. Mai M, Huang H, Reed C, Qian C, Smith J, Alderete B, Jenkins RB, **Smith DI**, Liu W. Genomic organization and mutation analysis of p73 in oligodendrogliomas with chromosome 1p-arm deletions. Amer. J. Hum. Genet. 1998, 63:A415.
16. Seelan RS, Qian C, **Smith DI**, Liu W. Characterization of 8p22, a chromosome region frequently deleted in prostate cancer. Amer. J. Hum. Genet. 1998, 63:A465.
17. Shridhar V, Staub J, Huntley B, Pass HI, Hartmann L, **Smith DI**. A novel region of deletion within chromosomal band 6q23.3 spanning less than 1 cM in high grade invasive epithelial ovarian cancer. Amer. J. Hum. Genet. 1998, 63:A472.
18. Yokomizo A, Mai M, Tindall DJ, Qian J, Cheng L, Bostwick DG, Jenkins RB, Naito S, **Smith DI**, Liu W. Mutation and expression analysis of the p73 gene in human bladder and prostate cancer. Amer. J. Hum. Genet. 1998, 63:A510.
19. Zhang J-S, Nelson M, Shridhar V, Bright R, **Smith DI**. High throughput screening for differentially expressed genes in matched normal/tumor prostate epithelial cell lines. Amer. J. Hum. Genet. 1998, 63:A515.
20. Jett JR, Halling A, Tazelaar H, Edell E, Midthun D, Marks R, Sloan J, Hillman S, Swensen S, Hartman T, Shridhar V, **Smith DI**. Screening for lung cancer: Pilot study of spiral CT chest scan and sputum cytology. 1999 ALA/ATS international conference.
21. Yokomizo A, Thibodeau SN, Tindall DJ, **Smith DI**, Liu W. Association of luteinizing hormone β, CYP17, glutathione S-transferase M1, T1 P1 and γ-glutamylcystein synthetase gene polymorphisms with familial prostate cancer. 1999 AACR Conference on "New research approaches in the prevention and cure of prostate cancer."
22. Shridhar V, Staub J, **Smith DI**, Jett JR. Methylation analysis of sputum from smokers lungs. AACR Annual Meeting, April 10-14, 1999.
23. Mai M, Qian C, Yokomizo A, **Smith DI**, Liu W. Cloning of the human homolog of conductin (AXIN2), a gene mapping to chromosome 17q23.23. AACR Annual Meeting, April 10-14, 1999.
24. Zhang J-S, Wang L, Huang H, Nelson M, **Smith DI**. Identification and characterization of HAIK1, a novel type I keratin, and a potential differentiation marker for pancreatic cancer. AACR Annual Meeting, April 10-14, 1999.
25. Huang H, Reed CP, Zhang J-S, Shridhar V, **Smith DI**. A novel carboxypeptidase A3 (CPA3) is highly inducible by histone deacetylase inhibitors in the differentiation of prostate epithelial cells. AACR Annual Meeting, April 10-14, 1999.
26. Krummel K, Kawakami M, Roberts LR, **Smith DI**. Cloning and characterization of the common fragile site, FRA16D, and its role in cancer. *Amer. J. Hum. Genet.* 65:A48, 1999.
27. Thorland EC, Myers S, Persing D, **Smith DI**. HPV16 preferentially integrates into the common fragile sites in cervical cancer. *Amer. J. Hum. Genet.* 65:A50, 1999.

28. Taniguchi K, Yang P, Marks T, Lesnick A, Yokomizo A, Sloan D, Miller J, Jett J, Tazelaar E, Edell E, **Smith DI**, Liu W. The effects of glutathione-related genes and cigarette smoking on lung cancer.

29. Callahan G, Shridhar V, Hartmann L, **Smith DI.** Characterization of a carboxypeptidase-A inhibitor identified by DD-PCR in primary ovarian tumors and cell lines. *Amer. J. Hum. Genet.* 65:A637, 1999.

30. Seelan RS, Qian C, Yokomizo A, **Smith DI**, Liu W. Human acid ceramidase located at 8p22 is overexpressed but not mutated in prostate cancer. *Amer. J. Hum. Genet.* 65:A1808, 1999.

31. Shridhar V, Staub J, Huang H, Callahan G, Bright RK, Yokomizo A, Wang L, Pass HI, Hartmann L, **Smith DI**. Loss of expression by deletion and hypermethylation of a new member of the DNAJ protein family on 13q14.1 in ovarian cancer. *Amer. J. Hum. Genet.* 65:A1817, 1999.

32. **Smith DI**, Thorland E, Krummel K, Kawakami M, Myers S, Roberts L. Role of the common fragile sites in cancer development. *Cancer Genetics and Epigenetics: Gordon Research Conference, Feb. 20-25, 2000.*

33. Shridhar V, Callahan G, Staub J, Avula R, Hartmann LC, **Smith DI**. Identification of novel genes not expressed in primary ovarian tumors and cell lines. *Cancer Res.* 41:A1983.

34. Callahan aG, Shridhar V, Bale LK, Kalli KR, Hartmann LC, Conover C, **Smith DI**. Loss of PAPP-A expression in ovarian epithelial carcinoma. *Cancer Res.* 41:A2214, 2000.

35. Huang H, Murillo H, **Smith DI**, Tindall DJ. Neuroendocrine-like survival of LNCAP prostate cancer cells under in vitro androgen ablation conditions is dependent upon PI3K-AKT. *Cancer Res.* 41:A2574, 2000.

36. Calhoun E, McGovern RM, **Smith DI**, Gostout BS, Pershing DH. Host genetic polymorphism analysis of squamous cell carcinoma of the cervix. *Cancer Res.* 41:A2785, 2000.

37. Taniguchi K, Krishnadath KK, Qian C, Yang P, **Smith DI**, Wang KK, Liu W. High sensitivity of denaturing high performance liquid chromatography (DHPLC) in detection of p53 mutations in adenocarcinoma of the esophagus. *Cancer Res.* 41:A3969, 2000.

38. Dong X, Seelan R, Qian C, **Smith DI**, Liu W. Human conductin (Axin2), like its mouse counterpart, binds to APC, G3K3β, and β-catenin. *Cancer Res.* 41:A4733, 2000.

39. Kawakami M, Zhang J-S, **Smith DI**. Identification of the human homolog of rat gene 33 as an androgen regulated gene in LNCAP cells and characterization of its promoter. *Cancer Res.* 41:A4753, 2000.

40. Asaf H, Scherer SW, Skaug J, Rahat A, **Smith DI**, Kerem B. DNA replication pattern along a broad region that contains FRA7G, a common fragile site on human chromosome 7. *Amer. J. Hum. Genet.* 67:A176, 2000.

41. Liu W, Dong X, Mai M, Seelan RS, Taniguchi K, Krishnadath KK, Halling KC, Cunningham JM, Qian C, Christensen E, Roche PC, **Smith DI**, Thibodeau SN. Altered Axin2 in colorectal cancer with defective mismatch repair. *Amer. J. Hum. Genet.* 67:A40, 2000.

42. Denison SR, Shridhar V, Ferber MJ, Becker NA, Callahan G, Lee J, Lillie J, **Smith DI**. Cloning and characterization of FRA6E. *Amer. J. Hum. Genet.* 67:A110, 2000.

43. Thorland EC, Myers SL, Gostout BS, **Smith DI**. HPV16 integrations in cervical tumors preferentially occur within the common fragile sites and cluster at specific sites. *Amer. J. Hum. Genet.* 67:A363, 2000.

44. Ferber MJ, Denison SR, Becker NA, Lee J, Lillie J, Hartmann LC, Shridhar V, **Smith DI**. Genes within the common fragile sites are down-regulated in ovarian cancer. *Amer. J. Hum. Genet.* 67:A447, 2000.

45. **Smith DI**, Sen A, Avula R, Staub J, Lee J, Hartmann L, Lillie J, Shridhar V. Identification of differentially expressed genes in early and late stage primary ovarian tumors by the construction of subtraction suppression hybridization cDNA libraries. *Amer. J. Hum. Genet.* 67:A505, 2000.

Presentations

Common fragile sites and cancer. Presented at the University of Istanbul. June 16, 1998

Common fragile sites and cancer. Presented at the Roswell Park Cancer Institute, July 20, 1998.

Common fragile sites and cancer. Presented to the Mayo Foundation Summer Students Program. July 22, 1998.

Cloning of other common fragile sites. Presented at the Expanded Fragile Site Consortium Meeting. Sept. 18, 1998.

Molecular genetics of prostate cancer. Presented to Urogenesys in Santa Monica, California. October 12, 1998.

Fragile sites and cancer. Presented at the University of Indiana. October 14, 1998.

Workshop on common fragile sites and cancer. Presented at the American Society of Human Genetics meeting, Denver, Colorado. October 28, 1998.

Allele-specific late replication and fragility in the FRA3B region. Presented at the American Society of Human Genetics meeting, Denver, Colorado. October 30, 1998.

Common fragile sites and cancer. Presented at Bilkent University in Ankara, Turkey. November 9, 1998.

Molecular genetics of prostate cancer. Presented at Bilkent University in Ankara, Turkey. November 11, 1998.

The role of the common fragile sites in cancer. Presented at Albert Einstein College of Medicine to the Department of Molecular Pharmacology, May 17, 1999.

Common fragile sites and cancer. Presented to the Frontiers in Clinical Genetics at George Washington University, Sept. 16, 1999.

Role of the Common Fragile Sites in Cancer Development. Presented at the Miami Winter Symposium on DNA, RNA and Cancer, February 6, 2000.

Common Fragile Sites and Cancer. Presented at the Common Fragile Sites, Gene Amplification and Cancer Meeting, Held at Mayo Foundation, August 25-26, 2000.

Common Fragile Sites and Cancer. Presented at the University of Nebraska in Omaha, Sept. 11, 2000.

Common fragile sites and the development of cancer. Presented to graduate students at Mayo, September 27, 2000.

Star Trek is here today: Impact of the human genome project on biology. Presented at the Women's Cancer Program, Mayo Foundation, October 6, 2000.

Impact of the Human Genome Project on Biology- Sigma Chi lecturer, Presented on October 17, 2000.

Star Trek is here today: Impact of the human genome project on biology. Presented at the Eagle's Award Dinner, Rochester, MN, October 23, 2000.

The human genome project and its impact on biology. Presented at the Clinical Coordinators Conference, Mayo Foundation, October 24, 2000.

HPV integration in common fragile sites and the development of cervical cancer. Presented at the Gyn/Onc grand rounds, Mayo Foundation, November 1, 2000.

Transcriptional Profiling of Ovarian Tumors. Presented at Eli Lilly, Indianapolis, IN, November 13, 2000.

Manuscripts Published Acknowledging DOD Support

Krummel et al. The characterization of the common fragile site FRA16D and its involvement in multiple myeloma translocations. *Genomics* 2000; 69:37-46.

Wang et al. Loss of expression of the DRR1 gene at chromosomal segment 3p21.1 in renal cell carcinoma. *Genes Chromosom Cancer* 2000; 27:1-10.

Kawakami et al. Involvement of H-cadherin (CDH13) on 16q in the region of frequent deletion in ovarian cancer. *Int J Oncol* 1999; 15:715-20.

Huang et al. Carboxypeptidase A3 (CPA3): A novel gene highly induced by histone deacetylase inhibitors during differentiation of prostate epithelial cancer cells. *Cancer Res.* 1999; 59:2981-8.

Wang et al. Allele-specific late replication and fragility of the most active common fragile site, FRA3B. *Human Molec. Genet.* 1999; 8:431-7.

Zhang et al. Keratin 23 (K23), a novel acidic keratin, is highly induced by histone deacetylase inhibitors during differentiation of pancreatic cancer cells. *Genes Chromosom Cancer* 2000; in press.

CONCLUSIONS

We have now cloned and characterized two very interesting chromosomal regions. The first is a region of approximately 300 Kb that contains the relatively inactive common fragile site, FRA7G. The markers which show the most frequent loss in prostate tumors (and in breast, ovarian, and hepatocellular tumors) are derived from the middle of this fragile region. None of the genes within this site (which includes caveolin-1, caveolin-2, TESTIN, and the distal c-maf gene) have any detectable mutations in our panel of primary prostate tumors. However, caveolin-1 and TESTIN are not frequently expressed in prostate tumors. We have found that the highly active common fragile site FRA16D shares many similarities to FRA3B, the most active common fragile site. This region spans over 1.5 megabases and there is a very

large gene that spans most of this unstable region. We have detected no alterations in this gene in any of our prostate tumor specimens. None of the genes analyzed from these regions appear to be functioning as "sensors" of genomic damage. However, the frequent loss of expression of these genes and genes identified as spanning other common fragile site regions continues to suggest that these regions and the genes contained within them play an important role in prostate cancer development.

Fish Mapping of YAC Clones at Human Chromosomal Band 7q31.2: Identification of YACS Spanning FRA7G Within the Common Region of LOH in Breast and Prostate Cancer

Haojie Huang, Chiping Qian, Robert B. Jenkins, and David I. Smith*

Division of Experimental Pathology, Department of Laboratory Medicine and Pathology, Mayo Foundation, Rochester, Minnesota

Loss of DNA sequences within human chromosomal band 7q31.2 is frequently observed in a number of different solid tumors including breast, prostate, and ovarian cancer. This chromosomal band also contains the common fragile site, FRA7G. Many of the common fragile sites occur within chromosomal regions that are frequently deleted during tumor formation but their precise position, relative to the chromosome breakpoints and deletions, has not been defined for the majority of the fragile sites. Because the frequency of expression of FRA7G is low, we analyzed the expression of FRA7G in a chromosome 7-only somatic cell hybrid (hamster-human). YAC clones defining a contig spanning 7q31.2 were then used as FISH probes against metaphase spreads prepared from the hybrid cells after aphidicolin induction. This analysis quickly revealed whether a specific YAC clone mapped proximal, distal, or actually spanned the region of decondensation/breakage of FRA7G. By using this approach, we have identified several overlapping YAC clones that clearly span FRA7G. Interestingly, these clones map precisely to the common region of LOH in breast cancer and prostate cancer. In addition, the *MET* oncogene is contained within the three YACs that span FRA7G. *Genes Chromosomes Cancer 21:152–159, 1998.* © 1998 Wiley-Liss, Inc.

INTRODUCTION

Chromosomal regions that form nonrandom gaps or breaks when exposed to specific growth conditions are known as fragile sites (Berger et al., 1985). The expression of all known fragile sites is dependent on specific chemical agents or modification of normal tissue culture conditions. The biochemical basis of induction and the relative frequency with which a specific fragile site is observed in the general population allow for further classification of 28 rare and 89 common fragile sites. The rare fragile sites, present in less than 5% of the population, can be subgrouped into sites that are folate-sensitive, distamycin A-sensitive, and BrdU-inducible. The common fragile sites, apparently present in all individuals, can be divided into those that are aphidicolin-inducible (Glover et al., 1984; Glover and Stein, 1988), 5 azacytidine-inducible, and BrdU-inducible (Berger et al., 1985).

Until recently, essentially nothing was known about the DNA sequences at the fragile sites. Verkerk et al. (1991) cloned the FRAXA fragile site, responsible for the fragile X syndrome, by standard positional cloning methods. A simple repeat, $(CGG)_n$, adjoining a CpG island, was found within the 5'-UTR in the first exon of the *FMR1* gene. This repeat shows sequence instability and a dramatic increase (to > 200 repeats) in fragile X patients. The increase of the $(CGG)_n$ repeat is associated with abnormal methylation within the CpG island, chromosome fragility, and the absence of expression of the *FMR1* gene (Fu et al., 1991; Pieretti et al., 1991; Yu et al., 1991). To date, four other folate-sensitive fragile sites (FRAXE, FRAXF, FRA16A, and FRA11B) have been cloned. All contain a CGG repeat that is amplified and methylated in individuals demonstrating fragility at these sites (Knight et al., 1993; Jones et al., 1994; Nancarrow et al., 1994; Ritchie et al., 1994). In vitro, CCG blocks of > 50 repeats display strong nucleosome exclusion and provide a possible explanation for the nature of these sites (Wang et al., 1996). Despite the molecular characterization of five folate-sensitive fragile sites, the relationship between the chemistry of fragile site induction and their DNA sequence composition is not yet clear. In an effort to gain a better understanding of this relationship, the distamycin A-sensitive fragile site, FRA16B, was isolated by positional cloning and found to be an expanded 33-bp AT-rich minisatellite (Yu et al., 1997).

Common fragile sites differ from rare fragile sites both in their frequency of expression and in their mode of expression. Most of the rare fragile sites are exquisitely sensitive to low levels of folic acid in the culture media. Common fragile sites are less sensitive to folate deficiency than the rare fragile sites (Glover et al., 1984; Yunis and Soreng, 1984), but most are strongly induced by aphidicolin (Berger et al., 1985). Aphidicolin is a specific inhibitor of the replicative DNA polymerases α and δ and has a high specificity for breakage at the constitutive fragile site at human chromosomal band 3p14.2 (FRA3B) (Glover and Stein, 1988). This is the most highly inducible common fragile site in the human genome (Smeets et al., 1986). Sequence analysis of 180 kb of DNA from the FRA3B region revealed no information as to why this region is sensitive to aphidicolin treatment (Boldog et al., 1997), but it is definitely not due to trinucleotide repeats or unstable minisatellites.

Yunis and Soreng (1984) first proposed, based upon cytogenetic examination, that the position of the fragile sites corresponded to hot spots for chromosomal breakage and rearrangement during carcinogenesis. FRA3B is frequently deleted in multiple tumor types (Rassool et al., 1992; Kastury et al., 1996; Pandis et al., 1997; Shridhar et al., 1997a) and lies very close to a hereditary renal cell carcinoma translocation breakpoint (hRCC) (Cohen et al., 1979; Boldog et al., 1994; Paradee et al., 1996). Recently, the fragile histidine triad (*FHIT*) gene was identified which crosses the hRCC and all of the FRA3B regions (Ohta et al., 1996; Zimonjic et al., 1997). Coquelle et al. (1997) found that intrachromosomal gene amplification may be triggered by the expression of fragile sites. Thus, fragile sites may play an important role in chromosomal loss of regions containing tumor suppressor genes as well as in amplification of chromosomal regions containing oncogenes.

Loss of heterozygosity (LOH) of microsatellite markers at human chromosomal band 7q31.2 has been detected in many solid tumors (Kuniyasu et al., 1994; Zenklusen et al., 1994a,b, 1995a; Takahashi et al., 1995; Lin et al., 1996; Devilee et al., 1997). Koike et al. (1997) observed LOH in this region in 50% of informative advanced ovarian cancers. It has been proposed that this region contains a tumor suppressor gene important in the development of prostate cancer (Zenklusen et al., 1994b; Latil et al., 1995; Takahashi et al., 1995), breast cancer (Champeme et al., 1995; Lin et al., 1996), and ovarian cancer (Zenklusen et al., 1995b; Koike et al., 1997). We analyzed LOH of 7q

microsatellites in sporadic renal cell carcinoma and found the highest allele loss at 7q31.2 loci D7S522 (24%) and D7S649 (30%) (Shridhar et al., 1997b). In addition, we identified a homozygous deletion in one renal cell carcinoma with a 7q31.1 marker. This provides further evidence that this region contains a tumor suppressor gene. FRA7G is an aphidicolin-inducible common fragile site at 7q31.2 (Berger et al., 1985). It is, however, possible that the frequent deletions observed in this region are due to the intrinsic instability in the fragile site and surrounding regions and not due to the presence of a tumor suppressor target in the region.

In this paper, we describe the mapping of YAC clones by FISH at 7q31.2 and the isolation of YACs crossing FRA7G within the common region of LOH in breast, prostate, and ovarian cancer. This will provide the starting point for characterizing the sequences surrounding FRA7G to determine its precise molecular relationship to chromosomal loss in this region in several tumor types and to compare its structure to that of other common fragile sites.

MATERIALS AND METHODS

Cell Line and Slide Preparation

The human-hamster hybrid cell line, 1HL11-G, was obtained from the NIGMS Human Genetic Mutant Cell Repository at the Coriell Institute for Medical Research in Camden, New Jersey (its repository number is GM10791). This cell line, which contains a single chromosome 7 as its only human component, has been described previously (Jones et al., 1990; Ledbetter et al., 1990; Green et al., 1991). Cell culture and chromosome preparation were modified from Kuwano et al. (1990). Briefly, cultures were grown in minimum essential medium (Eagle), Alpha modification (AMEM), containing 10% fetal calf serum, 4 mM glutamine, penicillin/streptomycin (100 units/ml, 100 μg/ml), and 3×10^{-5} mM mitomycin C. Aphidicolin, dissolved in 70% ethanol at a final concentration of 0.4 μM was added 24 hours after subculture. Cultures were maintained for another 17 hours and then washed twice in Hank's Balanced Salt Solution without aphidicolin. Cells were "recovered" for another 7 hours in fresh medium without aphidicolin. Cultures were treated with 0.04 μg/ml Colcemid for the last 1.5 hours, and cells were processed in the usual manner for the preparation of chromosomes.

Slide preparation was modified from the method described by Breen et al. (1992). After spreading, slide preparations were soaked in 3:1 methanol: acetic acid for 1 hour and then dehydrated in an

ethanol series at room temperature. Slides were aged at 42°C overnight and further treated in acetone for 10 minutes immediately prior to hybridization.

YAC Probe Preparation

YAC clones from the CEPH mega-YAC library (Bellane-Chantelot et al., 1992) were selected by markers known to be mapped to the region surrounding FRA7G at 7q31.2. Isolation of YAC DNA was performed using a modified procedure that was kindly provided by Dr. Harry Drabkin's laboratory (University of Colorado Health Sciences Center). PCR amplification of YAC recombinant DNA was carried out with four Alu primers in a manner similar to that described by Nelson et al. (1989). Four Alu primers, 450, 451, 153, and 154, were synthesized as described by Breen et al. (1992). PCR reactions were carried out with the conditions of 94°C, 5 min; 94°C, 1 min; 55°C, 1.5 min; and 72°C, 2 min for 35 cycles, and then a final extension at 72°C for 10 min. The Alu-PCR products from each YAC were pooled and precipitated. The DNA was labeled with biotin-16-dUTP (Boehringer-Mannheim, Indianapolis, IN) by using a Nick translation kit (Boehringer-Mannheim).

Fluorescence In Situ Hybridization

After precipitation, labeled DNA was dissolved in a final concentration of 15–25 ng/µl in a hybridization mixture which contained 50% formamide, 10% dextran sulfate, 2×SSC, 400–500 ng/µl human Cot-1 DNA (GIBCO, Grand Island, NY), and 0.5 µg/µl sheared herring sperm DNA. Probe DNA was denatured at 75°C for 10 min and then preannealed at 37°C for 20 minutes. Prior to hybridization, slides were denatured at 65°C in 70% (v/v) formamide in 0.6×SSC for 2–3 min, followed by passing through an alcohol series. Hybridizations were performed at 37°C for 17 hours. Post-washing was carried out at 42° under the following conditions: 50% formamide (v/v) in 2×SSC twice, 5 minutes, and 2×SSC twice, 5 minutes each. Hybridized probes were detected with a fluorescein detection kit (Oncor, Inc., Gaithersburg, MD). Cells were counterstained with propidium iodide (0.6 µg/µl) and the antifade compound p-phenylenediamine. Hybridization signals were observed with a Zeiss Axioplan microscope equipped with a triple-pass filter (102-104-1010; VYSIS). Pictures were taken with the LPLAB Spectrum P software on a computer.

TABLE 1. Observation of Gaps and Breaks Induced by Aphidicolin at Fragile Sites on Human Chromosome 7 in Human-Hamster Hybrid 1HL11-G[a]

Gene symbol[b]	Regional assignment	Number of gaps and breaks	Percent total aberrations
FRA7B (c)	7p22	3	1.1
FRA7C (c)	7p14.2	23	8.5
FRA7D (c)	7p13	0	0
FRA7A (r)	7p11.2	0	0
FRA7J (c)	7q11	7	2.6
FRA7E (c)	7q21.2	61	22.5
FRA7F (c)	7q22	68	25.1
FRA7G (c)	7q31.2	46	17.0
FRA7H (c)	7q32.3	59	21.7
FRA7I (c)	7q36	4	1.5
Total aberrations		271	100

[a]Values based on 9586 metaphase cells.
[b](c), common fragile site; (r), rare fragile site.

RESULTS

Expression of Fragile Sites on Human Chromosome 7 in Human-Hamster Hybrid 1HL11-G

The frequency of expression of FRA7G is significantly lower than that of FRA3B (Barbi et al., 1984; Yunis and Soreng, 1984; Kuwano et al., 1990; Hirsch, 1991). We therefore decided to analyze FRA7G expression in a human-hamster hybrid (1HL11-G). Prior to the FISH analysis with YAC clones from the 7q31.2 region, we performed a G/Q banding analysis and total human DNA painting with hybrid 1HL11-G. This analysis revealed that this cell line retains chromosome 7 as the only intact human chromosome in more than 90% of cells, which is consistent with other reports (Jones et al., 1990; Ledbetter et al., 1990). Hybrid cells were cultured in the presence of aphidicolin, metaphase spreads were prepared, and the gaps and breaks induced on the intact human chromosome 7 were scored after R-banding analysis. A total of 274 gaps and breaks were scored on chromosome 7 based on observation of 9,586 metaphase cells. Except for three gaps and breaks observed at 7p15, a non-fragile-site region, all other breakpoints were in the fragile-site regions. Of these aberrations on fragile sites, 1.1% was at FRA7B, 8.5% at FRA7C, 2.6% at FRA7J, 22.5% at FRA7E, 25.1% at FRA7F, 17% at FRA7G, 21.7% at FRA7H, and 1.5% at FRA7I (Table 1). The frequency of the gaps and breaks on chromosome 7 in this hybrid was not greater than the frequency that would have been observed in human cells. However, the ease of identifying chromosome 7's in hybrid 1HL11-G

TABLE 2. FISH Results of YACs on Chromosome 7
Surrounding FRA7G

YAC clones	Positive STS markers	Distal to break-point[a]	Cross break-point[a]	Proximal to break-point[a]
928C1	D7S635 (153 cM)	+	−	−
769G10	D7S680 (153 cM)	+	−	−
752H8	D7S686 (152 cM)	+	−	−
755A9	D7S1471 (151 cM)	+	−	−
763B7	D7S2471 (151 cM)	+	−	−
783G5	D7S487 (150 cM)	+	−	−
924B5	D7S490 (149 cM)	+	−	−
937B2	D7S480 (147 cM)	+	−	−
887D11	D7S633 (144 cM)	+	−	−
912D9	D7S2460 (144 cM)	+	−	−
831B12	D7S522 (144 cM)	−	+	−
746H5	D7S522 (144 cM)	−	+	−
921B4	D7S522 (144 cM)	−	+	−
757E10	D7S2502 (144 cM)	−	−	+
805E2	D7S2554 (143 cM)	−	−	+
847B10	D7S2554 (143 cM)	−	−	+

[a](+) indicates positive result; (−) indicates negative result.

made it much easier for us to analyze the large number of metaphases necessary to identify sufficient numbers of FRA7G gaps and breaks to conduct this study.

FISH Mapping of YACs at 7q31.2

In order to identify YACs crossing FRA7G, we selected YAC clones electronically based upon the markers that had been mapped surrounding 7q31.2 by genetic linkage analysis and physical mapping (Lin et al., 1996). These YACs cover 10 cM of the region within and surrounding 7q31.2 (see Table 2). FISH analysis, with these YACs, was performed on metaphase cells of the 1HL11-G cell line after aphidicolin treatment. YAC clones were scored as hybridizing distal to the region of a gap or break within FRA7G, proximal to that region or actually crossing the gap or break. All YAC clones that were genetically localized from 153 to 147 cM mapped distal to FRA7G. There is actually a gap of the YAC contig (between contigs WC7.6 and WC7.7) occurring around genetic position 144 cM, but clearly all YACs surrounding the gap always hybridize distal to FRA7G. However, YAC clones 757E10, 805E2, and 847B10 always hybridize proximal to FRA7G. Three of the YAC clones, 921B4, 831B12, and 746H5, hybridized to both sides of the gap or break within FRA7G. The markers that map to all three YAC clones include the *MET* oncogene, as well as D7S2460, D7S522, and D7S486. All of these markers map to a genetic position of 144 cM. A precise order of these markers was determined from a refined physical map of this region (Lin et al., 1996).

Figure 1A shows the FISH result obtained with YAC 757E10, demonstrating that this YAC hybridizes proximal to FRA7G. Figure 1B illustrates the FISH result obtained with YAC 831B12, clearly showing that this YAC clone hybridizes both proximal and distal to FRA7G, and Figure 1C shows the hybridization signal observed with YAC 912D9; this YAC is derived from the region immediately distal to YAC 831B12 and always hybridized distal to FRA7G. Figure 2 is a map of the 7q31.2 region between markers AFMA073ZB9 and D7S2554. Also included on this map are the YAC clones comprising part of the WC7.6 YAC contig and their relationship to the markers from this region. The region of overlap among YACs 921B4, 831B12, and 746H5 defines the FRA7G region. This is also the area defined as the common region of LOH in breast and prostate cancer; this is also indicated in Figure 1.

DISCUSSION

The strategy to use YAC clones derived from chromosomal bands known to contain fragile sites as FISH-based probes against aphidicolin-induced cells to look for YAC clones that span the region of aphidicolin-induced breakage has been used previously for successful cloning of sequences surrounding FRA3B (Boldog et al., 1994; Wilke et al., 1994). By using this method, we have isolated YAC clones that cross FRA7G within chromosomal band 7q31.2. Until recently, similar work has been laborious but, thanks to the current status of the physical map of the human genome, the work is much more straightforward. Electronic examination of the region surrounding 7q31.2 revealed an almost complete YAC contig for the region. On the basis of markers mapped to this region, we obtained 16 YAC clones (Table 2), which we used for our FISH-based mapping of FRA7G.

Because FRA7G is expressed at a very low level relative to the more active common fragile sites including FRA3B (3p14.2), FRA16D (16q23.2), and FRA6E (6q26) (Glover et al., 1984; Yunis and Soreng, 1984), we began this work with a hamster/human hybrid cell line, 1HL11-G, which contains a single human chromosome 7 as its only human component (Jones et al., 1990; Ledbetter et al., 1990; Green et al., 1991). Although the frequency of chromosome 7 fragile site breakpoints was not greater in this hybrid, the ease of identifying the human chromosome in the hybrid facilitated our analysis of sufficient metaphases to detect large
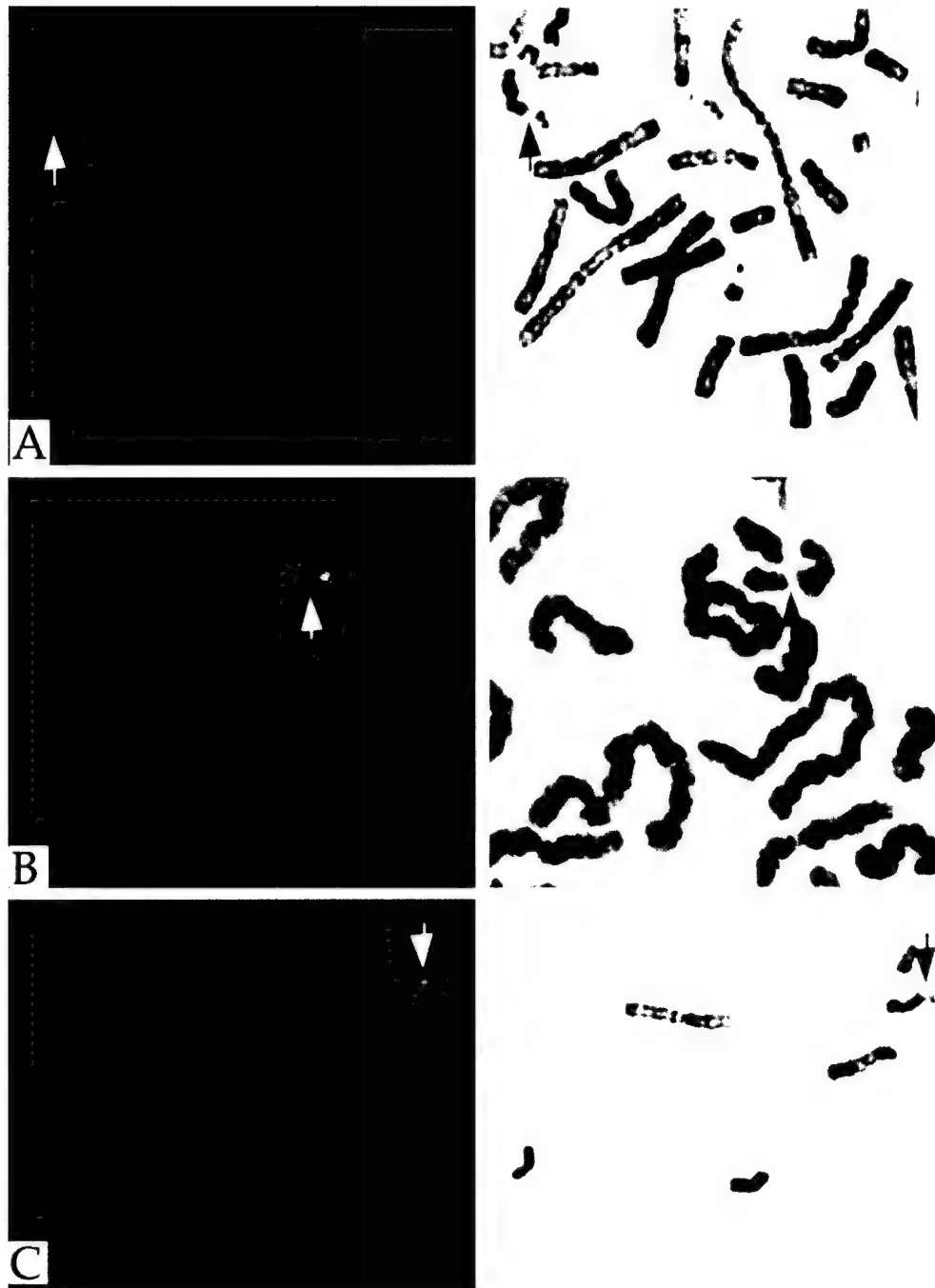
Figure 1. Combined fluorescence in situ hybridization of pooled Alu-PCR products (right) and R-banding analysis (left). **A:** Partial metaphase indicating FISH mapping of the YAC 757E10. This YAC signal localizes proximal to the gap of FRA7G. **B:** Representative metaphase spread showing FISH mapping of the YAC 831B12. This YAC hybridization is split by the breakage of FRA7G. **C:** Partial metaphase chromosome preparation illustrating FISH mapping of the YAC 912D9. This YAC maps distal to the breakpoint of FRA7G.

numbers of FRA7G breakpoints. We analyzed 9,586 metaphase cells from aphidicolin-treated 1HL11-G cells and found that 46 had gaps or breaks at FRA7G. A total of ten fragile sites are observed on chromosome 7 (Sutherland and Ledbetter, 1989). Fragility at FRA7A was not observed; this observa-

tion is consistent with the fact that FRA7A is a folate-sensitive, rare fragile site and thus would not be expected to be observed with aphidicolin induction. With the exception of FRA7D, all eight of the aphidicolin-inducible common fragile sites were induced in hybrid 1LH11-G (Table 1). It is possible
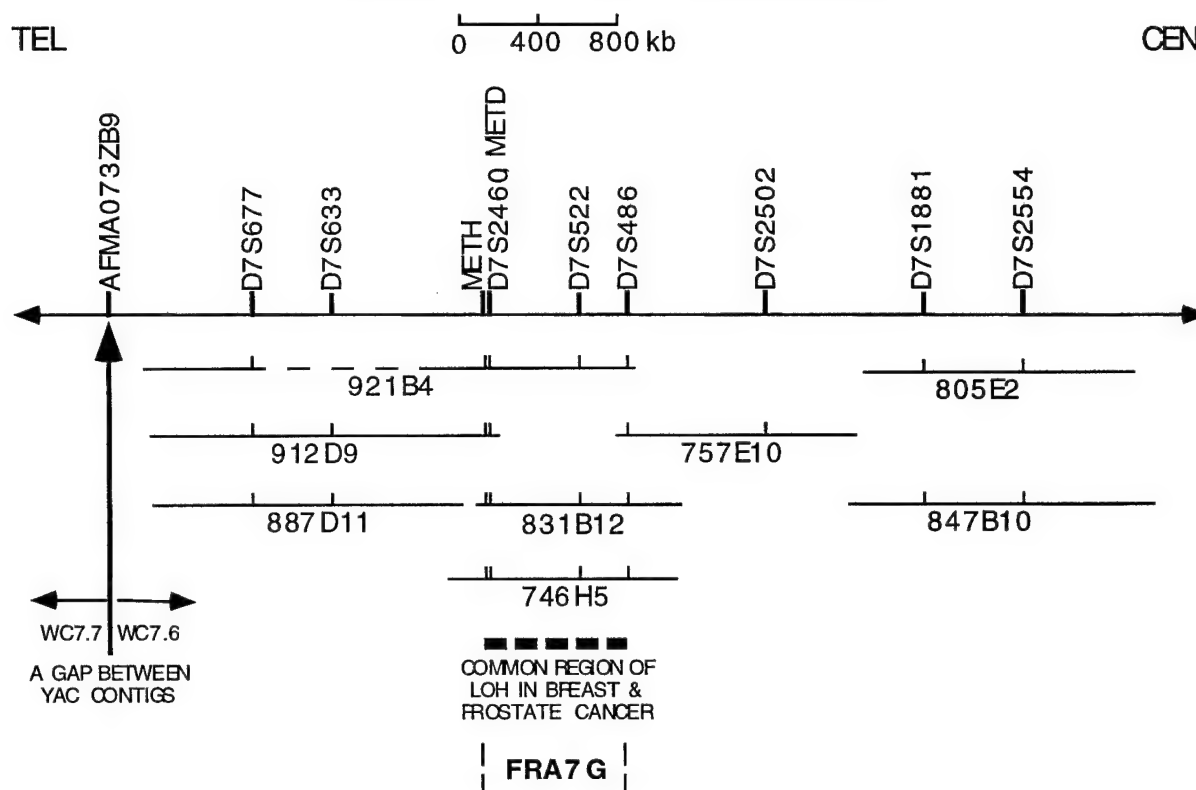
Figure 2. YAC map surrounding the FRA7G region. The top line represents approximate locations of known DNA markers. Each DNA marker contained with the YAC clone is shown by a small vertical bar. The dashed lines in the middle of YAC 921B4 represents a probable deletion in the middle of this YAC as marker D7S633 was not present on this YAC. The YACs were aligned based on FISH analysis and the genetic and physical position of their corresponding markers. FISH mapping shows that FRA7G falls into the region surrounding marker D7S522 between YACs 912D9 and 757E10. This region is also the common region of LOH in breast cancer and prostate cancer (Takahashi et al., 1995; Lin et al., 1996). YACs that flank a gap in a YAC contig around genetic position 144 cM were all mapped distal to FRA7G.

that FRA7D may be expressed at such a low level in the hybrid cells utilized that no breaks were observed.

Yunis and Soreng (1984) first hypothesized that the fragile sites might predispose the chromosomes to breakage and rearrangements in cancer cells, based upon cytogenetic observations. Chromosome segment 7q31.2 is indeed frequently deleted in many different tumor types including breast cancer (Zenklusen et al., 1994; Devilee et al., 1997), ovarian cancer (Zenklusen et al., 1995; Koike et al., 1997), and prostate cancer (Zenklusen et al., 1994b; Latil et al., 1995; Takahashi et al., 1995). The *MET* oncogene maps within this region and has been shown to be amplified in many tumors (Muleris et al., 1994; Wullich et al., 1994; Seruca et al., 1995). Our results with YACs derived from this region indicate that FRA7G is localized within the one megabase region that commonly shows LOH in breast and prostate cancer (Takahashi et al., 1995; Lin et al., 1996; Devilee et al., 1997). The *MET* oncogene is also contained within the three YACs that cross FRA7G. These results are thus consistent

with the preliminary cytogenetics-based hypothesis of Yunis and Soreng (1984) and suggest that FRA7G may play an important role in both deletion and amplification processes of this region in cancer development.

To date, we do not know why aphidicolin-inducible fragile sites are so unstable in cancer cells or why aphidicolin specifically induces frequent decondensation/breakage in these regions in cells grown in vitro. We also do not know whether the frequent deletions in this region in cancer cells are just due to the instability at this fragile site or whether there really is a tumor suppressor gene that is the target of the deletions. Further characterization of FRA7G at the molecular level will help us to understand the basis of its fragility and its relationship with tumorigenesis, especially when we compare it to FRA3B. As a direct result of the work done in analyzing metaphase cells from hybrid 1HL11-G treated with aphidicolin, we also have sufficient gaps and breakages on seven other chromosome 7-specific common fragile sites to isolate YAC clones spanning these sites. A comparison of

the regions surrounding each of these sites should give insights into the mechanism of instability at common fragile sites and the global relationship between common fragile sites and breakpoints in cancer.

ACKNOWLEDGMENTS

REFERENCES

Barbi G, Steinbach P, Vogel W (1984) Nonrandom distribution of methotrexate-induced aberrations on human chromosomes: Detection of further folic acid sensitive fragile sites. Hum Genet 68:290–294.

Bellanne-Chantelot C, Lacroix B, Ougen P, Billault A, Beautils S, Bertraut S, Georges I, Gilbert F, Lucotte G, Susm I, Jean-Jacques C, Gesnouin P, Pook S, Vaysseix G, Lu-Kuo J, Ried T, Ward D, Chumakov I, Le Paslier D, Barillot E, Cohen D (1992) Mapping the whole human genome by fingerprinting yeast artificial chromosomes. Cell 70:1059–1068.

Berger R, Bloomfield CD, Sutherland GR (1985) Report of the committee on chromosome rearrangements on neoplasia and on fragile sites (HGM8). Cytogenet Cell Genet 40:490–535.

Boldog FC, Wagoner B, Glover TW, Chumakov I, le Paslier D, Cohen D, Gemmill RM, Drabkin HA (1994) Integrated YAC contig containing the 3p14.2 hereditary renal carcinoma 3;8 translocation breakpoint and the fragile site FRA3B. Genes Chromosomes Cancer 11:216–221.

Boldog FC, Gemmill RM, West J, Robinson M, Robinson L, Li E, Roche J, Todd S, Waggoner B, Lundstrom R, Jacobson J, Mullokandov MR, Klinger H, Drabkin HA (1997) Chromosome 3p14 homozygous deletions and sequence analysis of FRA3B. Hum Mol Genet 6:193–203.

Breen M, Arveiler B, Murray I, Gosden JR, Porteous DJ (1990) YAC mapping by FISH using Alu-PCR-generated probes. Genomics 13:726–730.

Champeme M-H, Bieche I, Beuzelin M, Lidereau R (1995) Loss of heterozygosity on 7q31 occurs early during breast tumorigenesis. Genes Chromosomes Cancer 12:304–306.

Cohen AJ, Li FP, Berg S, Marchetto DJ, Tsai S, Jacobs SC, Brown RS (1979) Hereditary renal cell carcinoma associated with a chromosomal translocation. N Engl J Med 301:592–595.

Coquelle A, Pipiras E, Toledo F, Buttin G, Debatisse M (1997) Expression of fragile sites triggers intrachromosomal mammalian gene amplification and sets boundaries to early amplicons. Cell 89:215–225.

Devilee P, Hermans J, Eyfjord J, Borresen A-L, Lidereau R, Sobol H, Borg A, Cleton-Jansen A-M, Olah E, Cohen BB, Scherneck S, Hamann U, Peterlin B, Caligo M, Bignon Y-J, Maugard CH, the Breast Cancer Somatic Genetics Consortium (1997) Loss of heterozygosity at 7q31 in breast cancer: Results from an international collaborative study group. Genes Chromosomes Cancer 18:193–199.

Fu Y-H, Kuhl DPA, Pizzuti A, Pieretti M, Sutcliffe JS, Richards R, Verkerk AJMH, Holden JJA, Fenwick RG Jr, Warren ST, Oostra BA, Nelson DL, Caskey CT (1991) Variation of the CGG repeat at the fragile X site results in genetic instability: Resolution of the Sherman paradox. Cell 67:1047–1058.

Glover TW, Berger C, Coyle-Morris J, Echo B (1984) DNA polymerase inhibition by aphidicolin induces gaps and breaks at common fragile sites in human chromosomes. Hum Genet 67:882–890.

Glover TW, Stein CK (1988) Chromosome breakage and recombination at fragile sites. Am J Hum Genet 43:265–273.

Green ED, Mohr RM, Idol JR, Jones M, Buckingham JM, Deaven L, Moyzis RK, Olson MV (1991) Systematic generation of sequence-tagged sites for physical mapping of human chromosomes: Application to the mapping of human chromosome 7 using yeast artifical chromosomes. Genomics 11:548–564.

Hirsch B (1991) Sister chromid exchanges are preferentially induced at expressed and nonexpressed common fragile sites. Hum Genet 87:302–306.

Jones NJ, Stewart SA, Thompson LH (1990) Biochemical and genetic analysis of the Chinese hamster mutants *irs1* and *irs2* and their comparison to cultured ataxia telangiectasia cells. Mutagenesis 5:15–23.

Jones C, Slijepcevic P, March S, Baker E, Langdon WY, Richards RI, Tunnacliffe A (1994) Physical linkage of the fragile site FRA11B and Jacobsen syndrome chromosome deletion breakpoint in 11q23.3. Hum Mol Genet 3:2123–2130.

Kastury K, Baffa R, Druck T, Ohta M, Cotticelli MG, Inoue H, Negrini M, Rugge M, Huang D, Croce CM, Palazzo J, Huebner K (1997) Potential gastrointestinal tumor suppressor locus at the 3p14.2 FRA3B site identified by homozygous deletions in tumor cell lines. Cancer Res 56:978–983.

Knight SJL, Flannery AV, Hirst MC, Campbell L, Christodoulou Z, Phelps SR, Pointon J, Middleton-Price HR, Barnicoat A, Pembrey ME (1993) Tri-nucleotide repeat amplification and hypermethylation of a CpG island in FRAXE mental retardation. Cell 74:127–134.

Koike M, Takeuchi S, Yokota J, Park S, Hatta Y, Miller CW, Tsuruoka N, Koeffler HP (1997) Frequent loss of heterozygosity in the region of the D7S523 locus in advanced ovarian cancer. Genes Chromosomes Cancer 19:1–5.

Kuniyasu H, Yasui W, Yokozaki H, Akagi M, Kitahara K, Fujii K, Tahara E (1994) Frequent loss of heterozygosity of the long arm of chromosome 7 is closely associated with progression of human gastric carcinomas. Int J Cancer 59:597–600.

Kuwano A, Murano I, Kajii T (1990) Cell type-dependent difference in the distribution and frequency of excess thymidine-induced common fragile sites: T lymphocytes and skin fibroblasts. Hum Genet 84:527–531.

Latil A, Baron JC, Cussenot O, Fournier G, Soussi T, Boccon-Gibod L, Le Duc A, Rouesse J, Lidereau R (1995) Genetic alterations in localized cancers of the prostate: Identification of a common region of deletion on chromosome 18q. Bull Cancer 82:589–597.

Ledbetter SA, Garcia-Heras J, Ledbetter DH (1990) "PCR-karyotype" of human chromosomes in somatic cell hybrids. Genomics 8:614–622.

Lin JC, Scherer SW, Tougas L, Traverso G, Tsui L-C, Andrulis I, Jothy S, Park M (1996) Detailed deletion mapping with a refined physical map of 7q31 localizes a putative tumor suppressor gene for breast cancer in the region of MET. Oncogene 13:2001–2008.

Muleris M, Almeida A, Dutrillaux AM, Prochon E, Vega F, Delattre JY, Poisson M, Malfoy B, Dutrillaux (1994) Oncogene amplification in human gliomas: A molecular cytogenetic analysis. Oncogene 9:2717–2722.

Nancarrow JK, Kremer E, Holman K, Eyre H, Doggett NA, le Paslier D, Callen DF, Sutherland GR, Richards RI (1994) Implication of FRA16A structure for the mechanism of chromosomal fragile site genesis. Science 264:1938–1941.

Nelson DL, Ledbetter SA, Corbo L, Victoria MF, Ramirez-Solis R, Webster TD, Ledbetter DH, Caskey CT (1989) Alu polymerase chain reaction: A method for rapid isolation of human-specific sequences from complex DNA sources. Proc Natl Acad Sci USA 86:6686–6690.

Ohta M, Inoue H, Cotticelli MG, Kastury K, Baffa R, Palazzo J, Siprashvili Z, Mori M, McCue P, Druck T, Croce CM, Huebner K (1996) The FHIT gene, spanning the chromosome 3p14.2 fragile site and renal carcinoma-associated t(3;8) breakpoint, is abnormal in digestive tract cancers. Cell 84:587–597.

Pandis N, Bardi G, Mitelman F, Heim S (1997) Deletion of the short arm of chromosome 3 in breast tumors. Genes Chromosomes Cancer 18:241–245.

Paradee W, Wilke CM, Wang L, Shridhar R, Mullins CM, Hoge A, Glover TW, Smith DI (1996) A 350-kb cosmid contig in 3p14.2 that cross the t(3;8) hereditary renal cell carcinoma translocation breakpoint and 17 aphidicolin-induced FRA3B breakpoints. Genomics 35:87–93.

Pieretti M, Zhang F, Fu Y-H, Warren ST, Oostra BA, Caskey CT, Nelson DL (1991) Absence of expression of the FMR-1 gene in fragile X syndrome. Cell 66:817–822.

Rassool FV, Le Beau MM, Neilly ME, van Melle E, Espinosa R 3d, McKeithan TW (1992) Increased genetic instability of the common fragile site at 3p14 after integration of exogenous DNA. Am J Hum Genet 50:1243–1251.

Ritchie RJ, Knight SJL, Hirst MC, Crewal PK, Bobrow M, Cross GS, Davies KE (1994) The cloning of FRAXF: Trinucleotide repeat expansion and methylation at a third fragile site in distal Xqter. Hum Mol Genet 3:2115–2121.

Seruca R, Suijkerbuik RF, Gartner F, Criado B, Veiga I, Olde-Weghuis D, David L, Castedo S, Sobrinho-Simoes M (1995) Increased levels of MYC and MET co-amplification during tumor progression of a case of gastric cancer. Cancer Genet Cytogenet 82:104–145.

Shridhar R, Shridhar V, Wang X, Paradee W, Dugan M, Sarkar F, Wilke C, Glover TW, Vaitkevicius VK, Smith DI (1997a) Frequent breakpoints in the 3p14.2 fragile site, FRA3B, in pancreatic tumors. Cancer Res 56:4347–4350.

Shridhar V, Sun QC, Miller OJ, Kalemkerian GP, Petros J, Smith DI (1997b) Loss of heterozygosity on the long arm of human chromosome 7 in sporadic renal cell carcinomas. Oncogene, In Press.

Smeets DFCM, Scheres JMJC, Hustinx TWJ (1986) The most common fragile site in man is 3p14. Hum Genet 72:215–220.

Sutherland GR, Ledletter DH (1989) Report of the committee on cytogenetic markers. Cytogenet Cell Genet 51:452–458.

Takahashi S, Shan AL, Ritland SR, Delacey KA, Bostwick DG, Lieber MM, Thibodeau SN, Jenkins RB (1995) Frequent loss of heterozygosity at 7q31.1 in primary prostate cancer is associated with tumor aggressiveness and progression. Cancer Res 55:4114–4119.

Verkerk AJMH, Pieretti, Sutcliffe JS, Fu Y-H, Kuhl DPA, Pizzuti A, Reiner O, Richards S, Victoria MF, Zhang F, Eussen BE, van Ommen G-JB, Blonden LAJ, Riggins GJ, Chastain JL, Kunst GH, Caskey CT, Nelson DL, Oostra BA, Warren ST (1991) Identification of a gene (FMR-1) containing a CGG repeat coincident with a breakpoint cluster region exhibiting length variation in fragile X syndrome. Cell 65:905–914.

Wang YH, Gellibolian R, Shimizu M, Wells RD, Griffith J (1996) Long CCG triplet repeat blocks exclude nucleosomes: A possible mechanism for the nature of fragile sites in chromosomes. J Mol Biol 263:511–516.

Wilke CM, Guo S-W, Hall BK, Boldog F, Gemmill RM, Chandrasekharappa SC, Barcroft CL, Drabkin HA, Grover TW (1994) Multicolor FISH mapping of YAC clones in 3p14 and identification of a YAC spanning both FRA3B and the 7(3;8) associated with renal cell carcinoma. Genomics 22:319–326.

Wullich B, Sattler HP, Fisher U, Meese E (1994) Two independent amplification events on chromosome 7 in glioma: Amplification of the epidermal growth factor receptor gene and amplification of the oncogene MET. Anticancer Res 14:577–579.

Yu S, Pritchard M, Kremer E, Lynch M, Nancarrow J, Baker E, Holman K, Mulley JC, Warren ST, Schlessinger D, Sutherland GR, Richard RI (1991) Fragile X genotype characterized by an unstable region of DNA. Science 252:1179–1181.

Yu S, Mangelsdorf M, Hewett D, Hobson L, Baker E, Eyre H, Lapsys N, le Paslier D, Doggett NA, Sutherland GR, Richards RI (1997) Human chromosomal fragile site FRA16B is an amplified AT-rich minisatellite repeat. Cell 88:367–374.

Yunis JJ, Soreng AL (1984) Constitutive fragile sites and cancer. Science 226:1199–1204.

Zenklusen J, Bieche I, Lidereau R, Conti C (1994a) (C-A)$_n$ microsatellite repeat D7S522 is the most commonly deleted region in human primary breast cancer. Proc Natl Acad Sci USA 91:12155–12158.

Zenklusen JC, Thompson JC, Troncoso P, Kagan J, Conti CJ (1994b) Loss of heterozygosity in human prostate carcinomas: A possible tumor suppressor gene at 7q31.1. Cancer Res 54:6370–6373.

Zenklusen JC, Thompson JC, Klein-Szanto AJP, Conti CJ (1995a) Frequent loss of heterozygosity in human primary squamous cell and colon carcinomas at 1q31.1: Evidence for a broad range tumor suppressor gene. Cancer Res 55:1347–1350.

Zenklusen J, Weitzel J, Ball H, Conti C (1995b) Allelic loss at 7q31.1 in human primary ovarian carcinomas suggests the existence of a tumor suppressor gene. Oncogene 11:359–363.

Zimonjic DB, Druck T, Ohta M, Kastury K, Carlo MC, Popescu NC (1997) Positions of chromosome 3p14.2 fragile sites (FRA3B) within the FIHT gene. Cancer Res 57:1166–1170.

FRA7G extends over a broad region: coincidence of human endogenous retroviral sequences (HERV-H) and small polydispersed circular DNAs (spcDNA) and fragile sites

Haojie Huang[1], Junqi Qian[1], John Proffit[2], Kim Wilber[2], Robert Jenkins[1] and David I Smith[1]

[1]Division of Experimental Pathology, Department of Laboratory Medicine and Pathology, Mayo Foundation, 200 First Street, SW, Rochester, Minnesota; [2]Vysis Inc., Downer's Grove, Illinois, USA

FRA7G is an aphidicolin-inducible common fragile site at human chromosomal band 7q31.2. This region is frequently altered in a number of different tumor types including prostate, breast, and ovarian cancer. It has also been hypothesized that this region contains an important tumor suppressor gene which is mutated during the development of these cancers or an oncogene which is amplified. We previously used a FISH-based approach to isolate YAC clones which spanned FRA7G. In this report, we describe the isolation and restriction endonuclease mapping of three overlapping P1 clones which cover FRA7G and the region frequently altered in the different cancers. FISH-based analysis of these clones reveals that aphidicolin-induced breakage in the FRA7G region occurs over a region of at least 300 Kb in length. We have also localized a previously sequenced BAC clone to this region. The sequence obtained from this clone reveals the presence of an endogenous retroviral sequence (HERV-H) in the midst of the FRA7G region as well as sequences with homology to small polydispersed circular DNAs (spcDNAs). Thus for the first two cloned common fragile sites, FRA7G and FRA3B, there is an association with both spcDNAs and hot-spots for viral integration.

Keywords: chromosome fragility; FRA7G; spcDNA; human endogenous retroviral sequence; fluorescence *in situ* hybridization

Introduction

Fragile sites are chromosomal regions that form nonrandom gaps or breaks when exposed to specific chemicals or growth conditions (Sutherland and Hecht, 1985). The relative frequency that a specific fragile site is observed in the general population allow for further sub-classification of the fragile sites. Fragile sites that are observed in less than 5% of the population are referred to as rare fragile sites, whereas fragile sites that are observed in most individuals are known as common fragile sites. The specific chemical or growth condition which promotes fragile site expression allows for further groupings of the rare and common fragile sites.

To date, six rare fragile sites and one common fragile site have been cloned and characterized. Five folate-sensitive rare fragile sites have been cloned,

FRAXA, FRAXE, FRAXF, FRA16A, and FRA11B, and each contain a CGG repeat which is amplified and methylated in individuals that demonstrate fragility at these sites (Verkerk *et al.*, 1991; Knight *et al.*, 1993; Ritchie *et al.*, 1994; Jones *et al.*, 1994; Nancarrow *et al.*, 1994). The sixth cloned rare fragile site is FRA16B. This fragile site is induced by distamycin A, not by folate deficiency, and contains an expanded 33 bp AT-rich minisatellite sequence in individuals expressing the fragile site (Yu *et al.*, 1997). FRA3B is the only common fragile site which has been characterized at the molecular level (Paradee *et al.*, 1996; Rassool *et al.*, 1996; Wilke *et al.*, 1996; Boldog *et al.*, 1997). This fragile site is an aphidicolin-sensitive fragile site (Glover *et al.*, 1984), and the most highly inducible fragile site in the human genome (Smeets *et al.*, 1986). Breakpoints in FRA3B occur over a region of at least 300 Kb of DNA (Paradee *et al.*, 1996). Sequence analysis of 110 Kb of DNA from the FRA3B region revealed no information as to why this region is unstable to aphidicolin treatment (Boldog *et al.*, 1997); however, it is definitely not due to unstable trinucleotide or minisatellite repeat sequences. DNA sequence analysis of the FRA3B region did reveal several interesting features of the region. The first is the presence of an HPV16 viral integration site in the middle of the region of greatest aphidicolin-induced sensitivity (Wilke *et al.*, 1996). There are also three THE1 elements in the FRA3B region as well as sequences with homology to small polydispersed circular DNAs (spcDNA) (Boldog *et al.*, 1997; Wang *et al.*, 1997).

Although the molecular basis for instability in the rare fragile site regions is largely unknown, their fragility appears to be associated with expansions of the CGG or minisatellite sequences for each of the cloned rare fragile sites. Much less is known about why sequences within and surrounding the common fragile sites are sensitive when cells are exposed to aphidicolin. One possible explanation is the fragile sites replicate very late in the cell cycle and specific conditions which slow this replication effectively inhibit the ability of the common fragile site regions to complete their replication prior to cellular division (Laird *et al.*, 1987). Preliminary studies with clones throughout the FRA3B region have demonstrated that sequences in the fragile site region are indeed late replicating and that aphidicolin treatment can slow this replication even further (LeBeau *et al.*, 1998). However, late replication by itself cannot explain why fragile site regions show gaps and breaks after induction as there are many late replicating regions of the genome which do not show this sensitivity.

The association between fragile sites and disease is poorly understood, with the exception of a few of the rare fragile sites. The rare fragile site FRAXA is associated with the most common form of mental retardation (Kremer et al., 1991; Oberle et al., 1991; Verkerk et al., 1991; Yu et al., 1991), and FRAXE is associated with a milder form of mental retardation (Knight et al., 1993). FRA11B is located in the CBL2 proto-oncogene region and evidence now exists that breakage at 11q23.3 (the band containing FRA11B) in humans can give rise to a constitutional chromosomal deletion (11q-) resulting in Jacobsen's syndrome (Jones et al., 1995; Penny et al., 1995). This association shows that fragile sites can cause instability in vivo and lead to chromosome breakage. Yunis and Soreng (1984) first proposed that the position of the fragile sites corresponds to regions that showed frequent rearrangements and deletions during carcinogenesis. FRA3B is frequently deleted in multiple tumors (Rassool et al., 1992; Kastury et al., 1997; Pandis et al., 1997; Shridhar et al., 1997) and lies very close to the hereditary renal cell carcinoma translocation breakpoint (Cohen et al., 1979; Boldog et al., 1994; Paradee et al., 1996). Recently, the FHIT gene was identified which crossed the hereditary renal cell carcinoma translocation breakpoint and the FRA3B region (Ohta et al., 1996) and was found to have aberrant transcripts in 50% of gastrointestinal cancers (Ohta et al., 1996), 80% of small-cell lung cancers, and 40% of non-small cell lung cancers (Sozzi et al., 1996). Thus, FRA3B appears to be responsible for genomic instability in this region during carcinogenesis and also contains a putative tumor suppressor gene which may play a role in cancer development.

Loss of heterozygosity (LOH) of microsatellite markers at human chromosomal band 7q31.2 has been detected in many solid tumors (Kuniyasu et al., 1994; Zenklusen et al., 1994a, 1995a; Champeme et al., 1995;

Takahashi et al., 1995; Lin et al., 1996; Devilee et al., 1997). A recent FISH-based study of prostate cancer revealed triplication of this region (Jenkins et al., manuscript in preparation). This band also contains the common fragile site FRA7G. We previously reported on this isolation of three YAC clones which covered FRA7G (Huang et al., 1998). These YACs also contained the markers most frequently lost in breast, prostate, and ovarian cancer (Huang et al., 1998). Here we report the further localization of FRA7G to a region of at least 300 Kb surrounding the microsatellite D7S522. A P1 contig was constructed which covers the FRA7G region. We have also mapped a BAC clone, which has been completely sequenced, to this region. This clone, RG30H15, localizes near the center of frequent breakage in FRA7G. The sequence of this BAC reveals that FRA7G contains a human endogenous retroviral sequence. In addition, we found that FRA7G, like FRA3B, contains sequences with homology to small polydispersed circular DNAs (spcDNA).

Results

Restriction mapping of P1 clones in the FRA7G region

In our previous experiments using a FISH-based approach, we identified several YAC clones that spanned aphidicolin-induced decondensation/breakage within FRA7G and defined FRA7G to a region surrounding D7S522 and D7S486 (Huang et al., 1998). We have extended this approach to sublocalize the position of FRA7G by analysing P1 clones from this region.

PCR amplification using primers specific for D7S522 and D7S486 identified three P1 clones (see Figure 1a, b). P1 clones v203B and v203C generated the correct
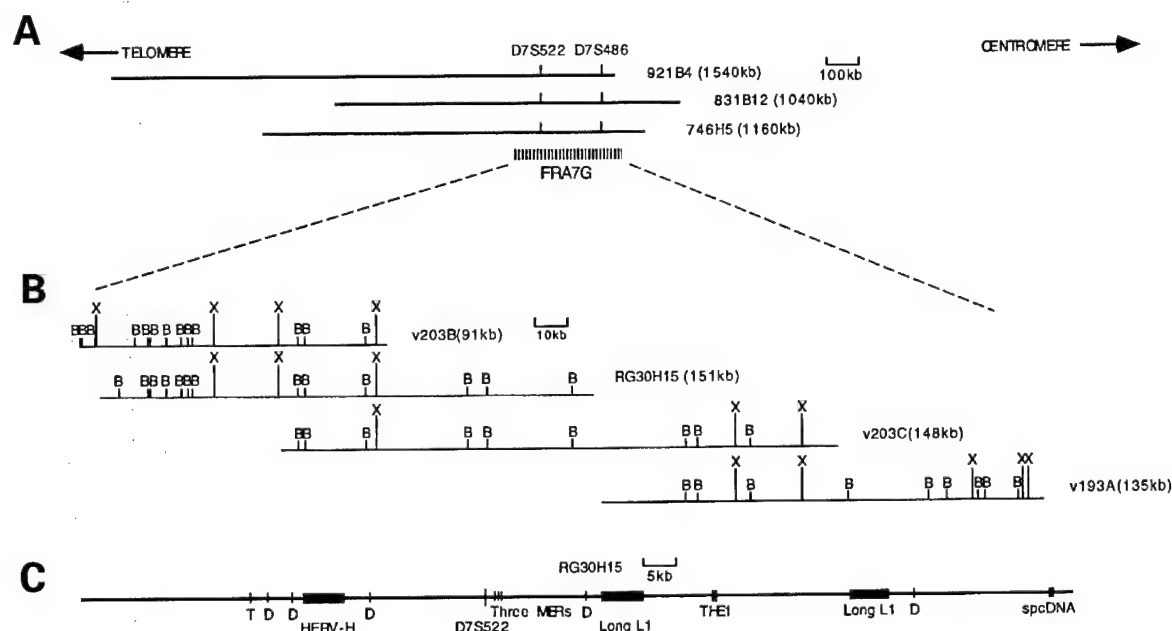
Figure 1 (a) Schematics showing the position of FRA7G relative to CEPH YACs 921B4, 831B12, and 746H5, and markers D7S522 and D7S486 (Huang et al., 1997). (b) Restriction maps of the three P1 clones and one BAC clone within the FRA7G region and the alignment of maps between these clones. (c) Localization of HER-V, MERs, spcDNA, THE-1, L1, and microsatellite sequences within BAC clone RG30H15 (GenBank AC002066): tetranucleotide repeat (T); dinucleotide repeat (D); MER family; THE1 family; long L1 repeat sequences; human endogenous retroviral sequence (HERV-H); and small polydispersed circular DNA (spcDNA)

PCR product with D7S522, and P1 clone v193A was identified with primers specific for D7S486. We then directly sequenced one end of P1 clone v203C using the T7 primer and this enabled us to develop PCR primers specific for that end of the clone. These primers generated the correct sized PCR product using DNA from P1 clones v203C and v193A demonstrating that these clones overlap (data not shown).

We then constructed a restriction map for the three P1 clones after linearizing the clones with *Pvu*I. *Pvu*I cuts the P1 cloning vector at three sites: 1213 bp, 7552 bp, and 10842 bp. When we performed a complete digestion of the three P1 clones with *Pvu*I and the DNA fragments were separated by pulsed-field gel electrophoresis, two small bands (which were ~6 Kb and ~3 Kb, respectively) and one large band (greater than 100 Kb) were observed for each of the clones. Thus, there are no *Pvu*I sites in the P1 clones. Similar analysis with *Sac*II and *Sgf*I revealed these enzymes also did not cleave the genomic DNA from this region.

We therefore linearized the three P1 clones with *Pvu*I and then digested the linearized DNA with various concentrations of *Bam*HI and *Xho*I to obtain partial digests of the genomic DNA contained within the clones. The digestion products were run on two different gels optimized for larger or smaller fragments and transferred to nylon membranes. We then hybridized these membranes with radioactively-labeled probes specific for the right and then the left end of the P1 cloning vector. Creation of the entire restriction map for each clone was accomplished by aligning the restriction site information from both the left and right end-specific probes. The restriction sites of each P1 clone and the alignment of them are shown in Figure 1b.

DNA isolated from the three P1 clones was digested with various restriction endonucleases, and the resulting restriction fragments were then resolved on agarose gels and transferred to nylon backed membranes. These membranes were hybridized with various oligonucleotides representing several of the potential trinucleotide and minisatellite repeats; none of the oligonucleotides hybridized to the three P1 clones. However, the CGG and CTG oligonucleotides did hybridize to the human androgen receptor cDNA in these experiments. Thus, the FRA7G region does not contain any of the repeats represented in the oligonucleotides used.

BAC clone, RG30H15, is derived from this region and has been completely sequenced

Our strategy for the characterization of the FRA7G region was to isolate clones covering this region, map them and then sequence them so that we could compare the sequence in the FRA7G region to the sequence already generated in the FRA3B region. However, a search of GenBank revealed that there was a BAC clone, RG30H15, which is derived from this region (this BAC clone was identified using D7S522) which had already been completely sequenced (GenBank Accession number AC002066). The complete sequence for this BAC clone enabled us to alight this BAC clone relative to the three P1 clones v203B, v203C, and v193A. The sequence obtained for RG30H15 also confirmed the restriction mapping of

P1 clones v203B and v203C. Figure 1b shows the alignment of this BAC clone relative to the three P1 clones.

Based upon the sequence information of the BAC clone, we found there was a tetranucleotide repeat $(AGGA)_{11}$ near the distal end of this BAC. We constructed primers flanking this repeat and found that the repeat is highly polymorphic. Five dinucleotide repeats were also found in this BAC clone. Positions of these repeats are shown in Figure 1c. Primers have been constructed flanking the dinucleotide repeats and determination of polymorphism of these repeats in the human population are ongoing in our laboratory.
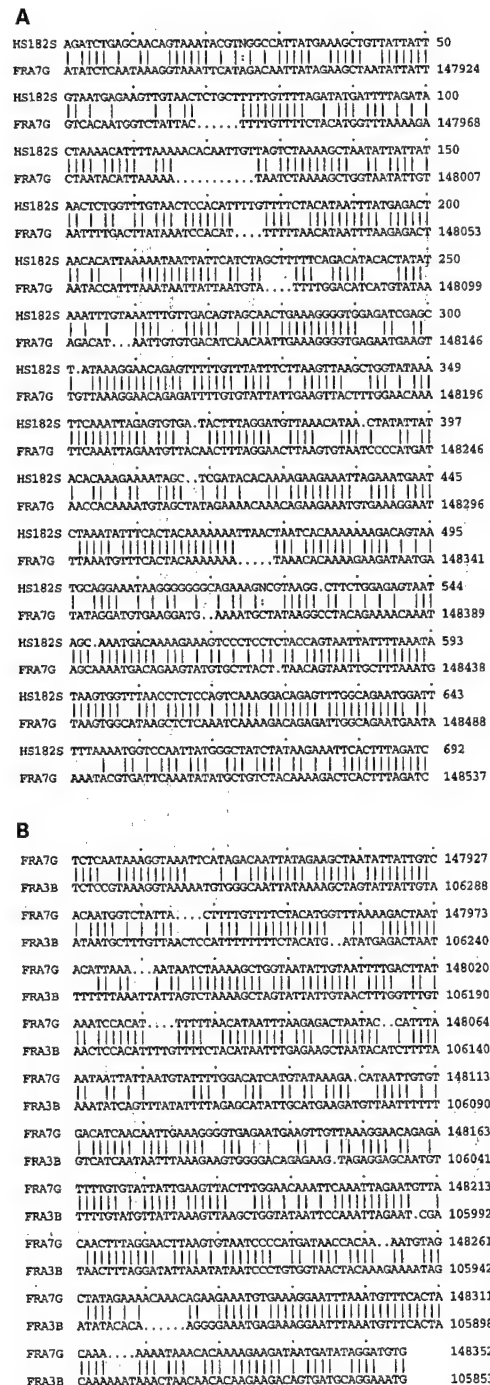
Figure 2 FASTA alignment of spcDNA clone HS182S relative to sequences within FRA7G (**a**), as well as spcDNA sequences in FRA7G relative to those in FRA3B (**b**)

These repeats should be very useful for the characterization of chromosomal loss in this region in various cancers. The BAC clone also contains other interesting repeats such as THE1, MER, and long L1 sequences (Figure 1c).

The sequence information for the BAC clone also revealed two very interesting sequences present in this region. We found a 5.8 Kb human endogenous retroviral sequence beginning at nucleotide position 33870 within RG30H15 (Figure 1c). This sequence was found to be 92.2% homologous to the human retroviral sequence HERV-H (GenBank Accession Number M18048). We also observed a sequence that was highly homologous to small polydispersed circular DNA (spcDNA) (GenBank X96885) beginning at nucleotide position 148040 within RG30H15 (Figure 1c). This may be very important as spcDNA sequences have been observed in the 110 Kb of sequence obtained within the FRA3B region (Boldog et al., 1997). Figure 2 shows a FASTA alignment between spcDNA clone 1-82 (HS182S), and spcDNA sequences obtained in the regions containing FRA3B and FRA7G. We found a 73.2% identity between spcDNA clone 1-82 and FRA7G (Figure 2a), and a 75.1% identity between an spcDNA sequence within FRA3B and the one identified in BAC RG30H15 (Figure 2b). There were no trinucleotide or minisatellite repeats present in the sequence from this BAC clone. This provides further evidence that repeats similar to those found at rare fragile sites are probably not responsible for fragility at the common fragile sites.

FISH-based analysis of P1 and BAC clones relative to FRA7G

FISH-based analysis within 3p14.2 revealed that breakage within the FRA3B region occurs over a region of at least 300 Kb (Wilke et al., 1996; Wang et al., 1997; Zimonjic et al., 1997). Cosmids in the middle of this region would hybridize proximal, distal, or across the region of aphidicolin-induced breakage in different metaphases at approximately equal frequencies. The center of this region of breakage was found to contain an HPV16 viral integration site, thus linking instability within a fragile site with a region that would preferentially integrate exogenous viral sequences.

We were therefore interested in analysing the FRA7G region to determine if breakage occurred over a large region and to define the apparent 'center' of such a region. The three P1 and one BAC clone were thus used as FISH-based probes against aphidicolin-induced FRA7G breakpoints to determine the frequency that they would hybridize proximal, distal, or actually cross the region of breakage. The first clone analysed was P1 clone v203B. When this clone was hybridized to 20 metaphases containing FRA7G breakpoints, it hybridized distal to the region of breakage in 16 metaphases. However, in two metaphases this P1 clone hybridized proximal to the region of breakage and in two metaphase it hybridized across the region of breakage. This demonstrates that breakage occurs over a relatively large region, but that this clone is clearly distal to the region where the majority of aphidicolin-induced breakage occurs.

P1 clone v203c, which is localized proximal to v203B, was hybridized to 31 metaphases that had

**Table 1** The positions of P1 and BAC clones relative to breaks of FRA7G by FISH analysis

Clones	N	%Prox	%Crossing	%Dist	%Prox-%Dist
v203B	20	10	10	80	−70
RG30H15	22	9.1	27.3	63.6	−54.5
v203C	31	25.8	32.3	41.9	−16.1
v193A	41	63.4	22	14.6	48.8

Note: N, the number scored of metaphase spreads with FRA7G expression. The %Prox, %Dist and %Crossing refer to the percentage of the time that FISH signals were seen proximal, distal, or across the breaks of FRA7G in different cells, respectively

FRA7G breakpoints. This clone hybridized proximal to the aphidicolin-induced breakpoint in 8 metaphases, distal in 13 metaphases, and crossed the region of breakage in 10 metaphases. P1 clone v193A, the most proximal of the clones analysed, was hybridized to 41 metaphases containing FRA7G breakpoints. This clone hybridized proximal to the aphidicolin-induced breakpoint in 26 metaphases, crossed the breakpoint in 9 metaphases, and hybridized distal in 6 metaphases. Finally BAC clone RG30H15, which covers most of P1 clone v203B and contains additional proximal sequences, was hybridized to 22 metaphases with FRA7G breakpoints. This clone hybridized proximal to the aphidicolin-induced breakpoint in 2 metaphases, crossed the breakpoint in 6 metaphases, and hybridized distal to the breakpoint in 14 metaphases. The results obtained with the three P1 clones and one BAC clone are very similar to results obtained with clones in the FRA3B region and demonstrate that aphidicolin-induced breakage in this region occurs across a region at least 300 Kb in size. All of these results are summarized in Table 1; also included on this Table is the difference between the incidence of probes hybridizing proximal and distal hybridization with each of the clones tested.

Figure 3 shows several representative hybridizations to aphidicolin-induced metaphases with breakage in the FRA7G region. Figure 3a shows one of the metaphases hybridized with P1 clone v193A where it can be clearly seen that the clone hybridizes proximal to the region of breakage. Figure 3b shows one of the metaphases hybridized with P1 clone v203B, and here the clone hybridized distal to the region of breakage. Figure 3c shows the result obtained when one of the metaphases was hybridized with P1 clone v203C; this clone clearly hybridized across the region of breakage. Figure 3d shows the R banding of the same metaphase seen in Figure 3c which demonstrates that the chromosome 7 breakage in this particular metaphase occurs in band 7q31.2, which is precisely where FRA7G resides.

Figure 4 is a histogram depicting the absolute value of the difference between the percent of the time that a particular clone hybridized proximal to the region of aphidicolin-induced breakage minus the percent of time that the clone hybridized distal to the region of breakage. This Figure demonstrates that clone v203C is approximately in the middle of the FRA7G region. The full size of the FRA7G region, or how large the region where aphidicolin-induced decondensations/breakage occurs, remains unknown as there are still a significant number of aphidicolin-induced breakpoints
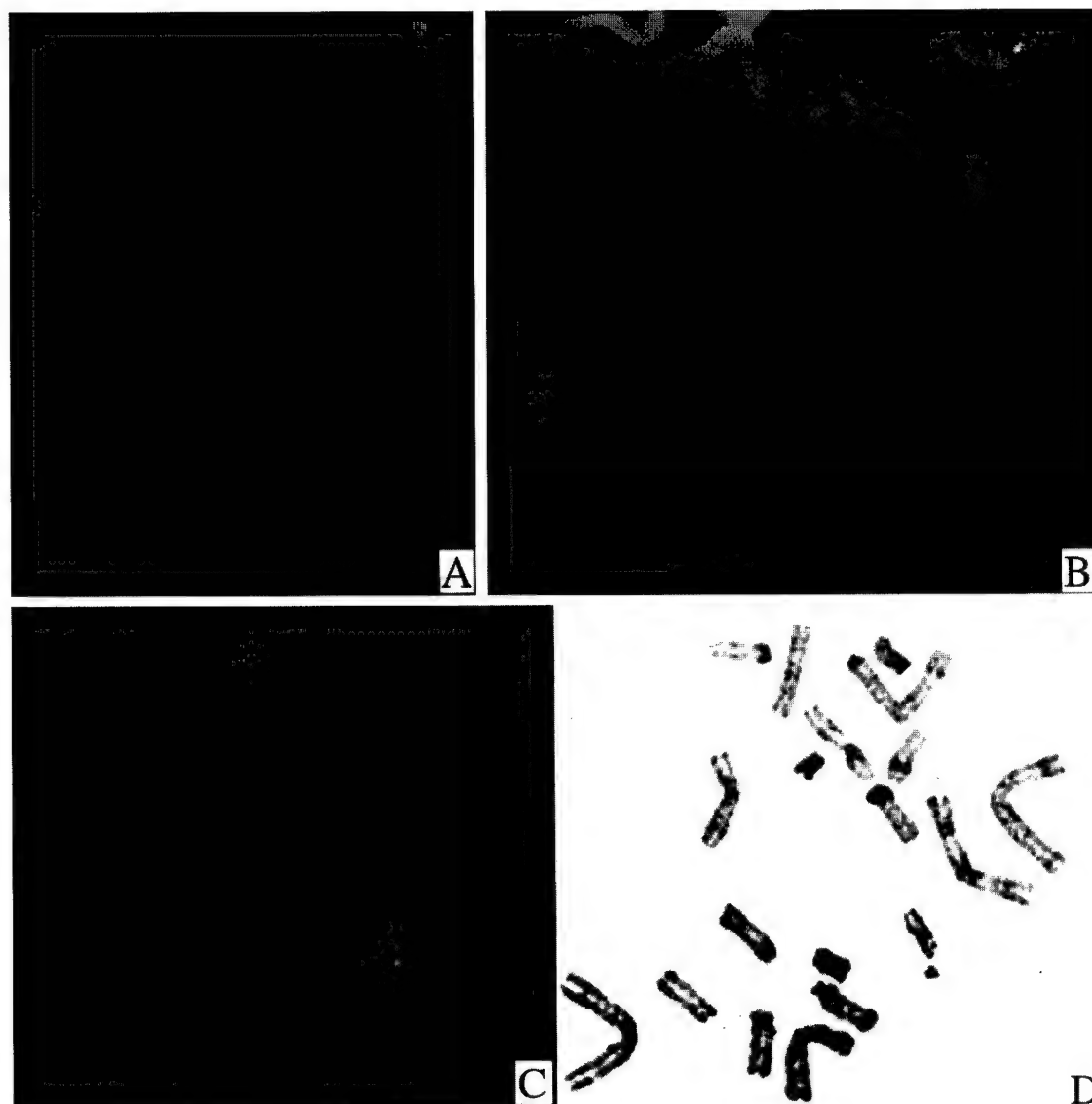
Figure 3 Representative FISH hybridizations to metaphase spreads of aphidicolin-induced chromosome 7-only somatic cell hybrid 1HL11-G: (**a**) A metaphase showing hybridization signal obtained with P1 clone v193A hybridizing proximal to FRA7G decondensation/breakdage; (**b**) Partial metaphase showing FISH hybridization of P1 clone v203B distal to the breakage of FRA7G; (**c**) A metaphase spread illustrating the FISH signal of P1 clone v203C is split by FRA7G breakage; (**d**) R-banding of the chromosomes shown in (**c**)

which occur proximal to clone v203B and distal to clone v193A. Also included on this Figure is a histogram showing the percent of time a particular clone hybridized across the region of FRA7G breakage. Although less striking, this too demonstrates that clone v203C is approximately in the middle of the FRA7G region.

Discussion

The mechanism for the instability of the common fragile sites and the role that these sites play in cancer development is unclear. Based upon the cytogenetic location of the common fragile sites and the position of breakpoints and rearrangements observed throughout the genome in human cancers, Yunis and Soreng (1984) first proposed that the fragile sites could be predisposing the chromosomes to breakage and thus could play a key role in cancer development. The

analysis of the sequence for much of FRA3B, the most active of the common fragile sites, has not revealed why the FRA3B region is so unstable. However, the molecular characterization of FRA3B has demonstrated that cancer breakpoints and rearrangements do indeed occur right within the FRA3B region at the molecular level (Boldog *et al.*, 1997; Shridhar *et al.*, 1996, 1997). We were therefore interested in analysing another common fragile site to determine if a comparison between different fragile sites would give insights into their mechanism of instability and also to determine if the position of cancer breakpoints at another fragile site coincided with the precise location of that fragile site.

We chose to characterize FRA7G, as alterations in the 7q31.2 region are frequently observed in a number of different tumors including breast (Zenklusen *et al.*, 1994a; Lin *et al.*, 1996; Devilee *et al.*, 1997), prostate (Zenklusen *et al.*, 1994b; Takahashi *et al.*, 1995; Latil *et al.*, 1995; Jenkins *et al.*, manuscript in preparation),
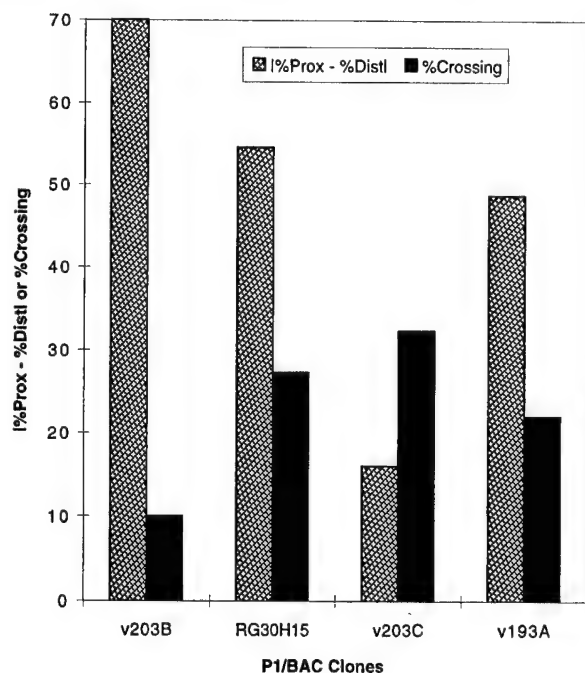
Figure 4 Histogram of the FISH analysis with P1 and BAC clones. The results are expressed in terms of the percentage of the time that FISH signals of each clone were observed across the region of breakage in FRA7G (black) and the absolute value of the difference between the percentage of the time that a individual clone hybridized distal or proximal to the gaps or breaks of the fragile site (grey shading). The lower the absolute value of the difference between the percentage of the time that a clone was distal or was proximal to the region of aphidicolin-induced breakage, the more often the hybridization signal was seen equally on both sides of FRA7G

and ovarian cancer (Zenklusen et al., 1995b; Koike et al., 1997). However, the FRA7G fragile site is expressed at considerably lower levels than FRA3B; thus, we concentrated our efforts on a chromosome 7-only somatic cell hybrid. The frequency of expression of FRA7G in this hybrid was not greater than what would have been observed in human lymphocytes, but the ease of identifying the chromosome 7 in the hybrid facilitated our analysis of the large number of metaphases which we needed to examine to find sufficient FRA7G breakpoints for our FISH-based analysis. By using a FISH-based mapping approach, we previously defined the FRA7G region within three YAC clones in the region surrounding a microsatellite marker that has been described as the most frequently deleted in a number of different tumors (Huang et al., 1998). In order to further characterize FRA7G, we identified three P1 clones from the FRA7G region. Restriction endonuclease mapping of these clones revealed that they overlap. In addition, we found that RG30H15, a BAC clone which has been completely sequenced, localized right in the middle of our P1 contig.

The five cloned folate-sensitive rare fragile sites each contain a CGG repeat which is amplified and methylated in individuals who demonstrate fragility at these sites (Verkerk et al., 1991; Knight et al., 1993; Ritchie et al., 1994; Jones et al., 1994; Nancarrow et al., 1994). The sixth cloned rare fragile site is the distamycin A-inducible fragile site, FRA16B. This

fragile site contains an expanded 33 bp AT-rich minisatellite sequence in individuals that express this site (Yu et al., 1997). We previously constructed a 350 Kb cosmid contig across the aphidicolin-inducible common fragile site FRA3B and found no evidence for the presence of any trinucleotide repeats in this region (Paradee et al., 1996). There were also no minisatellite repeats in the 110 Kb of sequence generated in this region by Boldog et al. (1997). The hybridization of various trinucleotide repeats to the P1 clones from the FRA7G region failed to detect any repeats, and there was no large extended repeat sequence present in the 150 Kb of sequence derived from BAC clone RG30H15. These results suggest that the mechanism of instability in the two cloned common fragile sites, FRA3B and FRA7G, are distinct from the instability which occurs in the rare fragile sites associated with expansions of tri- or mini-satellite repeat sequences.

The results of our FISH-based analysis of aphidicolin-induced breakage in the FRA7G region demonstrate that breakage occurs throughout this region. P1 clone v203B hybridized distal to FRA7G breakpoints in 16 out of 20 metaphases. However, this clone hybridized proximal to FRA7G breakpoints in 2 of 20 metaphases. Conversely, the most proximal P1 clone analysed, v193A, hybridized proximal to FRA7G breakpoints in 26 of 41 metaphases. This clone, however, hybridized distal to FRA7G breakpoints in 6 of 41 metaphases. These results demonstrate that breakage in the FRA7G region extends over a region of at least 300 Kb. This result is identical to the results obtained in the FRA3B region (Wilke et al., 1996; Wang et al., 1997; Zimonjic et al., 1997). Thus for two of the first cloned and characterized common fragile sites, there does not appear to be any repeat sequences responsible for fragility and aphidicolin-induced chromosomal breakage occurs over a region which is probably greater than 300 Kb. One of the cosmids in our 350 Kb contig surrounding the FRA3B region appears to lie within the center of that fragile site. It is thus very interesting to note that there was an HPV16 viral integration site within that cosmid and a sequence with considerable homology to spcDNA. The sequence obtained from BAC clone RG30H15 reveals the presence of another sequence with considerable homology to spcDNA as well as sequences corresponding to HERV-H DNA.

Evidence has been accumulating that spcDNA is associated with genomic instability in human cells (Cohen et al., 1997). spcDNAs can also be induced or increased by DNA damaging agents (Cohen and Lavi 1996; Cohen et al., 1997) and inhibitors of DNA synthesis, including the common fragile site inducer aphidicolin (Sunnerhagen et al., 1989). The presence of sequences with considerable homology to spcDNA right in the middle of two of the common fragile sites may therefore not be coincidental. While it is at present uncertain if spcDNA sequences are a primary cause of fragility in both FRA3B and FRA7G as well as other common fragile sites, it is attractive to speculate that these sequences may play some role in the instability in these regions.

It has been hypothesized that the regions containing fragile sites are late replicating (Laird et al., 1987). This was first demonstrated for FRAXA by Hansen et al. (1993). The normal FMR1 alleles replicate late in

S-phase, and this replication is further delayed in this region when there is expansion of the trinucleotide repeat (Hansen *et al.*, 1993). Aphidicolin is an inhibitor of DNA polymerases α and δ; an attractive hypothesis to explain fragility at the common fragile sites is that these regions are also late replicating and the inhibition of replication with aphidicolin further delays this replication resulting in instability in these regions. Using a FISH-based technique, we recently demonstrated FRA3B sequences are indeed late replicating, and that exposure to aphidicolin results in a further delay in the timing of replication (LeBeau *et al.*, 1998). Studies of DNA replication in the region of the cystic fibrosis gene at 7q31.2 showed that the region immediately proximal to the MET oncogene, which localizes precisely within the FRA7G region (Huang *et al.*, 1997), is a late replicating region (Selig *et al.*, 1992). This would support the hypothesis first proposed by Laird *et al.* (1987); however, not all late replicating regions are sensitive to aphidicolin and thus other factors must be playing a role in the exquisite sensitivity of most of the common fragile sites to aphidicolin treatment.

Although there are likely to be many different causes of chromosomal fragility, it has been shown in at least one case that a fragile site can correspond to a region of incompletely condensed chromatin (Durnam *et al.*, 1986). Agents that result in incomplete condensation in specific chromosomal regions could potentially explain why fragile sites are genetically recombinogenic and why certain fragile sites serve as preferential targets for viral or plasmid integration (Rassool *et al.*, 1991; Smith *et al.*, 1992; van der Drift *et al.*, 1994). Wilke *et al.* (1996) showed that a clone derived from the apparent center of the FRA3B region contains an HPV16 viral integration site. We have recently observed that the viral integration site is a hot spot for homozygous deletion in a number of different tumor-derived cell lines (Wang *et al.*, 1998). It has been observed that infection of human cells with adenovirus type 2 or 5 induces chromosomal fragility, and the virus infection and aphidicolin treatment have a synergistic effect on the expression of the common fragile sites (Caporossi *et al.*, 1991); this synergism suggests that both of these agents are targeting the same sequences within the fragile sites. FRA7G does not have an HPV16 viral integration site, as has been observed for FRA3B, but it does contain an HERV-H sequence. While we do not know if the HERV-H sequence is a major cause of fragility in the FRA7G region or simply a marker for this property, it is attractive to speculate that the common fragile sites are hot spots for the integration of exogenous DNA sequences, especially viral sequences. The association of specific types of cancer with viral infection, especially in the case of cervical cancer (Cannizzaro *et al.*, 1988; Wagatsuma *et al.*, 1990), suggests there may indeed be a direct link between viral integration and the initiation of carcinogenesis.

We now have the reagents in hand to begin to characterize two of the common fragile sites in greater detail. In addition, the maturity of the human genome mapping efforts has facilitated the more rapid cloning of additional common fragile sites. A comparison between a number of the common fragile sites should give greater insights into similarities between these sites

and the mechanism of instability in these regions. We are also characterizing chromosome breakpoints in the vicinity of these two common fragile sites in a number of different tumor types to determine the role these sites play in chromosome breakage and rearrangements during cancer development.

Materials and methods

Preparation of PAC and BAC DNAs

Three P1 clones (v193A, v203B, and v203C) were obtained from Vysis, Inc. (Downer's Grove, IL). These clones were identified by PCR screening of a P1 library using primers for D7S522 and D7S486. A BAC clone (RG30H15) was purchased from Research Genetics, Inc. (Huntsville, AL). P1 clones were maintained in *E. coli* strain NS3529 and the BAC clone was maintained in *E. coli* strain HB101/r. Both P1 and BAC clone DNAs were purified using the protocol recommended by QIAGEN using their QIAGEN-tip 100 column (QIAGEN, Chatsworth, CA). DNA preparations were analysed by agarose gel electrophoresis to be certain that there was no RNA present in the preparations and to assay for the presence of bacterial host DNA.

Restriction endonuclease mapping of the PAC clones

The restriction endonucleases used in these experiments (*Pvu*I, *Bam*HI, *Xho*I, *Sac*II, *Sgf*I, and *Eco*RI) were obtained from Promega (Madison, WI). The complete digestion of the P1 vector and partial restriction digestion of the genomic DNA in the P1 clones was performed using the procedure described by MacLaren and Clarke (1996). *Pvu*I restriction endonuclease (21 units) was added to 70 μl of reaction solution containing 3.5 μg P1 clone DNA. This mixture was then divided into 30 μl, 20 μl, and 20 μl portions in order to perform three serial dilutions of the restriction endonucleases which we wanted to generate partial digestion products. Restriction endonucleases (0.033 units) was added into the 30 μl sample. Ten microliters of this sample was transferred to the first 20 μl sample and mixed and then 10 μl of this mixture was transferred to the second 20 μl sample. All samples were then incubated at 37°C for 1 h and then mixed with 5 × type 1 gel loading buffer (Sambrook *et al.*, 1989). A 10 μl portion of each digested sample was fractionated by pulsed field gel electrophoresis on a 30-lane 1% agarose gel in 0.5 × TBE buffer (Sambrook *et al.*, 1989). The gel was run for 7 h with a linear ramp from 0.1 to 3.5 s for small fragments, and 17 h with a linear ramp from 0.2 to 9 s for large fragments. All the molecular weight standards were from Gibco-BRL (Gaithersberg, MD).

Southern blot analysis

DNA fragments were transferred to Hybond-N (Amersham) membranes using the downward blotting protocol (MacLaren and Clarke, 1996). Gels were not compressed with any weight. This method improves the transfer of large DNA fragments and DNA depurination is not necessary. The nylon membranes were washed for 5 min in 2 × SSC and baked in a vacuum oven at 84°C for 2 h. Southern blots were hybridized with random-primer ^{32}P-dCTP labeled probes ($>10^9$ c.p.m./μg) in a phosphate buffer-based Church buffer at 68°C as described by Schifman and Stein (1995).

Probes from the two ends of the P1 cloning vector were generated from PCR amplified fragments of the P1 vector. The left and right probe primer pairs (pLF, pLB; pRF, pRB) were the pairs described by MacLaren and Clarke (1996).

The PCR products for the left and right end probes were 780 bp and 470 bp, respectively. The PCR conditions to amplify these probes were: Final volume of 50 μl, final concentrations of $1 \times$ PCR buffer (50 mM KCl, 10 mM Tris-HCl, 0.1% Triton X-100, 1.5 mM MgCl$_2$) (Promega, Madison, WI), 0.1 mM of each of nucleotide, 1 ng P1 clone DNA, 12.5 pmol of primers, and 3 units Taq DNA polymerase (Promega) were combined. Reactions were cycled 35 times with 30 s at 94°C, 30 s at 55°C, and 1 min at 72°C.

Production of chromosome spreads and induction of FRA7G

The human-hamster hybrid cell line, 1HL11-G, was obtained from the Human Genetic Mutant Cell Repository at the Coriell Institute for Medical Research in Camden, New Jersey (repository number GM10791). This cell line contains a single chromosome 7 as its only human component (Jones et al., 1990; Ledbetter et al., 1990; Green et al., 1991). Chromosome preparation and fragile site induction were modified from published procedures (Kuwano et al., 1990; Hirsch, 1991; Green et al., 1994). Briefly, cells were cultured in MEM α medium with 10% fetal calf serum, 100 units/ml penicillin, and 100 μg/ml streptomycin. Aphidicolin dissolved in 70% ethanol was added to a final concentration of 0.2 μM and methotrexate (MTX) at a final concentration of 1×10^{-5} M was added 24 h after subculturing. Cultures were further maintained for another 17 h and then the cells were washed twice in Hank's solution, and cultured for another 7 h in medium with BrdU (25 μg/ml) without aphidicolin and MTX. Ethidium bromide (8 μg/ml) and colcemid (0.02 μg/ml) were added for the last 2 h. Cells were then processed using traditional cytogentic procedures for the preparation of metaphase spreads.

PAC and BAC clones used for FISH analysis

P1 and BAC clone DNAs were labeled with Biotin-16-dUTP (Boehringer-Mannheim, Indianapolis, IN) using a nick translation kit (Boehringer-Mannheim). Techniques for hybridization of labeled P1 and BAC DNA probes to metaphase spreads and FISH analysis were identical to those described by us previously (Huang et al., 1998).

Hybridization of trinucleotide and minisatellite repeats to the PAC contig across the FRA7G region

Oligonucleotide hybridizations to the PAC clones were performed by labeling oligonucleotides with ^{32}P-ATP using T4 polynucleotide kinase (Gibco-BRL) and hybridized overnight at 37°C to Southern transferred PAC DNA in oligo hybridization solution. The oligonucleotides used in this screening were synthesized by Gibco-BRL or in the Mayo Foundation Molecular Facility Core. These repeats include p(CGG)$_{11}$, p(CTG)$_{17}$, p(ATATATTATATATTA-TATCTAATAATAT^C/$_A$TA), p(CTA)$_{13}$, p(TAT)$_{17}$, p(GTA)$_{14}$, p(CCT)$_{13}$, p(TGG)$_{12}$, p(CGT)$_{14}$ and p(GAA)$_{17}$. As a positive control we included a cDNA for the human androgen receptor which has a (CGG) repeat and a (CAG) repeat in it.

References

Boldog FC, Wagoner B, Glover TW, Chumakov I, le Paslier D, Cohen D, Gemmill RM and Drabkin HA. (1994). Genes Chromosomes Cancer, **11**, 216–221.

Boldog FC, Gemmill RM, West J, Robinson M, Robinson L, Li E, Roche J, Todd S, Waggoner B, Lundstrom R, Jacobson J, Mullokandov MR, Klinger H and Drabkin HA. (1997). Hum. Mol. Genet., **6**, 193–203.

Cannizzaro LA, Durst M, Mendez MJ, Hecht BK and Hecht F. (1988). Cancer Genet. Cytogenet., **33**, 93–98.

Caporossi D, Bacchetti S and Nicoletti B. (1991). Cancer Genet. Cytogenet., **54**, 39–53.

Champeme M-H, Bieche I, Beuzelin M and Lidereau R. (1995). Genes Chromosomes Cancer, **12**, 304–306.

Cohen AJ, Li FP, Berg S, Marchetto DJ, Tasai S, Jacobs SC and Brown RS. (1979). New Eng. J. Med., **301**, 592–595.

Cohen S and Lavi S. (1996). Mol. Cell. Biol., **16**, 2002–2014.

Cohen S, Regev A and Lavi S. (1997). Oncogene, **14**, 977–985.

Devilee P, Hermans J, Eyfjord J, Borresen A-L, Lidereau R, Sobol H, Borg A, Cleton-Jansen A-M, Olah E, Cohen BB, Scherneck S, Hamann U, Peterlin B, Caligo M, Bignon Y-J and Maugard CH. (1997). Genes Chromosomes Cancer, **18**, 193–199.

Durnam DM, Smith PP, Menninger JC and McDougall JK. (1986). Cancer Cells, **4**, 349–354.

Glover TW, Berger C, Coyle-Morris J and Echo B. (1984). Hum. Genet., **67**, 882–890.

Green ED, Mohr RM, Idol JR, Jones M, Buckingham JM, Deaven L, Moyzis RK and Olson MV. (1991). Genomics, **11**, 548–564.

Green ED, Idol JR, Mohr-Tidwell RM, Braden VV, Peluso DC, Fulton RS, Massa HF, Magness CL, Wilson AM, Kimura J, Weissenbach J and Trask BJ. (1994). Hum. Mol. Genet., **3**, 489–501.

Hansen RS, Canfield TK, Lamb MM, Gartler SM and Laird CD. (1993). Cell, **73**, 1403–1409.

Hirsch B. (1991). Hum. Genet., **87**, 302–306.

Huang H, Qian C, Jenkins RB and Smith DI. (1998). Genes Chromosomes Cancer, In Press.

Jones C, Slijepcevic P, March S, Baker E, Langdon WY, Richards RI and Tunnacliffe A. (1994). Hum. Mol. Genet., **3**, 2123–2130.

Jones C, Penny L, Mattina T, Yu S, Baker E, Voullaire L, Langdon WY, Sutherland RG, Richards RI and Tunnacliffe A. (1995). Nature, **376**, 145–149.

Jones NJ, Stewart SA and Thompson LH. (1990). Mutagenesis, **5**, 15–23.

Kastury K, Baffa R, Druck T, Ohta M, Cotticelli MG, Inoue H, Negrini M, Rugge M, Huang D, Croce CM, Palazzo J and Huebner K. (1997). Cancer Res., **56**, 978–983.

Knight SJL, Flannery AV, Hirst MC, Campbell L, Christodoulou Z, Phelps SR, Pointon J, Middleton-Price HR, Barnicoat A and Pembrey ME. (1993). Cell, **74**, 127–134.

Koike M, Takeuchi S, Yokota J, Park S, Hatta Y, Miller CW, Tsuruoka N and Koeffler HP. (1997). Genes Chromosomes Cancer, **19**, 1–5.

Kremer E, Pritchard M, Lynch M, Yu S, Holman K, Baker E, Warren ST, Schlessinger D, Sutherland GR and Richards RI. (1991). Science, **252**, 1711–1714.

Kuniyasu H, Yasui W, Yokozaki H, Akagi M, Kitahara K, Fujii K and Tahara E. (1994). *Int. J. Cancer*, **59**, 597–600.

Kuwano A, Murano I and Kajii T. (1990). *Hum. Genet.*, **84**, 527–531.

Laird C, Jaffe E, Karpen G, Lamb M and Nelson R. (1987). *Trends Genet.*, **3**, 274–281.

Latil A, Baron JC, Cussenot O, Fournier G, Soussi T, Boccon-Gibod L, Le Duc A, Rouesse J and Lidereau R. (1995). *Bulletin Cancer*, **82**, 589–597.

Le Beau MM, Rassool FV, Neilly ME, Espinosa III R, Glover TW, Smith DI, Schumm PL and McKeithan TW. (1998). *Hum. Mol. Genet.*, In press.

Ledbetter SA, Garcia-Heras J and Ledbetter DH. (1990). *Genomics*, **8**, 614–622.

Lin JC, Scherer SW, Tougas L, Traverso G, Tsui L-C, Andrulis I, Jothy S and Park M. (1996). *Oncogene*, **13**, 2001–2008.

MacLaren DC and Clarke S. (1996). *Genomics*, **35**, 299–307.

Nancrarrow JK, Kremer E, Holman K, Eyre H, Doggett NA, le Paslier D, Callen DF, Sutherland GR and Richards RI. (1994). *Science*, **264**, 1938–1941.

Oberle I, Rousseau F, Heitz D, Kretz C, Devys D, Hanauer A, Boue J, Bertheas MF and Mandel J-L. (1991). *Science*, **252**, 1097–1102.

Ohta M, Inoue H, Cotticelli MG, Kastury K, Bafa R, Palazzo J, Siprashvili Z, Mori M, McCue P, Druck T, Croce CM and Huebner K. (1996). *Cell*, **84**, 587–597.

Pandis N, Bardi G, Mitelman F and Heim S. (1997). *Genes Chromosomes Cancer*, **18**, 241–245.

Paradee W, Wilke CM, Wang L, Shridhar R, Mullins CM, Hoge A, Glover TW and Smith DI. (1996). *Genomics*, **35**, 87–93.

Penny LA, Dell'Aquila M, Jones MC, Bergoffen J, Cunniff C, Fryns J-P, Grace E, Graham JM, Kouseff B and Mattina T. (1995). *Am. J. Hum. Genet.*, **56**, 676–683.

Rassool FV, McKeithan TW, Neilly ME, van Melle E, Espinosa R and Le Beau MM. (1991). *Proc. Natl. Acad. Sci. USA*, **88**, 6657–6661.

Rassool FV, Le Beau MM, Neilly ME, van Melle E, Espinosa R 3d and McKeithan TW. (1992). *Am. J. Hum. Genet.*, **50**, 1243–1251.

Rassool FV, Le Beau MM, Shen M-L, Neilly ME, Espinosa III R, Ong ST, Boldog F, Drabkin H, McCarroll R and McKeithan TW. (1996). *Genomics*, **35**, 109–117.

Ritchie RJ, Knight SJL, Hirst MC, Crewal PK, Bobrow M, Cross GS and Davies KE. (1994). *Hum. Mol. Genet.*, **3**, 2115–2121.

Sambrook J, Fritsch EF and Maniatis T. (ed). (1989). *Molecular Cloning: A Laboratory Manual*, Cold Spring Harbor Laboratory press: New York.

Selig S, Okumura K, Ward DC and Cedar H. (1992). *EMBO J.*, **11**, 1217–1225.

Shifman MI and Stein DG. (1995). *J. Neurosci. Methods*, **59**, 205–208.

Shridhar R, Shridhar V, Wang X, Paradee W, Dugan M, Sarkar F, Wilke C, Glover TW, Vaitkevicius VK and Smith DI. (1996). *Cancer Res.*, **56**, 4347–4350.

Shridhar V, Wang L, Rosati R, Paradee W, Shridhar R, Mullins C, Sakr W, Grignon D, Miller OJ, Sun QC, Petros J and Smith DI. (1997). *Oncogene*, **14**, 1269–1277.

Smeets DFCM, Scheres JMJC and Hustinx TWJ. (1986). *Hum. Genet.*, **72**, 215–220.

Smith PP, Friedman CL, Bryant EM and McDougall JK. (1992). *Genes Chromosomes Cancer*, **5**, 150–157.

Sozzi G, Veronese ML, Negrini M, Baffa R, Cotticelli MG, Inoue H, Tornielli S, Pilotti S, De Gregorio L and Pastorino U. (1996). *Cell*, **85**, 17–26.

Sunnerhagen P, Sjoberg RM and Bjursell G. (1989). *Somat. Cell. Mol. Genet.*, **15**, 61–70.

Sutherland GR and Hecht F. (1995). *Fragile sites on human chromosomes*. In *Oxford Monographs on Medical Genetics*, No. 13 Oxford University Press, New York.

Takahashi S, Shan AL, Ritland SR, Delacey KA, Bostwick DG, Lieber MM, Thibodeau SN and Jenkins RB. (1995). *Cancer Res.*, **55**, 4114–4119.

van der Drift P, Chan A, van Roy N, Laureys G, Westerveld A, Speleman F and Versteeg R. (1994). *Hum. Mol. Genet.*, **3**, 2131–2136.

Verkerk AJMH, Pieretti M, Sutcliffe JS, Fu Y-H, Kuhl DPA, Pizzuti A, Reiner O, Richards S, Victoria MF, Zhang F, Eussen BE, van Ommen G-JB, Blonden LAJ, Riggins GJ, Chastain JL, Kunst GH, Caskey CT, Nelson DL, Oostra BA and Warren ST. (1991). *Cell*, **65**, 905–914.

Wagatsuma M, Hashimoto K and Matsukura T. (1990). *Journal of Virology*, **64**, 813–821.

Wang L, Paradee W, Mullins C, Shridhar R, Rosati R, Wilke CM, Glover TW and Smith DI. (1998). *Genomics*, **41**, 485–488.

Wang L, Darling J, Zhang J-S, Qian C-P, Hartmann L, Conover C, Jenkins RB, Smith DI. (1998). *Oncogene*, In Press.

Wilke CM, Hall BK, Miller D, Hoge A, Paradee W, Smith DI and Glover TW. (1996). *Hum. Mol. Genet.*, **5**, 973–977.

Yu S, Pritchard M, Kremer E, Lynch M, Nancarrow J, Baker E, Holman K, Mulley JC, Warren ST, Schlessinger D, Sutherland GR and Richard RI. (1991). *Science*, **252**, 1179–1181.

Yu S, Mangelsdorf M, Hewett D, Hobson L, Baker E, Eyre H, Lapsys N, le Paslier D, Doggett NA, Sutherland GR and Richards RI. (1997). *Cell*, **88**, 367–374.

Yunis JJ and Soreng AL. (1984). *Science*, **226**, 1199–1204.

Zenklusen J, Bieche I, Lidereau R and Conti C. (1994a). *Proc. Natl. Acad. Sci. USA*, **91**, 12155–12158.

Zenklusen JC, Thompson JC, Troncoso P, Kagan J and Conti CJ. (1994b). *Cancer Res.*, **54**, 6370–6373.

Zenklusen JC, Thompson JC, Klein-Szanto AJP and Conti CJ. (1995a). *Cancer Res.*, **55**, 1347–1350.

Zenklusen J, Weitzel J, Ball H and Conti CJ. (1995b). *Oncogene*, **11**, 359–363.

Zimonjic DB, Druck T, Ohta M, Kastury K, Carlo MC and Popescu NC. (1997). *Cancer Res.*, **57**, 1166–1170.

The Characterization of the Common Fragile Site FRA16D and Its Involvement in Multiple Myeloma Translocations

Kurt A. Krummel,*,† Lewis R. Roberts,‡ Masako Kawakami,*
Thomas W. Glover,§ and David I. Smith*,1

*Division of Experimental Pathology, Department of Laboratory Medicine and Pathology, †Biochemistry and Molecular Biology
Program, Mayo Graduate School, and ‡Division of Gastroenterology and Hepatology, Department of Internal Medicine,
Mayo Foundation, Rochester, Minnesota 55905; and §Department of Pediatrics and Department of Human Genetics,
University of Michigan Medical School, Ann Arbor, Michigan 48109

Fragile sites appear as breaks, gaps, or decondensations on metaphase chromosomes when cells are grown under specific culture conditions. The breaks are nonrandom, appearing in defined, conserved locations throughout the mammalian genome. Common fragile sites, as their name implies, are present in virtually all individuals. With three common fragile sites cloned, their mechanism of expression and the role, if any, they play in human disease are still unclear. We have assembled a BAC contig of >1 Mb across the second most active common fragile site, FRA16D (16q23.2). We fluorescently labeled these BACs and used them as probes on metaphases from aphidicolin-induced lymphocytes and demonstrated that FRA16D decondensation/breakage occurs over a region of at least 1 Mb. Thus, this is the largest common fragile site cloned to date. Microsatellite markers that map within FRA16D show a very high loss in prostate, breast, and ovarian tumors, indicating that loss within this fragile site may be important in the development or progression of these tumors. In addition, a common t(14q32; 16q23) translocation is observed in up to 25% of all multiple myelomas (MM). We localized four of four such cloned t(14;16) MM breakpoints within the FRA16D region. This work further demonstrates that the common fragile sites may play an important role in cancer development. © 2000 Academic Press

INTRODUCTION

Fragile sites appear as breaks, gaps, or decondensations on metaphase chromosomes (Sutherland, 1979). These nonrandom breaks appear in defined locations on human chromosomes under appropriate conditions.

[1] To whom correspondence and reprint requests should be addressed at Mayo Clinic Cancer Center, Division of Experimental Pathology, Department of Laboratory Medicine and Pathology, Mayo Foundation, 200 First Street, S.W., Rochester, MN 55905. Telephone: (507) 266-0309. Fax: (507) 266-5193. E-mail: smith.david@mayo.edu.

Based on the relative frequency of occurrence in the general population, fragile sites have been divided into two classes, rare and common. Rare fragile sites (RFSs) are sites inherited in a Mendelian codominant fashion and are observed in less than 5% of the population. Common fragile sites (CFSs), as their name implies, are present in virtually all individuals. Variation in the means of induction allows for the additional subclassification of the currently recognized 28 rare and 89 common fragile sites. The rare fragile sites can be subdivided into sites that exhibit folic acid sensitivity or are inducible by such chemicals as distamycin A and bromodeoxyuridine (BrDU) (Sutherland et al., 1998). The CFSs are subdivided into three categories based on induction by aphidicolin, 5-azacytidine, or BrDU (Sutherland et al., 1985; Glover et al., 1984). The majority of the CFSs, however, are induced by aphidicolin, a DNA polymerase α/δ inhibitor.

Several groups cloned the first RFS, FRAXA, in 1991 (Oberle et al., 1991; Kremer et al., 1991; Verkerk et al., 1991; Yu et al., 1991). This work demonstrated that trinucleotide repeat expansion was responsible for the instability within FRAXA and established the paradigm of trinucleotide repeat instability in human disease (Sutherland et al., 1998). Since then, six other RFSs have been cloned and characterized (Hewett et al., 1998; Jones et al., 1995; Knight et al., 1993; Nancarrow et al., 1994; Parrish et al., 1994; Yu et al., 1997). These papers demonstrated that the expression of all the RFSs is associated with repeat expansions. The cloned folate-sensitive RFSs all have expanded trinucleotide repeats, whereas the distamycin A-sensitive RFS, FRA16B (Yu et al., 1997), and the bromodeoxyuridine-sensitive RFS, FRA10B (Hewett et al., 1998), have larger expanded minisatellite sequences at the center of their regions of instability.

A relationship between fragile sites and disease was documented with the rare fragile sites, FRAXA and FRAXE. These sites are associated with heritable mental retardation in humans, and FRA11B is implicated

37

in the genesis of the chromosomal deletion syndrome, Jacobsen syndrome. The clinical significance of the CFSs, however, has not yet been determined. Considerable interest in the CFSs has developed due to their potential role in the development of cancer. The cytogenetic locations of many of the CFSs map to regions that are frequently altered or rearranged during cancer development (Yunis and Soreng, 1984). There is also evidence to suggest that CFSs are preferred sites of sister chromatid exchange (Glover and Stein, 1987), chromosomal deletion and rearrangement (Wang et al., 1993; Glover and Stein, 1988), gene amplification (Coquelle et al., 1997), transfected plasmid DNA integration (Rassool et al., 1991), and viral integration (Popescu et al., 1990). These data initiated a substantial effort toward the cloning and characterization of the CFSs. Initial work was hampered by the lack of molecular markers, but the enormous progress of the Human Genome Project has greatly facilitated efforts to characterize these chromosomal regions. To date, three of the CFSs, FRA3B, FRA7G (Huang et al., 1998a,b), and FRA7H (Mishmar et al., 1998), have been cloned and characterized. The region of aphidicolin-induced decondensation/breakage at these CFSs extends for several hundred kilobases, but no particular sequences within these regions are directly associated with a preponderance of breakage/decondensation. In addition, the sequences from these regions show no unstable micro- or minisatellites. At least one group has suggested that the sequences at FRA3B and FRA7H exhibit high flexibility and low stability by computer modeling (Mishmar et al., 1998); however, the mechanism(s) responsible for CFS expression is still unclear.

FRA16D (16q23.2) is the second most frequently expressed CFS behind FRA3B (3p14.2). There are frequent deletions within 16q23 in a number of different cancers including prostate, breast, and ovarian cancers (Driouch et al., 1997; Lida et al., 1997; Chen et al., 1996; Dorion-Bonnet et al., 1995; Radford et al., 1995; Elo et al., 1997; Latil et al., 1997; Cooke et al., 1996; Saito et al., 1992; Lisitsyn et al., 1995) and hepatocellular carcinoma (Piao et al., 1999; Tsuda et al., 1990). In particular, three markers (D16S504, D16S516, and D16S518) have shown consistent loss of heterozygosity (LOH) across a number of tumors including breast, prostate, and hepatocellular carcinomas (Driouch et al., 1997; Lida et al., 1997; Chen et al., 1996; Elo et al., 1997; Piao et al., 1999). We wanted to determine whether the deletions within 16q23 corresponded at the molecular level to the position of FRA16D. We also wanted to compare and contrast the regions surrounding the two most active CFSs to aid in our understanding of the instability within these regions. Finally, we wanted to know whether genes within FRA16D are potential targets for the deletions observed in different cancers. Since no large regions of sequence or contigs were available for this region, we generated a series of overlapping clones and used them to characterize this chromosomal region.

The cytogenetic band 16q23 is not only associated with LOH in solid tumors, but it is implicated in the development of multiple myeloma as well. Multiple myeloma (MM) is a disease of plasma cells involving the overproliferation of terminally differentiated B-cells. In many cases, MM progresses through a stage known as monoclonal gammopathy of undetermined significance to malignant MM with increasing karyotypic instability (Hallek et al., 1998). Translocations in MM cells have been observed for some time. However, their frequency and importance have been underestimated due to technical limitations of cytogenetic observation. Specific MM translocations are found repeatedly in both primary tumors and cell lines and may have importance in MM initiation and progression. The most common translocations involve the IgH enhancer element locus (14q32.3). This element is a powerful enhancer and can highly upregulate genes many kilobases away (Chesi et al., 1998). In MM cell lines and primary tumors, IgH translocations occur with various partners such as bcl-1 or cyclin D1 (11q13), c-myc (8q24), or bcl-2 (18q21). In addition to these known 14q32 translocation partners, other regions with unknown gene partners have been observed including 16q23. The t(14q32;16q23) has been observed in many cell lines and their associated primary tumors. Chesi et al. (1998) estimate that this translocation may occur in up to 25% of all MMs. The total frequency of translocations involving an Ig region in MM are unknown, but Hallek et al. (1998) hypothesize that it may be a universal event. These translocations are found late in MM development, but are also thought to occur as an early event in normal plasma cell development when errors occur in IgH switch recombination (Chesi et al., 1998). Taken together, these data suggest an important role for FRA16D in MM translocations in the development of the disease.

MATERIALS AND METHODS

Cell culture and metaphase spread preparation. Human lymphocytes were cultured with 0.4 μM aphidicolin for 24 h after standard treatment as described by Verma and Babu (1989). Metaphase preparations were then affixed to slides according to standard procedures (Verma and Babu, 1989), and BAC probes were hybridized (see next section).

BAC probe preparation. The procedure for the purification of BAC DNA was adapted from the Qiagen plasmid maxi kit protocol as described by Qiagen. Briefly, a single BAC colony was inoculated into 500 ml of selective LB medium and cultured overnight at 37°C. The cultures were centrifuged, and the pelleted bacteria were then split into two parts. Each part was resuspended in 20 ml buffer P1 containing 100 μg/ml RNase A. Twenty milliliters of buffer P2 was added, and the mixture was incubated at room temperature for 5 min; 20 ml of buffer P3 was added, and each mixture was incubated on ice for 30 min. Each mixture was centrifuged at 20,000g for 30 min, and the supernatant was removed. Next, the supernatant was then applied to a Qiagen-tip 500 and eluted with 15 ml of buffer QF. The BAC DNA was precipitated with room temperature isopropanol and then resuspended in a suitable volume of TE. The typical yield

of a 150- to 250-kb BAC clone using this protocol was 125 μg. This BAC DNA was suitable for PCR, labeling for FISH analysis, sequencing, and complete and partial digestion by restriction endonucleases.

Fluorescence in situ hybridization (FISH). BAC DNA was labeled with biotin-16–dUTP (Boehringer Mannheim) using a nick-translation kit (Boehringer Mannheim) according to the manufacturer's protocol. After precipitation, labeled probe DNA was dissolved at a final concentration of 15–25 ng/μl in a hybridization mixture containing 50% formamide, 10% dextran sulfate, 2× SSC, 400–500 ng/μl Cot-1 DNA (Gibco BRL), and 0.5 μg/ml sheared herring sperm DNA. Probe DNA was denatured at 75°C for 10 min and preannealed at 37°C for 20 min. Prior to hybridization, slides with metaphase spreads were denatured at 65°C in 70% formamide in 0.6× SSC for 2–3 min, followed by passage through an alcohol series. Hybridizations were performed at 37°C for 17 h. After hybridization, washes were carried out at 42°C under the following conditions: 50% formamide v/v in 2× SSC twice for 5 min each, 2× SSC twice for 5 min each. Hybridized probes were detected with a fluorescein detection kit (Oncor). Cells were counterstained with propidium iodide (0.6 μg/ml) and antifade compound p-phenylenediamine. Hybridization signals were observed with a Zeiss Axioplan microscope equipped with a triple-pass filter (I02-104-1010, Vysis). Pictures were taken by IP LABSpectrum P software on a Macintosh computer system.

BAC sizing and Southern blot overlap using pulsed-field gel electrophoresis. To determine the sizes of the BACs in the contig, the BAC DNA, purified as described above, was digested to completion with the restriction endonuclease *Not*I. The digest was loaded onto a 1%, 0.5× TBE agarose gel at 14°C and electrophoresed for 30 h with a Bio-Rad CHEF pulsed-field gel box and controller using the following conditions: 120° angle, 1- to 6-s pulse time, linear ramping factor, and 6 V/cm voltage gradient. The gel was stained with ethidium bromide, and the insert sizes were determined by comparison to both the 2.5-kb ladder from Bio-Rad and the Mid-range PFG marker from New England Biolabs loaded on the same gel.

For determining overlap between BAC clones, DNA purified using Qiagen columns was completely digested with the restriction endonuclease, *Sal*I. The complete digestion of the BAC vector and the insert DNA and subsequent detection of overlap were performed as described by Hubert *et al.* (1997).

BAC end sequencing and primer construction. BAC sequencing was performed by the Mayo Clinic DNA sequencing core from 3 μg of BAC DNA prepared as previously described. Both T7 and SP6 primers, which are homologous to the pBeloBAC11 vector ends, were used to obtain sequence from the BAC genomic DNA. After sequence was obtained, primers with a T_m of around 55°C were designed in regions that were free of *Alu* repeats using the Oligo v3.0 software package. The primers were synthesized at the Mayo Clinic oligonucleotide core facility and then tested on three DNA sources: placental DNA, the BAC DNA from which the primers were designed, and a BAC from chromosome 7 as a negative control. The PCR was carried out under the following conditions for all primers: 2 cycles at 98, 55, and 72°C for 30 s each. This was followed by 28 cycles of 95, 55, and 72°C for 30 s each with a final extension of 72°C for 10 min. After the initial testing, the primers were used to screen the BAC pools to verify that they were specific to one point in the genome and to verify that the original BAC was again identified.

Multiple myeloma primer construction. Four sets of primers were used in screening for the positions of the multiple myeloma breakpoints in genomic DNA. These primers were designed from sequences submitted to GenBank for the t(14;16) for these cell lines. For the cell line KMS11 chromosome 16 breakpoint sequence, primers KMS11F and KMS11R are 5′-CCTGATAAATATTCAACACGAG-GAG-3′ and 5′-GCAGGTGCTTACACTGTCTGGT-3′, respectively. Cell line MM.1 primers MM.1F and MM.1R are 5′-CACCAG-CAAGCTGTGAAATG-3′ and 5′-AAAGGCTTTGGAGCTTCCTAA-3′, respectively. Cell line ANBL6 primers ANBL6F and ANBL6R are 5′-GAGAGCACATAACTCAGGCCTAATC-3′ and 5′-TTCCTTTC-CTCTGGTCCTCAGT-3′, respectively. Cell line JJN3 primers JJN3F

and JJN3R are 5′-TCAGGCCAAGTCTCTTTACTCA-3′ and 5′-TGTCCAGCCCCTACTCCTAAT-3′, respectively.

RESULTS

Construction of a BAC Contig across the FRA16D Region

When we began this project, there was very little information available about the genomic structure in this region, despite the region being implicated as an important region through LOH in several tumor types. We began with a YAC clone, 922_G_4, which had been shown to hybridize across the region of aphidicolin-induced decondensation/breakage in FRA16D (T. W. Glover, unpublished observations). Unfortunately, no known markers mapped to that YAC, and it was found to be chimeric. We utilized the Los Alamos YAC map that was available for chromosome 16 and were able to estimate which markers were in close proximity to 922_G_4, as well as others that seemed to flank the Los Alamos positioning of FRA16D. We also utilized the public databases available at the time including The Genome Database (GDB, 1990–2000) and The Whitehead Institute for Biomedical Research/MIT Center for Genome Research (Whitehead Institute for Biomedical Research, 2000) to identify markers in the region and assist us in physical positioning of the markers throughout the building of the contig.

We utilized markers from this region to screen the Research Genetics CITB BAC library (release IV). We tested single colonies to verify that they harbored the given STS, sized the clones, and labeled the DNA for use as FISH probes. We utilized our first set of BAC clones from this region in FISH analysis to determine where the clones and STSs resided in relation to the region of breakage. We analyzed at least 20 metaphases with FRA16D breakage/decondensation and a clearly distinguishable specific fluorescent signal for each BAC (Fig. 1). For metaphases of high quality, with breaks clearly defined, the signals were scored as proximal to, distal to, or crossing the region of breakage/decondensation. Using these data, we could determine the position of each clone relative to FS breakage (proximal/centromeric, distal/telomeric, or actually within the region of aphidicolin-induced decondensation/breakage).

Once the positions of the first set of clones were identified relative to FRA16D, we sequenced the ends of each BAC that mapped within the FS at some frequency (either crossing once or more or hybridizing proximal in some metaphases and distal in others). Based on the sequences from each end of the BACs, we made primers that would amplify a specific product from genomic DNA. In this way, we created two new STSs for many of the BACs from this region. Several BACs contained repetitive sequences at their ends; thus we could not derive specific PCR primers for the amplification of those ends. After testing the primers
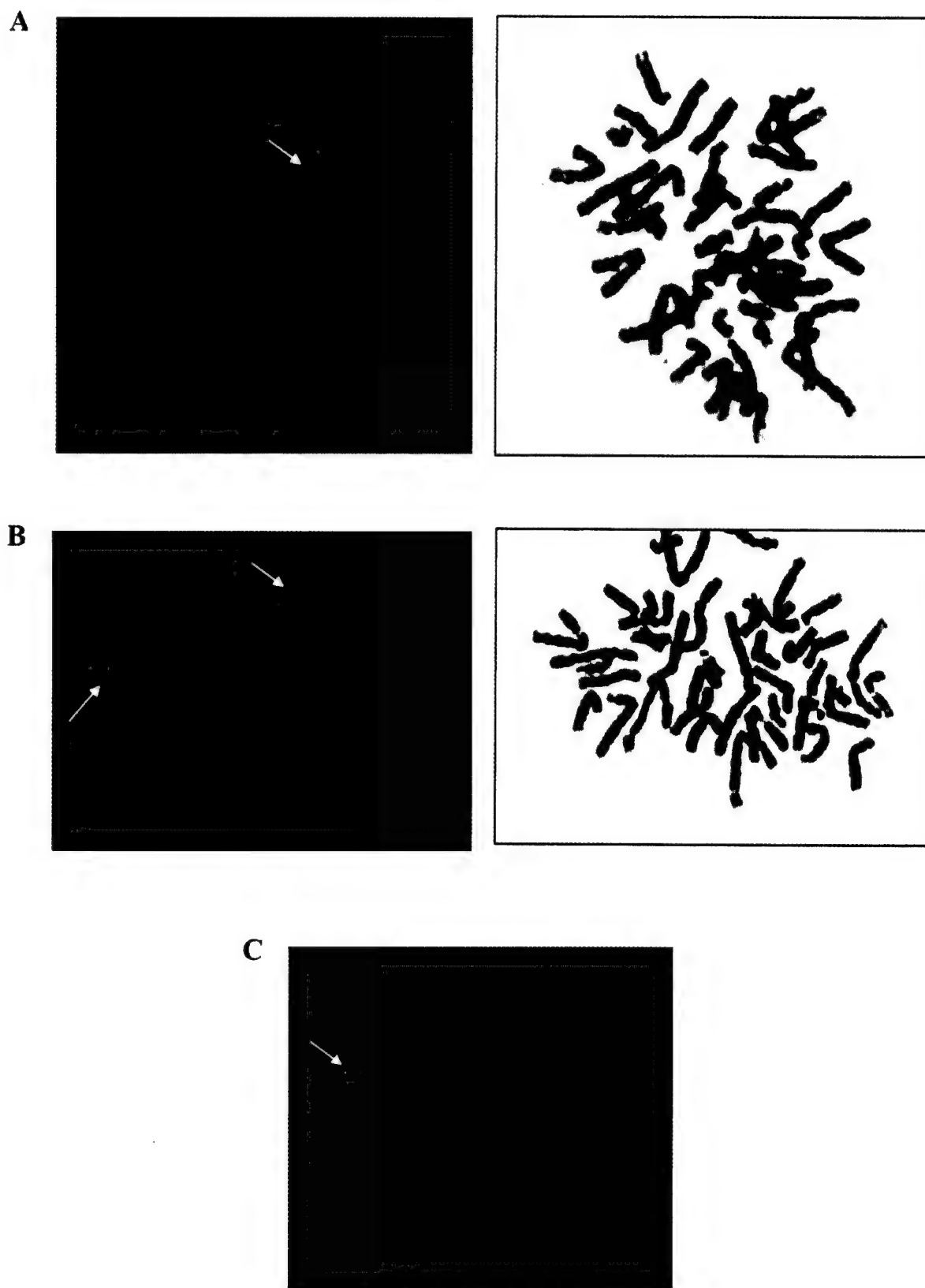
FIG. 1. FISH with human lymphocyte metaphases prepared by standard procedures after incubation with 0.4 μM aphidicolin for 24 h. The metaphases were hybridized with BAC 356_D_21 DNA labeled with biotin, visualized with avidin-FITC (green signal), and counterstained with either DAPI (**A** and **B**), or propidium idodide (**C**). The white arrows indicate breaks at FRA16D with the BAC signal distal (**A**), proximal in both chromosomes (**B**), or crossing the region of breakage (**C**).

for specificity, we began our strategy for determining BAC position and overlap in the contig.

We began by screening the BAC pools for clones that also contained the sequences from the end of a given BAC to identify overlapping clones. The new BACs retrieved in this way were tested by PCR to determine their overlap with other surrounding BAC ends and markers from the databases. This helped us to determine the orientation of the T7 and SP6 ends of each BAC and their positions relative to known STSs. The BACs that extended the contig in a desired direction without overlapping with many already identified clones (indicating a high degree of redundancy) were analyzed by Southern blot hybridization. Labeled BAC DNA was then used as a FISH probe to determine the position of the newly isolated BACs relative to FRA16D. These new BACs were sized and then subjected to end sequencing to make new primers. This strategy continued until all gaps had been filled and resulted in a contig of overlapping BAC clones that extended for >1 Mb around 16q23.2 (Fig. 2). As shown in Fig. 4, our clones confirmed the database marker and YAC orders established for this region.

Our FISH data indicated that our large contig covered the vast majority of FRA16D; however, FISH with BACs located on the centromeric edge of this contig continued to show infrequent hybridization on the centromeric side of FRA16D breakage. We therefore isolated another set of BAC clones that were centromeric to the first larger contig. This smaller contig contains the BAC 540_P_5. Listed in Table 1 are the sequences of the new STSs that we have generated in the construction of this contig. Figure 2 shows the total number of BAC clones isolated from this region, STSs, and polymorphic microsatellite markers that were used to isolate the BAC clones and the positions of the BACs.

FISH Characterization of the FRA16D Region

While constructing the BAC contig across the entire FRA16D region, we used FISH to position the BAC clones relative to the region of aphidicolin-induced decondensation/breakage. After the BAC contig was completed, FISH was performed with representative BAC clones from the contig to analyze the entire region for aphidicolin-induced decondensation/breakage. Figure 3 summarizes the results of this analysis, indicating the number of times a tested BAC clone hybridized proximal to, distal to, or across the region of breakage when analyzed with at least 20 metaphases with decondensation/breakage in FRA16D. The region of breakage extended throughout the entire BAC contig of over 1 Mb. Our most telomeric BAC clone, 484_H_2, hybridized distal to the region of breakage 19 times out of 20, crossed the region of breakage once, and never hybridized proximal to the break. These data indicate that this clone is on the very telomeric edge of this FS since it almost always hybridized distal to the breaks. These numbers do not reflect the exact physical posi-

tion since the FS breakage occurs throughout a region and is therefore subject to statistical fluctuation. The ratios of distal, proximal, and crossing do, however, give a relative idea of physical location relative to the FS. Physical locations of all the BACs have been verified by STS and other marker positions. On the centromeric end of the contig, BAC clone 313_F_8 hybridized proximal 11 times, crossed the breakage region 9 times, and never hybridized distal to the break. This clone appears to be on the proximal side of the contig, but the relative high frequency of crossing events suggested that we had not yet reached the centromeric border of the fragile site. We therefore isolated BAC clone 540_P_5, which is more centromeric to 313_F_8. Clone 540_P_5 hybridized on the proximal side of the break 20 of 20 times, indicating it is beyond the centromeric edge of the fragile site. The distance between 540_P_5 and the edge of our main contig is at this time unknown. However, the STSs that map to 540_P_5 (D16S3083 and D16S515) are estimated by public linkage databases to overlap with markers at the edge of our contig (D16S782, D16S3138, and D16S3125), including those contained in 313_F_8. This finding indicates that these markers are very close together.

Placement of MM Breakpoints

Translocation breakpoints involving 16q23 have been cloned and published for four different MM cell lines (Chesi et al., 1998). To determine whether these breakpoints occurred within FRA16D, we created primer pairs for sequences from the 16q23 portion of the four previously characterized translocations. When these primers were used to screen individual BACs from the contig, all four breakpoints fell within FRA16D. Figures 2 and 4 show the BAC contig for the FRA16D region and the positions of the four multiple myeloma translocation breakpoints within this region. We used our full contig map of this region, as well as estimated distances from STS mapping, to determine roughly the distances between the multiple myeloma breakpoints within our contig. We estimate that the distance from KMS11 to ANBL6 is 500 kb, that from KMS11 to MM.1 is about 300 kb, and that from MM.1 to JJN3 is about 200 kb, and since they are contained on the same BACs, the distance from JJN3 to ANBL6 is approximately 100 kb.

DISCUSSION

The data presented in this study indicate that FRA16D (16q23.2), the second most active common fragile site, covers the largest region yet analyzed. A contig of overlapping BAC clones was isolated from the 16q23.2 region and contains the majority of FRA16D. We have constructed a >1-Mb contig consisting of precisely sized BAC clones representing a sequence-ready group of clones for this chromosomal region. Of the metaphases analyzed, BAC 313_F_8 mapped 11 times proximal and 9 times across the region of aphidicolin-
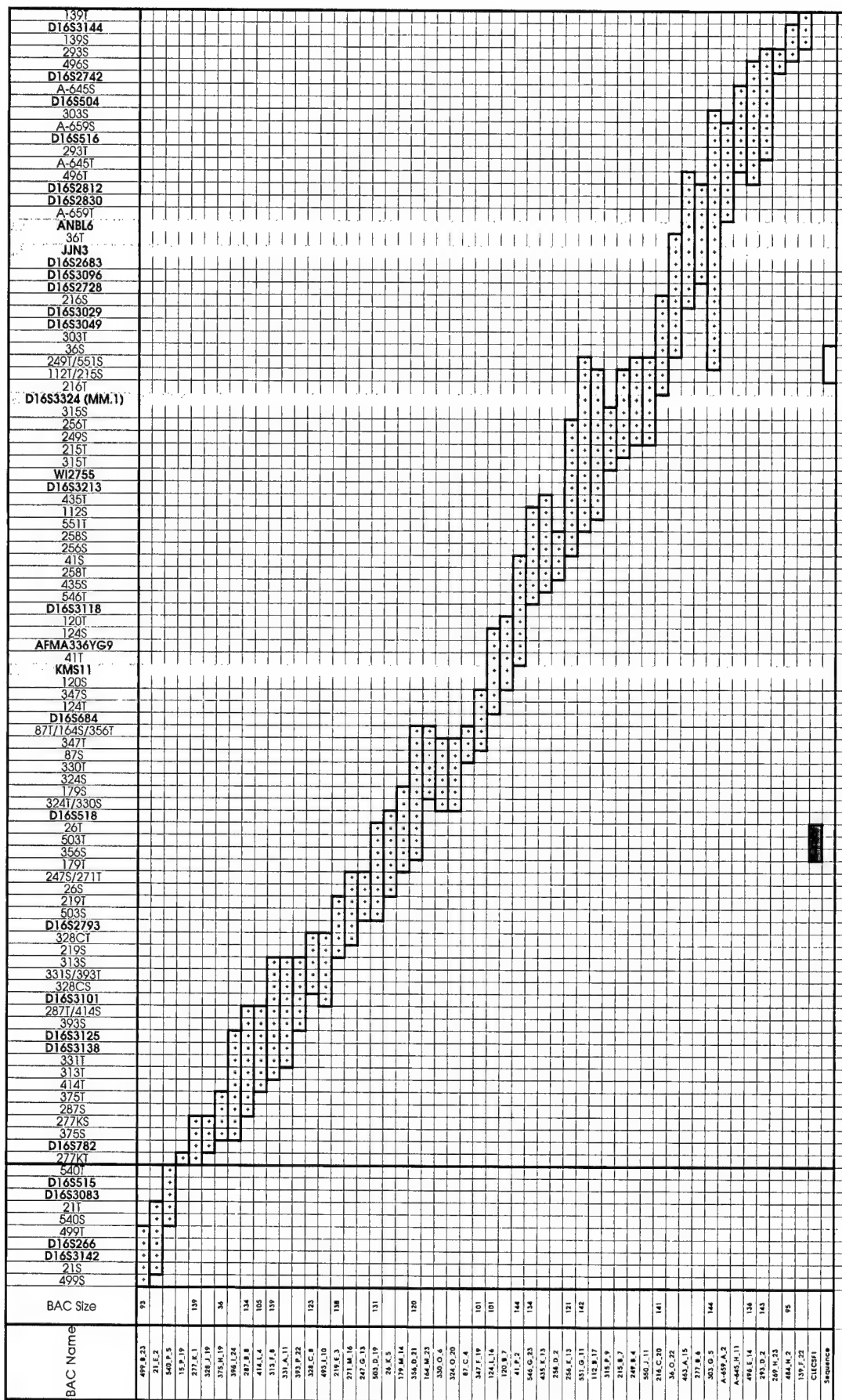
FIG. 2. FRA16D BAC contig. BAC names are indicated along the left side. Marker names are indicated along the top. A plus sign indicates the presence of the marker given along the top axis as determined by PCR in the BAC DNA given along the left axis. Shading indicates a region of sequence recently submitted to GenBank: Accession No. AF179633. The dark vertical line between markers 277KT and 540T represents a gap in the contig of undetermined distance. Gray vertical bars indicate multiple myeloma translocation breakpoints. The dark gray box indicates the approximate position of the C-type lectin gene (CLECSF1).

TABLE 1

New STS Markers Created and Positioned throughout FRA16D

Marker name	Product size	Primer F	Primer R	Marker name	Product size	Primer F	Primer R
26K5S	286	GCTTCAGTGCCACCAACTAC	GCTCCCTTAACCATAAACATCTA	328C8S	417	TTCCAAACGCGCAACA	TTGCTAACATCTGCGGTTCC
26K5T	191	TTTGGCCTATTTGCTCTCAATATCAGTT	TCTCCAAAGCATTCGACCACATT	328C8T	183	GCAGAAACTGAGTCCAGCGTC	AGCTAAGCATCCCGTAGAAA
36O22S	307	TAAATATGATAGCCAAAGGGTTTCAAAT	GCCAAGATGTTCACTCCATTGTC	328J19S	413	TTTTCAGTTGCAGGCACTTA	AAACAGAGCATGGGTCCTAC
36O22T	182	GCTTTGAAGGTGATACCATCTAGG	GTGTTAACTGAGTTTCGATAACGC	328J19T	499	GCATGCAAGCTTACCTCAGTGACCTAT	TTTTAATTTAGAGCACGAGAGTTCTCAATC
41P2S	410	TACAGGGCTCTAGCGGATTCT	TAATGGATGTTGGGCTTAATACCTA	330O6S	565	CTTAACATTTCAAACGGTCACCA	CCAAACCTTGAGCAATAATGCAAT
41P2T	189	CAGTGGATTATGAGTGCCTTCTAGC	GCCTTTCACCTTATAGCATGTACCC	330O6T	370	ATGCAAGCTTTAATGTGT	CTAGTGCAACCCTAAAGTCTATC
87C4S	172	TTTTGAAACCTGGGATAACC	CGCCTGCAATGATGAGTAGA	331A1S	378	AATGAACCCGCAAGTATGTGTGTA	CTGCGTGGCAAGTGAGTTTC
87C4T	191	CACTCTCAAAAGCCATGCAC	GGGATGGGGGAGCAGGTAAA	331A1T	553	AATGAATAGTAAGTTCCCTGGGTC	AAGGCTTCGGCAAACATAAAGTT
112B17S	369	CTCAGAGACATCACAGCCAAAG	AGGCCCTTCTTAGAATTCCAGAAA	347F19S	250	ACCACAGTGTGTAGACCCTTCATATCA	CAGACAATGCTGCCTAATATACACC
112B17T	193	TGCAAGCTTCCCAAATAC	CTGTTTATACCTTAGGCATTCTG	347F19T	395	AAATACGAGCCTCATGCCTGTCTAAGC	TGACAAATAATAGGACATTTTGCAACGC
120B7S	219	GGAGCACTGAAGCAGACACTGATTC	TCCCCTTCTCCTACAGCCATTAC	356D21S	167	CTCCCTGTCATCTTAGCAGTTTGA	TATTATGAGTAACCCAGCTATGCACATT
120B7T	246	CCCTCTGGAAAGTCATTTGACAATA	GCTTTGTGTTGGGTTTTAATCAGT	356D21T	308	CATACTATGACAAAGGGAGCGAGAG	TTCAATAATATACTTTAGGCAAAACTTGT
124L16S	480	TTACATGATGAGAGGCGAGGA	ATTTGTATTTCTTTGGACGTGACCC	375H19S	180	TGCTGGAATTTGGTTTGC	ATTGGTCTTTGGGATTATGCTT
124L16T	349	GATCCTTAGAGTCGACCTGC	CTTCCTGGTTGCACATTCACAACAC	375H19T	290	GGCATGCAAGCTTAAGTATAAATGCTAT	TGGCTTAGGCTCTAGAAATCTGTCTAAAA
179M14S	431	GGTAAGCCATCTGTCTCTGTCTC	ATTTAGTAACCCATTGCCTTCCATTATTT	393P22S	168	GGTACATTTGCTTTGCCATA	GCAGAAGAATGAAACCGATCT
179M14T	329	TCATGTTACGCATCCCAGACTCC	GACCTGTGGCGTTCGAAGACA	393P22T	396	TGAGTTCTTATCTACATGCC	CCTTTTCTCCCTGGACTGTC
216C20S	210	CCATCTTAAGCTCTGTCCAAGGGTTGA	TGGTTCTGATTGAAAGGAAAGAAGGAGG	414L4S	175	GGCCAAATCAAGTCACCTAGTCATA	CAACACCTCCCAAGAAGATGC
216C20T	277	TTCCCAATCACACAGTCAGGAGA	ACAGTCTTGGGTATGTCTTTATCAGCAG	414L4T	326	TTCAATCAAGTGGAAGAAAGGGTAT	ACAATTATGTGTCTCGGGGTAGTTC
219E3S	216	CGAGGCCCTCTGTTTTACATA	CCAGAAAGTTCTCCCCAAAGA	435K13S	227	GGCTTGTAAATCAATGAAGGTTACT	CAAAGCAGCAGCTGTGATGACCCAC
219E3T	268	TGCAGGGCTGCCTCTAATCT	TGCAAAGGGCCTCATATGT	435K13T	480	CATGCAAGCTTTGGGGTCTGTAAAC	TATTGCTGCAGGGGAATAAACCAGT
256K13S	173	GACAGGCTATACGCGGACA	CCTGGCCTAACACTTAAATGAAG	484H2S	150	AAAAGTCACACAGGGTGGCAA	TTTTTAAATCCCCTGGGTTG
256K13T	415	TATGGGGCACAGTGAGGAA	CTGGCTAGAATGTGTAGGAGACG	484H2T	388	TGCAGCCTACATTGGTGATA	GCTCCATAAGCTCGGGTAAA
258D2S	416	AGCTTCCATAGGATACGGAGTCT	GAAAATCCCATTAAGGTCTTAC	496E14S	338	TCCCAAGGAAGGTGTTACGA	TTGGAGTGGGCATGATAATG
258D2T	311	AGAGAGCCAAAGTCTTGATAGA	TGCCAATCTGTGCTGAGCATCC	496E14T	403	GGCCTCTACCCACTAGATGC	AGTGAGCGATAATGCCAATG
277K1S	360	ATCATTCAGAAGGCTAGTTTT	TTCATCACCCCATATACTCAG	503D19S	381	AGGAAGCAAGCAGCACAC	CATTCTCTGGCCTCTTATTCATTC
277K1T	311	CAGGACAACGCATAACTGTAG	TCTTTACCTCCATTTCGCAGAC	503D19T	465	GGCACAGAAAATCCTTGAAATGG	AGTAGTGTGTCTGGCATGAGGTG
277B6S	166	ACCACAGGACAAGGCACA	CCCAGAACACTTAAACTTTGGAG	540P5S	550	GGGCCTTTAATTAAACGAAATA	TTTACCCCTCCCGGCACACCC
277B6T	185	CGGGAGACACATTTATGGAGTCA	ACCTCTACCTATGGCATCTTTGT	540P5T	188	GGATCCTCTAGAGTCGACCT	TGAAGCAATTAAAACACAATGG
287B8S	185	AACTATCAGGCTCAAAGCTCTGGAA	CGCTAAGTTTGTGGCAACTGGTT	546G223S	355	GGAGTCGGGAAGCATAG	TAGGGCTTTTCTGGATAATTG
287B8T	208	TTTAATTGCGTTGGGAGGTGCCTTCT	CGCTACGCCTGGTTGGAGACTGTTTA	546G223T	231	TAGAACATCAGGATTTTTATGCACG	TGGTTGGGCACCTCTAATCTCAACTA
303G5S	287	ACCTTCAGCAAOCGCCAACT	CCCAGACCCACCGCAATAAA	551G11S	170	GAATGTTTGTGTCCCTCTACC	CCAGCCCCCTTGTCCTCTTCT
303G5T	273	GCGTTGCTGCTCCTTCTCTAT	AGCGTGCATACTTGAGTGACAG	551G11T	166	GGGATCCTCTAGAGTCGACCT	CCCATCTTCCTCTGAAAOCT
313F8S	428	TGTCTGAATGAATGAACCCGCAAGT	TAGTGGAGTTGGGAAAGGTGTGGAA	570G9S	413	GGGATCCTCTAAACTGAGAGTAA	GCCATCATCACCACTGCCACC
313F8T	251	GCTTCAGCAAAGGCAACCACTA	AGCCCTATTTAACATTCTCCATCCA	570G9T	492	GGGATCCTCTAGAGTCGACCT	CCTCGCTTGGCCTCTCATTCTC
315P9S	172	AGTGTTGCTCTTCTTTGCTTACCCA	CGTGAGCCACTGTGTATTTCTATTACCA	A645H11S	178	AAAGCATTTCCTTCTTTAGGTTCCCATA	GGTTTGGTGGATCACACAGGGATTCAG
315P9T	158	AGAAACTCTGTGTGCCCATCCATTATGT	CATTTAGAATTGGACTCTTGTTGTGCCTGC	A645H11T	239	AGGCATGCAAGCTTTATAGG	CATGAGGGTGTCTTTTACGC
324O20S	539	AGCTTCAACATTTCAAACG	CTCATGTAACAAATCTGCATAAG	A659A2S	463	CCCAAACCTTCAGCAACC	TACAAAGAAAACGCTTCACAG
324O20T	397	ATGGTTGTTGGTGTTCCCTTTC	CAGAGTTTGCTTAGAGGCCACTT	A659A2T	183	GGAAACGCCATTCTGCAAATCTACA	GGTGATGATTCCCAAAGAAAGGCGAGTT

Note. Names, sizes of PCR products in bp, and primers are listed.

FIG. 3. FRA16D FISH data with selected BAC clones. Twenty human lymphocyte metaphase chromosomal preparations with clear breaks and signals were analyzed for each BAC clone designated on the lower axis. The number of occurrences in each of three categories (1) proximal to the break, (2) distal to the break, or (3) crossing the break, are designated on the left axis. Hybridization events scored as proximal are indicated by the bars with diagonal stripes, the solid black bars indicate distal events, and the solid white bars indicate crossing events.

induced fragility (Fig. 3), but was never found to hybridize distal to the FRA16D region. Though this clone is considered to map centromeric to FRA16D, the fact that almost half of the metaphases had decondensation/breakage within BAC 313_F_8 indicates that the FRA16D region extends proximal to this BAC clone. We therefore identified the BAC 540_P_5 further centromeric to this clone and found that it always hybridized proximal to FRA16D. As previously stated, the markers associated with this clone are thought to exist in the same region as 313_F_8. While this is not precisely accurate, we feel that the distance between these two clones should be relatively small and the proximal edge of the fragile site lies in between these two clones. Nevertheless, of the four CFSs that have now been characterized (FRA3B, FRA7G, FRA7H, and FRA16D), FRA16D represents the most expansive region of chromosomal fragility identified. FRA7G and FRA3B may cover areas as large as FRA16D, but until more analysis is completed, FRA16D appears to be the largest common fragile site.

Aside from FRA16D covering a large region, and being expressed frequently, this CFS is of particular interest as it resides within a cytogenetic band suspected to harbor a tumor suppressor gene involved in breast, prostate, hepatocellular, and ovarian cancers. Polymorphic markers from the 16q23.2 region have been shown to be frequently lost in all four cancers. A comparison of the markers with the highest LOH in these tumors to the BAC contig containing FRA16D indicates that three of these markers (D16S504, D16S516, and D16S518) map within the FRA16D region. As these markers are in one of the regions of greatest instability in these cancers, the correlation of the molecular position of this fragile site and this region of instability provides further evidence for a causal relationship between chromosomal fragility and cancer.

FIG. 4. FRA16D minimal tiling BAC contig and Whitehead YAC mapping with multiple myeloma translocation breakpoints denoted. Plus signs indicate PCR detection of the marker along the top axis for that DNA sample. BAC names are indicated along the left side. Vertical shading indicates multiple myeloma translocation breakpoints. The order of the STS markers in our contig corresponded exactly with The Whitehead Database YAC STS mapping information as indicated.

Chromosomal band 16q23.2 not only contains markers that are frequently lost during tumor development, but is also the location of a frequent translocation observed in multiple myeloma patients. Approximately 25% of multiple myelomas have been shown to contain a balanced reciprocal translocation between 14q32 and 16q23.2. This rearrangement juxtaposes the IgH switch region and its very powerful enhancer element to sequences and possibly genes in the 16q23.2 region. To determine whether the chromosome 16 breakpoints were contained within the FRA16D region, sequence data for four breakpoints that had been previously cloned and characterized by Chesi *et al.* (1998) were utilized to screen the FRA16D BAC contig. Sequence data for these breakpoints indicated that all four translocations map within the FRA16D fragile site. Thus, not only is the instability within FRA16D potentially involved in the chromosomal loss seen in solid tumors, but also in the generation of balanced reciprocal translocations important in the development or genesis of multiple myeloma.

There are also data to suggest that at least one gene, located downstream of the most telomeric of the four chromosome 16 breakpoints characterized, is upregulated in cell lines containing the t(14q;16q) translocation (Chesi *et al.,* 1998). The proto-oncogene c-maf, which is <500 kb from our most telomeric BAC, has been shown to be upregulated in the multiple myeloma cell lines from which the breakpoints have been cloned. Therefore, any genes that reside within the fragile site, between the multiple myeloma breakpoints and c-maf, are not only potential targets for upregulation in multiple myelomas, but may also prove oncogenic for other cancers.

The relationship between chromosomal fragile sites and cancer remains enigmatic. The correlation of FRA16D with markers that show frequent loss in breast, prostate, hepatocellular, and ovarian cancers and with the four translocation breakpoints identified in multiple myeloma further suggests that CFSs do potentially play a role in cancer and cancer development. However, there are many questions that remain unanswered. What is the mechanism of instability within FRA16D and the other CFSs that have already been characterized? What are the functions of CFSs within the normal cell and how does the instability within these regions play a role in cancer development? The progressive sequencing of the human genome will greatly increase information about the DNA sequences within and surrounding each of the CFSs and provide insights into these important questions. Future study of the FRA16D region may lead to the identification of genes that are critical targets in the initiation and progression of breast, ovarian, prostate, and hepatocellular carcinomas.

ACKNOWLEDGMENTS

Note added in proof. We would also like to mention that while this publication was in review, two other papers were published on the cloning and characterization of FRA16D (Paige *et al.,* 2000; Mangelsdorf *et al.,* 2000).

REFERENCES

Chen, T., Sahin, A., and Aldaz, C. M. (1996). Deletion map of chromosome 16q in ductal carcinoma in situ of the breast: Refining a putative tumor suppressor gene region. *Cancer Res.* **56:** 5605–5609.

Chesi, M., *et al.* (1998). Frequent dysregulation of the c-maf proto-oncogene at 16q23 by translocation to an Ig locus in multiple myeloma. *Blood* **91**(12): 4457–4463.

Cooke, I. E., *et al.* (1996). Allele loss on chromosome arm 6q and fine mapping of the region at 6q27 in epithelial ovarian cancer. *Genes Chromosomes Cancer* **15**(4): 223–233.

Coquelle, A., *et al.* (1997). Expression of fragile sites triggers intrachromosomal mammalian gene amplification and sets boundaries to early amplicons. *Cell* **89**(2): 215–225.

Dorion-Bonnet, F., Mautalen, S., Hostein, I., and Longy, M. (1995). Allelic imbalance study of 16q in human primary breast carcinomas using microsatellite markers. *Genes Chromosomes Cancer* **14:** 171–181.

Driouch, K., *et al.* (1997). Loss of heterozygosity on chromosome arm 16q in breast cancer metastases. *Genes Chromosomes Cancer* **19:** 185–191.

Elo, J. P., *et al.* (1997). Loss of heterozygosity at 16q24.1–q24.2 is significantly associated with metastatic and aggressive behavior of prostate cancer. *Cancer Res.* **57:** 3356–3359.

GDB (Human Genome Database) (1990–2000). The Hospital for Sick Children, Johns Hopkins University, Baltimore, MD. Available from the Internet at URL http://www.gdb.org/. [Online database, updated daily]

Glover, T. W., Berger, C., Coyle, J., and Echo, B. (1984). DNA polymerase alpha inhibition by aphidicolin induces gaps and braks at common fragile sites in human chromosomes. *Hum. Genet.* **67:** 136–142.

Glover, T. W., and Stein, C. K. (1987). Induction of sister chromatid exchanges at common fragile sites. *Am. J. Hum. Genet.* **41**(5): 882–890.

Glover, T. W., and Stein, C. K. (1988). Chromosome breakage and recombination at fragile sites. *Am. J. Hum. Genet.* **43**(3): 265–273.

Hallek, M., Leif Bergsagel, P., and Anderson, K. C. (1998). Multiple myeloma: Increasing evidence for a multistep transformation process. *Blood* **91**(1): 3–21.

Hewett, D. R., *et al.* (1998). FRA10B structure reveals common elements in repeat expansion and chromosomal fragile site genesis. *Mol. Cell* **1:** 773–781.

Huang, H., *et al.* (1998a). FRA7G extends over a broad region: Coincidence of human endogenous retroviral sequences (HERV-H) and small polydispersed circular DNAs (spcDNA) and fragile sites. *Oncogene* **16**(18): 2311–2319.

Huang, H., Qian, C., Jenkins, R. B., and Smith, D. I. (1998b). Fish mapping of YAC clones at human chromosomal band 7q31.2: Identification of YACs spanning FRA7G within the common region of LOH in breast and prostate cancer. *Genes Chromosomes Cancer* **21:** 152–159.

Hubert, R. S., *et al.* (1997). BAC and PAC contigs covering 3.5 Mb of the Down syndrome congenital heart. *Genomics* **41**(2): 218–226.

Jones, C., *et al.* (1995). Association of a chromosome deletion syndrome with a fragile site within the proto-oncogene CBL2. *Nature* **376:** 145–149.

Knight, S. J. L., *et al.* (1993). Trinucleotide repeat amplificaiton and hypermethylation of a CpG island in FRAXE metal retardation. *Cell* **74:** 127–134.

Kremer, E., *et al.* (1991). Mapping of DNA instabillity at the Fragile X to a trinucleotide repeat sequence p(CCG)n. *Science* **252:** 1711–1714.

Latil, A., *et al.* (1997). Loss of heterozygosity at chromosome 16q in prostate adenocarcinoma: Identification of three independent regions. *Cancer Res.* **57**(6): 1058–1062.

Lida, A., *et al.* (1997). Localization of a breast cancer tumor-suppressor gene to a 3-cM interval within chromosomal region 16q22. *Br. J. Cancer* **75**(2): 264–267.

Lisitsyn, N. A., *et al.* (1995). Comparative genomic analysis of tumors: Detection of DNA losses and amplification. *Proc. Natl. Acad. Sci. USA* **92**(1): 151–155.

Mangelsdorf, M., *et al.* (2000). Chromosomal fragile site FRA16D and DNA instability in cancer. *Cancer Res.* **60**(6): 1683–1689.

Mishmar, D., *et al.* (1998). Molecular characterization of a common fragile site (FRA7H) on human chromosome 7 by the cloning of a simian virus 40 integration site. *Proc. Natl. Acad. Sci. USA* **95**(14): 8141–8146.

Nancarrow, J. K., *et al.* (1994). Implications of FRA16A structure for the mechanism of chromosomal fragile site genesis. *Science* **264:** 1938–1941.

Oberle, I., *et al.* (1991). Instability of a 550bp DNA segment and abnormal methylation in fragile X syndrome. *Science* **252:** 1097–1102.

Paige, A. J., *et al.* (2000). A 700-kb physical map of a region of 16q23.2 homozygously deleted in multiple cancers and spanning the common fragile site FRA16D. *Cancer Res.* **60**(6): 1690–1697.

Parrish, J. E., *et al.* (1994). Isolation of a GCC repeat showing expansion in FRAXF, a fragile site distal to FRAXA and FRAXE. *Nat. Genet.* **8:** 229–235.

Piao, Z., Park, C., Kim, J. J., and Kim, H. (1999). Deletion mapping of chromosome 16q in hepatocellular carcinoma. *Br. J. Cancer* **80**(5–6): 850–854.

Popescu, N. C., Zimonjic, D., and DiPaolo, J. A. (1990). Viral integration, fragile sites, and proto-oncogenes in human neoplasia. *Hum. Genet.* **84**(5): 383–386.

Radford, D. M., *et al.* (1995). Allelotyping of ductal carcinoma in situ of the breast: Deletion of loci on 8p, 13q, 16q, 17p, and 17q. *Cancer Res.* **55:** 3399–3405.

Rassool, F. V., *et al.* (1991). Preferential integration of marker DNA into the chromosomal fragile site at 3p14: An approach to cloning fragile sites. *Proc. Natl. Acad. Sci. USA* **88**(15): 6657–6661.

Saito, S., *et al.* (1992). Fine-scale deletion mapping of the distal long arm of chromosome 6 in 70 human ovarian cancers. *Cancer Res.* **52**(20): 5815–5817.

Sutherland, G. R. (1979). Heritable fragile sites on human chromosomes I. Factors affecting expression in lymphocyte culture. *Am. J. Hum. Genet.* **31**(2): 125–135.

Sutherland, G. R., Baker, E., and Richards, R. I. (1998). Fragile sites still breaking. *Trends Genet.* **14**(12): 501–506.

Sutherland, G. R., Parslow, M. I., and Baker, E. (1985). New classes of common fragile sites induced by 5-azacytidine and bromodeoxyuridine. *Hum. Genet.* **69**(3): 233–237.

Tsuda, H., *et al.* (1990). Allele loss on chromosome 16 associated with progression of human hepatocellular carcinoma. *Proc. Natl. Acad. Sci. USA* **87**(17): 6791–6794.

Verkerk, A. J. M. H., *et al.* (1991). Identification of a gene (FMR-1) containing a CGG repeat coincident with a breakpoint cluster region exhibiting length variation in fragile X syndrome. *Cell* **65:** 905–914.

Verma, R. S., and Babu, A. (1989). "Human Chromosomes: Manual of Basic Techniques." p. 240, Pergamon, New York.

Wang, N. D., Testa, J. R., and Smith, D. I. (1993). Determination of the specificity of aphidicolin-induced breakage of the human 3p14.2 fragile site. *Genomics* **17**(2): 341–347.

Whitehead Institute for Biomedical Research/MIT Center for Genome Research (2000). Cambridge, MA. Available from the Internet at URL http://www-genome.wi.mit.edu/. [Online database, updated daily]

Yu, S., *et al.* (1991). The fragile X genotype is characterised by an unstable region of DNA. *Science* **252:** 1179–1182.

Yu, S., *et al.* (1997). Human chromosomal fragile site FRA16B is an amplified AT-rich minisatellite repeat. *Cell* **88**(3): 367–374.

Yunis, J. J., and Soreng, A. L. (1984). Constitutive fragile sites and cancer. *Science* **226**(4679): 1199–1204.

A Molecular Cytogenetic Analysis of 7q31 in Prostate Cancer[1]

Robert B. Jenkins,[2] Junqi Qian, Hyun K. Lee, Haojie Huang, Kiyoshi Hirasawa, David G. Bostwick, John Proffitt, Kim Wilber, Michael M. Lieber, Wanguo Liu, and David I. Smith

Departments of Laboratory Medicine and Pathology [R. B. J., J. Q., H. K. L., H. H., D. G. B., W. L., D. I. S.], and Urology [K. H., M. M. L.], Mayo Clinic, Rochester, Minnesota 55905, and Vysis Inc., Downers Grove, Illinois 60515 [J. P., K. W.]

ABSTRACT

Gains of chromosome 7 and alterations of the 7q-arm have been frequently observed in multiple cancers using various cytogenetic and molecular genetic techniques. Using PCR analysis of microsatellite markers, we have previously reported that allelic imbalance of 7q31 is common in prostate cancer and is associated with higher tumor grade and advanced pathological stage. In an effort to better understand the chromosome 7 alterations in prostate cancer, we undertook a molecular cytogenetic study of 25 prostate specimens using fluorescence *in situ* hybridization (FISH) with DNA probes for the chromosome 7 centromere and for 5 loci mapped to 7q31 (D7S523, D7S486, D7S522, D7S480, and D7S490) and 1 locus at 7q11.23 (ELN). Six tumors had no apparent anomaly for any chromosome 7 probe. Nine tumors showed apparent simple gain of a whole chromosome 7, whereas one tumor had apparent simple loss of a whole chromosome 7. Four tumors had gain of the chromosome 7 centromere and additional overrepresentation of the 7q-arm. One tumor had overrepresentation of 7q31 without any apparent anomaly of the chromosome 7 centromere, and one tumor had apparent loss of the chromosome 7 centromere with no apparent anomaly of the 7q-arm. Three tumors had gain of the chromosome 7 centromere and loss of the 7q31 region. Gain of 7q31 was strongly correlated with tumor Gleason score. Multiplex PCR studies of these specimens supported these FISH observations. Mutation screening and DNA sequencing of the MET gene, which is mapped to 7q31, revealed only the presence of simple sequence polymorphisms but no apparent acquired disease-associated mutations. FISH analysis of metaphases from an aphidicolin-induced, chromosome 7 only, somatic cell hybrid demonstrated that the DNA probe for D7S522 spans the common fragile site FRA7G at 7q31. Our data indicate that the 7q-arm, particularly the 7q31 region, is genetically unstable in prostate cancer, and some of the gene dosage differences observed may be due to fragility at FRA7G.

INTRODUCTION

FISH[3] studies have demonstrated that aneusomy of chromosome 7 is frequent in prostate cancer and is associated with higher tumor grade, advanced pathological stage, and early patient death from prostate cancer (1–5). Cytogenetic analyses have demonstrated that gain, deletion, and translocation of 7q22-q31 are common in prostate adenocarcinoma (6, 7). In addition, several independent studies have indicated that genes important for tumorigenesis are mapped to 7q31 (8–10). Using PCR analysis of microsatellite markers, we and others have identified frequent imbalance of alleles mapped to 7q31 in prostate and other cancers (9–14). In prostate cancer, this allelic imbalance is strongly correlated with tumor aggressiveness, progres-

sion, and cancer-specific death (12–14). These findings suggest that genetic alterations of the 7q-arm play an important role in the development of prostate cancer (11–14). However, the allelic imbalance detected by PCR has been assumed to be a result of chromosomal loss or deletion (11, 12), whereas FISH studies have uniformly observed gain of the chromosome 7 centromere (2, 3–5). Resolving this discrepancy is critically important for the definition of the 7q31 anomalies in prostate cancer.

FISH analysis of interphase cells with region-specific and centromere-specific probes is useful for the detection of gene copy number alterations and numerical chromosomal anomalies in solid tumors such as prostatic carcinoma that are often difficult to analyze by conventional cytogenetic analysis (2, 15, 16). FISH can easily distinguish chromosomal centromere gain and loss. With appropriate probes, the dosage of specific chromosomal regions can also be determined. Moreover, when FISH is applied to histological sections, tumor cells can be precisely evaluated. The effects of normal cell infiltration are reduced, and the genetic heterogeneity of tumor foci can be assessed (2, 15, 16). Furthermore, normal ranges of FISH signals can be determined by studying regions of apparently normal prostate. However, interphase FISH studies of gene dosage in paraffin-embedded materials require relatively large probes that target one locus or, at most, a few loci at a time (17).

PCR analysis of microsatellite markers has been very useful for the detection of allelic imbalance, especially for the mapping of imbalance of specific chromosomal regions in many tumors. In addition, by their very nature, individual PCR studies evaluate a much smaller region than the typical FISH studies. However, PCR analyses are limited by the difficulty of characterizing allelic imbalance as loss or gain (11–14). Applying both PCR and FISH to the same specimens can be extremely useful to clarify discrepancies observed by either FISH or PCR alone.

Chromosome band 7q31 also contains the common fragile site, FRA7G (18). Recently, we identified several overlapping YAC clones spanning FRA7G within the common allelic imbalance region that includes the D7S522 locus (19). To determine the precise molecular relationship of FRA7G with the 7q31 alterations we observed, we analyzed metaphases from an aphidicolin-induced, chromosome 7 only, somatic hybrid using a FISH probe for D7S522.

MATERIALS AND METHODS

Patient Selection and Histopathological Evaluation

Twenty-five cases were selected from the surgical pathology files at the Mayo Clinic from patients who had undergone radical retropubic prostatectomy and bilateral pelvic lymphadenectomy between 1991 and 1994. All patients had clinically localized prostate cancer, and none had received preoperative hormone or radiation therapy. Fresh tissue blocks of primary prostate cancer and paired benign tissue from all 25 patients were harvested, frozen, and microdissected for DNA extraction as described previously (13). Prostate specimens adjacent to those that had been frozen were also formalin-fixed and paraffin-embedded for routine surgical pathology. Ten serial 5-μm sections and three serial 50-μm sections were prepared from a representative tissue block for FISH analysis and flow cytometric DNA ploidy analysis (5), respectively. Gleason score was determined for each focus of cancer (2), and

pathological stage for each case was assigned using the TNM system (1992 revision). The Gleason scores of carcinoma foci were 4–6 (6 foci), 7 (7 foci), and 8–10 (12 foci). Pathological tumor stages were $T_2N_0M_0$ (10 cases), $T_3N_0M_0$ (11 cases), and $T_3N_1M_0$ (4 cases).

FISH with Chromosome Enumeration Probe and Region-specific Probes

Our method for FISH analysis of paraffin-embedded prostate tissues has been described previously (16). Briefly, tissue sections were deparaffinized, dehydrated, treated with microwave in citrate buffer (pH 6.0) for 10 min, digested in pepsin solution [4 mg/ml in 0.9% NaCl (pH 1.5)] for 15 min at 37°C, rinsed in 2× SSC at room temperature for 5 min, and air dried. Because previous work showed a high frequency of genetic changes on 7q31, directly labeled fluorescent DNA LSPs for five 7q31 loci (*D7S523, D7S486, D7S522, D7S480*, and *D7S490*) and one 7q11.23 locus (*ELN*) were chosen for study. Each of the LSPs was composed of a contig of clones ≤225 kb in length. Dual-probe hybridization was performed on the serial 5-μm sections using a SpectrumGreen-labeled chromosome 7 centromere (CEP7) probe together with a SpectrumOrange-labeled LSP. Probes and target DNA were denatured simultaneously in an 80°C oven for 5 min, and each slide was incubated at 37°C overnight. Posthybridization washes were performed in 1.5 M urea/0.1× SSC at 45°C for 30 min and in 2× SSC at room temperature for 2 min. Nuclei were counterstained with DAPI and antifade compound p-phenylenediamine.

The number of FISH signals was counted with a Zeiss Axioplan microscope equipped with a triple-pass filter (DAPI/Green/Orange; Vysis, Downers Grove, IL). For each probe, 300 nonoverlapping interphase nuclei from foci of benign epithelium and prostatic carcinoma were enumerated. Nuclei from stromal elements were not counted. The number of signals for the CEP7 and the LSP were counted for each nucleus and tabulated for each probe pair for each normal and tumor focus.

We have previously reported our method for the interpretation of FISH data from paraffin-embedded materials (16). In the present study, we simplified our data interpretation method (see below) and criteria for FISH anomalies (see

"Results"). Typical hybridization images and tabulated data for a representative tumor focus from case 38 for the *D7S522*/CEP7 and the *D7S523*/CEP7 probe pairs are illustrated in Fig. 1 and Table 1. The rows in the tables demonstrate the percentage of nuclei with different numbers of CEP7 signals. The nuclei with 0–1 and ≥3 CEP7 signals defined those cells with apparent loss (−CEP7) and gain of CEP7 (+CEP7), respectively. The columns in the tables demonstrate the percentage of nuclei with different numbers of LSP signals. The nuclei with 0–1 and ≥3 LSP signals defined those cells with apparent loss (−LSP) and gain of the LSP (+LSP), respectively. Finally, a mean LSP:CEP7 signal ratio was calculated for each LSP for each focus. These variables (−CEP7, +CEP7, −LSP, −LSP, and the mean LSP:CEP ratio) can be used to determine if the chromosomal centromere and/or chromosomal regions are gained or lost. Importantly, normal ranges for each of these variables can be established by evaluating apparently normal prostate epithelium (see "Results").

Evaluation of Allelic Imbalance by Multiplex PCR

We used multiplex PCR analysis of microsatellite alleles for marker *D7S522* to independently evaluate allelic imbalance of this locus. DNA extraction from microdissected frozen tissue of these 25 specimens was performed as reported previously (13). The extracted DNA was subjected to multiplex PCR using *D7S522* and a control marker of *D14S615* (chromosome 14 is rarely altered in prostate cancer). The PCR conditions were the same as those described previously (13), except 28 cycles were used instead of 35 cycles. The PCR products were analyzed on 6% polyacrylamide gels. The intensities of the bands were quantified using densitometry and the image analysis software program NIH Image (Ver0.1.47). Quantitation of the band intensities was performed by the area integration method (with subtraction of local background).

To evaluate gene deletions or overrepresentation in tumor samples, we normalized the amount of tumor DNA loaded in gel with the following index: $I = (A1n + A2n)/(A1t + A2t)$, in which A1n and A2n represent the intensity of upper and lower alleles at *D14S615* for the normal sample, and A1t and A2t
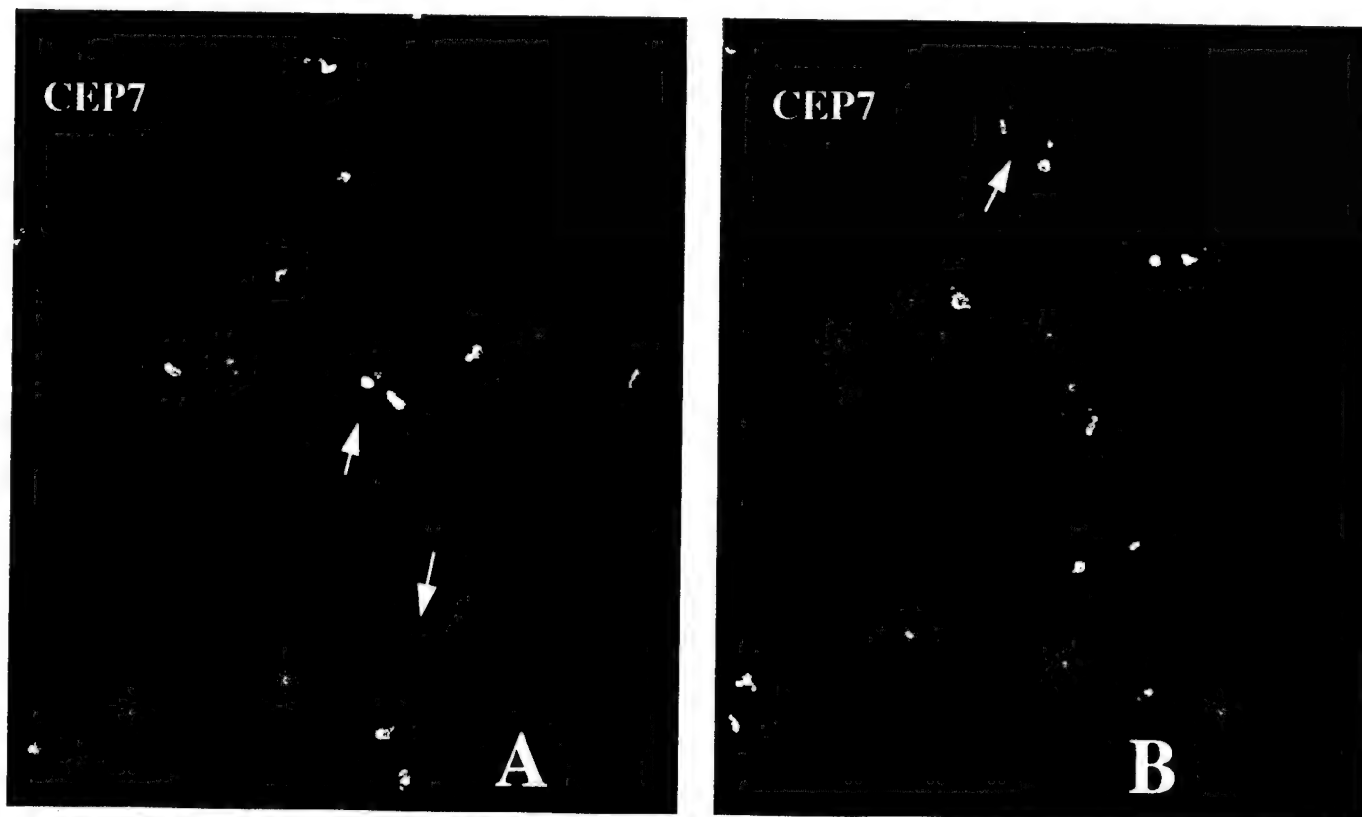

Fig. 1. Results of dual-probe FISHs using a centromere probe for chromosome 7 (CEP7, *green signals*) and a LSP (*orange signals*) for a stage $T_3N_1M_1$ prostate cancer (case 38). Nuclei are counterstained with DAPI. *A*, two nuclei with three green signals for CEP7 and one orange signal for the *D7S522* locus are illustrated (*yellow arrows*). *B*, a nucleus with two green signals for CEP7 and two orange signals for the *D7S523* locus is illustrated (*yellow arrow*). Another nucleus demonstrates three green signals for CEP7 and three orange signals for the *D7S523* locus (*green arrow*).

Table 1 *Distribution of D7S522, D7S523, and CEP7 copy numbers in a prostate cancer focus from case 38*

A. CEP7 copy no.	D7S522 copy no.[a]						
	0	1	2	3	4	≥5	Total (%)
0	0.0	1.3	0.0	0.0	0.0	0.0	1.3
1	4.6	13.1	0.7	0.0	0.0	0.0	18.4
2	1.3	53.4	11.8	0.0	0.0	0.0	66.5
3	0.7	3.2	4.6	0.7	0.0	0.0	9.2
4	0.0	0.7	3.3	0.6	0.0	0.0	4.6
≥5	0.0	0.0	0.0	0.0	0.0	0.0	0.0
Total (%)	6.6	71.7	20.4	1.3	0.0	0.0	100.0

B. CEP7 copy no.	D7S523 copy no.[b]						
	0	1	2	3	4	≥5	Total (%)
0	0.3	0.0	0.0	0.0	0.0	0.0	0.3
1	0.0	14.9	4.3	0.0	0.0	0.0	20.5
2	0.0	6.0	51.3	4.3	0.0	0.0	61.6
3	0.0	0.6	1.7	13.9	0.3	0.0	16.6
4	0.0	0.0	0.0	0.0	1.0	0.0	1.0
≥5	0.0	0.0	0.0	0.0	0.0	0.0	0.0
Total (%)	0.3	21.5	57.3	19.5	1.3	0.0	100.0

[a] Mean D7S522:CEP7 ratio = 0.59. Average D7S522 signals/nucleus = 1.15. Average CEP7 signals/nucleus = 1.96. +CEP7 = 13.8%, −CEP7 = 19.7%. +D7S522 = 1.3%, −D7S522 = 78.3%.

[b] Mean D7S523:CEP7 ratio = 1.01. Average D7S523 signals/nucleus = 2.00. Average CEP7 signals/nucleus = 1.97. +CEP7 = 17.6%, −CEP7 = 20.8%. +D7S523 = 20.8%, −D7S523 = 21.8%.

represent the intensity of upper and lower alleles at *D14S615* for the tumor sample. The corrected intensity of upper and lower alleles for the tumor sample at the *D7S522* locus was calculated by multiplying the original intensity by the index. The corrected intensity of tumor sample was compared with paired normal sample. Based on an analysis of the intensity ratio distribution for all informative microsatellite analyses of 84 cases (data not shown), we selected conservative cutoffs to define allelic loss or gain. If the intensity ratio of tumor sample:normal sample was 1.30 or more, an allele was defined as being gained. If the ratio was 0.75 or less, the allele was defined as being lost.

FISH Mapping of Chromosome Breakage at *FRA7G*

The method of cell line and metaphase slide preparation has been described elsewhere (19). Briefly, a human-hamster hybrid cell line (1HL11-G) that contains a single chromosome 7 as its only human genetic component was cultured in MEM-α containing 10% FCS, 4 mM glutamine, 100 units/ml penicillin/streptomycin, and 3×10^{-5} mM mitomycin C. Aphidicolin dissolved in 70% ethanol at a final concentration of 0.4 μM was used to induce the expression of fragile sites. The aphidicolin-treated cultures were harvested for cytogenetic analysis, and the resultant metaphases were examined for chromosome 7 fragility and subjected to FISH analysis.

The identical *D7S522* FISH probe (Vysis) used in interphase FISH was applied to the metaphase preparations. Before hybridization, the DNA probe and slides were denatured separately. Hybridizations were performed at 37°C. After washing and counterstaining, the slides were examined with a Zeiss Axioplan microscope, and the number of metaphases with the *D7S522* probe hybridizing proximal to, spanning, and hybridizing distal to the fragile site was enumerated.

Mutation Analysis of the *MET* Gene

We evaluated portions of the *MET* proto-oncogene for mutations in all 25 tumor samples. Exons 5–7, containing the cysteine-rich region, and exons 15–21, containing the tyrosine kinase domain, were studied. Heteroduplex analysis by ion-paired, reversed-phase DHPLC (DNASep column, alkylated polystyrene-divinylbenzene packing; Sarasep Inc., San Jose, CA) was used for mutation screening as reported previously (20). Heteroduplex analysis by DHPLC is a new mutation screening method with high throughput specificity and sensitivity (21). A pilot study demonstrated that heteroduplex analysis by

DHPLC missed 1 of 100 known polymorphisms or mutations in 8 different genes.[4]

All cases with possible sequence alterations detected by heteroduplex analysis by DHPLC were subjected to mutation analysis using the Thermo Sequenase kit (Amersham Life Science, Inc., Cleveland, OH). Nucleotides were numbered according to the scheme in GenBank. Intronic sequences surrounding the known exons of the *MET* proto-oncogene were determined and kindly provided by Dr. Laura S. Schmidt (National Cancer Institute-Frederick Cancer Research & Development Center, Frederick, MD).

Statistical Analysis

The software program Statview version 4.0 was used for statistical analysis. The relationships of FISH anomalies with Gleason score and pathological stage were evaluated by the Pearson χ^2 test. The significance level was 0.05.

RESULTS

Anomalies of 7q Locus Copy Number in Prostate Cancer Detected by FISH

Normal Value Study. To accurately ascertain the copy number alterations of the chromosome 7 centromere and chromosome 7q-arm regions in prostate cancer, we undertook a detailed normal value study. This normal value study was necessary, because the FISH analysis was performed using 5-μm sections from paraffin-embedded prostate specimens. Nuclear truncation and nuclear overlap can cause false signal loss and false signal gain in such specimens. For the normal value study, each of the LSP/CEP7 dual probe pairs was hybridized to 10 apparently benign prostate regions. Only normal epithelial cells were enumerated. For each normal region, the FISH data were tabulated, and the FISH variables were calculated as described in "Materials and Methods." Table 2 summarizes the mean ± 3 SD for each of the FISH variables for the 10 normal prostate regions we evaluated. In benign epithelia, the mean LSP:CEP7 ratio for the six LSPs ranged from 0.97–1.01. The mean percentage of epithelial nuclei with −CEP7 and +CEP7 ranged from 19.4–22.2 and 1.6–3.7%, respectively. The mean percentage of epithelial nuclei with −LSP and +LSP ranged from 20.2–24.6 and 0.9–3.2%, respectively.

Criteria for FISH Anomalies. Based on the normal value study and an inspection of the distribution of FISH signals among the carcinoma foci, we developed the following conservative criteria for LSP copy number anomalies: (*a*) simple gain of both the chromosome 7q-arm and the centromere, without any relative increase of LSP copy number, required an overall mean LSP:CEP7 signal ratio of 0.90–1.10 and ≥10% epithelial nuclei with ≥3 signals for each LSP and for CEP7. The percentage of cells with ≥3 signals must also be similar for each probe; (*b*) low additional increases of LSP copy number relative to centromere copy number (LAI) required a mean LSP:CEP7 signal ratio of >1.10 and <1.35 and ≥10% epithelial nuclei with ≥3 signals for each LSP. Most of these cases also had ≥10% epithelial nuclei with ≥3 signals for CEP7. LAI identifies cancer foci whose nuclei might have relative LSP duplication; (*c*) high additional increases of LSP copy number relative to centromere copy number (HAI) required a mean LSP:CEP7 ratio of ≥1.35 and ≥10% epithelial nuclei with ≥3 signals for each LSP. All of these cases also had ≥10% epithelial nuclei with ≥3 signals for CEP7. HAI identifies cancer foci whose nuclei might have relative LSP triplication or overt LSP amplification (*e.g.*, relative LSP quadruplication or greater); (*d*) simple loss of both the chromosome 7q-arm and the centromere without any relative increase of LSP copy number required an overall mean LSP:CEP7 signal ratio of 0.90–1.10 and ≥55% of epithelial

Table 2 *Summary of the mean values ± 3 SD for analyzed FISH variables in 10 regions of apparently benign prostate[a]*

Probe	LSP:CEP7 ratio	+CEP7[b]	−CEP7[b]	+LSP[b]	−LSP[b]
ELN	0.97 ± 0.04	3.7 ± 5.8	22.0 ± 13.5	2.8 ± 4.9	21.2 ± 11.8
D7S523	1.01 ± 0.03	2.7 ± 5.0	19.4 ± 11.7	3.2 ± 5.7	22.4 ± 13.5
D7S486	1.00 ± 0.01	2.6 ± 5.3	20.0 ± 12.5	3.0 ± 5.9	20.4 ± 12.5
D7S522	0.98 ± 0.05	1.6 ± 2.5	21.8 ± 24.2	0.9 ± 2.5	24.6 ± 22.0
D7S480	0.99 ± 0.04	3.3 ± 5.3	19.9 ± 22.4	2.9 ± 4.5	20.2 ± 17.6
D7S490	1.00 ± 0.03	3.1 ± 5.1	22.2 ± 23.7	3.0 ± 5.0	21.8 ± 16.0

[a] See Fig. 1 and the text for definition of variables.
[b] +CEP7, −CEP7, +LSP, −LSP, percentage of cells with gain (≥3) or loss (0–1) of CEP7 or LSP signals.

nuclei with 0–1 signals for each LSP and for CEP7. The percentage of cells with 0–1 signals must also be similar for each probe. Keep in mind that this percentage is high because of nuclear truncation; (*e*) relative loss of LSP copy number (RL) required a mean LSP:CEP7 signal ratio ≤ 0.90. RL defined cancer foci whose nuclei might have actual deletion of the LSP or decreased LSP copy number relative to CEP7 copy number; and (*f*) high level proliferation (HLP) was suspected when a focus had a mean LSP:CEP7 ratio of >1.1, and the percentage of nuclei in the S phase/G_2-M phase determined by flow cytometry was similar to the percentage of nuclei with relative LSP duplication.

The category of HLP was added because chromatid separation may occur in cells in the S phase and G_2-M phase of the cell cycle. HLP would result in a falsely elevated LSP:CEP7 ratio in the absence of the LSP overrepresentation. One cancer focus (case 33) clearly had evidence of high proliferative activity. This tumor had 38% of cells in the S phase/G_2-M phase and 37% of nuclei with relative LSP duplication.

Summary of FISH Anomalies in 25 Stage $T_{2-3}N_{0-1}M_0$ Prostate Cancer Specimens. Table 1 and Fig. 1 illustrate typical FISH images and enumeration data derived from case 38. Fig. 1A and Table 1 show the FISH results for the D7S522/CEP7 probe pair for a cancer focus of case 38. For this cancer focus, 13.8 and 19.7% of nuclei had +CEP7 and −CEP7, respectively. The percentage of nuclei with +D7S522 and −D7S522 was 1.3 and 78.3%, respectively. The mean D7S522:CEP7 signal ratio was 0.59. On the basis of our abnormal criteria, we defined this focus as having +CEP7 and −D7S522. Fig. 1B and Table 1 show the FISH results for the D7S523/CEP7 probe pair for the same cancer focus of case 38. Unlike the results for the D7S522/CEP7 probe pair, this cancer focus had a similar level of +CEP7 (17.6%) and +D7S523 (20.8%), a similar level of −CEP7

(20.8%) and −D7S523 (21.8%), and a mean D7S523:CEP7 signal ratio of 1.01. On the basis of our abnormal criteria, we defined this focus as having +CEP7 and +D7S523. The remaining four probe pairs were hybridized to the same cancer focus, and the data were analyzed as described above. The FISH data for D7S486 were similar to D7S522, and the FISH data for ELN, D7S480, and D7S490 were similar to D7S523 (data not shown). Based on our criteria, we defined this focus as having an apparent gain of most of the chromosome 7q-arm (including the centromere) together with loss of the region containing D7S486 and D7S522.

We performed FISH and analyzed the data for each cancer focus as described for case 38. Fig. 2 and Table 3 summarize the chromosome 7 FISH anomalies detected in 25 tumors. Six tumors (24%, cases 13, 17, 29, 34, 50, and 52) had no apparent anomaly of chromosome 7. Nine tumors (36%, cases 7, 10, 12, 14, 19, 26, 33, 44, and 51) showed apparent simple gain of both the chromosome 7q-arm and the centromere, consistent with whole chromosome 7 gain. For example, in case 10, the mean LSP:CEP7 ratio for the six LSPs ranged from 0.98–1.09, and 26–29% of nuclei had three or more signals for CEP7 and the LSPs. In addition to gain of the 7q-arm, case 33 also had evidence of high proliferative activity (see criteria for FISH anomalies). Three tumors (12%, cases 6, 11, and 54) had LAI. Two of these (cases 6 and 11) also had gain of the centromere. For example, in case 6, the mean LSP:CEP7 ratio for the six LSPs was very similar for all probes and ranged from 1.10–1.16. The percentage of nuclei with +CEP7 and +LSP was 20% for CEP7 and approximately 34% for the six LSPs. In case 11, the mean LSP:CEP7 ratio for the six LSPs ranged from 1.10–1.13. The percentage of nuclei with +CEP7 and +LSP was 74% for CEP7 and approximately 81% for the six LSPs. Two tumors (8%, cases 46 and 47) had HAI. For example, in case 46, the mean
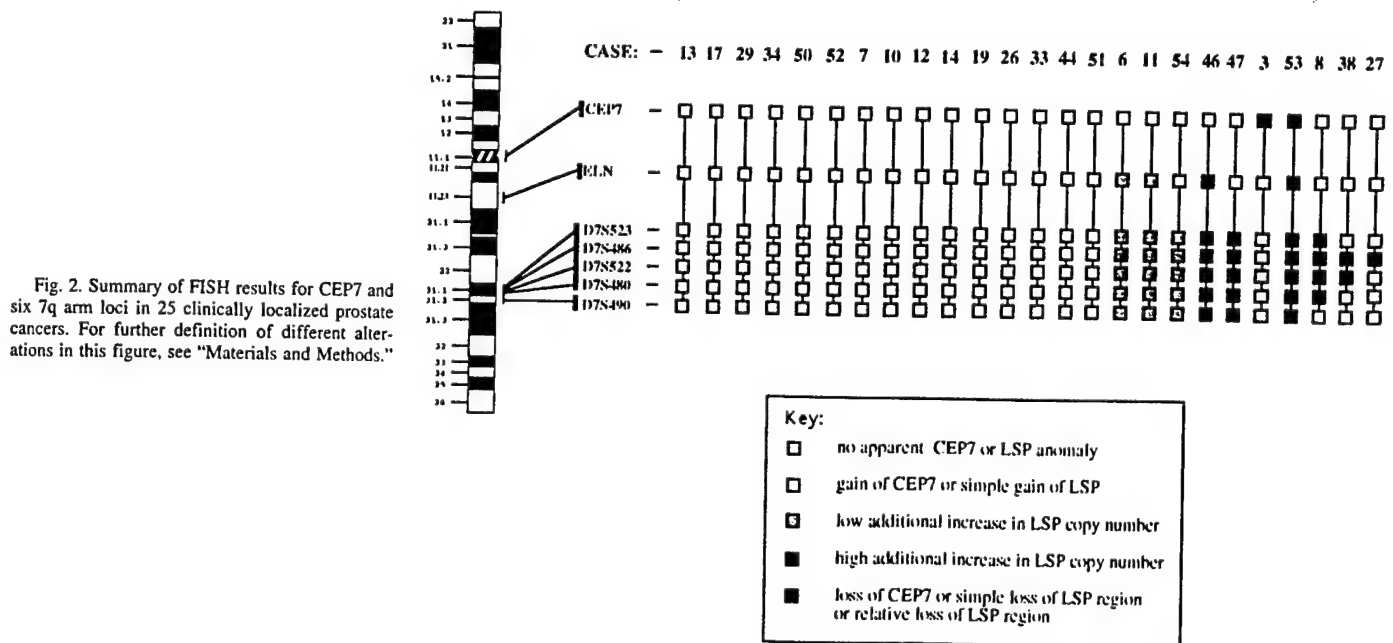

Fig. 2. Summary of FISH results for CEP7 and six 7q arm loci in 25 clinically localized prostate cancers. For further definition of different alterations in this figure, see "Materials and Methods."

Key:
☐ no apparent CEP7 or LSP anomaly
☐ gain of CEP7 or simple gain of LSP
◪ low additional increase in LSP copy number
■ high additional increase in LSP copy number
■ loss of CEP7 or simple loss of LSP region or relative loss of LSP region

762

Table 3 *A summary of the chromosome 7 FISH results and a comparison of FISH and PCR analyses of D7S522 in 25 stage $T_{2-3}N_{0-1}M_0$ prostate cancers*

Case no.	Chromosome 7[a]	FISH results					PCR results
		+CEP7 (%)	+D7S522 (%)	D7S522:CEP7 signal ratio	CEP7[b]	D7S522[b]	D7S522[b]
3	−CEP7	1.6	4.6	1.21	−	N	N
6	+7q, LAI of 7q11.21-31	20.4	34.7	1.15	+	+	+
7	+7q	47.3	46.6	1.02	+	+	NI
8	+7q, RL of 7q31	60.6	34.4	0.73	+	−	−
10	+7q	25.7	28.6	1.04	+	+	+
11	+7q, LAI of 7q11.21-31	73.8	80.6	1.12	+	+	+
12	+7q	63.7	74.6	1.08	+	+	+
13	N	6.3	7.2	1.00	N	N	N
14	+7q	54.2	53.0	1.02	+	+	+
17	N	5.0	4.4	1.02	N	N	N
19	+7q	24.5	23.8	0.99	+	+	+
26	+7q	50.6	52.6	1.01	+	+	+
27	+7q, RL of D7S522	45.3	33.8	0.90	+	+	+
29	N	2.6	1.7	0.98	N	N	N
33	+7q	78.7	82.2	1.07	+	+	NI
34	N	2.6	2.2	1.01	N	N	N
38	+7q, RL of D7S522 and D7S486	13.8	1.3	0.59	+	−	−
44	+7q	38.1	37.3	1.03	+	+	N
46	+7q, HAI of 7q11.21-31	21.2	49.7	1.36	+	+	+
47	+7q, HAI of 7q31	70.3	90.5	1.63	+	+	+
50	N	6.6	5.1	1.00	N	N	N
51	+7q	36.8	34.3	0.98	+	+	NI
52	N	6.0	4.3	0.99	N	N	N
53	−7q	3.1	2.3	1.00	−	−	NI
54	+7, LAI of 7q31	6.2	29.8	1.24	N	+	N

[a] Summary of all FISH changes for chromosome 7 (see Fig. 2). Alterations are abbreviated as follows: N, no apparent chromosomal anomaly; +7q, simple gain of the chromosome 7q arm, including the centromere; −7q, simple loss of the chromosome 7q-arm, including the centromere.

[b] +, increased dosage for indicated chromosome regions; −, decreased dosage for indicated chromosome regions; NI, noninformative.

LSP:CEP7 ratio for the six LSPs ranged from 1.35–1.46, and the percentage of nuclei with +CEP7 and +LSP was 21% for CEP7 and approximately 50% for the six LSPs. Very few of nuclei from these two cases with HAI had evidence of relative LSP quadruplication or greater, suggesting that overt LSP amplification was rare. One tumor (4%, case 53) had a simple loss of both the chromosome 7q-arm and the centromere, consistent with whole chromosome 7 loss. Three tumors (12%, cases 8, 27, and 38) had evidence of gain of some LSPs and relative loss of other LSPs. For example, case 8 had gain of CEP7, ELN, and D7S490 together with relative loss of D7S523, D7S486, D7S522, and D7S480. In this tumor, 21% of the nuclei had +CEP7, and the mean LSP:CEP7 ratio for ELN, D7S523, D7S486, D7S522, D7S480, and D7S490 was 1.06, 0.79, 0.73, 0.73, 0.80, and 0.91, respectively. One tumor (4%, case 3) had a normal range of copy numbers for the six LSPs studied and an apparent loss of CEP7.

The location of the commonly altered regions can be inferred by the pattern of locus dosage determined by FISH analyses of these 25 tumors (Fig. 2). The most commonly overrepresented region is defined by cases 54 and 47 and includes all loci evaluated in the 7q31.1–31.2 region. The minimal deletion region is defined proximally by cases 38 and 27 and distally by case 27. The most commonly deleted region lies between D7S523 and D7S522.

Relationships of 7q31 Alterations with Pathological Factors. Table 4 shows that overrepresentation of the 7q31 region (simple + 7q, LAI, and HAI) increased in frequency with increasing Gleason score ($P = 0.01$). An additional increase in LSP copy number

(LAI and HAI) accounted for much of this increase. No positive correlation for overrepresentation of 7q31 with pathological stage could be identified (data not shown). There was no positive relationship of 7q31 deletion with either Gleason score or pathological stage (data not shown).

Comparison of FISH Results with Multiplex PCR Results

To obtain independent evidence that the critical region of chromosome 7 was both gained and lost in these tumors, we performed multiplex PCR analysis of microsatellite alleles using D7S522 and a control marker, D14S615. Fig. 3 shows representative data from tumors 6, 8, and 46. Tumor 8 was interpreted to have loss of the lower D7S522 allele, whereas tumors 6 and 46 were interpreted to have gain of the lower D7S522 allele. Table 3 summarizes the comparison of FISH results with multiplex PCR results. Of 21 informative cases, FISH and multiplex PCR assessments of D7S522 dosage were concordant in 19 cases (90.5%) and discordant in 2 cases (9.5%). Seven cases (cases 3, 13, 17, 29, 34, 50, and 52) showed no apparent anomaly of 7q31 by both FISH and PCR. Ten cases (cases 6, 10, 11, 12, 14, 19, 26, 27, 46, and 47) showed evidence of increased D7S522 dosage by both FISH and PCR. Two cases (cases 8 and 38) showed evidence of decreased D7S522 dosage by both FISH and PCR. Two cases (cases 44 and 54) showed evidence of increased D7S522 dosage by FISH and normal D7S522 dosage by PCR.

FISH Mapping of Chromosome Breakage at Fragile Sites at 7q31

Aphidicolin was used to induce fragile site expression in a chromosome 7 only somatic cell hybrid (1HL11-G). A total of 159 chromosome 7 gaps and breaks were observed on examination of 4817 metaphase cells. Of these 159 gaps and breaks, 27 (17%) were located at 7q31 (FRA7G). The D7S522 FISH probe was hybridized to the metaphase preparations, and typical FISH images are illustrated in Fig. 4. Fig. 4A shows a metaphase in which D7S522 probe hybridizes distal to FRA7G. Fig. 4B illustrates a metaphase in which the D7S522 probe hybridizes proximal to FRA7G. Among 27 metaphase cells with

Table 4 *Relationship of overrepresentation of 7q31 with Gleason score in 25 clinically localized prostate carcinomas*

Gleason score	n	Cases with indicated anomalies (%)			
		+7q	LAI	HAI	+7q31[a]
4–6	6	0	0	0	0
7	7	43	0	0	43
8–10	12	50	25	17	92
P[b]		0.1	0.16	0.31	0.01

[a] +7q31, the sum of simple gain of 7q, LAI and HAI.

[b] P, Gleason score 4–6 versus 7 versus 8–10.

Case 8   Case 6   Case 46

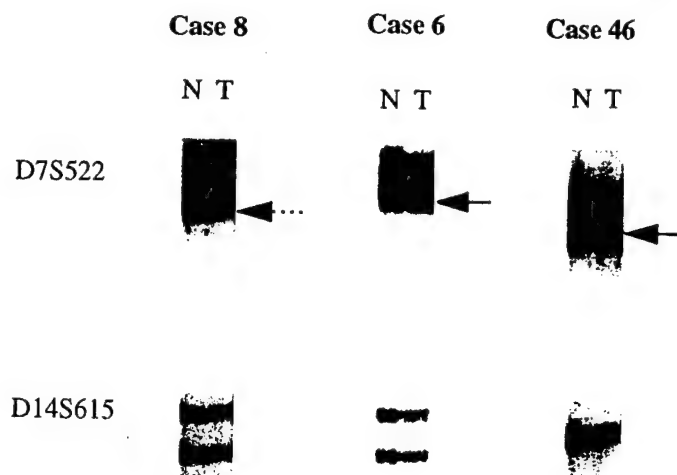N T   N T   N T

D7S522

D14S615

Fig. 3. Examples of comparative multiplex PCR for cases 8 and 46. An internal control marker (*D14S615*) indicates that almost equal amounts of DNAs were amplified in the PCR reaction and loaded in the tumor (*T*) and noncancerous (*N*) lanes. Case 8 shows a loss of the lower *D7S522* allele (*dashed arrow*). The intensity ratio of tumor sample:normal sample for case 8 was 0.43. Cases 6 and 46 show a gain of the lower band *D7S522* allele (*solid arrows*). The intensity ratios were 1.35 for case 6 and 1.46 for case 46, respectively.

breaks at 7q31, 10 (37%) showed FISH hybridization distal to *FRA7G*, 5 (19%) showed FISH hybridization proximal to *FRA7G*, and 12 (44%) showed FISH hybridization spanning *FRA7G*.

Mutation Analysis of the *MET* Gene

The *MET* proto-oncogene is mapped to 7q31 and is within 500 kb of *D7S522* (19, 22). Mutations in the tyrosine kinase domain of the *MET* proto-oncogene have been identified in papillary renal carcinomas (22), tumors that frequently have a gain of chromosome 7 (21). To detect mutations of the *MET* gene in the 25 tumor DNA specimens, we scanned exons 5–7 and exons 15–21, containing the cysteine-rich and tyrosine kinase domains of *MET*, respectively. The heteroduplex DHPLC mutation screening procedure detected 28 alterations among the 10 exons. DNA sequence alterations were detected for 27 of these 28 DHPLC changes, and none were nonsense, missense, or truncating mutations. All were apparently silent polymorphisms; 13 and 14

tumor DNA specimens contained I1357I and Y649Y alterations, respectively.

DISCUSSION

Frequent allelic imbalance on chromosome 7q31 has been shown in a number of tumors including breast cancer, head and neck cancer, prostate cancer, colon cancer, malignant myeloid disorder, ovarian cancer, and T-cell malignancies (9–13, 23–26). Breast cancer patients with allelic imbalance at 7q31.1 (the *MET* locus) have been reported to show significantly higher risk of relapse and shorter metastasis-free survival and overall survival compared to patients without this alteration (27, 28). In a recent study from our laboratory, allelic imbalance for *D7S522* at 7q31 was found to correlate more strongly with prostate cancer progression and patient death from prostate cancer (14). Lin *et al.* reported a minimum deletion of 1000 kb at 7q31 in breast cancer (29), and Edelson *et al.* (25) identified a 1300-kb deletion unit at 7q31 in invasive epithelial ovarian carcinomas. Taken together, these findings suggest that 7q31 is the location of a gene significant for certain malignancies. But in many of the studies mentioned above, multiplex PCR was not performed to carefully control the amount of tumor and nontumor DNA amplified by the PCR and then loaded onto gels. Previous loss of heterozygosity studies of chromosome 7 in prostate cancer may be misleading when they suggest that a tumor suppressor gene resides at 7q31.

Cytogenetic and FISH centromeric studies have demonstrated that chromosome 7 was often gained and/or 7q22-q31 was often duplicated in prostate cancer (2–7). In the present study, using closely linked locus specific probes, we confirmed that 7q31 is frequently altered in prostate cancer. We also found that apparent simple gain of the chromosome 7q-arm including the centromere and additional gain of the 7q-arm relative to the centromere were more common than simple loss of the chromosome 7q arm or deletion of 7q31. Based on FISH dosage in two tumors (cases 47 and 54), we hypothesize that the most commonly overrepresented region includes all of 7q31.1–31.2. Because our proximal probe was the *ELN* gene and we did not use a more distal probe in this study, the actual extent of the region of overrepresentation cannot be determined. Using comparative genomic hybridization, Visakorpi *et al.* (23) found that gain of chromosome 7 was much more common in recurrent prostate cancer than in primary
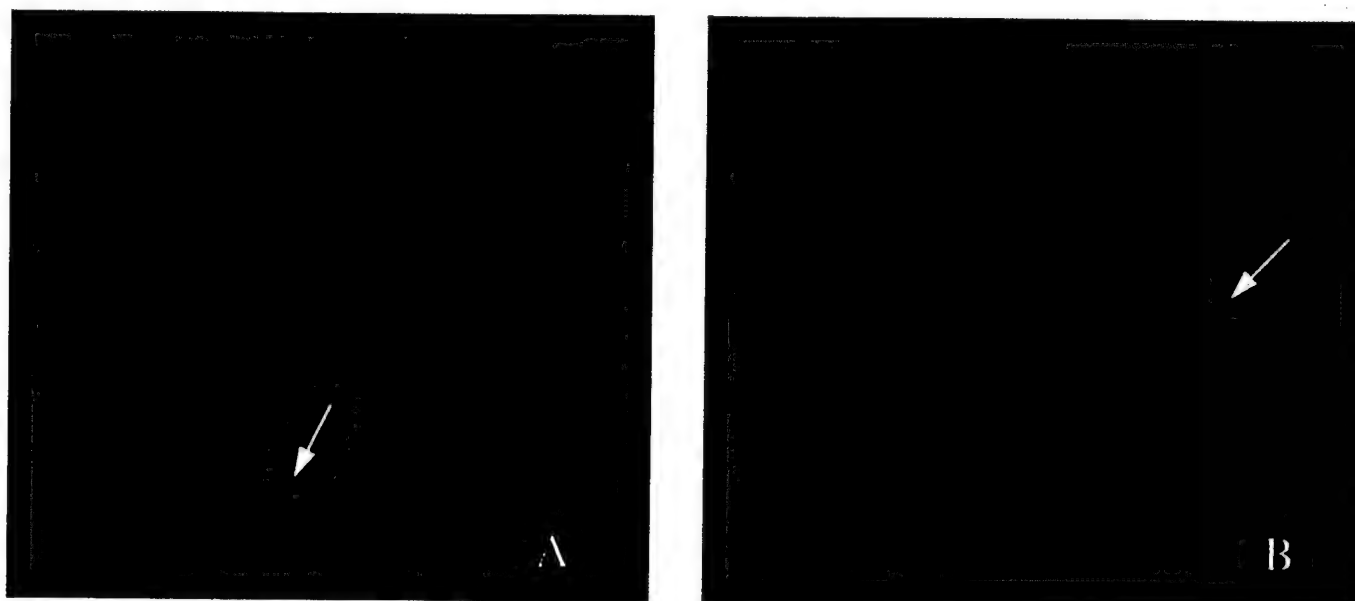

Fig. 4. Hybridization to metaphases containing aphidicolin-induced 7q31 breakage with a FISH probe for *D7S522*. *A*, probe hybridization distal to the 7q31 break (*FRA7G*). *B*, probe hybridization proximal to the 7q31 break (*FRA7G*).

prostate cancer. They observed that the most commonly gained region on the 7q-arm extended from the centromere to band 7q31 (23). By comparative genomic hybridization, Cher *et al.* (24) also detected frequent gain of the chromosome 7q-arm, and overrepresentation of the region from band 7q21 to 7q32 was especially common in metastatic and androgen-independent prostate cancer. In this study, we found that overrepresentation of the 7q31 region was strongly correlated with Gleason score of prostate cancer. All of these findings suggest that overrepresentation of the 7q-arm and possibly the 7q31 region is important for the progression of prostate cancer. Our FISH data also suggest that this overrepresentation is a result of simple relative duplication and/or triplication of the 7q-arm or the 7q31 region.

In this study, we also observed three cases of prostate cancer with the deletion of a specific 7q31 region. Among these three cases, the most commonly deleted region was between loci *D7S523* and *D7S522*. Because we used relatively small FISH probes (≤225 kb in length) to map the genetic changes at the 7q-arm, we suspect that we detected most of the genetic deletions. However, we have not excluded the presence of deletions smaller than the size of our probes. Interestingly, the commonly deleted region is within the most commonly gained region, suggesting that the 7q31 region is genetically unstable in prostate cancer.

Our multiplex PCR studies supported our FISH observations. The multiplex PCR analysis did not detect more *D7S522* deletions than FISH. This indicates that FISH with an appropriate LSP is a reliable approach for determining the dosage of specific chromosome regions. However, in two cases, FISH analysis showed evidence of increased *D7S522* dosage, whereas PCR analysis suggested a normal *D7S522* dosage. A possible explanation for this discrepancy is that PCR analysis of gene dosage using DNA extracted from tumor tissue is limited by normal cell contamination.

Many of the common fragile sites occur at chromosome regions that are frequently altered in tumors (30). Because we observed both gains and deletions of 7q31, we hypothesized that these alterations could be due to fragility at the common fragile site, *FRA7G*. Recently, we identified several overlapping YAC clones spanning *FRA7G* (19). These clones map to the commonly altered region and contain both the *D7S522* locus and the *MET* oncogene (19). In the present study, we performed FISH analysis of aphidicolin-induced chromosome breakage in a chromosome 7-containing somatic cell hybrid. Our results demonstrate that *FRA7G* breakage occurs throughout the *D7S522* region, because the *D7S522* FISH probe hybridized both proximally and distally to the 7q31.2 fragile site. This result is similar to previous findings for *FRA3B*, the most active of the common fragile sites (31, 32), in which it was demonstrated that breakage occurs over a region of at least 300 kb in size. The coincidence of *FRA7G* with the region showing the greatest allelic imbalance suggests that instability of this fragile site may be responsible for both the gains and losses of this region. Interestingly, Coquelle *et al.* (33) have recently observed that intrachromosomal gene amplification may be triggered by the expression of fragile sites in cells cultured *in vitro*. A similar phenomenon may be occurring in 7q31 *in vivo*.

The *MET* proto-oncogene is distal to *FRA7G* and is within 500 kb telomeric of *D7S522* (19, 22, 29). *MET* has been shown to be overexpressed in papillary carcinoma of the thyroid and in carcinomas of the colon, pancreases, ovary, and prostate (19, 34–39). In addition, mutations in the tyrosine kinase domain of the *MET* proto-oncogene have been identified in papillary renal carcinomas (22); tumors that frequently have gain of chromosome 7 (22). Thus, *MET* is an excellent candidate target gene in band 7q31. In this study, we scanned both of the tyrosine kinase and cysteine-rich domains of *MET*. Only silent polymorphisms were identified, indicating that these domains of *MET*

are rarely mutated in prostate cancer. However, it should be noted that we have not excluded alterations in other regions of *MET*. It is also possible that amplification or overrepresentation of the 7q31 region may result in overexpression of *MET*. In this study, we rarely observed nuclei with overt amplification of the LSPs we evaluated, even in the two tumors with HAI. Thus, it is unlikely that *MET* is amplified in prostate cancer to a greater extent than the levels we measured for the 7q31 region, because most amplicons are reported to be greater than 5 Mb in size (40, 41).

In summary, we have evaluated the genetic changes of the 7q-arm in prostate cancer using both FISH and multiplex PCR. Our data suggest that the 7q-arm is genetically unstable in prostate cancer and is subject to both deletion and duplication (or additional overrepresentation) events. Overrepresentation of 7q31 is strongly correlated with increased tumor grade. Some of the gene dosage differences observed in this region may be due to fragility of *FRA7G*. Our observations have two possible implications: (*a*) it is possible that overrepresentation of the 7q-arm, 7q31, and/or genes in these regions may be important for the development and/or progression of a significant proportion of prostate cancer. If this is so, then our data suggest that *MET* is unlikely to be the target gene; and (*b*) conversely, it is also possible that prostate cancer progression is associated with increased chromosomal fragility, perhaps as a result of other genetic alterations (28). If this is so, then fragility at *FRA7G* may be why the 7q-arm and 7q31 are frequently altered in prostate cancer, rather than there being an important tumor suppressor gene or oncogene in these regions.

ACKNOWLEDGMENTS

REFERENCES

1. Bandyk, M. G., Zhao, L., Troncoso, P., Pisters, L. L., Palmer, J. L., von Eschenbach, A. C., Chung, L. W. K., and Liang, J. C. Trisomy 7: a potential cytogenetic marker of human prostate cancer progression. Genes Chromosomes Cancer, 9: 19–27, 1994.
2. Qian, J., Bostwick, D. G., Takahashi, S., Borell, T. J., Herath, J. F., Lieber, M. M., and Jenkins, R. B. Chromosomal anomalies in prostatic intraepithelial neoplasia and carcinoma detected by fluorescence *in situ* hybridization. Cancer Res., 55: 5408–5414, 1995.
3. Takahashi, S., Qian, J., Brown, J. A., Alcaraz, A., Bostwick, D. G., Lieber, M. M., and Jenkins, R. B. Potential markers of prostate cancer aggressiveness detected by fluorescence *in situ* hybridization. Cancer Res., 54: 3574–3579, 1994.
4. Alcaraz, A., Takahashi, S., Brown, J. A., Herath, J. F., Bergstralh, E., Larson-Keller, J., Lieber, M. M., and Jenkins, R. B. Aneuploidy and aneusomy of chromosome 7 detected by fluorescence *in situ* hybridization are markers of poor prognosis in prostate cancer. Cancer Res., 54: 3998–4002, 1994.
5. Persons, D. L., Gibney, D. J., Hatzmann, J. A., Lieber, M. M., Farrow, G. M., and Jenkins, R. B. Use of fluorescence *in situ* hybridization for deoxyribonucleic acid ploidy analysis of prostatic carcinoma. J. Urol., 150: 120–125, 1993.
6. Brothman, A. R., Peehl, D. M., and McNeal, J. E. Frequency and pattern of karyotypic anomalies in human prostate cancer. Cancer Res., 50: 3795–3803, 1990.
7. Lundgren, R., Mandahl, N., Heim, S., Limon, J., Henrikson, H., and Mitelman, F. Cytogenetic analysis of 57 primary prostatic adenocarcinomas. Genes Chromosomes Cancer, 4: 6–24, 1992.
8. Collard, J. G., van de Poll, M., Scheffer, A., Roos, E., Hopman, A. H. M., Geurts van Kessel, A. H. M., and van Dongen, J. J. M. Location of genes involved in invasion and metastasis on human chromosome 7. Cancer Res., 47: 6666–6670, 1987.
9. Zenklusen, J. C., Bieche, I., Lidereau, R., and Conti, C. J. (C-A)ₙ microsatellite repeat *D7S522* is the most commonly deleted region in human primary breast cancer. Proc. Natl. Acad. Sci. USA, 91: 12155–12158, 1994.
10. Zenklusen, J. C., Thompson, J. C., Klein-Szanto, A. J. P., and Conti, C. J. Frequent loss of heterozygosity in human primary squamous cell and colon carcinomas at 7q31.1: evidence for a broad range tumor suppressor gene. Cancer Res., 55: 1347–1350, 1995.
11. Zenklusen, J. C., Thompson, J. C., Troncoso, P., Kagan, J., and Conti, C. J. Loss of heterozygosity in human primary prostate carcinomas: a possible tumor suppressor gene at 7q31.1. Cancer Res., 54: 6370–6373, 1994.
12. Latil, A., Cusseno, O., Fournier, G., Baron, J. C., and Lidereau, R. Loss of heterozygosity at 7q31 is a frequent and early event in prostate cancer. Clin. Cancer Res., 1: 1385–1389, 1995.
13. Takahashi, S., Shan, A. L., Ritland, S. R., Delacey, K. A., Bostwick, D. G., Lieber, M. M., Thibodeau, S. N., and Jenkins, R. B. Frequent loss of heterozygosity at 7q31.1

in primary prostate cancer is associated with tumor aggressiveness and progression. Cancer Res., 55: 5115–5119, 1995.

14. Jenkins, R. B., Takahashi, S., Delacey, K. A., Bergstralh, E., and Lieber, M. M. Prognostic significance of allelic imbalance of chromosome regions 7q, 8p, 16q, and 18q in stage $T_3N_0M_0$ prostate cancer. Genes Chromosomes Cancer, in press, 1998.

15. Alers, C. A., Krijtenburg, P. J., Vissers, K. J., Bosman, F. T., van der Kwast, T. H., and Dekken, H. Interphase cytogenetics of prostatic adenocarcinoma and precursor lesions: analysis of 25 radical prostatectomies and 17 adjacent prostatic intraepithelial neoplasias. Genes Chromosomes Cancer, 12: 241–250, 1995.

16. Jenkins, R. B., Qian, J., Lieber, M. M., and Bostwick, D. G. Detection of c-myc oncogene amplification and chromosomal anomalies in metastatic prostatic carcinoma by fluorescence in situ hybridization (FISH). Cancer Res., 57: 524–531, 1997.

17. Qian, J., Bostwick, D. G., Takahashi, S., Brown, J. A., Lieber, M. M., and Jenkins, R. B. Comparison of fluorescence in situ hybridization analysis of isolated nuclei and routine histologic sections from paraffin-embedded prostatic adenocarcinoma specimens. Am. J. Pathol., 149: 1193–1199, 1996.

18. Berger, R., Bloomfield, C. D., and Sutherland, G. R. Report of the committee on chromosome rearrangements in neoplasia and on fragile sites (HGM8). Cytogenet. Cell Genet., 40: 490–535, 1985.

19. Huang, H., Qian, C., Jenkins, R. B., and Smith, D. I. FISH mapping of YAC clones at human chromosomal band 7q31.2: identification of YACS spanning FRA7G within the common region of LOH in breast and prostate cancer. Genes Chromosomes Cancer, in press, 1998.

20. Liu, W., James, D. C., Frederick, L., Alderete, B. E., and Jenkins, R. B. PTEN/ MMAC1 mutations and epidermal growth factor receptor amplification in glioblastomas. Cancer Res., 57: 5254–5257, 1997.

21. Hayward-Lester, A., Oefner, P. J., Sabatini, S., and Doris, P. A. Accurate and absolute quantitative measurement of gene expression by single-tube RT-PCR and HPLC. Genome Res., 5: 494–499, 1995.

22. Schmidt, L., Duh, F. M., Chen, F., Kishida, T., Glenn, G., Choyke, P., Scherer, S. W., Zhuang, Z., Lubensky, I., Dean, M., Allikmets, R., Chidambaram, A., Bergerheim, U. R., Feltis, J. T., Casadevall, C., Zamarron, A., Orcutt, M. L., Stackhouse, T., Lipan, J., Slife, L., Brauch, H., Decker, J., Niehans, G., Hughson, M. D., Moch, H., Storkel, S., Lerman, M. I., Linehan, W. M., and Zbar, B. Germline and somatic mutations in the tyrosine kinase domain of the MET proto-oncogene in papillary renal carcinomas. Nat. Genet., 16: 68–73, 1997.

23. Visakorpi, T., Kallioniemi, A. H., Syvanen, A. C., Hyytinen, E. R., Karhu, R., Tammela, , Isola, J. J., and Kallioniemi, O. P. Genetic changes in primary and recurrent prostate cancer by comparative genomic hybridization. Cancer Res., 55: 342–347, 1995.

24. Cher, M. L., Bova, G. S., Moore, D. H., Small, E. J., Carroll, P. R., Pin, S. S., Epstein, J. I., Isaacs, W. B., and Jensen, R. H. Genetic alterations in untreated metastases and androgen-independent prostate cancer detected by comparative genomic hybridization and allelotyping. Cancer Res., 56: 3091–3102, 1996.

25. Edelson, M. I., Scherer, S. W., Tsui, L. C., Welch, W. R., Bell, D. A., Berkowitz, R. S., and Mok, S. C. Identification of a 1300-kilobase deletion unit on chromosome 7q31.3 in invasive epithelial ovarian carcinomas. Oncogene, 14: 2979–2984, 1997.

26. Abrahamson, G. M., Rack, K., Oscier, D. G., Fichett, M., Buckle, V. J., and Wainscoat, J. S. Comparison of cytogenetic and restriction fragment length polymorphism analyses for the detection of loss of chromosome material in clonal hemopoietic disorders. Am. J. Hematol., 42: 171–176, 1993.

27. Bieche, I., Champeme, M. H., Matifas, F., Hacene, K., Callahan, R., and Lidereau, R.

Loss of heterozygosity on chromosome 7q and aggressive primary breast cancer. Lancet, 339: 139–143, 1992.

28. Deng, G., Chen, L. C., Schott, D. R., Thor, A., Bhargava, V., Ljung, B. M., Chew, K., and Smith, H. S. Loss of heterozygosity and p53 gene mutations in breast cancer. Cancer Res., 54: 499–505, 1994.

29. Lin, J. C., Scherer, S. W., Tougas, L., Traverso, G., Tsui, L., Andrulis, I. L., Jothy, S., and Park, M. Detailed deletion mapping with a refined physical map of 7q31 localizes a putative tumor suppressor gene for breast cancer in the region of MET. Oncogene, 13: 2001–2008, 1996.

30. Yunis, J. J., and Soreng, A. L. Constitutive fragile sites and cancer. Science (Washington DC), 226: 1199–1204, 1984.

31. Paradee, W., Wilke, C. M., Wang, L., Shridhar, R., Mullins, C. M., Hoge, A., Glover, T. W., and Smith, D. I. A 350-kb cosmid contig in 3p14.2 that crosses the t(3;8) hereditary renal cell carcinoma translocation breakpoint and 17 aphidicolin-induced FRA3B breakpoints. Genomics, 35: 87–93, 1996.

32. Zimonjic, D. B., Druck, T., Ohta, M., Kastury, K., Carlo, M. C., and Popescu, N. C. Positions of chromosome 3p14.2 fragile sites (FRA3B) within the FIHT gene. Cancer Res., 57: 1166–1170, 1997.

33. Coquelle, A., Pipiras, E., Toledo, F., Buttin, G., and Debatisse, M. Expression of fragile sites triggers intrachromosomal mammalian gene amplification and sets boundaries to early amplifications. Cell, 89: 215–225, 1997.

34. Hofstra, R. M., Landsvater, R. M., Ceccherini, I., Stulp, R. P., Stelwagen, T., Luo, Y., Pasini, B., Hoppener, J. W. M., van Amstel, H. K. P., Romeo, G., Lips, C. J. M., and Buys, C. H. C. M. A mutation in the RET proto-oncogene associated with multiple endocrine neoplasia type 2B and sporadic medullary thyroid carcinoma. Nature (Lond.), 367: 375–376, 1994.

35. Eng, C., Smith, D. P., Mulligan, L. M., Healey, C. S., Zvelebil, M. J., Stonehouse, T. J., Ponder, M. A., Jackson, C. E., Waterfield, M. D., and Ponder, B. A. A novel point mutation in the tyrosine kinase domain of the RET proto-oncogene in sporadic medullary thyroid carcinoma and in a family with FMTC. Oncogene, 10: 509–513, 1995.

36. Ponzetto, C., Giordano, S., Peverali, F., Della Valle, G., Abate, M. L., Vaula, G., and Comoglio, P. M. C-met is amplified but not mutated in a cell line with an activated met tyrosine kinase. Oncogene, 6: 553–559, 1991.

37. Bremner, R., and Balmain, A. Genetic changes in skin tumor progression: correlation between presence of a mutant ras gene and loss of heterozygosity on mouse chromosome 7. Cell, 61: 407–417, 1990.

38. Wirchubsky, Z., Wiener, F., Spira, J., Sumegi, J., and Klein, G. Triplication of one chromosome no. 15 with an altered c-myc homologue in a T-cell lymphoma line of AKR origin (TIKAUT). Int. J. Cancer, 33: 477–481, 1984.

39. Humphery, P. A., Zhu, X., Zarnegar, R., Swanson, P. E., Ratliff, T. L., Vollmer, R. T., and Day, M. L. Hepatocyte growth factor and its receptor (c-MET) in prostatic carcinoma. Am. J. Pathol., 147: 386–396, 1995.

40. Kallioniemi, A., Kallioniemi, O. P., Piper, J., Tanner, M., Stokke, T., Chen, L., Smith, H. S., Pinkel, D., Gray, J. W., and Waldman, F. M. Detection and mapping of amplified DNA sequences in breast cancer by comparative genomic hybridization. Proc. Natl. Acad. Sci. USA, 91: 2156–2160, 1994.

41. Tanner, M. M., Tirkkonen, M., Kallioniemi, A., Isola, J., Kuukasjarvi, T., Collins, C., Kowbel, D., Guan, X. Y., Trent, J., Gray, J. W., Meltzer, P., and Kallioniemi, O. P. Independent amplification and frequent co-amplification of three nonsyntenic regions on the long arm of chromosome 20 in human breast cancer. Cancer Res., 56: 3441–3445, 1996.

Loss of Expression of the *DRR 1* Gene at Chromosomal Segment 3p21.1 in Renal Cell Carcinoma

Liang Wang,[1] John Darling,[1] Jin-San Zhang,[1] Wanguo Liu,[1] Junqi Qian,[1] David Bostwick,[2] Lynn Hartmann,[3] Robert Jenkins,[1] Walter Bardenhauer,[4] Jochen Schutte,[4] Bertram Opalka,[4] and David I. Smith[1]*

[1]Division of Experimental Pathology, Department of Laboratory Medicine and Pathology, Mayo Clinic, Rochester, Minnesota
[2]Department of Laboratory Medicine and Pathology, Mayo Clinic, Rochester, Minnesota
[3]Division of Medical Oncology, Mayo Clinic, Rochester, Minnesota
[4]Innere Klinik und Poliklinik (Tumorforschung), Universitätsklinikum Essen, Westdeutsches Tumorzentrum, Essen, Germany

Consistent deletion of DNA sequences in chromosomal band 3p21 observed in a variety of human tumors suggests the presence of one or more tumor suppressor genes within this region. Previously, we reported on the construction of two distinct cosmid contigs and our identification of several new genes within 3p21.1. In our search for tumor suppressor genes from this region, we have cloned a gene that we have called *DRR 1* (downregulated in renal cell carcinoma). The gene was first mapped to 3p21.1 by fluorescence in situ hybridization analysis. Further analysis of yeast artificial chromosome clones in 3p14.2–p21.1 refined its localization. *DRR 1* spans about 10 Kb of genomic DNA with a 3.5-Kb mature transcript. The putative protein encoded by this gene is 144 amino acids and includes a nuclear localization signal and a coiled domain. The gene showed loss of expression in eight of eight renal cell carcinoma cell lines, one of seven ovarian cancer cell lines, one of one cervical cancer cell line, one of one gastric cancer cell line, and one of one non–small-cell lung cancer cell line. Southern blot analysis did not show any altered bands, indicating that gross structural changes or deletions did not cause the loss of expression. This gene was also found to have reduced expression in 23 of 34 paired primary renal cell carcinomas. Mutational analysis detected three polymorphic sites within the gene, but no point mutations were identified in the 34 primary tumors. However, we did detect base substitutions in 4 of 12 cell lines that had undetectable expression of the gene. We also transfected the gene into *DRR 1*–negative cell lines and observed clear growth retardation. Our results suggest that loss of expression of the *DRR 1* gene may play an important role in the development of renal cell carcinoma and possibly other tumors. *Genes Chromosomes Cancer 27:1–10, 2000.*   © 2000 Wiley-Liss, Inc.

INTRODUCTION

Consistent loss of DNA sequences from several regions on the short arm of human chromosome 3 has suggested that there may be multiple tumor suppressor genes on this chromosomal arm (Kok et al., 1997). Chromosomal band 3p21 is believed to harbor tumor suppressor genes based on the observation of frequent deletions in this region in several types of tumors, including lung, kidney, breast, and ovarian carcinomas (Killary et al., 1992; Daly et al., 1993; Satoh et al., 1993). DNA sequences from 3p21 have also been reported to suppress the growth of tumor cells (Killary et al., 1992; Rimessi et al., 1994).

Previously, we described the isolation of two cosmids from human chromosomal band 3p21.1, which contained clusters of unmethylated, rare restriction endonuclease sites and DNA sequences that were found to be evolutionarily conserved. Cosmid walking identified two distinct contigs of overlapping cosmids surrounding the two cosmids (Smith et al., 1989). We also described the identifi-

cation of three new genes from the proximal contig and two from the distal contig (Shridhar et al., 1994). One of the five genes, called *ARP* (Arginine-Rich Protein), was evolutionarily conserved and encodes a novel, ubiquitously expressed, arginine-rich protein (Shridhar et al., 1996). The coding portion of this gene contains an imperfect trinucleotide repeat that encodes multiple arginines. Sequence analysis detected point mutations of the gene in several human cancers (Shridhar et al., 1996). However, subsequent analysis revealed that many of these changes could potentially be explained by polymorphisms in the imperfect trinucleotide repeat region (Evron et al., 1997).

The aminoacylase-1 (*ACY1*) gene and a gene called *RIK* are also located at 3p21.1 (Erlandsson et

al., 1990; Cook et al., 1993). Expression of these two genes has been demonstrated to be highly reduced in human cancers. However, Southern and Northern analyses failed to demonstrate any gross abnormalities of these genes in cancer cell lines and primary tumors.

In this article, we describe the identification of another cDNA clone derived from chromosomal segment 3p21.1. We found a complete loss of expression of this gene by reverse transcription-polymerase chain reaction (RT-PCR) in 8/8 renal cell carcinoma (RCC) cell lines. For further characterization of the function of the gene and its relationship to RCC development, we cloned the full-length cDNA for this gene and screened for alterations in the gene in human cancers. The gene spans about 10 kb of genomic DNA, with a final processed transcript of 3.5 kb capable of encoding a 144-amino acid protein. Because the gene showed significant loss of expression in RCC cell lines, as well as in primary tumors, we have termed the gene *DRR 1* for downregulated in renal cell carcinoma.

MATERIALS AND METHODS

Cloning Strategy to Identify Gene

Five expressed sequence tags (ESTs) on the human gene map (Schuler et al., 1996) derived from 3p21 and flanking regions were ordered from Genome Systems and completely sequenced. The clones were then labeled and hybridized to a multiple tissue Northern blot (Clontech, Palo Alto, CA). Hybridization was performed according to the manufacturer's recommendations. The clones with clear signals on the Northern blot were analyzed for expression in RCC cell lines. We then used the EST clones with reduced expression in these cell lines to construct EST contigs using the software Sequencher 3 (Gene Codes, Ann Arbor, MI). Whole contigs were sequenced twice. The integrity of the full-length cDNAs was confirmed by PCR analysis using primers flanking each junction between two EST clones.

Tumor Cell Lines and Primary Renal Cell Carcinomas

A total of 17 tumor cell lines were analyzed, including eight RCC cell lines (HTB-44, HTB-45, HTB-46, HTB-47, HTB-49, CRL-1611, CRL-1932, and CRL-1933), one cervical cancer cell line (C-33A), one gastric cancer (AGS), one non–small-cell lung cancer (NSCLC, CRL-8403), and seven ovarian cancer cell lines (OV167, OV177, OV202, OV207, OV266, OV675, and OVCAR-3). The ovar-

ian cancer cell lines except for OVCAR-3 were established at the Mayo Clinic; other cell lines were purchased from the American Type Culture Collection. The cell lines were cultured based on the provider's recommendation. Thirty-four pairs of fresh RCCs and their normal adjacent kidney tissues were obtained from the Mayo Clinic. All patients had conventional clear cell renal cell carcinoma; clinical information was obtained by chart review. The mean follow-up was 2.6 years (range, 0.1–4.4 years). Tumor and matched normal samples were immediately frozen in liquid nitrogen and stored at -70°C.

DNA and RNA Extraction

DNA was extracted from these cell lines and tissues by standard phenol-chloroform extraction. Total RNA was extracted using Trizol reagent (Life Technologies, Gaithersburg, MD). Five micrograms of each RNA sample was subjected to electrophoresis in 1.2% denaturing agarose gels to make certain that we obtained undegraded RNA. Then 1 µg of the total RNA was treated with 1 unit of RNase-free DNase I for 30 min at room temperature to eliminate contaminating DNA, followed by heating for 10 min at 65°C to inactivate the DNase I. Reverse transcription was performed as previously described (Wang et al., 1998).

Polymerase Chain Reaction and RT-PCR

Several PCR primers were designed based on the full-length cDNA. The primer pairs are listed below: DRR 1F, 5'-TGGAATCCACTCTTGCCTG-3'; DRR 1R, 5'-CGCTGGTCAGTGTGGCAATTG-3'; DRR-2F, 5'-GCCATGTACTCGGAGATCCAG-3'; DRR-2R, 5'-AGCCTCGGAGATTCCTGG-TG-3'; DRR-2811R, 5'-CTGTGGTTCATGAG-CAGC-3'.

Primer pair 2F/2R is expected to give an 804-bp RT-PCR product. Primer pair 1F/2811R generates a 590-bp RT-PCR product. Primer pairs 2F/1R and 2F/2811R generate amplified products from genomic DNA that are 421 bp and 171 bp, respectively.

PCR and RT-PCR were performed in a 12.5-µl reaction volume containing 10 µM of each primer, 1 × PCR buffer (Qiagen, Santa Clarita, CA) with Q-solution, 1.5-mM MgCl$_2$, and 0.5 unit of Taq DNA polymerase (Qiagen). After 3 min of initial denaturation at 95°C, amplification was performed for 30 cycles (94°C for 20 sec, 60°C for 30 sec, and 72°C for 30 sec). To quantitate the relative expression level of the gene in tumor cell lines, we utilized duplex PCR with *GAPDH* primers as an

internal control. The *GAPDH* primers are: *GAPDH* (forward), 5′-ACCACAGTCCATGCCATCAC-3′, and *GAPDH* (reverse), 5′-TCCACCACCCTGTT-GCTGTA-3′.

We mixed the primer pairs DRR-2F/2R at a 10-μM final concentration and *GAPDH* (F/R) at a 0.20-μM final concentration. The PCR conditions were the same as above except that a series of diluted RT products (1.1:10 and 1:100) were used for accurate quantitation.

The *FHIT* gene is a potential tumor suppressor gene for various human tumors (Ohta et al., 1996; Druck et al., 1997). The gene was localized at 3p14.2, where a t(3;8)(p14.2;q24.13) breakpoint was identified in a hereditary renal cell carcinoma family (Cohen et al., 1979). To determine the possible role of the gene in RCC development, we amplified the *FHIT* coding sequences from the tumor samples for sequence analysis. The primer pairs were: FHIT-231, 5′-AAGGGAGAGAAAGAG-AAAGAAG-3′ and FHIT-954,5′-TCACTGGTTGAA-GAATACAGGA-3′.

Duplex PCR was also performed to quantitate the relative expression of this gene in these samples. PCR conditions for this were described previously (Wang et al., 1998).

Mutational Analysis

RT-PCR or PCR products were denatured at 95°C for 5 min and then gradually reannealed to room temperature in 30 min. Denaturing high-performance liquid chromatography (DHPLC) was used to screen possible mutations within the coding region of this gene (Liu et al., 1998). PCR products with potential mutations were cut from agarose gels and purified using a Gel Extraction Kit (Qiagen). Purified products (100–200 ng) were mixed with 3.2-pmol primer and then submitted for sequencing to the Mayo Clinic Molecular Core Facility. A BigDye Terminator Cycle Sequencing Kit (PE Biosystems, Foster City, CA) was used for the sequencing analysis. Sequencing products were separated and analyzed on an ABI 377 sequencer (PE Biosystems).

In Vitro Protein Translation and Cellular Localization

For protein translation in vitro, the full-length *DRR 1* cDNA was directionally cloned into the expression vector pcDNA3.1(+) (Invitrogen, Carlsbad, CA). The TNT-coupled transcription/translation system (Promega, Madison, WI) was used for protein translation. For cellular localization, the full coding region of this gene was cloned into vector

pcDNA3.1(+)/myc-His (version A; Invitrogen). The vector is expected to produce a fusion protein containing 144 amino acids of DRR 1, 10 amino acids of epitope from MYC, and a polyhistidine. The vectors with/without the insert were used to transfect a tumor cell line, HTB-46. Transfection was performed using Lipofectamine Plus reagent (Life Technologies) according to the manufacturer's recommendation. After a 48-hr transfection, the cells were fixed in 4% formaldehyde and detected by an immunofluorescence procedure.

Transfection Analysis of *DRR 1*–Negative Cell Lines

Two *DRR 1*–negative cancer cell lines, HTB-44 and HTB-46, were transfected with 15 μg of pcDNA3.1 (Invitrogen) without insert or pcDNA3.1 with *DRR 1* insert in Opti-MEM I medium (Life Technologies). At the indicated times, cells were trypsinized, collected, and subjected to cell counting. For each group, three dishes were run at each time point.

Chromosomal Localization of *DRR 1*

YAC clones at 3p14.3–p21.1 (Michaelis et al., 1995) were grown, and the DNA was isolated. The primer pair DRR-2F/2811R was then used to determine which YAC clones would produce amplification products with this primer pair. One positive YAC clone, 777F8, was identified. This clone was then used for FISH analysis to localize the gene on chromosome 3. Probe labeling and hybridization conditions were described previously by Huang et al. (1998). Slides were analyzed under a Zeiss fluorescence microscope with a CCD camera.

Southern and Northern Blot Analysis

For Southern blots, 10 μg of genomic DNA was digested with 50 units of restriction enzyme (*Eco*RI, *Sac*I, *Bam*HI, or *Hin*dIII) at 37°C overnight. Digested DNAs were resolved on 1% agarose gels, transferred to Hybond-N$^+$ filters (Amersham), and baked at 80°C for 2 hr. The full-length cDNA was labeled with [^{32}P]-dCTP using random priming and hybridized to the filter at 68°C overnight in hybridization solution [7% SDS, 1-mM EDTA, and 250-mM NaHPO$_4$ (pH 7.2)]. For Northern blot analysis, 10 μg of total RNA was run on 1.2 % denaturing agarose gels, transferred to Hybond-N$^+$ filters (Amersham), and baked at 80°C for 2 hr. Hybridization conditions were the same as those used for the Southern blots.
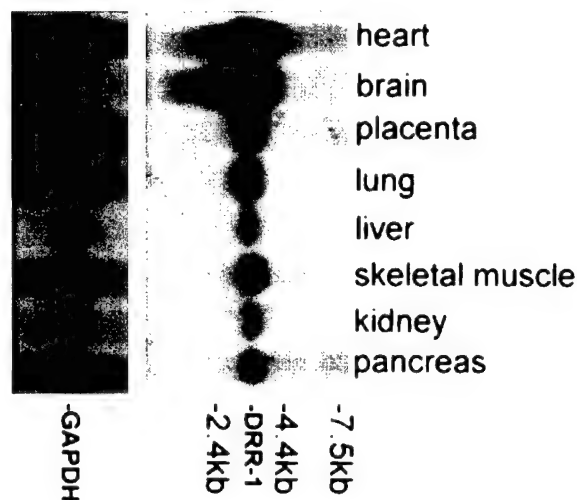
Figure 1. Expression of the *DRR 1* gene in different tissues. A 2.1-kb fragment from DRR 1 cDNA or 452-bp fragment from *GAPDH* cDNA was labeled with [³²P]-dCTP and hybridized to a multiple tissue Northern blot (Clontech). The result shows that the *DRR 1* gene is expressed in all tissues, with a 3.5-kb transcript, although at variable levels in different tissues. The highest detectable expression was found in brain. Kidney tissue expresses this gene at a moderate level.

RESULTS

Cloning the Full-Length cDNA for *DRR 1*

Five EST clones around 3p21.1 were sequenced, including R06759, H67375, D80522, H90388, R19427 (GenBank dbEST accession numbers). One of the ESTs (R19427) showed a loss of expression in the RCC cell lines. To determine the size of the complete mature transcript, we hybridized the 2.1-Kb EST insert to a multiple-tissue Northern blot (Clontech). The Northern blot showed that the transcript was about 3.5 Kb (Fig. 1). cDNA computer-based walking using Sequencher linked two UniGenes (Hs.8022 and Hs.7915) together, which generated a 3.5-Kb cDNA. The complete sequence of this 3.5-Kb cDNA was determined by sequencing of different clones and RT-PCR products. The final full-length processed mRNA from this gene was found to be 3,538 bp with an open reading frame encoding 144 amino acids (GenBank accession number AF089853; Fig. 2). A BLAST search did not find any proteins with significant homology in the database. However, a motif search of the putative 144-amino acid protein showed that it contained a nuclear localization signal as well as a coiled region (Fig. 2B).

To determine the size of the *DRR 1* gene at the genomic level, we digested genomic DNA with four different enzymes and separated the resulting fragments on a 1% agarose gel for Southern blot analysis. The full-length cDNA was labeled with [³²P]-dCTP and used as a hybridization probe. The
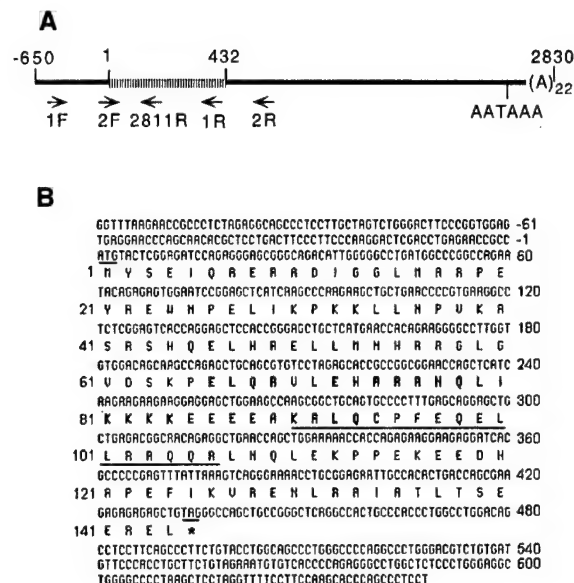
Figure 2. cDNA and protein sequence of *DRR 1* gene. **A:** Schematic structure of *DRR 1* gene, including open reading frame (shaded area), polyadenylation signal (AATAAA), and position of various primers used in the experiment. **B:** Partial cDNA and predicted protein sequence of the *DRR 1* gene (GenBank accession number AF089853 for the full-length cDNA). The gene encodes a small protein consisting of 144 amino acids. The protein is predicted to contain a nuclear localization signal (underlined) and a coiled domain (shaded).
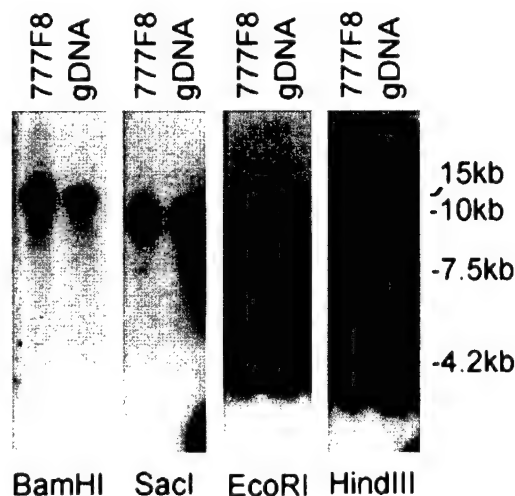
Figure 3. Southern blot analysis of *DRR 1* gene in YAC 777F8 and genomic DNA (placenta) digested with *Bam*HI, *Sac*I, *Eco*RI, and *Hind*III. *Bam*HI and *Sac*I generated a single fragment that hybridized with the full-length cDNA. *Eco*RI and *Hind*III cut the gene into two and three pieces, respectively. The maximum size of this gene at the genomic level is thus less than 10 Kb (defined by *Sac*I).

Southern blot demonstrated that the maximum size of this gene can be no greater than the 10-Kb genomic fragment observed with *Sac*I digestion (Fig. 3).

The full-length *DRR 1* cDNA was cloned and transcribed/translated in a cell-free system. The
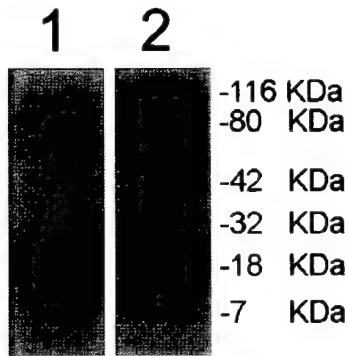
Figure 4. In vitro translation of the *DRR I* mRNA. Lane I, vector containing the full-length *DRR I* cDNA produced a protein with a molecular weight of 18 kDa; lane 2, vector containing the *DRR I* coding region and an MYC epitope produced a fusion protein with a molecular weight of 20 kDa.
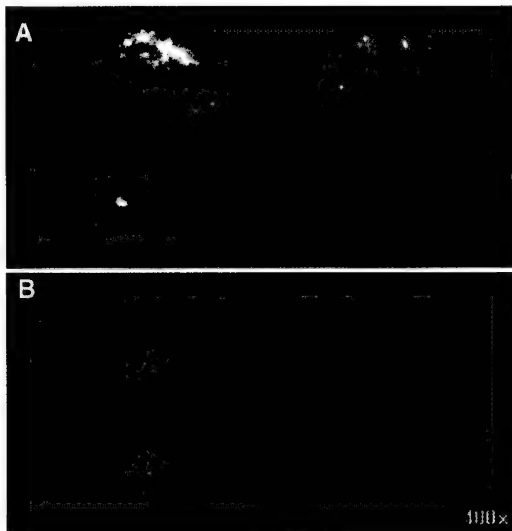
Figure 5. Cellular localization of *DRR I* protein. The cells were transfected with expression vector pcDNA3.1/myc-His, which expresses a fusion protein consisting of *DRR I* and MYC epitope, and then fixed for immunofluorescence detection. Propidium iodide was used for counterstaining. Included in the picture are four cells, three of which show the fusion protein (green) in nuclei.

Figure 6, **A:** Localization of the *DRR I* gene on chromosomes by FISH analysis. DNA from YAC 777F8 was labeled and hybridized to a normal metaphase cell. Arrows show the hybridization signals. **B:** Localization of *DRR I* gene relative to YAC clones from the 3p14.3–p21.1 region.

translated protein was labeled with [^{35}S] methionine and separated on a 4%–20% polyacrylamide gel. The result showed a clear band around 18 kDa, which is consistent for a protein with an expected molecular weight of 144 amino acids (Fig. 4).

Cellular Localization of the DRR I Protein

After a 48-hr transfection, a fusion protein containing DRR 1 and an MYC epitope was detected using an MYC antibody (Invitrogen) and a fluorescein-labeled anti-IgG antibody (Calbiochem, San Diego, CA). We randomly counted 100 cells and found 58 cells expressing the fusion protein (green color in nuclei and/or cytoplasms). Of the 58 transfected cells, 50 showed a strong green signal in nuclei (Fig. 5), demonstrating that the DRR 1 protein is a nuclear protein.

Chromosomal Localization of DRR 1

For FISH analysis, YAC 777F8 was labeled with biotin-dUTP and hybridized to metaphase cells. As expected, hybridization signals were clearly localized at 3p21.1 among 32 chromosomes 3 in 16 metaphases analyzed (Fig. 6A). *DRR 1* was further localized by PCR analysis of more precisely localized YAC clones from the 3p14.3–p21.1 region. YAC clones that tested positive for several *DRR 1* primers were 777F8, 825A4, 947B1, and 961F12. This result places *DRR 1* between the markers D3S3040 and D3S1067 (Fig. 6B). This also places *DRR 1* proximal to the translocation breakpoint associated with hematologic malignancies, t(3; 6)(p21.1; p11) (Smith et al., 1993).

Expression of DRR 1 in Normal and Tumor Tissues

Because *DRR 1* localized to a chromosomal region where other genes have been identified with altered expression in cancers (Erlandsson et al., 1990; Cook et al., 1993),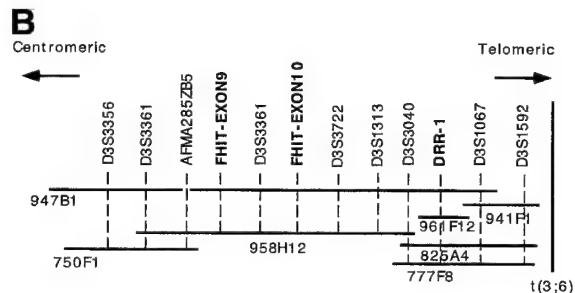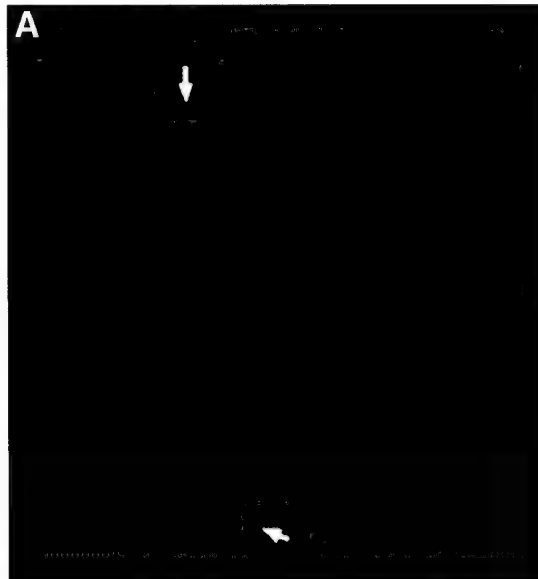 we decided to analyze whether this gene also showed altered expression in human cancers. A multiple tissue Northern blot showed that the *DRR 1* gene was expressed in all tissues tested, although at different levels (Fig. 1). The highest detectable expression was found in brain. The gene was expressed in normal kidney at a moderate level, although which type of kidney cells express the gene is unknown. We then tested the expression level of *DRR 1* in 17 tumor cell lines. RT-PCR showed loss of expression of this gene in eight of eight RCC cell lines (one derived from a papillary RCC, and three derived from clear cell RCC), one of seven ovarian cell lines, one of one cervical cell line, one of one gastric cell line, and one of one NSCLC cell line. To confirm this, we performed semiquantitative RT-PCR using as an internal control the housekeeping gene *GAPDH*. This analysis demonstrated decreased expression of *DRR 1* in many of the cell lines (Fig. 7A). This result was further confirmed using Northern blot analysis (Fig. 7B). To elucidate whether the loss of expression was caused by deletion of genomic sequences or inactivation of the gene, we used the full-length cDNA as a probe to detect possible structural changes of the gene in DNA samples from the 17 cell lines digested with *Eco*RI, *Hin*dIII, and *Bam*HI, respectively. Southern blot analysis did not identify any gross changes within the gene in any of the cell lines tested (data not shown). We also tested the expression of the *DRR 1* gene in 34 paired primary RCCs by semiquantitative RT-PCR; 23 of the 34 RCC samples showed de-
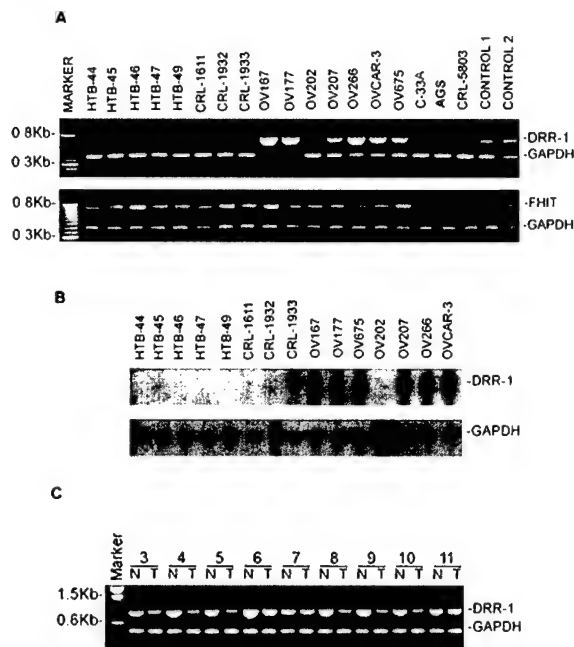
Figure 7. Downregulation of *DRR 1* gene in renal cell carcinomas. Duplex PCRs were performed by mixing gene-specific primers 2F/2R and internal control primers for the *GAPDH* gene (**A** and **C**). The RT-PCR products were resolved on 1.5% agarose gel. Loss of expression of *DRR 1* and *FHIT* was observed in several cell lines (A). The loss of expression of the *DRR 1* gene was confirmed by Northern blot analysis (**B**). Downregulation of the *DRR 1* gene was found in 23 of 34 primary RCC samples (C).

creased expression of the gene (Fig. 7C). When samples were diluted 1:10 and 1:100, we obtained the same results. However, the expression of *DRR 1* in the primary RCC samples was higher than that observed in the tumor-derived cell lines. A possible reason for this is normal cell contamination in the primary tumors.

We also analyzed the *FHIT* gene to determine whether it showed altered expression in any of the cell lines. We amplified the full coding sequence of *FHIT* and determined the level of expression by semiquantitative PCR, and we also analyzed the amplified sequence for mutations in these samples. We did not identify any mutations within the coding region. The results also showed no change of expression in the samples tested except for one cervical tumor cell line, one gastric cancer cell line, and one NSCLC cell line (Fig. 7A). The first two cell lines had previously been reported to have partial deletions of the *FHIT* gene (Druck et al., 1997).

Mutational Analysis of DRR 1 in Tumor Samples

Primers DRR 2F/2R were used to amplify the full-length coding region of *DRR 1* mRNA in 17 tumor cell lines, 34 primary RCC tumors and their

TABLE I. Expressional and Mutational Analysis of DRR 1 Gene in Human Tumors[a]

Samples	Tumor origin	Expression	Base substitution	Polymorphism	Amino acid
HTB-44	RCC, papillary	Loss			
HTB-45	RCC	Loss	CCA to CTA at codon 19		Pro to Leu
HTB-46	RCC, clear cell	Loss			
HTB-47	RCC, clear cell	Loss	CCA to CTA at codon 19		Pro to Leu
HTB-49	RCC, clear cell	Loss	CTG to ATG at codon 15		Leu to Met
CRL-1611	RCC	Loss	CCA to CTA at codon 19		Pro to Leu
CRL-1932	RCC	Loss		TCC/GCC at codon 89	Ser to Ala
CRL-1933	RCC	Loss		CAG/CAA at codon 104	
OV167	OC	Normal		CAG/CAA at codon 104	
OV177	OC	Normal	98bp insert at nt455		
OV202	OC	Loss	CCA to CTA at codon 19		Pro to Leu
OV207	OC	Normal			
OV266	OC	Normal			
OVCAR-3	OC	Normal			
OV675	OC	Normal		CAG/CAA at codon 104	
C-33A	CC	Loss			
AGS	GC	Loss			
CRL-5803	NSCLC	Loss			
RCC1	RCC	Normal			
RCC2	RCC	Normal			
RCC3	RCC	Decrease			
RCC4	RCC	Decrease		CAG/CAA at codon 104	
RCC5	RCC	Decrease			
RCC6	RCC	Decrease			
RCC7	RCC	Normal			
RCC8	RCC	Decrease		TCC/GCC at codon 89	Ser to Ala
RCC9	RCC	Decrease			
RCC10	RCC	Decrease			
RCC11	RCC	Decrease			
RCC12	RCC	Normal			
RCC13	RCC	Normal		TCC/GCC at codon 89	Ser to Ala
RCC14	RCC	Decrease			
RCC15	RCC	Decrease		CAG/CAA at codon 104	
RCC16	RCC	Decrease			
RCC17	RCC	Normal			
RCC18	RCC	Decrease			
RCC19	RCC	Normal			
RCC20	RCC	Decrease			
RCC21	RCC	Normal			
RCC22	RCC	Normal			
RCC23	RCC	Decrease			
RCC24	RCC	Decrease			
RCC25	RCC	Normal		CAG/CAA at codon 104	
RCC26	RCC	Decrease			
RCC27	RCC	Decrease		CAG/CAA at codon 104	
RCC28	RCC	Decrease			
RCC29	RCC	Normal			
RCC30	RCC	Decrease			
RCC31	RCC	Decrease		CAG/CAA at codon 104	
RCC32	RCC	Decrease			
RCC33	RCC	Decrease			
RCC34	RCC	Decrease			

[a]RCC: renal cell carcinoma; OC: ovarian cancer; NSCLC: non–small-cell lung cancer; CC: cervical cancer; GC: gastric cancer.

corresponding normal kidney tissues, and 28 normal cDNA samples derived from different sources. The RT-PCR products were screened for mutations using the DHPLC system (Liu et al., 1998). RT-PCR products with potential mutations as determined by DHPLC were directly used for sequence analysis (ABI 377 sequencer). By comparing normal and tumor tissues, we identified several polymorphic sites within the gene (Table 1). Due to the almost complete absence of expression of *DRR 1* in
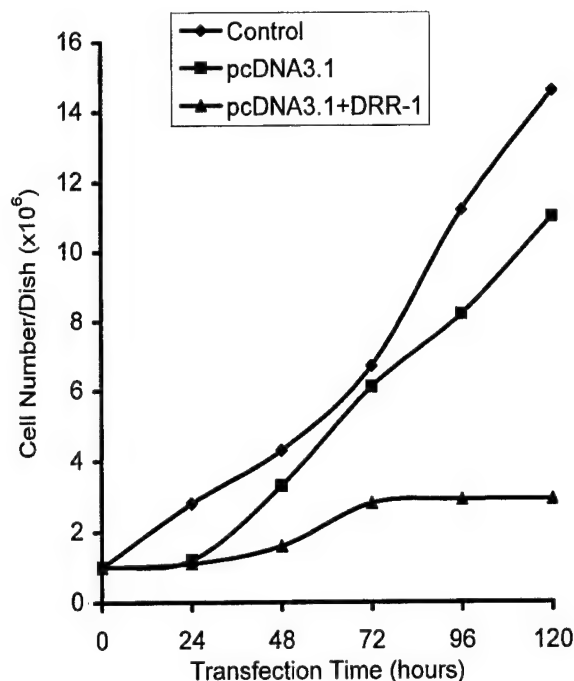
Figure 8. Suppression of cell growth by reexpression of the *DRR 1* gene. The *DRR 1* gene was transfected into an RCC cell line, HTB-44. At the indicated time points, the cells were collected and counted. The cells transfected with the *DRR 1* gene were clearly suppressed.

12 of 17 tumor cell lines, we were forced to use primers 2F/1R to amplify genomic DNA from those samples for sequence analysis. Of the 12 tumor cell lines examined, four (HTB-45, HTB-47, CRL-1611, and OV202) showed a base substitution at codon 19, producing an amino acid change from Pro to Leu, and one (HTB-49) had a heterozygous base substitution at codon 15, causing an amino acid change from Leu to Met. These alterations were not observed in an analysis of 34 normal kidney tissues and 28 normal individuals. We also detected an extra band by using primer pairs DRR 1F/2811R for RT-PCR in the ovarian cell line OV177. Sequence analysis demonstrated that 98 bp of unknown sequence (GenBank accession number AF089854) was inserted into the transcript just five nucleotides before the start codon in the cell line.

Expression of DRR 1 Gene and Cancer Cell Growth

We compared the cell growth rate after the *DRR 1* gene was transiently transfected into cells. The cell growth curves of cell line HTB-44 are shown in Figure 8. Included in this figure are untransfected cells (control) and vector-transfected cells (pcDNA3.1 only) as well as gene-transfected cells (pcDNA3.1 + *DRR 1*). This figure indicates that the transfection of *DRR 1* into HTB-44 cells definitely resulted in growth suppression of these

cells. The suppression of cell growth was also observed in another *DRR 1*–negative cell line, HTB-46 (data not shown). Thus, this gene appears to have definite growth suppression activity when transfected into cell lines lacking expression of this gene.

DISCUSSION

Several types of experimental evidence suggest that there are multiple tumor suppressor genes that map to the short arm of chromosome 3. Loss of heterozygosity (LOH) studies, as well as functional analyses, have demonstrated that a candidate tumor suppressor gene is located at 3p21 (Killary et al., 1992; Daly et al., 1993; Satoh et al., 1993). The transfer of a chromosome 3 could suppress ovarian tumor cell lines, but this suppression was lost if one of three small segments of 3p were lost. Two of these segments were located in 3p23–p24.2, and one was in 3p21.1–p21.2, suggesting that these chromosomal bands are important for suppression of tumorigenicity of ovarian carcinoma cells (Rimessi et al., 1994). However, large scale sequencing and positional cloning efforts within 3p21 thus far have not resulted in the discovery of a classical tumor suppressor gene that shows frequent mutations and/or deletions in human cancers (class I tumor suppressors) (Zou et al., 1994).

The aminoacylase 1 gene at 3p21.1 was reported to show low or undetectable enzymatic activity in 18 of 29 small cell lung cancer (SCLC) cell lines (Cook et al., 1993). *RIK*, another gene at 3p21.1, had low or undetectable expression in 11 of 15 primary RCCs (Erlandsson et al., 1990). Similar to the other two genes in 3p21.1, *DRR 1* in this study also showed low or undetectable expression in human tumors. It is very interesting that these three genes share a common feature, inactivation or downregulation in different tumors. These genes with low expression in tumors, combined with a decrease in tumorigenicity when expressed in cell lines, have been characterized as class II tumor suppressors (Zou et al., 1993). Our results indicate that *DRR 1* may be a class II tumor suppressor for RCC because of undetectable expression in all 8 RCC cell lines and low expression in 23 of 34 primary tumors, and the absence of any detectable mutations in *DRR 1* in any of these samples. Although no classical tumor suppressor gene has been identified from the 3p21 region, a number of genes have already been identified from this chromosomal band that show loss of expression in different tumor types. It is thus attractive to speculate that perhaps the regional inactivation of mul-

tiple genes from this chromosomal band contributes to tumor formation (Zou et al., 1994). Growth suppression by transfecting *DRR 1* into cancer cell lines further suggests that loss of expression of *DRR 1* correlates with growth advantage during RCC development.

The strong nuclear localization signal within the putative protein suggests that the *DRR 1* gene encodes a nuclear protein. We have demonstrated that this protein is indeed present in the nucleus. This small protein may interact with other proteins or DNA to regulate gene expression, because it contains a coiled region (Fig. 2). Several mechanisms may contribute to inactivation of a gene in human tumors, such as methylation and mutation. Cook et al. (1998) reported that point mutations within the coding region of the *ACY1* gene could cause inactivation of the gene in an SCLC cell line. Because Southern blots did not identify any gross structural change in the 12 tumor cell lines with undetectable expression of *DRR 1*, the loss of expression is probably caused by another mechanism. Our result shows that 4 of the 12 cell lines have a base substitution at codon 19 (Table 1). As a control, DNA samples from 62 unrelated normal individuals did not show the same nucleotide change, indicating that this nucleotide substitution is not a common polymorphism, and thus could possibly be responsible for inactivation of the gene in the four cell lines. The substitution may provide a selective advantage to these RCC cell lines. Whether the remaining eight cell lines with undetectable *DRR 1* transcripts have any other mutation within the noncoding region is unknown.

A 98-bp insert was identified just five nucleotides before the putative start codon ATG of the gene in RNA rather than DNA from the ovarian cancer cell line OV177. Therefore, it could be caused by a splicing error. The insert has no homology to any known DNA sequence. Because the open reading frame and expression of the gene seem not to be influenced by this insertion, and the wild-type form of this gene is coexistent in the cell line, the biological significance of the insertion of this unknown DNA fragment into the *DRR 1* CDNA remains to be determined.

DRR 1 was localized immediately telomeric to the *FHIT* gene, which is a frequent target of deletions in a number of different tumors (Huebner et al., 1998). This gene was localized to several YAC clones that overlap a YAC that contains the 3′ end of the *FHIT* gene. The *FHIT* gene spans the 3p14.2 common fragile site (FRA3B), which is the most active common fragile site in the human genome (Smeets et al., 1987). In contrast to other tumor suppressor genes, however, the potential mechanism of *FHIT* inactivation appears to be large chromosomal deletions, and no point mutations have been detected in this gene to date. This is a chromosomal region that shows frequent LOH that extends considerably beyond the *FHIT* gene; thus, *DRR 1* is definitely within a region that is also a frequent target of deletions in a number of different cancers. However, our mutational studies have demonstrated that this gene is not a mutational target. Instead, this gene could be inactivated by other mechanisms such as methylation. We are presently isolating the promoter sequences of this gene to determine whether there is methylation of this gene in tumors that lack expression of *DRR 1*.

In summary, we have cloned and characterized a gene called *DRR 1* at 3p21.1. The gene was found to have frequent loss of expression in several tumor cell lines and low expression in primary RCC tumors. The putative protein contains a nuclear localization signal and a coiled domain, suggesting that it has a potential role in the regulation of gene transcription and signal transduction. Suppression of cell growth by reexpression of *DRR 1* in these cells indicates that the gene has a potential role in the development of several cancers, including RCC.

REFERENCES

Cohen AJ, Li FP, Berg S, Marchetto DJ, Tasai S, Jacobs SC, Brown RS. 1979. Hereditary renal-cell carcinoma associated with a chromosomal translocation. N Engl J Med 301:592–595.

Cook RM, Burke BJ, Buchhagen DL, Minna JD, Miller YE. 1993. Human aminoacylase-1. Cloning, sequence, and expression analysis of a chromosome 3p21 gene inactivated in small cell lung cancer. J Biol Chem 268:17010–17017.

Cook RM, Franklin WA, Moore MD, Johnson BE, Miller YE. 1998. Mutational inactivation of aminoacylase-I in a small cell lung cancer cell line. Genes Chromosomes Cancer 21:320–325.

Daly MC, Xiang RH, Buchhagen D, Hensel CH, Garcia DK, Killary AM, Minna JD, Naylor SL. 1993. A homozygous deletion on chromosome 3 in a small cell lung cancer cell line correlates with a region of tumor suppressor activity. Oncogene 8:1721–1729.

Druck T, Hadaczek P, Fu TB, Ohta M, Siprashvili Z, Baffa R, Negrini M, Kastury K, Veronese ML, Rosen D, Rothstein J, McCue P, Cotticelli MG, Inoue H, Croce CM, Huebner K. 1997. Structure and expression of the human FHIT gene in normal and tumor cells. Cancer Res 57:504–512.

Erlandsson R, Bergerheim US, Boldog F, Marcsek Z, Kunimi K, Lin BY, Ingvarsson S, Castresana JS, Lee WH, Lee E. 1990. A gene near the D3F15S2 site on 3p is expressed in normal human kidney but not or only at a severely reduced level in 11 of 15 primary renal cell carcinomas (RCC). Oncogene 5:1207–1211.

Evron E, Cairns P, Halachmi N, Ahrendt SA, Reed AL, Sidransky D. 1997. Normal polymorphism in the incomplete trinucleotide repeat of the arginine-rich protein gene. Cancer Res 57:2888–2889.

Huang H, Qian C, Jenkins RB, Smith DI. 1998. FISH mapping of YAC clones at human chromosomal band 7q31.2: identification of YACS spanning FRA7G within the common region of LOH in breast and prostate cancer. Genes Chromosomes Cancer 21:152–159.

Huebner K, Druck T, Siprashvili Z, Croce CM, Kovatich A, McCue PA. 1998. The role of deletions at the FRA3B/FHIT locus in carcinogenesis. Recent Results Cancer Res 154:200–215.

Killary AM, Wolf ME, Giambernardi TA, Naylor SL. 1992. Definition of a tumor suppressor locus within human chromosome 3p21–p22. Proc Natl Acad Sci USA 89:10877–10881.

Kok K, Naylor SL, Buys CH. 1997. Deletions of the short arm of chromosome 3 in solid tumors and the search for suppressor genes. Adv Cancer Res 71:27–92.

Liu W, Smith DI, Rechtzigel KJ, Thibodeau SN, James CD. 1998. Denaturing high performance liquid chromatography (DHPLC) used in the detection of germline and somatic mutations. Nucl Acids Res 26:1396–1400.

Michaelis SC, Bardenheuer W, Lux A, Schramm A, Gockel A, Siebert R, Willers C, Schmidtke K, Todt B, van der Hout AH, Buys HCMC, Heppell-Parton A, Rabbitts P, Smith DI, LePaslier D, Cohen D, Opalka B, Schutte J. 1995. Characterization and chromosomal assignment of yeast artificial chromosomes containing human 3p13–p21 specific sequence tagged sites. Cancer Genet Cytogenet 81:1–12.

Ohta M, Inoue H, Cotticelli MG, Kastury K, Baffa R, Palazzo J, Siprashvili Z, Mori M, McCue P, Druck T, Croce CM, Huebner K.1996. The FHIT gene, spanning the chromosome 3p14.2 fragile site and renal carcinoma-associated t(3;8) breakpoint, is abnormal in digestive tract cancers. Cell 84:587–597.

Rimessi P, Gualandi F, Morelli C, Trabanelli C, Wu Q, Possati L, Montesi M, Barrett JC, Barbanti-Brodano G. 1994. Transfer of human chromosome 3 to an ovarian carcinoma cell line identifies three regions on 3p involved in ovarian cancer. Oncogene 9:3467–3474.

Satoh H, Lamb PW, Dong JT, Everitt J, Boreiko C, Oshimura M, Barrett JC. 1993. Suppression of tumorigenicity of A549 lung adenocarcinoma cells by human chromosomes 3 and 11 introduced via microcell-mediated chromosome transfer. Mol Carcinogen 7:157–164.

Schuler GD, Boguski MS, Stewart EA, Stein LD, Gyapay G, Rice K, White RE, Rodriguez-Tome P, Aggarwal A, Bajorek E, Bentolila S, Birren BB, Butler A, Castle AB, Chiannilkulchai N, Chu A, Clee C, Cowles S, Day PJ, Dibling T, Drouot N, Dunham I, Duprat S, East C, Hudson TJ. 1996. A gene map of the human genome. Science 274:540–546.

Shridhar R, Shridhar V, Rivard S, Siegfried JM, Pietraszkiewicz H, Ensley J, Pauley R, Grignon D, Sakr W, Miller OJ, Smith DI. 1996. Mutations in the arginine-rich protein gene, in lung, breast, and prostate cancers, and in squamous cell carcinoma of the head and neck. Cancer Res 56:5576–5578.

Shridhar V, Golembieski W, Kamat A, Smith SE, Phillips N, Miller OJ, Miller Y, Smith DI. 1994. Isolation of two contigs of overlapping cosmids derived from human chromosomal band 3p21.1 and identification of 5 new 3p21.1 genes. Somat Cell Mol Genet 20:255–265.

Smeets DF, Scheres JM, Hustinx TW. 1986. The most common fragile site in man is 3p14. Hum Genet 72:215–220.

Smith DI, Golembieski W, Drabkin H, Kiousis S. 1989. Identification of two cosmids derived from within chromosomal band 3p21.1 that contain clusters of rare restriction sites and evolutionarily conserved sequences. Am J Hum Genet 45:443–447.

Smith SE, Joseph A, Nadeau S, Shridhar V, Gemmill R, Drabkin H, Knuutila S, Smith DI. 1993. Cloning and characterization of the human t(3;6)(p14;p11) translocation breakpoint associated with hematologic malignancies. Cancer Genet Cytogenet 71:15–21.

Wang L, Darling J, Zhang JS, Qian CP, Hartmann L, Conover C, Jenkins R, Smith DI. 1998. Frequent homozygous deletions in the FRA3B region in tumor cell lines still leave the FHIT exons intact. Oncogene 16:635–642.

Zou Z, Anisowicz A, Hendrix MJ, Thor A, Neveu M, Sheng S, Rafidi K, Seftor E, Sager R. 1994. Maspin, a serpin with tumor-suppressing activity in human mammary epithelial cells. Science 263:526–529.

Involvement of H-cadherin (CDH13) on 16q in the region of frequent deletion in ovarian cancer

MASAKO KAWAKAMI[1], JULIE STAUB[1], WILLIAM CLIBY[3], LYNN HARTMANN[2], DAVID I. SMITH[1] and VIJI SHRIDHAR[1,4]

[1]Department of Experimental Pathology and Laboratory Medicine, [2]Department of Medical Oncology, Mayo Foundation; [3]Division of Gynecological Surgery, Mayo Clinic, Rochester, MN; [4]Department of Surgery, Wayne State University School of Medicine, and Karmanos Cancer Institute, Detroit, MI, USA

Abstract. Ovarian cancer is one of the leading causes of mortality unique to women. Deletions within chromosome 6q are the most frequent events in high-grade invasive epithelial ovarian cancer (IEOC). While previous reports seem to indicate that there is loss of 16q sequences in IOEC, only a very small number of markers (single marker in two different reports) were used. In order to more precisely define the regions of deletions on 16q, we first analyzed LOH with 13 polymorphic markers on 16q in 10 benign, 3 low-grade and 21 high-grade invasive ovarian cancer samples. There was no loss with any of the markers with the benign ovarian samples and loss of one marker in one of three low-grade tumors. In contrast, 14 of 21 (67%) high-grade invasive ovarian tumors showed loss of one or more markers. Detailed deletion mapping revealed three distinct commonly deleted regions on this chromosomal arm: 10/21 (48%) of high-grade tumors showed loss at 16q23.1-23.2 (D16S518, D16S3049 and D16S3029). The second region of loss at 16q23.3-16q24.1 (D16S3144, D16S504, HSD17B2 and D16S507) was observed in 11/21 (52%) of the tumors. The highest frequency of loss was seen at 16q24.2-16q 24.3 (D16S422, D16S402 and D16S520) in 12/21 (57%) of tumors. The genomic map of CDH13 indicates that the marker D16S422 that was lost in 5 of these 12 tumors is part of this gene. Three of these 5 tumors showed very low levels of CDH13 expression. Three tumors with LOH of other markers in this region also showed lower levels of CDH13 expression. Analysis of the methylation status of CDH13 in tumors with low levels of expression with methylation-specific PCR revealed that four of six (67%) tumors had methylation of one of the CDH13 alleles. These results suggest that a combination of hyper-methylation and deletion cause the inactivation of CDH13 in ovarian tumors.

Introduction

Ovarian cancer is a frequent cause of cancer death in women. The five-year survival rate for women with this cancer is only about 15-20% (1). The reason for this poor prognosis is due to the fact that 70% of ovarian cancers are not diagnosed until the disease is advanced in stage. It is therefore imperative to identify genes responsible for the development and progression of ovarian cancer that may have diagnostic and therapeutic value and which can be used to detect this cancer at earlier, more potentially treatable stages.

In common with other types of tumors, inactivation of tumor suppressor genes and activation of oncogenes are most likely involved in the multi-step process of ovarian carcinogenesis. Loss of heterozygosity (LOH) studies have led to the cloning of a number of tumor suppressor genes involved in the development and progression of several different types of cancer (2,3). LOH studies in ovarian tumors have delineated chromosomal regions on 1p, 3p, 5q, 6q, 7q, 8p, 9p, 13q, and 17p that may be involved in the development of this cancer (4-6). However, no ovarian cancer tumor suppressor gene has thus far been identified. Of the tumor suppressor genes identified thus far, only TP53 has been reported to have frequent mutations in ovarian cancer (7). While mutations in BRCA1 are more frequently observed in familial ovarian cancer, only 10% of sporadic cases of ovarian cancer have mutations in this gene (8).

Allele loss on 16q has been reported in a number of different cancers including breast cancer (9), prostate cancer (10), and hepatocellular carcinoma (11). In fact, LOH of 16q is one of the most consistent genetic alterations seen in sporadic prostate cancer (12). However, few markers have been tested on 16q for loss in ovarian cancer. Sato *et al* (1991) has shown 37% (11/30) loss with the marker D16S7 by RFLP analysis in ovarian tumors (13). In a similar analysis, Cliby *et al* (1993) used a single marker on 16q22.1 and observed a similar percentage of loss (35%; 6/17) (14). With the availability of closely spaced markers throughout the entire genome, it is now possible to more precisely define the specific chromosomal regions of allele loss in any type of tumor.

Correspondence to: Dr Viji Shridhar, Division of Experimental Pathology, Department of Laboratory Medicine and Pathology, Mayo Foundation, 200 First Street SW, Rochester, MN 55905, USA

Table I. Result of microsatellite analysis of the 24 epithelial ovarian samples with 13 polymorphic 16q markers.

Marker Sample	Grade	D16S512	D16S395	1			2				3			
				D16S518	D16S3049	D16S3029	D16S3144	D16S504	HSD17B2	D16S507	D16S422	D16S402	D16S520	D16S413
1	1	□	ND	□	□	□	UI	UI	□	□	■	□	□	□
2	2	□	UI	UI	□	ND	UI	UI	□	□	□	□	UI	□
3	2	□	□	□	□	□	UI	□	□	□	□	□	□	□
4	3	□	UI	■	UI	UI	□	■	■	□	UI	UI	■	■
5	3	UI	UI	□	■	ND	■	UI	□	□	■	■	□	ND
6	3	ND	□	□	ND	□	UI	UI	□	UI	UI	□	ND	□
7	3	□	□	□	UI	□	UI	□	□	□	□	□	■	□
8	3	□	□	□	□	□	UI	UI	□	□	UI	□	□	□
9	3	□	ND	□	□	□	□	UI	UI	□	□	□	□	□
10	3	ND	□	■	UI	■	■	UI	■	ND	□	■	■	ND
11	3	■	□	□	■	■	□	UI	UI	■	■	■	■	■
12	3	UI	ND	□	UI	UI	□	□	ND	ND	□	ND	■	□
13	3	□	□	□	□	□	□	□	UI	□	UI	□	UI	□
14	3	UI	□	□	■	□	□	UI	□	■	■	■	■	■
15	3	□	UI	□	□	□	□	□	■	UI	□	UI	■	■
16	3	UI	□	□	UI	UI	□	UI	□	UI	UI	UI	■	□
17	4	UI	□	□	□	ND	□	UI	□	ND	UI	UI	□	UI
18	4	UI	□	□	ND	□	UI	UI	□	ND	UI	□	□	ND
19	4	■	ND	■	□	■	□	UI	■	■	■	■	■	■
20	4	■	ND	UI	□	■	■	■	■	UI	□	UI	□	□
21	4	□	ND	UI	■	□	UI	■	□	UI	■	□	■	□
22	4	□	□	□	□	UI	UI	UI	□	UI	□	UI	UI	UI
23	4	□	■	■	□	□	UI	UI	■	UI	□	UI	□	□
24	4	■	ND	■	UI	UI	■	■	■	■	□	■	■	■

■, LOH; □, retained; UI, uninformative. The bars with numbers represent the three minimally deleted regions defined by the markers in specific regions of chromosome 16q.

H-cadherin (CDH13) is a candidate tumor suppressor gene belonging to the family of cell adhesion molecules. Loss of expression of CDH13 has been shown to be connected with breast cancer progression (3). More recently, Sato *et al* demonstrated the inactivation of CDH13 in lung tumorigenesis (15). In this study we report the inactivation of CDH13 by a combination of both deletion and hypermethylation in high-stage ovarian cancers.

Materials and methods

Materials. Tumors were collected from patients undergoing surgery for ovarian cancer at the Mayo Clinic (Rochester, MN). Fresh tumor samples were snap frozen at -70˚C until processed for DNA extraction. Tumor specimens were cryostat sectioned before DNA extraction. The sections were reviewed by a pathologist (Dr G. Keeney) to assess the tumor content in each section and for determination of histopathological subtype and grade. Only sections containing >90% tumor cells were used for DNA extraction. For constitutional DNA, blood samples were used from each patient.

LOH analysis. The markers used in this study are listed in Table II along with their chromosomal locations. The PCR reaction mix contained 50 ng of genomic DNA, 50 mM KCl, 10 mM Tris-HCl (pH 8.3), 1.5 mM $MgCl_2$, 200 µM concentration of each primer, 0.05 µl of α-^{32}P CTP (10 µci/µl),

Table II. Chromosomal locations of the markers used. Also included are the cumulative results of 16q LOH in the 24 epithelial ovarian samples.

Marker	LOH %	16q	cM distance
D16S512	19	16q22.2	78.62
D16S395	8	16q23.1	84.86
D16S518	24	16q23.1	85.43
D16S3049	25	16q23.2	87.83
D16S3029	25	16q23.2	87.83
D16S3144	29	16q23.3	91.6
D16S504	44	16q23.3	92.6
HSD17B2	35	16q24.1	93.976
D16S507	31	16q24.1	94.48
D16S422	35	16q24.2	96.59
D16S402	38	16q24.2	96.91
D16S520	55	16q24.3	97.645
D16S413	32	16q24.3	97.764

and 0.5 units of Taq polymerase (Promega) in a 10 μl reaction volume. The conditions for amplification were 94°C for two min, then 30 cycles of 94°C for 30 sec, 52-57°C for 30 sec, and 72°C for 30 sec in a Perkin Elmer-Cetus 9600 Gene-Amp PCR system in a 96-well plate. The PCR products were denatured and run on 6% polyacrylamide sequencing gels containing 8 M urea. The gels were dried and autoradiographed for 16-24 h and scored for LOH. Multiple exposures were used before scoring for LOH. Allelic imbalance indicative of LOH were scored when there was more than 50% loss of intensity of one allele in the tumor sample with respect to the matched allele from normal tissue. The evaluation of the intensity of the signal between the different alleles was determined by visual examination by two independent viewers (M. Kawakami and V. Shridhar).

Expression of CDH13 by RT-PCR. Five tumors with LOH at D16S422 locus (#5, 11, 14, 19, and 21) and three other tumors with no LOH at this locus (#7, 10, and 24) were selected for analysis of the expression of CDH13 by RT-PCR. RNA was extracted from the primary tumors with Trizol (Gibco BRL) following the manufacturer's instructions. The integrity of the RNA in these samples was confirmed by denaturing agarose gel electrophoresis. One μg of total RNA was used in a reverse transcription reaction after DNase treatment. The conditions for the reverse transcription reactions were as previously described (16). Then 1 μl of the synthesized cDNA was added to 24 μl of reaction solution, and RT-PCR was performed as described by Sato *et al* (15). The conditions for amplification were 94°C for 2 min for the initial denaturation followed by 30 cycles of 94°C for 30 sec, 55°C for 30 sec, and 72°C for 30 sec with a final elongation of 5 min at 72°C.

HCAD-sense primer (5'-TTCAGCAGAAAGTGTTCCATA T-3') and the HCAD anti-sense primer (5'-GTGCATGGAC GAACAGAGT-3') are within exons 2 and 3 of the CDH13 gene respectively. As a control, GAPDH was amplified from 1 μl of the synthesized cDNA at the same time in separate reactions under the same conditions. Equal volumes of the GAPDH and CDH13 reactions from each sample were pooled before resolving the products on a 2% agarose gel.

Methylation-specific PCR (MS-PCR). The methylation state of CDH13 was determined using the recently described technique of MS-PCR (17). DNA was modified with sodium bisulfite as described by Herman *et al*, with the following modifications: 1-1.5 μg of DNA was digested with EcoRI in a 50 μl reaction overnight. The digested DNA was extracted once with phenol-chloroform-isoamyl alcohol (25:24:1) and precipitated with 1/10 volume of 5.0 M ammonium acetate and 100% ethanol in the presence of 1 μl of 20 mg/ml glycogen (Boehringer-Mannheim). The DNA pellet was washed twice with 70% ethanol and the DNA was taken up in 90 μl of TE. Ten μl of freshly prepared 3.0 M NaOH was added to each sample and the DNA was denatured at 42°C for 30 min. After the addition of 10 μl of distilled water, 1020 μl of 3.0 M sodium bisulfite (pH 5.0) and 60 μl of 10 mM hydroquinone, the samples were incubated in the dark at 55°C overnight (16-20 h). Modified DNA was purified using the Wizard purification system (Promega, Cat# A7548) according to the manufacturer's instructions, followed by a final denaturation step with 0.3 M NaOH for 15 min at 37°C. The DNA was eluted in 50-100 μl of TE and stored at -20°C in the dark.

The primers for amplifying methylated sequences for CDH13 were from Sato *et al* (15) and were: H-cad-MF: 5'-T CGCGGGGTTCGTTTTTCGC-3'; H-cad-MR: 5'-GACTTTT CATTCATACACGCG-3'.

PCR was performed by 'hot-start' method using Taq-Gold from Perkin-Elmer with an initial denaturation of 10 min at 95°C to activate the enzyme, followed by 35 cycles at 95°C for 30 sec, 60°C for 30 sec, and 72°C for 30 sec, with a final extension cycle at 72°C for 10 min with primers amplifying methylated sequences. Controls with unmodified DNA were performed for each set of reactions.

Results and Discussion

We examined loss of heterozygosity (LOH) using 13 polymorphic microsatellite markers on the long arm of chromosome 16 in 10 benign, 3 low-grade (1 and 2), and 21 high-grade (3 and 4) ovarian tumors (Table I). With the exception of tumor #22 (stage IIB), the other 23 tumors were late-stage (IIIC to IV) tumors. The map positions and the genetic distance between the markers are based on the LDB database (Genetic Location Database at the University of Southampton, UK) (Table II). None of the 10 benign tumors showed any loss of alleles with the tested markers (data not shown). The single grade 1 tumor had a loss with one of the markers (D16S422, which maps to 16q24.2). Grade 2 tumors showed no loss with any of the tested markers.

Of the 21 high-grade tumors, 13 were grade 3 tumors and 8 were grade 4; 14 of 21 (67%) high-grade tumors had loss
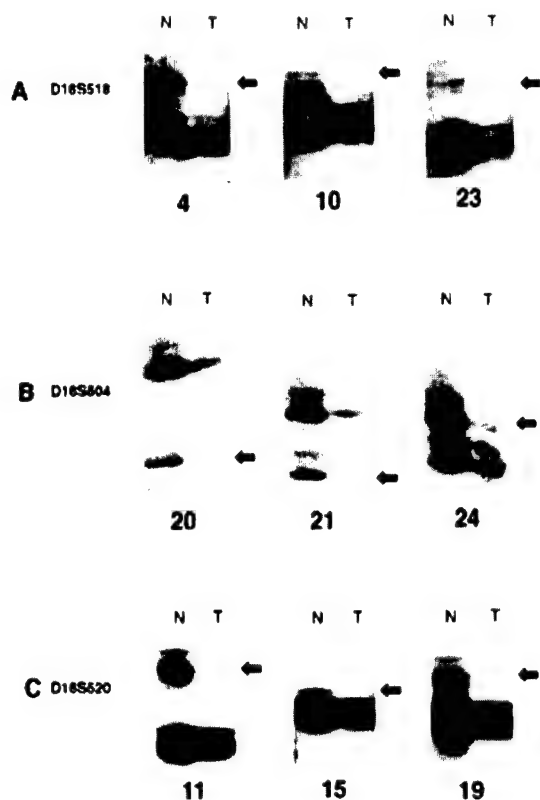
Figure 1. Representative examples of LOH in epithelial ovarian tumors. Autoradiographs of LOH results of selected tumor samples in three distinct regions of 16q. For each panel, the tumor # is shown below and the individual markers are on the side. A, Marker D16S518 shows loss of allele in tumors 4, 10, and 23. B, Marker D16S504 shows loss of allele in tumors 20, 21 and 24. Marker D16S520 shows loss of allele in tumors 11, 15, and 19. N, normal DNA; T, tumor DNA. Arrows indicate loss of allele in the tumor sample.

of one or more marker on 16q. We did not find loss of the whole chromosomal arm in any of the tumors analyzed. The 14 high-grade tumors that showed LOH were found to have one or more interstitial deletions as evidenced by allelic loss at some loci and retention of flanking loci (Table I). The LOH analysis defined three regions of loss on 16q. Tumors 10, 11, 19, and 23 showed loss of a common region in 16q23.1-23.2 between markers D16S395 and D16S3029. The estimated recombination distance between these markers is about 3 cM. Tumors 4, 5, 14, 21, and 24 also showed allele loss of at least one of the markers mapped to this region. Taken together this accounts for 43% (9/21) of the tumors showing loss in this region. Tumors 4, 10, 19, 20, and 24 define a second minimally deleted region in 16q 23.3-24.1 defined by markers D16S3144, D16S504, HSD17B2 and D16S507 (Fig. 1). Tumors 5, 11, 14, 15, 21, and 23 showed loss of at least one of the markers in this region. Marker D16S504 showed 44% loss while the flanking marker HSD17B2, which is 1.7 cM telomeric to D16S504, showed the second highest frequency of loss (35%) in this region (Fig. 2). The gene product of HSD17B2 converts 17-hydroxysteroids into 17-keto forms. This inactivates male and female sex steroids in both peripheral and target tissues (18). Recently Elo *et al* showed the highest frequency of LOH with HSD17B2 (63%) in prostate tumors (19).

The third region of deletion is seen with the markers D16S422, D16S402, D16S520, and D16S413 that are derived from 16q24.2-24.3. Tumors 5, 10, 11, 14, 19, 21, and 24 showed loss of alleles of D16S422 and D16S402, while tumors 4, 7, 12, 15, and 16 had lost either one of the distal markers D16S520 and D16S413 or both. The distance between markers D16S402 and D16S422 is only 320 kb. Tumors 4 and 15 had lost only the distal markers D16S520 and D16S413 that were separated by a distance of less than 150 kb. The single grade 1 tumor also showed loss of D16S422. We found that 57% (12/21) of the high-grade tumors showed loss in this region. The genetic mapping information (LDB database) suggests that the genetic distance between D16S422 and D16S413 is 1.1 cM. Since we did not test markers distal to D16S413, we do not know whether tumors with LOH of this marker have terminal deletions.

Candidate tumor suppressor genes mapped to this third region of allele loss include HSD17B2 and H-cadherin (CDH13). The genomic map of H-cadherin (CDH13) indicates that the marker D16S422 is part of this gene (15). H-cadherin belongs to a super-family of cell-adhesion molecules. Sato *et al* showed loss of expression of this gene in 57% of lung cancer cell lines and Lee *et al* showed reduced levels of expression of CDH13 in breast cancer (15,20). We examined the expression of CDH13 by RT-PCR as described by Mori *et al* (21). The primers used for this analysis amplified a product that includes exons 2 and 3 in the region of marker D16S422 (15). The conditions for amplification of CDH13 and GAPDH are as described in the Materials and methods section. Our attempts to co-amplify CDH13 and GAPDH gave inconsistent results with regard to both products. This kind of analysis clearly indicated that while the expression of GAPDH was consistent in all the samples analyzed, the expression of CDH13 was variable (Fig. 3A). Tumors 7, 10, 14, and 19 clearly had very low levels of expression of CDH13 compared to GAPDH. In addition tumors 21 and 24 showed decreased levels of expression in comparison to tumors 5, and 11. The samples with LOH of D16S422 and lower levels of expression of CDH13 are 14, 19 and 21. Samples 5 and 11 expressed CDH13 and had LOH of the D16S422 locus. The results from the study of Sato *et al* suggests that a combination of deletion and hyper-methylation leads to the inactivation of CDH13 gene in the lung cancer tumors analyzed (15). In our samples, we did not observe a complete loss of expression of CDH13. However, we could not rule out the possibility of methylation of one of the alleles in samples that showed lower levels of CDH13 expression with no concomitant loss of the D16S422 locus.

In order to test this, we performed methylation-specific PCR (MS-PCR) on two sets of tumor samples, one tumor group that showed LOH with the marker D16S422 and the other group that had no loss with this marker but did have allele loss in a more proximal region. All the tumors analyzed showed lower levels of expression of CDH13. The first set of tumors with LOH of D16S422 and lower levels of CDH13 expression were tumors 14, 19, and 21. Two of the three tumors (tumors 14 and 19) amplified a specific product with H-cadherin methyl-specific primers. The presence of contaminating normal cells could probably explain why these three tumors did not show a complete loss of expression of
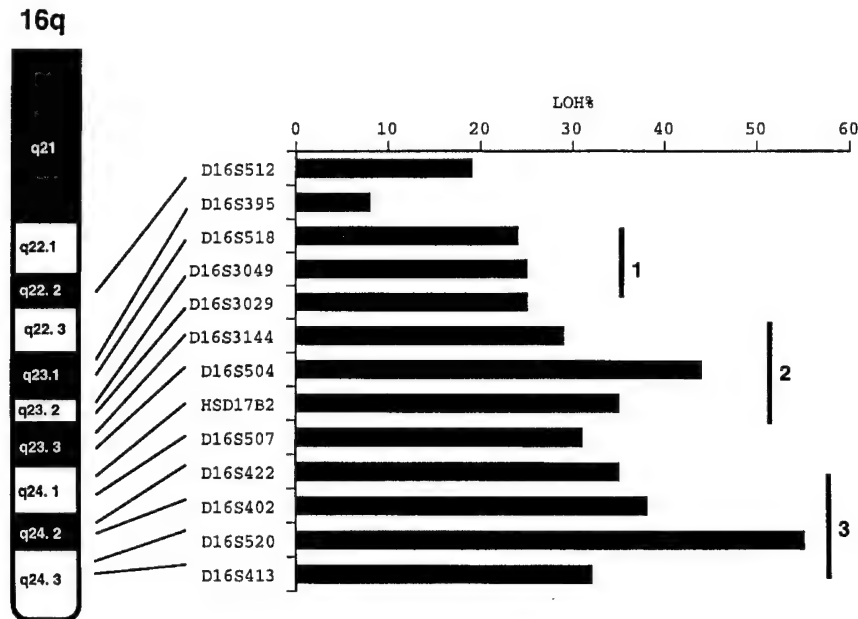
Figure 2. Graphic representation of the frequency of LOH with specific 16q markers. X-axis, markers used; Y-axis, percentage of tumors showing LOH. The bars with numbers above each peak of loss represent the three different regions of loss.
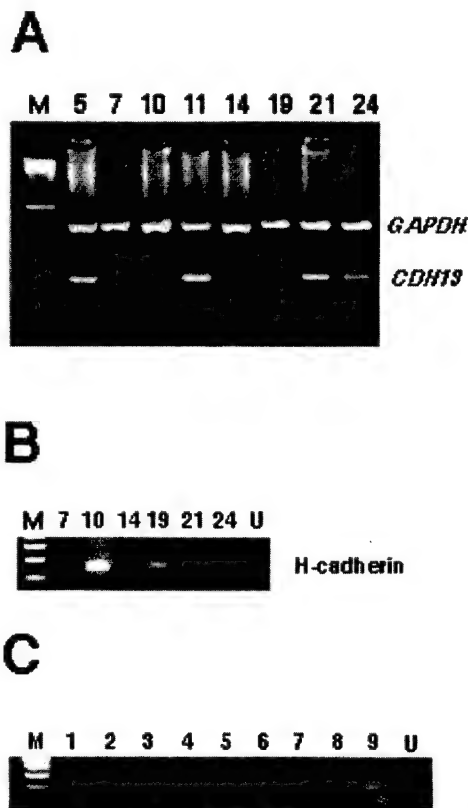
Figure 3. The results of RT-PCR (A) and MSP-PCR (B and C) in selected tumors. A, GAPDH, Glyceraldehyde-3 phosphate; CDH13, Cadherin 13. Note lower levels of expression of CDH13 in tumors 7, 10, 14, 19, and 24 in comparison to GAPDH in respective tumors. B and C, Methylation-specific PCR (MSP) analysis of H-cadherin. Amplification of bisulfite modified DNA from B (high grade tumors) and C (benign tumors). U, unmodified DNA control; M, 100 bp ladder. The tumor numbers are indicated on top of the panel.

CDH13. Two other tumors (tumor 10 and 24) with lower levels of expression but no LOH at D16S422 also amplified a methylation-specific product. This seems to indicate that the lower level of expression of CDH13 seen in these tumors is probably due to methylation of one of the HCAD alleles. Thus overall four of six tumors (67%) with lower levels of CDH13 expression also had methylation of one of the CDH13 alleles.

In order to evaluate the methylation status of CDH13 in benign tumors that had no loss with any of the markers tested, we performed MSP-PCR with H-cadherin primers in nine benign tumors. Only one of nine benign tumors amplified with H-cadherin primers (Fig. 3C). Although only three low-grade tumors were analyzed, the observation that none of the benign tumors or any of the three low-grade tumors showed loss on 16q probably indicates that LOH on 16q may be a late event (which may be associated with metastasis) as seen in prostate cancer. Interestingly, the same three low-grade tumors showed a very high frequency of LOH on 6q (22). Also, eight of nine benign tumors did not reveal any methylation-specific product with MSP-PCR with H-cadherin. Thus, methylation of H-cadherin is also probably a later event in the development of ovarian cancer.

In conclusion, our data shows the existence of three independent regions of deletion in ovarian cancer with the most frequently deleted region of loss at 16q24.2-24.3. LOH detected here was observed only in high-grade tumors. While our data do not conclusively prove the involvement of CDH13 as a tumor suppressor in ovarian carcinogenesis, the methylation analysis coupled with the LOH data with the D16S422 marker indicates that H-cadherin may be a gene involved in the progression of ovarian cancer. In addition to observing frequent deletions in this region, we have also found two distinct regions on 16q that also have frequent deletions in high-grade ovarian tumors. Thus, there is the

possibility that multiple tumor suppressor genes exist that map to this chromosomal arm.

Acknowledgements

References

1. Landis S, Murray T, Bolden S and Wingo P: Cancer statistics. Cancer J Clin 48: 6-29, 1998.
2. Latif F, Tory K, Gnarra J, Yao M, Duh F, Orcutt M, Stackhouse T, Kuzmin I, Modi W, Geil L, Schmidt L, Zhlu F, Li H, Wei M, Chen F, Glenn G, Choyke P, Walther M, Weng Y, Duan D, Dean M, Glavac D, Richards F, Crossey P, Lee W, Bookstein R, Hong F, Young L, Shew J and Lee E: Identification of the von Hippel-Lindau disease tumor suppressor gene. Science 260: 1317-1320, 1993.
3. Lee S: H-cadherin, a novel cadherin with growth inhibitory functions and diminished expression in human breast cancer. Nat Med 2: 776-782, 1996.
4. Jiang X, Hitchcock A, Bryan E, Watson R, Englefield P, Thomas E and Campbell I: Microsatellite analysis of endometriosis reveals loss of heterozygosity at candidate ovarian tumor suppressor gene loci. Cancer Res 56: 3534-3539, 1996.
5. Foulkes W, Ragoussis J, Stamp G, Allan G and Trowsdale J: Frequent loss of heterozygosity on chromosome 6 in human ovarian carcinoma. Br J Cancer 67: 551-559, 1993.
6. Saito S, Sirahama S, Matsushima M, Suzuki M, Sagae, Kudo R, Saito J, Noda K and Nakamura Y: Definition of a commonly deleted region in ovarian cancers to a 300-kb segment of chromosome 6q27. Cancer Res 56: 5586-5589, 1996.
7. Kupryjanczyk J, Thor A, Beauchamp R, Merritt V, Edgerton S, Bell D and Yandell D: P53 gene mutations and protein accumulation in human ovarian cancer. Proc Natl Acad Sci USA 90: 4961-4965, 1993.
8. Takahashi H, Behbakht K, McGovern P, Chiu H, Couch F, Weber B, Friedman L, King M, Furusato M, Li Volsi V, Menzin A, Liu P, Benjamin I, Morgan M, King S, Rebane B, Cardonick A, Mikuta J, Rubin S and Boyd J: Mutation analysis of the BRCA1 gene in ovarian cancers. Cancer Res 55: 2998-3002, 1995.
9. Hansen L, Yilmaz M, Overgaard J, Andersen J and Kruse T: Allelic loss of 16q23.2-24.2 is an independent marker of good prognosis in primary breast cancer. Cancer Res 58: 2166-2169, 1998.
10. Latil A, Cussenot O, Fournier G, Driouch K and Lidereau R: Loss of heterozygosity at chromosome 16q in prostate adenocarcinoma: identification of three independent regions. Cancer Res 57: 1058-1062, 1997.
11. Piao Z, Park C, Park JH and Kim H: Allelotype analysis of hepatocellular carcinoma. Int J Cancer 75: 29-33, 1998.
12. Jenkins R, Takahashi S, De Lacey K, Bergstrahl E and Lieber M: Prognostic significance of allelic imbalance of chromosome arms 7q, 8p, 16q, and 18q in stage T3N0M0 prostate cancer. Genes Chromosomes Cancer 21: 131-143, 1998.
13. Sato T, Saito H, Morita R, Koi S, Lee J and Nakamura Y: Allelotype of human ovarian cancer. Cancer Res 51: 5118-5122, 1991.
14. Cliby W, Ritland S, Hartmann L, Dodson M, Halling K, Keeney G, Podratz K and Jenkins R: Human epithelial ovarian cancer allelotype. Cancer Res 53: 2393-2398, 1993.
15. Sato M, Mori Y, Sakurada A, Fujimura S and Horii A: The H-cadherin (CDH13) gene is inactivated in human lung cancer. Hum Genet 103: 96-101, 1998.
16. Kawakami M, Okaneya T, Furihata K, Nishizawa O and Katsuyama T: Detection of prostate cancer cells circulating in peripheral blood by reverse transcription-PCR for hKLK2. Cancer Res 57: 4167-4170, 1997.
17. Herman G, Graff R, Myohanen S, Nelkin D and Baylin B: Methylation-specific PCR: a novel PCR assay for methylation status of CpG islands. Proc Natl Acad Sci USA 93: 9821-9826, 1996.
18. Elo J, Akinola L, Poutanen M, Vihko P, Kyllonen A, Lukkarinen O and Vihko R: Characterization of 17 beta-hydroxysteroid dehydrogenase isoenzyme expression in benign and malignant human prostate. Int J Cancer 66: 37-41, 1996.
19. Elo J, Harkonen P, Kyllonen A, Lukkarinen O, Poutanen M, Vihko R and Vihko P: Loss of heterozygosity at 16q24.1-q24.2 is significantly associated with metastatic and aggressive behavior of prostate cancer. Cancer Res 57: 3356-3359, 1997.
20. Lee W, Bookstein R, Hong F, Young L, Shew J and Lee E: Human retinoblastoma susceptibility gene: cloning, identification, and sequence. Science 235: 1395-1399, 1987.
21. Mori Y, Shiwaku H, Fukushige S, Wakatsuki S, Sato M, Nukiwa T and Horii A: Alternative splicing of hMSH2 in normal human tissues. Hum Genet 99: 590-595, 1997.
22. Shridhar V, Staub J, Huntley B, Cliby W, Jenkins R, Pass H, Hartmann L and Smith D: A novel region of deletion on chromosome 6q23.3 spanning less than 500 Kb in high-grade invasive epithelial ovarian cancer. Oncogene (In press).

Carboxypeptidase A3 (CPA3): A Novel Gene Highly Induced by Histone Deacetylase Inhibitors during Differentiation of Prostate Epithelial Cancer Cells[1]

Haojie Huang, Christopher P. Reed, Jin-San Zhang, Viji Shridhar, Liang Wang, and David I. Smith[2]

Division of Experimental Pathology, Department of Laboratory Medicine and Pathology, Mayo Foundation, Rochester, Minnesota 55905

ABSTRACT

Butyrate and its structural analogues have recently entered clinical trials as a potential drug for differentiation therapy of advanced prostate cancer. To better understand the molecular mechanism(s) involved in prostate cancer differentiation, we used mRNA differential display to identify the gene(s) induced by butyrate. We found that the androgen-independent prostate cancer cell line PC-3 undergoes terminal differentiation and apoptosis after treatment with sodium butyrate (NaBu). A novel cDNA designated carboxypeptidase A3 (CPA3), which was up-regulated in NaBu-treated PC-3 cells, was identified and characterized. This gene expresses a 2795-bp mRNA encoding a protein with an open reading frame of 421 amino acids. CPA3 has 37–63% amino acid identity with zinc CPs from different mammalian species. It also shares 27–43% amino acid similarity with zinc CPs from several nonmammalian species, including *Escherichia coli*, yeast, *Caenorhabditis elegans*, and *Drosophila*. The structural similarity between CPA3 and its closest homologues indicates that the putative CPA3 protein contains a 16-residue signal peptide sequence, a 95-residue NH_2-terminal activation segment, and a 310-residue CP enzyme domain. The consistent induction of CPA3 by NaBu in several prostate cancer cell lines led us to investigate the signaling pathway involved in the induction of CPA3 mRNA. Trichostatin A, a potent and specific inhibitor of histone deacetylase, also induced CPA3 mRNA expression, suggesting that *CPA3* gene induction is mediated by histone hyperacetylation. We demonstrated that CPA3 induction was a downstream effect of the treatment with butyrate or trichostatin A, but that the induction of $p21^{WAF1/CIP1}$ occurred immediately after these treatments. We also demonstrated that the induction of CPA3 mRNA by NaBu was inhibited by $p21^{WAF1/CIP1}$ antisense mRNA expression, indicating that p21 transactivation is required for the induction of CPA3 by NaBu. Our data demonstrate that the histone hyperacetylation signaling pathway is activated during NaBu-mediated differentiation of PC-3 cells, and the new gene, *CPA3*, is involved in this pathway.

INTRODUCTION

Prostate cancer is the most commonly diagnosed cancer and the second leading cause of cancer-related deaths in men in the United States. Within the prostate, androgens are capable of stimulating proliferation, as well as inhibiting the rate of epithelial cell death. Androgen withdrawal triggers the programmed cell death pathway in both normal prostate epithelium and androgen-dependent prostate cancer cells. Currently, the ablation of testosterone remains the most effective systemic therapy of advanced carcinoma of the prostate and is believed to induce apoptosis in these tumors (1). However, tumor cells that were formerly sensitive to androgen ablation therapy almost always emerge as androgen-independent tumors after 1–3 years of treatment (2). The development of resistance to androgen ablation

therapy acquired by prostate tumor cells remains a severe obstacle to the effective treatment of metastatic prostate cancer (3, 4). Androgen-independent prostate cancer cells do not initiate the programmed cell death pathway on androgen ablation; however, they do retain the cellular machinery necessary to activate the differentiation and programmed cell death cascade when these cellular processes are sufficiently initiated by injury to the cell induced by various exogenous damaging agents (*e.g.*, radiation, chemicals, viruses) or by changes in the levels of a series of endogenous signals (*e.g.*, hormones or growth/survival factors). Therefore, differentiation therapy or apoptosis therapy has been proposed as a method for the treatment of advanced prostate cancer (5–7).

Butyrate, a four-carbon short-chain fatty acid, is naturally produced by bacterial fiber fermentation within the colon and is found in the plasma of mammals (8). The biological significance of this compound is its ability to regulate cell growth and differentiation. Several studies have established that this agent has the ability to induce *in vitro* differentiation of prostate cancer, breast cancer, pancreatic cancer, and hematopoietic cells (9–12). The concentrations of butyrate that cause growth inhibition *in vitro* are similar to those measured within the mammalian colon (13), and it has been found to inhibit the growth of colon carcinoma cells *in vivo* (14). Although the molecular mechanisms by which butyrate mediates its effects are not well understood, it is known to induce a variety of changes within the nucleus, including histone hyperacetylation and the changes are secondary to hyper- or hypo-methylation of DNA (15, 16). Histone acetylation has been shown to have a permissive effect on mRNA transcription (17), possibly by relaxing specific segments of tightly coiled DNA and thereby facilitating the binding of transcription factors to selectively activate expression of genes (18, 19). Numerous epidemiological and experimental studies have found an association between a high-fiber diet and a decreased incidence and growth of colon cancer (20). The molecular link between a high-fiber diet and the arrest of colon carcinogenesis has been investigated, and it has been established that butyrate mediates growth inhibition of colon cancer cells by inducing $p21^{WAF1/CIP1}$ expression through histone hyperacetylation (21). Recently, the product of certain oncogenes was shown to suppress transcription of their target genes by recruiting histone deacetylase (22–24), which cleaves acetyl groups from histones and blocks their ability to induce DNA conformational changes. This transcriptional block can be overcome by agents that inhibited histone deacetylase, and, clinically, transcription targeting therapy for leukemia has been achieved by using butyrate to inhibit histone deacetylases to relieve the transcriptional repression caused by certain oncogenes (25).

Butyrate and its structural analogues recently entered clinical trials for prostate cancer at the National Cancer Institute (26). In the present study, we sought to investigate the molecular mechanisms by which butyrate mediates growth arrest and differentiation of androgen-independent prostate cancer cells and to identify potential markers for the diagnosis and treatment of androgen-independent prostate cancer. We first treated the androgen-independent prostate cancer cell line PC-3

with NaBu[3] and confirmed that they underwent typical differentiation and apoptosis. We then used the DD-PCR technique to identify a new gene, designated *CPA3*, which was up-regulated in PC-3 cells induced by NaBu. A homology search indicated that CPA3 belongs to the CP family that includes prostate-specific membrane antigen. We also demonstrate that the induction of CPA3 is due to the histone hyper-acetylation pathway.

MATERIALS AND METHODS

Cell Culture and Treatment. The prostate cancer cell lines PC-3, DU145, and LNCaP and the pancreatic cancer cell lines AsPC-1, BXPC-3, Capan-1, HS.766, PANC-1, and SU.86 were purchased from the American Type Culture Collection (Manassas, VA). Dr. Donald J. Tindall (Department of Urologic Research, Mayo Foundation, Rochester, MN) kindly provided the BPH1 benign prostatic hyperplasia cell line. All cells were maintained at 37°C as monolayers in a humidified atmosphere containing 5% CO_2. Cells were passaged at confluence by trypsinization. Tissue culture medium for each cell line was as follows. PC-3, DU145 and LNCaP were grown in RPMI 1640 (Life Technologies, Inc., Grand Island, NY) containing 10% fetal bovine serum, 100 units/ml penicillin, and 100 μg/ml streptomycin; BPH1 was cultured in RPMI 1640 containing 5% fetal bovine serum, 100 units/ml penicillin, and 100 μg/ml streptomycin. Chemical treatments were performed on cells that were 60–80% confluent. Cells were treated with various concentrations of NaBu or TSA as indicated. Some cells were pretreated with actinomycin D (4 μM) or concomitantly treated with CHX (10 μg/ml). All these chemicals mentioned were obtained from Sigma Chemical Co. (St. Louis, MO).

Analysis of Apoptotic DNA. To determine whether DNA fragmentation occurred after treatment with NaBu, all cells were collected and the DNA was extracted by the method described by Borner *et al.* (27). Attached cells were detached from the culture dishes with 5 mM EDTA, pooled with detached cells, spun down, and lysed in 5 mM Tris (pH 7.4), 5 mM EDTA, and 0.5% Triton X-100 for 2 h on ice. The lysate was centrifuged at 27,000 $\times$ g for 20 min. The supernatant was incubated with 200 μg/ml proteinase K for 1 h at 50°C and extracted with phenol/chloroform; then the DNA was precipitated overnight at −20°C in 2 volumes of ethanol and 0.13 M NaCl with 20 μg glycogen. Nucleic acids were treated with 1 mg/ml boiled bovine pancreatic RNase A for 1 h at 50°C, then the DNA was loaded onto a 2% (w/v) agarose gel containing 0.3 μg/ml ethidium bromide, and run in 1 x TBE buffer at 2.5 V/cm.

mRNA DD. The DD-PCR technique was used to identify genes up-regulated or down-regulated by butyrate treatment (28, 29). Total RNA was extracted from PC-3 cells exposed to NaBu (10 mM) for different periods of time using Trizol (Life Technologies, Inc.) and treated with RNase-free DNase I (Life Technologies, Inc.) to eliminate genomic DNA contamination. mRNA DD-PCR was performed using the RNAimage Kit (GenHunter, Corp., Nashville, TN). After isolation of potentially interesting cDNA fragments from the differential display gel, each fragment was reamplified and cloned into the pGEM-T vector (Promega, Madison, WI). Cloned cDNAs were then sequenced, followed by database analysis, Northern blot hybridization, and RACE.

5'-RACE. To obtain the full-length cDNA sequence of CPA3, the 5'-RACE procedure was used. cDNA was synthesized from poly(A)$^+$ RNA isolated from NaBu-treated PC-3 cells. Adaptor ligation and PCR were performed using the Marathon cDNA Amplification Kit following the manufacturer's recommendations (Clontech, Palo Alto, CA).

Northern Blot Analysis. Total cellular RNA (10–15 μg) was applied to and run on 1.2% denaturing formaldehyde-agarose gels and transferred onto positively charged nylon membranes. Filters were hybridized first with [^{32}P]dCTP-labeled target cDNA (CPA3, p21, and Actin) and, after stripping, rehybridized with [^{32}P]dCTP-labeled GAPDH and 18S rRNA as controls. Human multiple tissue Northern blots were purchased from Clontech (numbers 7759-1 and 7760-1). According to the manufacturer's information, each lane

was loaded with ~2 μg of poly(A)$^+$ RNA prepared from different normal human tissues. The premade blots were hybridized with the CPA3 full-length cDNA probe and, after stripping, rehybridized with a human actin cDNA probe as a control.

Construction and Transient Transfection with the Antisense p21$^{WAF1/CIP1}$ Expression Vector. On the basis of the p21$^{WAF1/CIP1}$ cDNA sequence (GenBank number U03106), two primers were designed to amplify a 530-bp fragment of p21$^{WAF1/CIP1}$ (from base 66–595). A *Bam*HI (Promega) cut site (*underlined*) was inserted into the forward primer AGGA*GGATC-C*ATGTCAGAA, and a *Hin*dIII (Promega) cut site (*underlined*) was inserted into the reverse primer GGACTGC*AAGCTT*CCTGTGG. The PCR product was digested with both *Bam*HI and *Hin*dIII, and a 517-bp cDNA fragment from the 5' end of the p21$^{WAF1/CIP1}$ coding region that includes the start ATG codon was isolated, then subcloned into the cloning sites of the mammalian expression vector pcDNA3.1(+) (Invitrogen, Carlsbad, CA) and transformed into *Escherichia coli* DH5α (Life Technologies, Inc.). Mini-preparations of ampicillin-resistant clones were sequenced and analyzed for the orientation of the inserts. Transient transfections were accomplished by using the LipofectAmine Plus system (Life Technologies, Inc.). To examine the effects of p21$^{WAF1/CIP1}$ transactivation on CPA3 mRNA induction by NaBu, PC-3 cells were transfected with a p21$^{WAF1/CIP1}$ antisense expression plasmid before treatment with NaBu. For controls, cells were similarly transfected with pcDNA3.1(+). Exponentially growing cells in 100-mm culture dishes were washed with serum-free medium, then a mixture of 5 μg of plasmid, 30 μl of LipofectAmine, and 20 μl of Plus was added. After a 3-h incubation, we added complete medium with serum, and then the cells were incubated at 37°C; 24 h
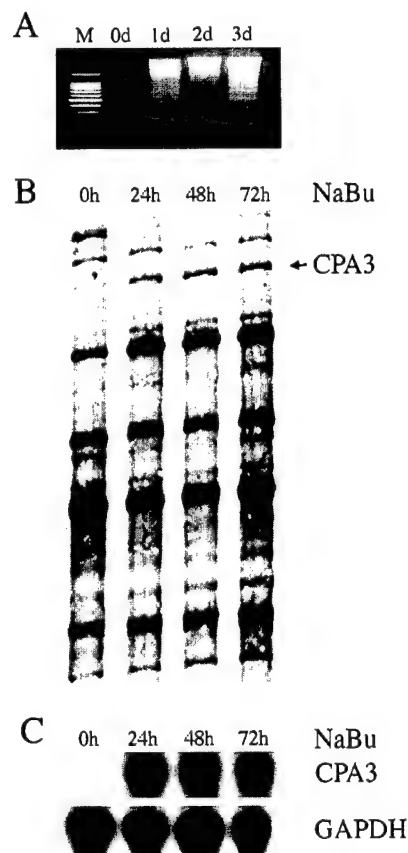
Fig. 1. *A*, agarose gel electrophoresis of DNA from NaBu-treated PC-3 cells demonstrating the DNA fragmentation associated with apoptosis in these cells. Cells were treated with 10 mM NaBu for 0, 1, 2, and 3 days. *Lane 1* (*M*) was loaded with a 100-bp DNA ladder from Life Technologies Inc. (Grand Island, NY) as a marker. *B*, mRNA DD of samples recovered from PC-3 cells treated with 10 mM NaBu for 0, 24, 48, and 72 h was performed by conducting PCR with primer pairs of H-T11G (5'-AAGCTTTTTTTTTTTTG-3') and AP10 (5'-AAGCTTCTGGGGT-3'). The CPA3 cDNA fragment identified is marked with an *arrow*. *C*, Northern blot analysis of CPA3 expression in PC-3 cells treated with NaBu (10 mM) for 0, 24, 48, and 72 h. Also shown is the hybridization with a GAPDH cDNA as a control for the normalization of RNA loaded.

[3] The abbreviations used are: NaBu, sodium butyrate; DD-PCR, differential display-PCR; CP, carboxypeptidase; RACE, rapid amplification of cDNA ends; GAPDH, glyceraldehyde-3-phosphate dehydrogenase; UTR, untranslated region; CHX, cycloheximide; ACLP, aortic carboxypeptidase-like protein; TSA, trichostatin A; RT-PCR, reverse transcription-PCR; EST, expressed sequence tag; ActD, actinomycin D.

```
                                                             CGGGGAC      7
ATGAGGTGGATACTGTTCATTGGGGCCCTTATTGGGTCCAGCATCTGTGGCCGAGAAAAATTTTTTGGGGACCAAGTTTTGAGGATTAAT    97
  1 M  R  W  I  L  F  I  G  A  L  I  G  S  S  I  C  G  R  E  K  F  F  G  D  Q  U  L  R  I  N
GTCAGAAATGGAGACGAGATCAGCAAATTGAGTCAACTAGTGAATTCAAACAACTTGAAGCTCAATTTCTGGAAATCTCCCTCCTCCTTC    187
 31 U  R  N  G  D  E  I  S  K  L  S  Q  L  U  N  S  N  N  L  K  L  N  F  W  K  S  P  S  S  F
AATCGGCCTGTGGATGTCCTGGTCCCATCTGTCAGTCTGCAGGCATTTAAATCCTTCCTGAGATCCCAGGGCTTAGAGTACGCAGTGACA    277
 61 N  R  P  U  D  U  L  U  P  S  U  S  L  Q  A  F  K  S  F  L  R  S  Q  G  L  E  Y  A  U  T
ATTGAGGACCTGCAGGCCCTTTTTAGACAATGAAGATGATGAAATGCAACACAATGAAGGGCAAGAACGGAGCAGTAATAACTTCAACTAC    367
 91 I  E  D  L  Q  A  L  L  D  N  E  D  D  E  M  Q  H  N  E  G  Q  E  R  S  S  N  N  F  N  Y
GGGGCTTACCATTCCCTGGAAGCTATTTACCACGAGATGGACAACATTGCCGCAGACTTTCCTGACCTGGCGAGGAGGGTGAAGATTGGA    457
121 G  A  Y  H  S  L  E  A  I  Y  H  E  M  D  N  I  A  A  D  F  P  D  L  A  R  R  U  K  I  G
CATTCGTTTGAAAACCGGCCGATGTATGTACTGAAGTTCAGCACTGGGAAAGGCGTGAGGCGGCCGGCCGTTTGGCTGAATGCAGGCATC    547
151 H  S  F  E  N  R  P  M  Y  U  L  K  F  S  T  G  K  G  U  R  R  P  A  U  W  L  N  A  G  I
CATTCCCGAGAGTGGATCTCCCAGGCCACTGCAATCTGGACGGCAAGGAAGATTGTATCTGATTACCAGAGGGATCCAGCTATCACCTCC    637
181 ■  S  ■  ■  W  I  S  Q  A  T  A  I  W  T  A  R  K  I  U  S  D  Y  Q  R  D  P  A  I  T  S
ATCTTGGAGAAAATGGATATTTTCTTGTTGCCTGTGGCCAATCCTGATGGATATGTGTATACTCAAACTCAAAACCGATTATGGAGGAAG    727
211 I  L  E  K  M  D  I  F  L  L  P  U  A  N  P  D  G  Y  U  Y  T  Q  T  Q  N  R  L  W  ■  K
ACGCGGTCCCGAAATCCTGGAAGCTCCTGCATTGGTGCTGACCCAAATAGAAACTGGAACGCTAGTTTTGCAGGAAAGGGAGCCAGCGAC    817
241 T  R  S  R  N  P  G  S  S  C  I  G  A  D  P  ■  ■  N  W  N  A  S  F  A  G  K  G  A  S  D
AACCCTTGCTCCGAAGTGTACCATGGACCCCACGCCAATTCGGAAGTGGAGGTGAAATCAGTGGTAGATTTCATCCAAAAACATGGGAAT    907
271 N  P  C  S  E  U  Y  H  G  P  H  A  N  S  E  U  E  U  K  S  U  U  D  F  I  Q  K  H  G  N
TTCAAGGGCTTCATCGACCTGCACAGCTACTCGCAGCTGCTGATGTATCCATATGGGTACTCAGTCAAAAAGGCCCCAGATGCCGAGGAA    997
301 F  K  G  F  I  D  L  ■  S  Y  S  Q  L  L  M  Y  P  Y  G  Y  S  U  K  K  A  P  D  A  E  E
CTCGACAAGGTGGCGAGGCTTGCGGCCAAAGCTCTGGCTTCTGTGTCGGGCACTGAGTACCAAGTGGGTCCCACCTGCACCACTGTCTAT   1087
331 L  D  K  U  A  R  L  A  R  K  A  L  A  S  U  S  G  T  E  Y  Q  U  G  P  T  C  T  T  U  ■
CCAGCTAGCGGGAGCAGCATCGACTGGGCGTATGACAACGGCATCAAATTTGCATTCACATTTGAGTTGAGAGATACCGGGACCTATGGC   1177
361 P  A  S  G  S  S  I  D  W  A  Y  D  N  G  I  K  F  A  F  T  F  ■  L  R  D  T  G  T  Y  G
TTCCTCCTGCCAGCTAACCAGATCATCCCCACTGCAGAGGAGACGTGGCTGGGGCTGAAGACCATCATGGAGCATGTGCGGGACAACCTC   1267
391 F  L  L  P  A  N  Q  I  I  P  T  A  E  E  T  W  L  G  L  K  T  I  M  E  H  U  R  D  N  L
TACTAGGCGATGGCTCTGCTCTGTCTACATTTATTTGTACCCACACGTGCACGCACTGAGGCCATTGTTAAAGGAGCTCTTTCCTACCTG   1357
421 Y  *
TGTGAGTCAGAGCCCTCTGGGTTTGTGGAGCACACAGGCCTGCCCCTCTCCAGCCAGCTCCCTGGAGTCGTGTGTCCTGGCGGTGTCCCT   1447
GCAAGAACTGGTTCTGCCAGCCTGCTCAATTTTGGTCCTGCTGTTTTTGATGAGCCTTTTGTCTGTTTCTCCTTCCACCCTGCTGGCTGG   1537
GCGGCTGCACTCAGCATCACCCCTTCCTGGGTGGCATGTCTCTCTCTACCTCATTTTTAGAACCAAAGAACATCTGAGATGATTCTCTAC   1627
CCTCATTCACATCTAGCCAAGCCAGTGACCTTTGCTCTGGTGGCACTGTGGGAGACACCACTTGTCTTTAGGTGGGTCTCAAAGATGATG   1717
TAGAATTTCCTTTAATTTCTCGCAGTCTTCCTGGAAAATATTTTCCTTTGAGCAGCAAATCTTGTAGGGATATCAGTGAAGGTCTCTCCC   1807
TCCCTCCTCTCCTGTTTTTTTTTTTTTGAGGCAGAGTTTTGCTCTTGTTGCCCAGGCTGGAGTGTGATGGGCTCGATCTTGGCTCACCACA   1897
ACCTCTGCCTCCTGGGTTCAAGCAATTCTCCTGCCTCAGCCTCTTGAGTAGCTTGGTTTATAGGCGCATGCCACCATGCCTGGCTAATTT   1987
TGTGTTTTTAGTAGAGACAGGGTTTCTCCATGTTGGTCAGGCTGGTCTCAAACTCCCAACCTCAGGTGATCTGCCCTCCTTGGCCTCCCA   2077
GAGTGCTGGGATTACAGGGGGAGCCACTGTGCCGGTCCCGTCCCCTCCTTTTTTAGGCCTGAATACAAAGTAGAAGATCACTTTCCTTCA   2167
CTGTGCTGAGAATTTCTAGATACTACAGTTCTTACTCCTCTCTTCCCTTTGTTATTCAGTGTGACCAGGATGGGCGGGAGGGGATCTGTG   2257
TCACTGTAGGTACTGTGCCCAGGAAGGCTGGGTGAAGTCCCCATCTAAATTGCAGGATGGCGAAATTATCCCCATCTGTCCTAATGGGCT   2347
TCCCTCCTCTTTGCCTTTTGAACTCACTTCAAAGATGTAGGCCTCATCTTACAGGTCCTAAATCACTCATCTGGCCTGGATAATCTCACT   2437
GCCCTGGCACATTCCCATTTGTGCTGGGGTATCCTGTGTTTCCTTGTCCTGGTTTGTGTGTGTGTGTGTGTGTGTGTGTGTGTGTGTGTG   2527
TGTTTGTGTGTGTGTGTCTGTCTATTTTGATCCGGCCCAAGTTCCTAAGTAGAGCAAGAATTCATCAACCAGCTGCCTTTGTTTCATTTC   2617
ACCTCAGCACGTACCATCGTCCTTTGGGGGGTTGTTTGTTTTTGTTTTTTGCTTTAACCAAAATGTTTGTAAATCTTAACCTCCTGCCTA   2707
GGATTTGTACAGCATTTGGTGTGTGCTTATAAGCCAATAAATATTCAATGTGAGTTCCAAAAAAAAAAAAAAAAAAAAAAAAAAAAAAAA   2795
```

Fig. 2. Full nucleotide sequence and corresponding amino acid sequence of the human CPA3. The nucleotide sequence is numbered on the *right*, and the amino acid sequence is numbered on the *left*. The CPA3 cDNA contains a 5′ UTR (7 bp), 3′ UTR (1522 bp), and a 1266-bp open reading frame encoding a 421-amino acid protein. The polyadenylation signal consensus sequence AATAAA is *underlined* within the 3′ UTR. Within the deduced CPA3 amino acid sequence, a putative signal peptide region is *underlined*, and two CP zinc binding signature domains are marked by *dark lines*. Key catalytic residues implicated for Zn^{2+} binding, substrate positioning, and catalytic activity are *shaded*. The *asterisk* at the end of the amino acid sequence of CPA3 corresponds to and is directly over the TGA stop codon.

after the start of transfection, cells were treated with or without 10 mM NaBu for 12 h, cells were harvested, and total RNA was isolated. Northern blot analysis was performed using p21$^{WAF1/CIP1}$ and CPA3 cDNAs as probes.

RESULTS

Identification and Cloning of CPA3. The androgen-independent prostate cancer cell PC-3 began to show dramatic morphology changes after exposure to 10 mM NaBu for 24 h. The treated cells demonstrated a differentiation phenotype of cellular spreading and flattening and extension of pseudopodia (data not shown). Simultaneously, DNA fragmentation indicative of apoptosis was detected by agarose gel electrophoresis analysis (Fig. 1A). DD-PCR was used to isolate cDNAs up-regulated and down-regulated after NaBu treatment of the PC-3 cells. In the course of this work, one 330-bp fragment was identified using DD-PCR, which was induced by NaBu treatment (Fig. 1B). As is shown in Fig. 1B, expression of the fragment corre-

Table 1 *Homology (amino acid identity) among CPA3 and other members of the metallocarboxypeptidase gene family*

Gene	Identities (%)	Positives (%)
Mammalian metallocarboxypeptidase		
Human CPA2	63	76
Rat CPA2	61	74
Bovine CPA	55	73
Human CPA1	54	72
Rat CPA1	52	70
Pig CPB	52	72
Bovine CPB	49	66
Human CPB	40	60
Rat CPB	40	60
Dog CPB	39	60
Human CPA-MC	38	58
Rat CPA-MC	37	58
Mouse CPA-MC	37	56
Human pCPB	37	54
Nonmammalian metallocarboxypeptidase		
Black fly Zinc-CP	43	60
C. elegans Zinc-CP	35	55
Humus earthworm Zinc-CP	33	52
Baker's yeast Zinc-CP	32	50
Drosophila CPA	30	55
Cotton bollworm CPA	30	52
E. coli Zinc-CPT	30	48
Fission yeast Zinc-CP	28	46

sponding to CPA3 was very highly induced by the treatment with NaBu (more so than any of the other fragments detected by DD-PCR). Therefore, we selected this fragment for further characterization. The differential expression of CPA3 between parental and differentiated cells was further confirmed by Northern blot hybridization using the 330-bp fragment as a probe (Fig. 1C). The 330-bp fragment hybridized to a 3.0-kb message on these Northern blots. Sequence analysis and database searching revealed that this cDNA belonged to a novel gene. To clone the full length of this gene, we isolated poly(A)$^+$ mRNA from the PC-3 cells after they were treated with NaBu for 2 days. cDNA was synthesized for 5'-RACE. From RACE experiments, we obtained an additional 2.5-kb cDNA fragment for this gene. These two clones collectively define a 2795-bp full-length cDNA sequence. The nucleotide sequence and the corresponding amino acid sequence of the protein are shown in Fig. 2. The analyzed full-length cDNA contained a very short 5'-UTR, a large 3'-untranslated region, a poly(A) tail, and an open reading frame of 1266 bp capable of encoding a 421-amino acid protein. Computer-based analysis predicted that the putative protein encoded by this gene contained two zinc-binding signature domains of metallocarboxypeptidases (Fig. 2). Similar to some of the other CP mRNAs (30), the 5' UTR is only several bp in length (7 bp). However, distinct from other CP mRNAs, the 3' UTR of CPA3 mRNA is quite long and has a 1.5-kb segment containing the consensus polyadenylation signal sequence AATAAA, located 17 nucleotides upstream from the poly(A) tail. By using TMAP (software for the identification of transmembrane segments on a protein sequence; EMBL-Heidelberg) analysis, we found a 16-amino acid signal peptide present at the NH_2 terminus of the putative protein encoded by this cDNA (Fig. 2).

CPA3 Belongs to the Metallocarboxypeptidase Family. Computer-assisted homology comparison revealed that although the CPA3 cDNA sequence shares very low homology with other genes in the database (data not shown), the CPA3 amino acid sequence shares significant homology with metallocarboxypeptidases in different species from human to *E. coli* (Table 1). The overall homology of the putative CPA3 protein is highest to human and rat CPA2, with 63% and 61% amino acid identity, respectively. CPA3 also shows very high amino acid similarity with bovine CPA, human CPA1, and rat CPA1. Both CPA1 and CPA2 exist as procarboxypeptidases with a structure containing an NH_2-terminal signal peptide, a COOH-terminal CP domain, and an activation segment in the middle. As shown in Fig. 3, CPA3 shares significant structural similarity with CPA2 and CPA1. Residues known to be involved in Zn^{2+} binding (His^{69}, Glu^{72}, and His^{196}, using the CPA1 numbering system), substrate anchoring and positioning (Arg^{71}, Arg^{127}, Asn^{144}, Arg^{145}, and Tyr^{248}), and catalysis (Arg^{127} and Glu^{270}) are present in comparable positions in

Fig. 3. Comparison of the amino acid sequence of human CPA3 with those of human CPA1 and CPA2. The human CPA1 numbering system is shown on the top of the amino acid sequences and residues within the CP moiety are numbered as positive, whereas residues in the signal and activation regions are numbered as negative. *Arrows*, the boundaries between the signal peptide, activation segment, and enzyme domain. Residues for Zn^{2+} binding, substrate positioning, and catalytic activity preserved in the corresponding positions of these CPs are *shaded*. The amino acid sequence of each individual enzyme is also numbered on the *right*.
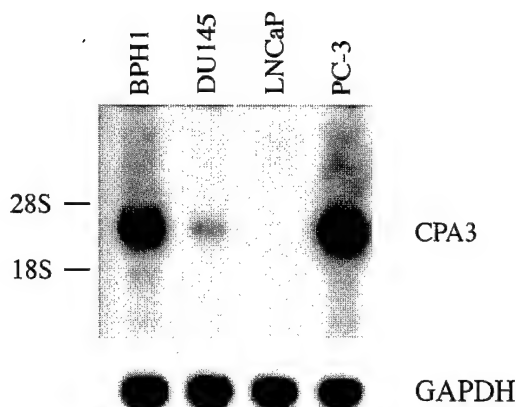
Fig. 4. Basal levels of CPA3 mRNA in various prostate cell lines. Northern blots were made from three prostate cancer cell lines and one benign prostatic hyperplasia cell line and probed with CPA3 cDNA. The molecular weight markers shown on this gel are 18S and 28S rRNAs. Also shown is the hybridization with the GADPH cDNA to control for loading of RNA in the different lanes.

CPA3 in its COOH-terminal enzyme domain (Figs. 2 and 3). On the basis of this data, we named this gene *CPA3*.

Expression of CPA3 in Different Tissues and Cells. We analyzed expression of CPA3 mRNA in 16 human normal tissues by using Clontech's Multiple Tissue Northern blots #1 and #2. However, we did not detect any Northern hybridization signal in tissues including heart, brain, placenta, lung, liver, skeletal muscle, kidney, pancreas, spleen, thymus, prostate, testis, ovary, small intestine, colon, and peripheral blood lymphocytes. However, we did detect very strong hybridization signals on the blots made from prostate cell lines in the same hybridization experiment (Fig. 4). Hybridization with an actin cDNA demonstrated that the quality of the mRNA on the commercial multiple tissue Northern blots was good. We, therefore, analyzed the expression status of CPA3 in different human tissues using RT-PCR analysis. Using RT-PCR, we did observe low expression of CPA3 in some of aforementioned tissues, including normal prostate, as compared with the expression of GAPDH (data not shown). There are very few ESTs homologous to CPA3 cDNA in the database, and all these ESTs were obtained from normalized cDNA libraries made from fetal brain, melanocyte, and pregnant uterus, respectively. Thus, it seems that CPA3 mRNA could be an extremely rare transcript in normal human cells. Because the two homologous CPs CPA1 and CPA2 are of pancreatic origin, we also analyzed expression of CPA3 mRNA in pancreatic cells. In normal pancreatic tissues, no expression of CPA3 mRNA was observed by Northern hybridization, although low expression was detected by RT-PCR analysis (data not shown). Similar very low expression levels of CPA3 were observed in seven pancreatic cancer cell lines (data not shown).

CPA3 Is Inducible in Various Prostate Cell Lines by NaBu. Previous data indicated that CPA3 mRNA was preferentially expressed in specific types of tissues or cells. We then sought to establish whether CPA3 mRNA was inducible by NaBu in other prostate cell lines. CPA3 induction by NaBu was found to be dosage-dependent in PC-3 cells (Fig. 5A). It is considered that the half-life of NaBu is quite short, and no cytotoxic effect was found after cells were treated with 20 mM NaBu. Therefore, we selected to use 10 mM NaBu to treat PC-3, DU145, LNCaP, and BPH1 cells for the time-course study. In PC-3 cells, CPA3 can be induced as early as 3 h after NaBu treatment and was highly induced from 12 h to 48 h (Fig. 5B). In DU145 cells, CPA3 expression was slightly higher after 6 h of NaBu treatment and extremely high after 48 h of treatment (Fig. 5C). Induction of CPA3 mRNA by NaBu was detected in the BPH1 cell line, although the induction pattern of this gene was slightly different from PC-3 and DU145 (Fig. 5D). CPA3 could not be induced in the androgen-sensitive cell line LNCaP (data not shown). We also tested the inducibility of CPA3 in several pancreatic cancer cell lines (see "Materials and Methods"). No induction of CPA3 mRNA by NaBu was detected in any of the seven tested cell lines (data not shown).

CPA3 mRNA Expression Is Induced by Histone Hyperacetylating Agents. Because butyrate is known to be a histone deacetylase inhibitor, we wonder if another histone hyperacetylating agent could induce the *CPA3* gene. TSA is a potent and specific inhibitor of histone deacetylase and, like butyrate, has been shown to cause G_1 cell cycle arrest and differentiation of various cell types (31, 32). We found that in PC-3 cells, TSA induces CPA3 expression in a dosage-dependent manner, with maximal effects occurring at 0.6 μM and 1.2 μM (Fig. 6A). Similar to NaBu, the effects of TSA on CPA3 occur as early at 3 h, but distinct from NaBu, the expression level of CPA3 comes down by 48 h of TSA treatment (Fig. 6B). To investigate whether CPA3 induction by either NaBu or TSA was due to an increase in the rate of CPA3 mRNA synthesis or an enhancement of its stability, the transcriptional inhibitor ActD was used. Pretreatment with 4 μM ActD for 30 min completely abolished CPA3 induction by NaBu and TSA (Fig. 6, C and D), thus, indicating that induction of CPA3 is dependent on transcriptional activity of cells. Because induction of CPA3 occurs at 3 h by treatment of NaBu and TSA (Figs. 5B and 6B), we tested whether CPA3 was induced by an early drug response mechanism. As shown in Fig. 6E, the induction of CPA3 was inhibited by simultaneous treatment with CHX, indicating that other proteins mediate CPA3 induction by NaBu or TSA.

Requirement of Transactivation of p21^WAF1/CIP1 in CPA3 Induction by NaBu. Induction of p21$^{WAF1/CIP1}$ by NaBu and TSA in the colorectal cancer cell line HT-29 cannot be blocked by the protein synthesis inhibitor CHX. Instead, the mRNA expression level of p21$^{WAF1/CIP1}$ increases slightly, indicating that p21$^{WAF1/CIP1}$ was induced by these chemicals as an immediate-early gene (21). We

Fig. 5. Effect of NaBu on CPA3 expression in several prostate cell lines. *A*, PC-3 cells were treated with 0, 0.1, 0.5, 2.5, 10, or 20 mM NaBu for 24 h; Total RNA (15 μg) was applied for Northern blot analysis and hybridized with CPA3 and GAPDH cDNAs as probes. *B-D*, PC-3, DU145, and BPH1 cells were treated with 10 mM NaBu for various times, respectively. Total RNA (15 μg) was applied to the gels for Northern blot analysis. GAPDH cDNA was used as a control for the normalization of RNA loaded in these experiments.
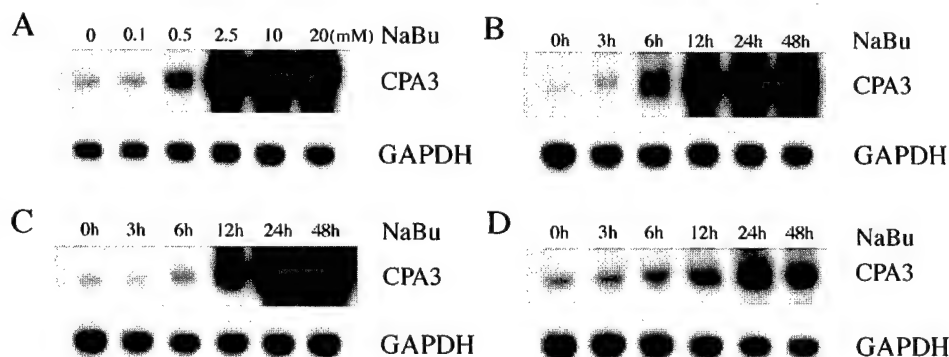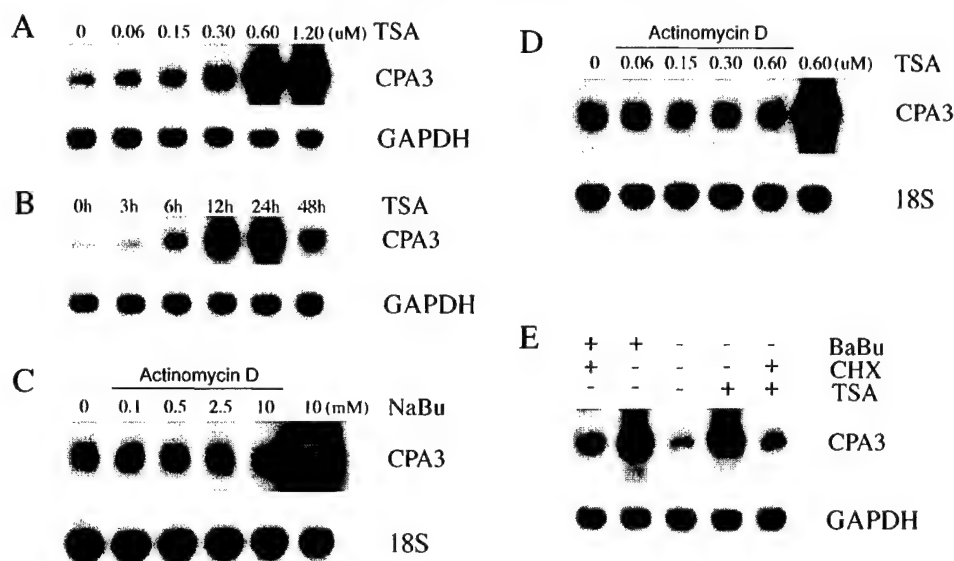
Fig. 6. NaBu and TSA induce CPA3 expression in PC-3 cells in a drug late-response manner. *A*, dose response for CPA3 induction by TSA. PC-3 cells were treated with various concentrations of TSA, 0–1.2 μM for 24 h, and CPA3 mRNA expression was examined by Northern blot analysis. *B*, time-course for induction of CPA3 by TSA. Cells were treated with 0.6 μM TSA for varying lengths of time, from 0–48 h, and induction of CPA3 expression was examined by Northern blot analysis. *C*, effect of ActD on CPA3 induction by NaBu. PC-3 cells were pretreated with 4 μM ActD for 30 min before a 24-h exposure to the indicated doses of NaBu *(Lanes 2–5)* or not pretreated with ActD *(Lane 6)*. Expression of CPA3 mRNA in PC-3 cells without any chemical treatment was included as a control *(Lane 1)*. 18S rRNA was used as a control for the normalization of RNA loaded in these experiments. *D*, effect of ActD on CPA3 induction by TSA. PC-3 cells were pretreated with 4 μM ActD for 30 min before a 24-h exposure to the indicated doses of TSA *(Lane 2–5)* or not pretreated with ActD *(Lane 6)*. Expression of CPA3 mRNA in PC-3 cells without any chemical treatment was analyzed as a control *(Lane 1)*. 18S rRNA was used as a control for the normalization of RNA loaded in these experiments. *E*, CPA3 induction by NaBu and TSA is blocked by a protein synthesis inhibition. Cells were treated simultaneously with 10 mM NaBu or 0.6 μM TSA and 10 μg/ml CHX for 12 h. RNA was isolated and applied to the gels for Northern blot analysis. GAPDH cDNA probe was used as a control for the normalization of RNA loaded in the experiments.

obtained the same result when the PC-3 cell line was simultaneously treated with NaBu or TSA and CHX (data not shown). This result suggests that p21$^{WAF1/CIP1}$ also acts as an immediate-early gene in the *in vitro* differentiation of PC-3 cells due to treatment with NaBu or TSA. Because the induction of CPA3 was mediated by a late response mechanism, we investigated whether there was any effect of p21$^{WAF1/CIP1}$ transactivation on CPA3 induction by NaBu. An antisense p21$^{WAF1/CIP1}$ expression vector was transiently transfected into PC-3 cells, and the cells were treated with NaBu. As is shown in Fig. 7, expression of antisense p21$^{WAF1/CIP1}$ not only completely blocked expression of p21$^{WAF1/CIP1}$, but also almost completely inhibited induction of CPA3 by NaBu. For a control, PC-3 cells were transfected with only the expression vector pcDNA3.1. Similar to the PC-3 cells, both p21$^{WAF1/CIP1}$ and CPA3 can be highly induced in these cells by NaBu treatment (Fig. 7). Therefore, induction of CPA3 by NaBu requires the transcription activity of p21$^{WAF1/CIP1}$.

DISCUSSION

In this study, we describe the isolation and characterization of a novel CP, CPA3, that shares significant homology with the CPA subfamily of metalloprecarboxypeptidases. CPA3 was highly induced by NaBu treatment of several prostate cancer cell lines, and it was also induced by TSA, which is a potent and specific inhibitor of histone deacetylase. We also demonstrated that the specific induction of CPA3 by NaBu was specifically inhibited by antisense p21^{WAF1}.

GenBank searches indicated that CPA3 shares significant homology to the members of the CPA and CPB subfamily of metallocarboxypeptidases. As shown in Table 1, CPA3 not only has 37–63% amino acid identity with other zinc CPs from different mammalian species, but also shares 27–43% of amino acid similarity with zinc CPs from a number of nonmammalian species. CPA3 shows the highest homology with CPA1 and CPA2, indicating that it is a new member of the CPA subfamily. CPA1 and CPA2 are also known as

pancreatic CPs, the digestive enzymes involved in the hydrolysis of alimentary proteins, which are expressed and secreted into the pancreatic juices. We, therefore, examined the expression of CPA3, but did not find expression of CPA3 in either normal pancreas or pancreatic tumor cells by Northern analysis. We previously showed that several pancreatic cancer cell lines also undergo differentiation and apoptosis on exposure to NaBu (11), but, in this study, we did not detect any induction of CPA3 in seven pancreatic cancer cell lines
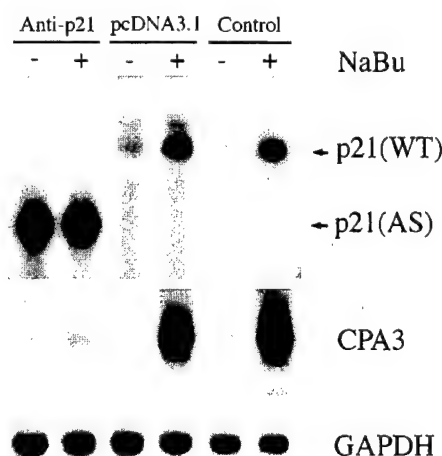

Fig. 7. Expression of antisense p21$^{WAF1/CIP1}$ RNA inhibits induction of CPA3 mRNA by NaBu. The antisense p21$^{WAF1/CIP1}$ expression vector was constructed and transiently transfected into PC-3 (see "Materials and Methods"). Twenty-four hours later, cells were subjected to treatment with 10 mM NaBu for 12 h. Total RNA (15 μg) was applied to gels for Northern blot analysis using p21$^{WAF1/CIP1}$, CPA3, and GAPDH cDNAs as probes. As controls, PC-3 cells without any transfection and transiently transfected with an empty pcDNA3.1(+) expression vector were treated with 10 mM NaBu for 12 h, and RNA was isolated for Northern blot analysis. *p21(WT)*, wild type transcript of p21$^{WAF1/CIP1}$ (2.1 kb); *p21(AS)*, antisense transcript of p21$^{WAF1/CIP1}$ (0.8 Kb). This figure is representative of results from three experiments.

after exposure to NaBu for more than 2 days. We detected extremely low levels of CPA3 expression in normal prostate tissue by RT-PCR analysis. However, expression of CPA3 was easily detectable in untreated prostate cancer cell lines by Northern hybridization analysis (Fig. 4), and CPA3 mRNA was highly induced by NaBu in these cancer cell lines (Fig. 5). These data indicate that CPA3 is a nondigestive pancreatic-like CPA.

Although, generally, similarities in primary structure between digestive and nondigestive CPs are quite low (33), sequence alignments clearly show that key catalytic residues are common to these enzymes, His^{69}, Glu^{72}, and His^{196} (using the CPA1 numbering system) for the Zn^{2+} binding; Arg^{71}, Arg^{127}, Asn^{144}, Arg^{145}, and Tyr^{248} for substrate anchoring and positioning; and Arg^{127} and Glu^{270} for catalytic activity (30, 33, 34). All of the residues essential for the coordination of the Zn^{2+} active site, substrate peptide anchoring, and CP activity are also preserved in comparable positions in the putative CPA3 protein (Figs. 2 and 3). The NH_2-terminal domains of most metallocarboxypeptidases contain a signal peptide critical for the proper targeting of the protein. Motif analysis predicts that CPA3 contains an NH_2-terminal sequence of 16 amino acids that resembles the signal peptide consensus sequence (35) and, thus, CPA3 is similar to other CP family members. Further analysis shows that similar to other metallocarboxypeptidases (including CPA1, CPA2, CPB, CPA-MC, pCPB, and CPE), CPA3 contains a pro-peptide between the NH_2-terminal signal peptide sequence and COOH-terminal CP moiety (Fig. 3). Thus, CPA3 is a proprecarboxypeptidase.

A number of nondigestive pancreatic-like CPs have been reported in the recent literature. AEBP1 has CP activity and has also been shown to be a new type of transcription factor (36). In addition to a CP domain, CPZ and ACLP contain the frizzled (fz) and discoidin-like domains, respectively, indicating that these two proteins might have other functions distinct from CP activity (34, 37). CPs catalyze the removal of the COOH-terminal basic amino acids arginine or lysine from peptides or proteins. The natural substrates of these enzymes seem to be peptide hormones including kinins, enkephalin hexapeptides, and anaphylatoxins, or proteins such as creatinine kinase (38). The removal of the COOH-terminal arginine or lysine results in modulation or inactivation of peptide hormone activity, and this might play an essential role in cell growth and differentiation. Induction of ACLP message and protein was observed as Monc-1 cells differentiate into smooth muscle cells, indicating that ACLP may play a role in the differentiation of vascular smooth muscle cells (37). Expression of CP M is associated with monocyte to macrophage differentiation (38). In this study, we found that induction of CPA3 mRNA expression was associated with in vitro differentiation of prostate epithelial cells.

Butyrate and its structural analogues are known cell growth and differentiation regulators and are currently under clinical consideration as a tool for the management of prostate cancer (5, 26). However, the molecular link between butyrate treatment and prostate cell differentiation is not well understood. By investigating mechanisms by which induction CPA3 mRNA is mediated in NaBu-induced in vitro differentiation of prostate cancer cells, this study strongly supports the existence of a link between histone deacetylase activity and butyrate-mediated differentiation in prostate cancer cells.

Differentiation and apoptosis induced by NaBu was observed in three androgen-independent prostate cells including PC-3 (Fig. 1A), DU145, and BPH1 (data not shown). We, therefore, believe that this is an ideal model to study gene expression and regulation during differentiation and apoptosis of androgen-independent prostate cells. CPA3 expression was highly up-regulated during NaBu-induced differentiation of PC-3 cells (Fig. 1C). Similar up-regulation was also observed in two other androgen-independent prostate cancer cell lines (Fig. 5), suggesting that a common signal pathway seems to be

involved in induction of CPA3 mRNA. Butyrate is known to induce general histone acetylation through a noncompetitive inhibition of the histone deacetylation enzyme. This action likely occurs in vivo because rats fed a high-fiber diet have high butyrate levels, which were found to be associated with histone hyperacetylation in colon epithelial cells (39). Further investigation showed that CPA3 mRNA expression was also induced by TSA in a time- and dosage-dependent manner (Fig. 6). TSA is a potent and specific histone deacetylase inhibitor. Thus, our data indicates that CPA3 mRNA induction is mediated by the mechanism of histone hyperacetylation.

Induction of CPA3 mRNA expression by histone inhibitors can be blocked by CHX, indicating that CPA3 is a downstream gene in response to the hyperacetylating activity of histones. The mechanism by which CPA3 is induced by NaBu and TSA was further investigated in this study. Hyperacetylation of histones neutralizes their positive charge, disrupting their ionic interaction with DNA, and thereby allowing transcription factors to access and activate specific genes (17). During in vitro differentiation of colon cancer cells, it was shown that $p21^{WAF1/CIP1}$ mRNA is consistently induced by NaBu and TSA in an immediate-early manner through a mechanism involving histone hyperacetylation (21). We observed the same results in the differentiation of prostate cancer cells. By performing transient transfection assays with antisense $p21^{WAF1/CIP1}$, we discovered that antisense expression of $p21^{WAF1/CIP1}$ completely inhibits the induction of CPA3 by butyrate (Fig. 7). We do not know how NaBu and TSA induce expression of CPA3, but a plausible model is that butyrate and TSA inhibit histone deacetylase at the level of the $p21^{WAF1/CIP1}$ gene. This leads to changes in the chromatin that allow transcriptional activation of this gene (21), and transactivation of the $p21^{WAF1/CIP1}$ gene further mediates induction of CPA3 mRNA. Whether $p21^{WAF1/CIP1}$ directly interacts with CPA3 through the binding to its promoter or through other proteins is still unknown and needs to be determined.

Proliferation and differentiation of prostate cancer cells is hormone-related. Several studies have suggested that various factors including androgen and peptide growth factors, play a major role in the pathogenesis as well as in the promotion of prostate cancer (40–42). Prostate-specific membrane antigen was originally identified as a marker of prostate cancer (43). Recently, it was found to function as a glutamate CP (42), indicating that like androgen, peptide hormones such as neuropeptides might also be involved in the cell growth and differentiation of prostate epithelial cells. Of the five ESTs that were found to be homologous to the CPA3 cDNA in the DNA sequence databases, one was derived from a pregnant mouse uterus library, and another was derived from a pregnant human uterus library. We have identified the mouse CPA3, and its expression pattern was different between pregnant and nonpregnant mouse uterus (data not shown). Therefore, it seems that expression of CPA3 is associated with hormone-regulated tissues. The removal of the COOH-terminal amino acid results in modulation or inactivation of peptide hormone activity that could play an essential role in cell growth and differentiation. The structural similarity of CPA3 with other CPs suggests that it might modulate the function of peptide hormones that play an essential role in the growth and/or differentiation of prostate epithelial cells. However, the exact substrate of CPA3, and its function within the cell, is presently unknown.

REFERENCES

1. Kyprianou, N., English, H. F., and Isaacs, J. T. Programmed cell death during regression of PC-82 human prostate cancer following androgen ablation. Cancer Res., 50: 3748–3753, 1990.
2. Crawford, E. D., Eisenberger, M. A., McLeod, D. G., Spaulding, J. T., Benson, R., Dorr, F. A., Blumentein, B. A., Davis, M. A., and Goodman, P. J. A controlled trial

of leuprolide with and without flutamide in prostatic carcinoma. N. Engl. J. Med., *321:* 419–424, 1989.

3. Catalona, W. J. Management of cancer of the prostate. N. Engl. J. Med., *331:* 996–1004, 1994.

4. McDonnell, T. J., Navone, N. M., Troncoso, P., Pisters, L. L., Conti, C., von Eschenbach, A. C., Brisbay, S., and Logothetis, C. J. Expression of bcl-2 oncoprotein and p53 protein accumulation in bone marrow metastases of androgen independent prostate cancer. J. Urol., *157:* 569–574, 1997.

5. Thibault, A., Cooper, M. R., Figg, W. D., Venzon, D. J., Sartor, A. O., Tompkins, A. C., Weinberger, M. S., Headlee, D. J., McCall, N. A., Samid, D., and Myers, C. E. A phase I and pharmacokinetic study of intravenous phenylacetate in patients with cancer. Cancer Res., *54:* 1690–1694, 1994.

6. Denmeade, S. R., Lin, X. S., and Isaacs J. T. Role of programmed (apoptotic) cell death during the progression and therapy for prostate cancer. Prostate, *28:* 251–265, 1996.

7. Tang, D. G., and Porter, A. T. Target to apoptosis: a hopeful weapon for prostate cancer. Prostate, *32:* 284–223, 1997.

8. Rivero, J. A., and Adunyah, S. E. Sodium butyrate stimulates PKC activation and induces differential expression of certain PKC isoforms during erythroid differentiation. Biochem. Biophys. Res. Commun., *248:* 664–668, 1998.

9. Carducci, M. A., Nelson, J. B., Chan-Tack, K. M., Ayyagari, S. R., Sweatt, W. H., Campbell, P. A., Nelson, W. G., and Simons, J. W. Phenylbutyrate induces apoptosis in human prostate cancer and is more potent than phenylacetate. Clin. Cancer Res., *2:* 379–387, 1996.

10. Mandal, M., and Kumar, R. Bcl-2 expression regulates sodium butyrate-induced apoptosis in human MCF-7 breast cancer cells. Cell Growth Differ., *7:* 311–318, 1996.

11. Zhang, J. S., Nelson, M., Wang, L., Liu, W., Qian, C. P., Shridhar, V., Urrutia, R., and Smith, D. I. Identification and chromosomal localization of CTNNAL1, a novel protein homologous to α-catenin. Genomics, *54:* 149–154, 1998.

12. Niitsu, N., Yamamoto-Yamaguchi, Y., Miyoshi, H., Shimizu, K., Ohki, M., Umeda, M., and Honma, Y. AML1a but not AML1b inhibits erythroid differentiation induced by sodium butyrate and enhances the megakaryocytic differentiation of K562 leukemia cells. Cell Growth Differ., *8:* 319–326, 1997.

13. McIntyre, A., Young, G. P., Taranto, T., Gibson, P. R., and Ward, P. B. Different fibers have different regional effects on luminal contents of rat colon. Gastroenterology, *101:* 1274–1281, 1991.

14. McIntyre, A., Gibson, P. R., and Young, G. P. Butyrate production from dietary fiber and protection against large bowel cancer in a rat model. Gut, *34:* 386–391, 1993.

15. Candido, E. P., Reeves, R., and Davie, J. R. Sodium butyrate inhibits histone deacetylation in cultured cells. Cell, *14:* 105–113, 1978.

16. de Haan, J. B., Gevers, W., and Parker, M. I. Effects of sodium butyrate on the synthesis and methylation of DNA in normal cells and their transformed counterparts. Cancer Res., *46:* 713–716, 1986.

17. Grunstein, M. Histone acetylation in chromatin structure and transcription. Nature (Lond.), *389:* 349–352, 1997.

18. Lee, D. Y., Hayes, J. J., Pruss, D., and Wolffe, A. P. A positive role for histone acetylation in transcription factor access to nucleosomal DNA. Cell, *72:* 73–84, 1993.

19. Wolffe, A. P. Histone deacetylase: a regulator of transcription. Science (Washington DC), *272:* 371–372, 1996.

20. Trock, B., Lanza, E., and Greenwald, P. Dietary fiber, vegetables, and colon cancer: critical review and meta-analyses of the epidemiologic evidence. J. Natl. Cancer Inst., *82:* 650–661, 1990.

21. Archer, S. Y., Meng, S., Shei, A., and Hodin, R. A. p21[WAF1/CIP1] is required for butyrate-mediated growth inhibition of human colon cancer cells. Proc. Natl. Acad. Sci. USA, *95:* 6791–6796, 1998.

22. Yang, X. J., Ogryzko, V. V., Nishikawa, J., Howard, B. H., and Nakatani, Y. A. p300/CBP-associated factor that competes with the adenoviral oncoprotein E1A. Nature (Lond.), *382:* 319–324, 1996.

23. Ogryzko, V. V., Schiltz, R. L., Russanova, V., Howard, B. H., and Nakatani, Y. The transcriptional coactivators p300 and CBP are histone acetyltransferases. Cell, *87:* 953–959, 1996.

24. Bannister, A. J., and Kouzarides, T. The CBP co-activator is a histone acetyltransferase. Nature (Lond.), *384:* 641–643, 1996.

25. Warrell, R. P. Jr., He, L. Z., Richon, V., Calleja, E., and Pandolfi, P. P. Therapeutic targeting of transcription in acute promyelocytic leukemia by use of an inhibitor of histone deacetylase. J. Natl. Cancer Inst., *90:* 1621–1625, 1998.

26. Samid, D., Hudgins, W. R., Shack, S., Liu, L., Prasanna, P., and Myers, C. E. Phenylacetate and phenylbutyrate as novel, nontoxic differentiation inducers. Adv. Exp. Med. Biol., *400A:* 501–505, 1997.

27. Borner, M. M., Myers, C. E., Sartor, O., Sei, Y., Toko, T., Trepel, J. B, and Schneider, E. Drug-induced apoptosis is not necessarily dependent on macromolecular synthesis or proliferation in the p53-negative human prostate cancer cell line PC-3. Cancer Res., *55:* 2122–2128, 1995.

28. Liang, P., and Pardee, A. B. Differential display of eukaryotic messenger RNA by means of the polymerase chain reaction. Science (Washington DC), *257:* 967–971, 1992.

29. Liang, P., Averboukh, L., and Pardee, A. B. Distribution and cloning of eukaryotic mRNAs by means of differential display: refinements and optimization. Nucleic Acids Res., *21:* 3269–3275, 1993.

30. Catasus, L., Vendrell, J., Aviles, F. X., Carreira, S., Puigserver, A., and Billeter, M. The sequence and conformation of human pancreatic procarboxypeptidase A2. cDNA cloning, sequence analysis, and three-dimensional model. J. Biol. Chem., *270:* 6651–6657, 1995.

31. Yoshida, M., Nomura, S., and Beppu, T. Effects of trichostatins on differentiation of murine erythroleukemia cells. Cancer Res., *47:* 3688–3691, 1987.

32. Ogryzko, V. V., Hirai, T. H., Russanova, V. R., Barbie, D. A., and Howard, B. H. Human fibroblast commitment to a senescence-like state in response to histone deacetylase inhibitors is cell cycle dependent. Mol. Cell. Biol., *16:* 5210–5218, 1996.

33. Aviles, F. X., Vendrell, J., Guasch, A., Coll, M., and Huber, R. Advances in metallo-procarboxypeptidases: emerging details on the inhibition mechanism and on the activation process. Eur. J. Biochem., *211:* 381–389, 1993.

34. Song, L., and Fricker, L. D. Cloning and expression of human carboxypeptidase Z, a novel metallocarboxypeptidase. J. Biol. Chem., *272:* 10543–10550, 1997.

35. von Heijne, G. Signal sequences: the limits of variation. J. Mol. Biol., *184:* 99–105, 1985.

36. He, G. P., Mulse, A., Li, A. W., and Ro, H. S. A eukaryotic transcriptional repressor with carboxypeptidase activity. Nature (Lond.), *378:* 92–96, 1995.

37. Layne, M. D., Endege, W. O., Jain, M. K., Yet, S. F., Hsieh, C. M., Chin, M. T., Perrella, M. A., Blanar, M. A., Haber, E., and Lee, M. E. Aortic carboxypeptidase-like protein, a novel protein with discoidin and carboxypeptidase-like domains, is up-regulated during vascular smooth muscle cell differentiation. J. Biol. Chem., *273:* 15654–15660, 1998.

38. Rehli, M., Krause, S. W., Kreutz, M., and Andreesen, R. Carboxypeptidase M is identical to the MAX.1 antigen and its expression is associated with monocyte to macrophage differentiation. J. Biol. Chem., *270:* 15644–15649, 1995.

39. Boffa, L. C., Lupton, J. R., Mariani, M. R., Ceppi, M., Newmark, H. L., Scalmati, A., and Lipkin, M. Modulation of colonic epithelial cell proliferation, histone acetylation, and luminal short chain fatty acids by variation of dietary fiber (wheat bran) in rats. Cancer Res., *52:* 5906–5912, 1992.

40. Qiu, Y., Robinson, D., Pretlow, T. G., and Kung. H. J. Etk/Bmx, a tyrosine kinase with a pleckstrin-homology domain, is an effector of phosphatidylinositol 3′-kinase and is involved in interleukin 6-induced neuroendocrine differentiation of prostate cancer cells. Proc. Natl. Acad. Sci. USA, *95:* 3644–3649, 1998.

41. Kremer, R., Goltzman, D., Amizuka, N., Webber, M. M., and Rhim, J. S. ras activation of human prostate epithelial cells induces overexpression of parathyroid hormone-related peptide. Clin. Cancer Res., *3:* 855–859, 1997.

42. Carter, R. E., Feldman, A. R., and Coyle, J. T. Prostate-specific membrane antigen is a hydrolase with substrate and pharmacologic characteristics of a neuropeptidase. Proc. Natl. Acad. Sci. USA, *93:* 749–753, 1996.

43. Israeli, R. S., Powell, C. T., Fair, W. R., and Heston, W. D. Molecular cloning of a complementary DNA encoding a prostate-specific membrane antigen. Cancer Res., *53:* 227–230, 1993.

Allele-specific late replication and fragility of the most active common fragile site, FRA3B

Liang Wang, John Darling, Jin-San Zhang, Haojie Huang, Wanguo Liu and David I. Smith*

Division of Experimental Medicine, Department of Laboratory Medicine and Pathology, Mayo Clinic/Foundation, 200 First Street SW, Rochester, MN 55905, USA

FRA3B at 3p14.2 is the most active of the common fragile sites in the human genome and is expressed when cells are exposed to the DNA replication inhibitor, aphidicolin. Several lines of evidence suggest that fragile sites are regions of late replication. To elucidate the relationship between the timing of replication across the FRA3B region and its corresponding fragility, we labeled cells with 5-bromo-2′-deoxyuridine (BrdU) and adopted an immunofluorescent procedure to visualize late replicating DNA (BrdU-substituted DNA) in metaphase chromosomes. We also chose 21 markers along the FRA3B region and analyzed the timing of replication using BrdU-labeled DNA from different stages of the cell cycle sorted by flow cytometry. Our results show that there are two distinct alleles that replicate at different stages in the cell cycle and that breaks/gaps preferentially occurred on the chromosome 3 with the late replication allele. These results provide direct evidence that allele-specific late replication is involved in the fragility of the most active common fragile site, FRA3B.

INTRODUCTION

FRA3B is the most highly inducible fragile site in the human genome (1). Deletions in the FRA3B region are observed in a number of different solid tumors (2–6). Ohta *et al.* (7) identified the fragile histidine triad (*FHIT*) gene from this region, and they identified alterations in this gene using nested RT–PCR analysis in a number of different tumor types (7–9). The human *FHIT* gene spans an estimated 1 Mb of DNA at chromosome 3p14.2 and encompasses the entire FRA3B region and a t(3;8) translocation breakpoint observed in a family with hereditary renal cell carcinoma (the hRCC breakpoint). In contrast to its large genomic size, the final processed transcript of this gene is only 1.1 kb and it encodes a 16.8 kDa protein with diadenosine triphosphate hydrolase activity (10).

The molecular basis for the fragility in the FRA3B region is not yet known. Previous studies (11,12) have suggested that the common fragile site FRA3B is distinct from the cloned rare

fragile sites. First, no repeat motifs, such as trinucleotide or minisatellite repeats, characteristic of rare fragile sites have been identified. Second, genomic breakage and instability occur over a large genomic region (at least 500 kb). It has been hypothesized that gaps at fragile sites arise as a result of replication failure at chromosomal points that are unusually sensitive to interference during DNA synthesis (13). Using a fluorescence *in situ* hybridization (FISH)-based procedure to analyze replication timing, Le Beau *et al.* (14) reported that FRA3B sequences are late replicating and that replication was delayed further by aphidicolin, an inhibitor of DNA polymerases α and δ (15).

Although the function of the *FHIT* gene has not yet been determined, the gene can be used as a biomarker to analyze DNA replication around the *FHIT*/FRA3B region. We treated cell lines with aphidicolin and analyzed replication timing in the *FHIT* region using multiplex PCR analysis with human *FHIT* exon-specific primers as well as markers throughout the FRA3B region including several polymorphic markers. We also adopted an immunofluorescent procedure to visualize 5-bromo-2′-deoxy-uridine (BrdU)-substituted DNA in metaphase chromosomes. Our data show that replication timing in the *FHIT*/FRA3B region is asynchronous and that there are two distinct alleles that replicate at different times in the cell cycle. Breaks/gaps within the FRA3B region preferentially occurred on the chromosome with the late replicating (LR) allele. To our knowledge, this is the first report to demonstrate allele-specific late replication in this region.

RESULTS

FRA3B expression and DNA replication in the *FHIT*/FRA3B region

To visualize the replication pattern across the FRA3B region, we labeled the cells with BrdU for 3 h and then collected them for chromosome preparation. Indirect immunofluorescence was used for detection of BrdU-substituted DNA in metaphases. Since BrdU was incorporated into DNA in the last 3 h before the cells entered M phase, the detected BrdU should represent the LR region on chromosomes. Preliminary data from cell line GM03715 and two normal blood samples showed that LR signals were observed mostly on one of the two chromosomes 3 and that breaks/gaps in the FRA3B region occurred preferentially on the chromosome with LR signals. These data raise an important

---

*To whom correspondence should be addressed. Tel: +1 507 266 0311; Fax: +1 507 266 5193; Email: smith.david@mayo.edu

question, which is whether FRA3B expression occurs randomly between the chromosome 3 homologs or preferentially on one homolog. To answer this question, we chose another cell line (GM11428) with abnormalities on both chromosomes 3, which were easily differentiable as one had a partial deletion, del(3), and the other had a partial duplication, dup(3). We analyzed 660 metaphases from this cell line, comprising 278 metaphases from cells with aphidicolin induction and 382 metaphases from cells without aphidicolin induction. We first analyzed late replication and compared the results obtained between aphidicolin-induced cells and cells not exposed to aphidicolin. After aphidicolin induction, a total of 75 LR signals out of 278 metaphases were identified in the FRA3B region while 48 of 382 metaphases from untreated cells showed LR signals in this fragile site. The difference between the two groups is statistically significant ($P_1 = 0.0001$, χ^2 test) (Table 1), demonstrating a delay of replication at FRA3B after aphidicolin induction. Figure 1 shows some representative metaphases with LR and/or fragile site breakage on one chromosome 3 while the other chromosome 3 did not have a BrdU LR signal or a fragile site break.

Table 1. Preferential breaks at chromosome 3 with the late replication allele

	Metaphases analyzed	LR signals del(3)/dup(3)	Breaks del(3)/dup(3)
Aphidicolin induction	278	75 (63/12)	33 (31/2)
Control (no induction)	382	48 (48/0)	8 (8/0)

LR, late replication; del(3), chromosome 3 with deletion; dup(3), chromosome 3 with duplication.

Since the cell line utilized has two distinct homologs, del(3) and dup(3), it was very easy to differentiate them. We next analyzed LR and breaks/gaps between the two chromosome 3 homologs. Interestingly, 84% (63/75) of LR signals were detected on the chromosome 3 with the partial deletion in aphidicolin-treated cells (Table 1). A similar result was also obtained in the cells without aphidicolin treatment (Table 1). The difference between the two distinguishable chromosomes 3 in this cell line was significant ($P_2 = 0.035$, χ^2 test). These results indicate that replication at FRA3B is asynchronous. One chromosome 3 contains an LR allele and the other contains an earlier replicating allele. More interestingly, the chromosome with the LR allele showed more breaks/gaps at FRA3B than its homolog, especially after aphidicolin induction (Table 1), suggesting that late replication is associated with fragility of the fragile site FRA3B.

### Profile of replication timing in the *FHIT*/FRA3B region

BrdU-labeled human DNAs from six fractions of the cell cycle were isolated by co-immunoprecipitation with BrdU-labeled hamster DNA. To test the quality of the isolated DNA, we performed control experiments by analyzing control PCR products in the cell line GM03715. First, the hamster-specific PCRs from hypoxanthine–guanine phosphoribosyltransferase (*HXGPRT*) and transducin (*TRANA*) genes showed constant bands across the six fractions of cell cycle, suggesting that BrdU-labeled human DNAs were co-precipitated successfully (data not shown). Secondly, human-specific PCR primers derived from regions with known replication profiles showed late

(*DXS297* and *DXS7857*) and early replication (*HPRT*) as expected, further suggesting that the DNA did indeed represent different fractions in the cell cycle (Fig. 2A). We then used the BrdU-substituted DNAs as templates to analyze the replication timing of *FHIT* exons and other markers along the *FHIT*/FRA3B region. The results showed that replication was clearly asynchronous in at least six of seven *FHIT* exons, including exons 3, 4, 6, 7, 8 and 9 (Fig. 3A). For example, replication of exon 8 started at S_1, stopped at S_2, and restarted at S_3. After aphidicolin induction, the replication was delayed but still remained asynchronous (Fig. 3B). To determine if this actually represented asynchronous replication between two alleles, we analyzed three polymorphic markers from this region (*D3S4260, D3S1600* and *D3S1313*) against the BrdU-substituted DNA. The result of this analysis demonstrated that there are indeed two distinct alleles with independent replication timing in the cell line analyzed (Fig. 2B).

To better understand the replication profile in the *FHIT*/FRA3B region, we scanned all of the signals and compared the relative density of each signal. We chose the two cell cycle stages that gave the greatest amplification with each respective marker to represent the replication timing of the early and late alleles for that specific marker. Figure 4 includes all markers tested within the *FHIT*/FRA3B region and shows the replication pattern of the two respective alleles for each marker. Also included in this figure is the replication of the two alleles for each marker in the presence of aphidicolin. It can be clearly seen that most of the markers replicate later (for both alleles) in the presence of aphidicolin. The LR allele of *FHIT*, which usually replicates very late, replicates extremely late in the presence of aphidicolin: 15 of 21 markers tested showed replication of the LR allele in the G_2/M phase in the presence of aphidicolin (Fig. 4). We also repeated this experiment in another cell line GM00546. Although the data are not shown here, the results from this cell line were similar to those from GM03715, suggesting that the allele-specific late replication within the *FHIT*/FRA3B region was not limited to one cell line.

DISCUSSION

Chromosome replication is under stringent temporal and spatial control to ensure accurate duplication of the genome. Timing of DNA replication appears to be an important epigenetic regulator of gene expression during development. Using a FISH-based procedure, Le Beau *et al.* (14) reported LR in the FRA3B region and this replication was delayed further in the presence of aphidicolin. By detecting BrdU-labeled DNA, we cytologically and molecularly demonstrate not only late replication but also allele-specific replication within the *FHIT*/FRA3B region, especially after aphidicolin induction (Table 1 and Fig. 4). After induction, the chromosomes with LR signals within the FRA3B region increased from 12.6 (48/382) to 27.0% (75/278), and chromosomes with breaks/gaps at the same region increased from 2.1 (8/382) to 11.9% (33/278) (Table 1). This demonstrates a coincidence between a delay of replication and breaks/gaps at FRA3B. More importantly, our data also show that the chromosome with the LR allele had more breaks/gaps than its homolog (Table 1), suggesting that indeed late replication and possibly incomplete replication may lead to breaks/gaps in the *FHIT*/FRA3B region. It is hypothesized that unreplicated DNA regions would affect the localized chromatin structure, and this might lead to the unstable as well as recombinogenic properties of this
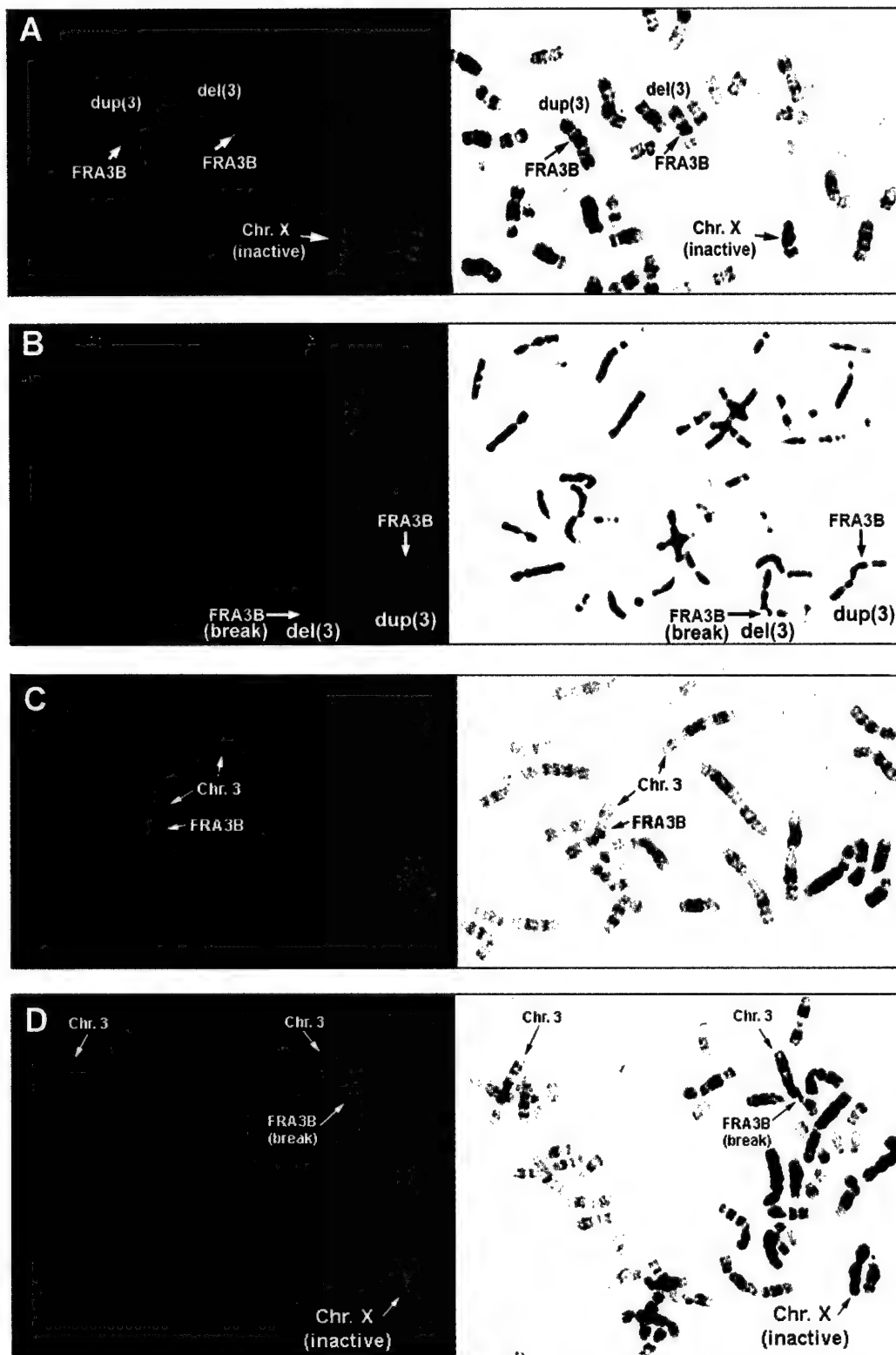
Figure 1. Visualization of late replication in the FRA3B region. Cultured cells were treated with aphidicolin for 24 h and labeled by BrdU for 3 h before harvest for chromosome preparation. BrdU-labeled DNA in the metaphase chromosomes was detected by an immunofluorescent procedure (see Materials and Methods). The green/light blue spots represent the late replicating region (BrdU-substituted DNA) on the chromosomes. The metaphase spreads were obtained from cell lines GM11428 (**A** and **B**) and GM03715 (**C** and **D**), respectively. (A) and (C) show late replication of one chromosome 3 homolog without fragile site breakage in either homolog. (B) and (D) show late replication of one homolog with fragile site breakage. Two of the metaphases (A and D) also showed very strong signals (late replication) on the inactive chromosomes X. del(3), chromosome 3 with partial deletion; dup(3), chromosome 3 with duplication.
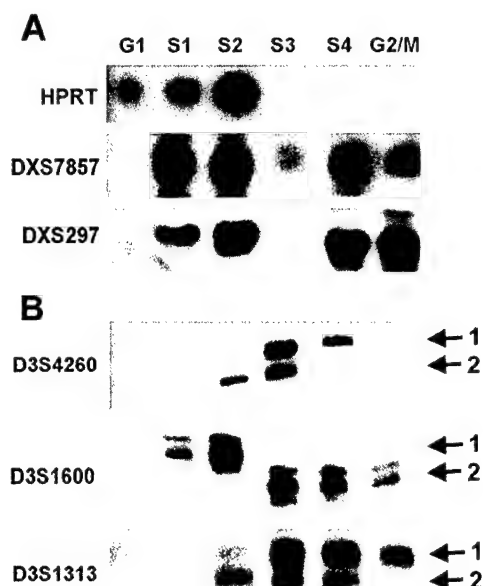
Figure 2. Allele-specific replication in the *FHIT*/FRA3B region. PCR products were labeled and separated on sequencing gels. (**A**) A control experiment was performed to ensure the high quality of isolated DNAs. The PCR products from known replication pattern markers produced early (*HPRT*) and late (*DXS297* and *DXS7857*) replication signals as expected. Note: both of the late replication markers also showed early replication bands since the DNAs were isolated from female cells with only one late replicated chromosome X (inactivated). (**B**) Three polymorphic markers from the *FHIT*/FRA3B region displayed asynchronous replication of their two distinct alleles. The arrows demonstrate the two different replicating alleles for each polymorphic marker.
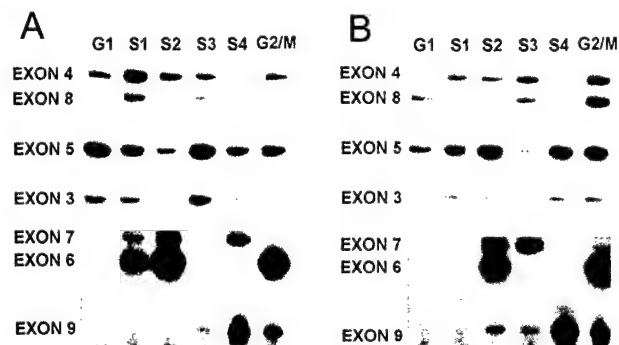
Figure 3. Replication timing profile of the *FHIT* gene. BrdU-labeled DNA from six different fractions of cell cycle were subjected to multiplex PCR by direct labeling with [α-^{32}P]dCTP followed by separation on sequencing gels (see Materials and Methods). (**A**) Replication profile before aphidicolin induction. (**B**) Replication profile after aphidicolin induction. Asynchronous replication timing can be seen with most of the *FHIT* exons.

fragile site. The data herein provide direct evidence linking late replication and breaks/gaps to the common fragile site FRA3B.

Asynchronous DNA replication has been reported in imprinted regions such as 15q11–13, 11q23 and 11p15.5 (16–19). Imprinted regions appear to be unstable in the human genome since frequent deletions and rearrangements were observed in these regions in human cancers and also in several genetic diseases. So far, the molecular basis of the instability at imprinted regions is not yet

known. Imprinted regions and the FRA3B region share several common features such as asynchronous replication and frequent deletion in cancers. Preliminary studies in our laboratory have shown that one allele of the *FHIT* gene in cancer cell lines is deleted preferentially (unpublished data) whereas the other allele appears to be unperturbed. This could explain why full-length RT–PCR products were still observed in cell lines with heterogeneous deletions in *FHIT* exons (20). Asynchronous replication may be associated with frequent splicing alterations within the *FHIT* gene, as seen in a variety of tumors and some normal tissues (21,22), since altered RNA splicing in other regions with asynchronous replication has been reported (23,24). More interestingly, *FMR1* and *FMR2*, the two cloned genes at rare fragile sites, also demonstrated altered RNA splicing and late replication (25–28). Further analysis will help to address any relationship between DNA replication and RNA splicing.

The data presented here show that the markers throughout this region replicate at different times in the cell cycle (Fig. 4). This does not seem consistent with what we know about DNA replication, replicons and replication domains in other regions. This asynchronous replication pattern could be one of the important factors leading to fragility in the FRA3B region. Thus far, we are not sure what mechanism causes this unique replication pattern. Previous studies have shown that the DNA sequences in this region are high in A–T content, LINEs and MER repeats, whereas the number of Alu elements is reduced (12). Further studies are needed to determine what kind of DNA sequences or three-dimensional structures are associated with the asynchronous replication timing across this region.

In summary, we report here that there is allele-specific replication of the *FHIT*/FRA3B region. The expression of fragility in the FRA3B region preferentially occurred on the chromosome with the late replicating allele. The results herein provide evidence that allele-specific late replication is related to the fragility of the common fragile site FRA3B. It will be interesting to see if the genes that reside on the 87 other common fragile sites show allele-specific replication. Such an observation would suggest that this is the mechanism underlying the common fragile sites: a very late replicating allele, which cannot finish replication before cell division in the presence of aphidicolin or some other cellular stress, predisposes that homolog to breakage and rearrangement.

MATERIALS AND METHODS

Cell lines and reagents

Human lymphoblastoid cell lines GM03715, GM00546 and GM11428 were purchased from NIGMS. The former two cell lines are karyotypically normal. GM11428, came from a 6-year-old female with the following karyotype: 46, XX, del(3)(p25pter),der(3)add(3)(pter)dup(3)(q21qter). The two chromosomes 3 in this patient are easily distinguishable from each other, thus facilitating our analyses of chromosome-specific late replication. The culture conditions were based on recommendations from the supplier. In addition, two peripheral blood samples were obtained from two females with normal karyotypes. Aphidicolin and BrdU were purchased from Sigma (St Louis, MO). Mouse anti-BrdU antibody and fluorescein-labeled secondary antibody (anti-IgG) were obtained from Calbiochem (La Jolla, CA).
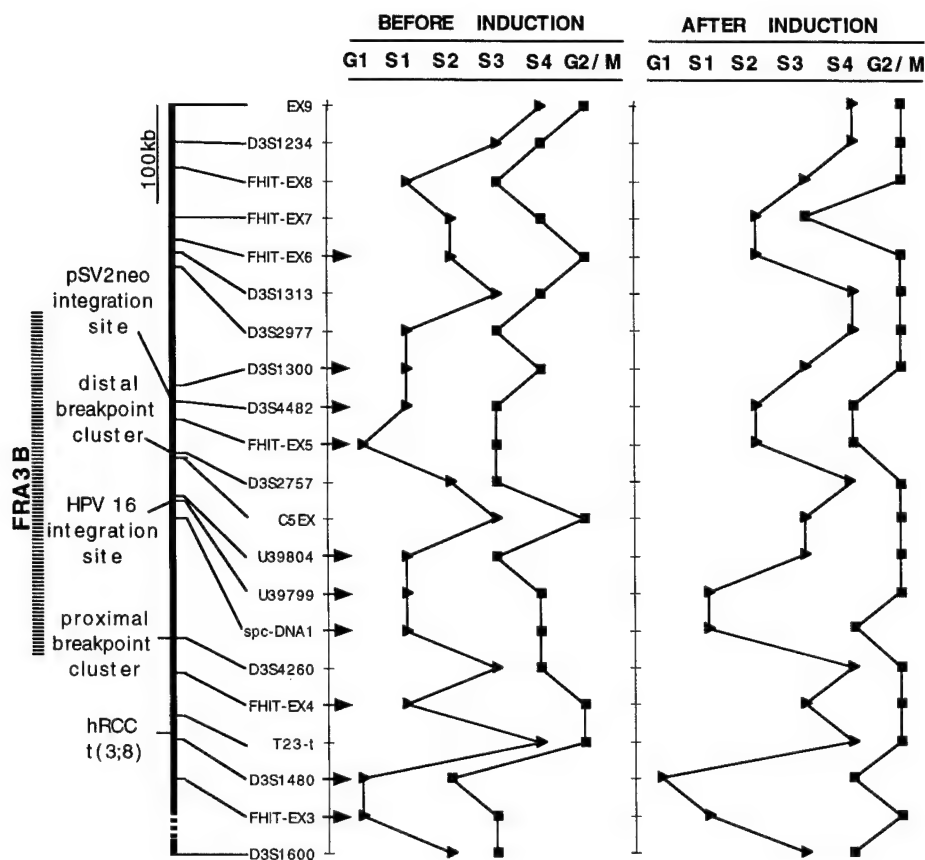
Figure 4. Timing of the replication profile across the *FHIT*/FRA3B region in cell line GM03715 in the absence and presence of aphidicolin. A total of 21 markers across the *FHIT*/FRA3B region were analyzed. The approximate position of each marker within the *FHIT*/FRA3B region is shown on the left. Also included in this figure is the region where aphidicolin-inducible breakage occurs (the FRA3B region), as well as important landmarks in that region including the hRCC breakpoint, the proximal and distal clusters of aphidicolin-induced breakpoints, the position of the HPV16 viral integration site and the position of pSV2neo insertions into the FRA3B region in the presence of aphidicolin. The two strongest signals were chosen to represent the replication timing for each allele for that marker. The curved lines represent replication timing for each allele across this region. The most significant asynchronous replication between the two alleles occurred at *FHIT* exon 6, *D3S1300*, *D3S4482*, *FHIT* exon 5, *U39804*, *U39799*, spc-DNA1, *FHIT* exon 4, *D3S1480* and *FHIT* exon 3 (arrows beside each marker).

Visualization of late replication in the FRA3B region

Cell lines GM03715 and GM11428 and two whole blood samples were cultured in RPMI-1640 with 10% fetal bovine serum (FBS) and treated with aphidicolin (0.4 μM) for 24 h. The cells were then labeled with BrdU at a final concentration of 10 μM (for GM03715 and GM11428) or 50 μM (for the two whole blood samples) for 3 h and treated with colcemid at a final concentration of 0.4 μM for 1 h before harvesting. The cells were collected and subjected to chromosome preparation. Chromosomes from metaphase spreads were denatured by incubation for 2 min in a mixture of ethanol/0.1 M NaOH (2:5) (29). BrdU-labeled chromosomes were visualized by using an indirect immuno-fluorescence procedure. Briefly, the denatured slides were permeabilized with 0.1% NP-40 for 15 min followed by incubation with 10% goat serum in phosphate-buffered saline (PBS) (pH 7.4) for 20 min. The slides were incubated with 5 μg/ml of anti-BrdU antibody in PBS-FCS solution (1× PBS, 5% fetal calf serum) for 1 h. After three 3 min washes with PBS, the slides were incubated with 1 μg/ml of fluorescein-labeled anti-mouse IgG for 1 h. The slides were then washed three times for 5 min each with PBS before counterstaining with 4′,6-diami-dino-2-phenylindole (DAPI) (0.03 μg/ml). The slides were

analyzed under a Zeiss fluorescence microscope with a CCD camera.

Flow cytometry and DNA isolation

Two different lymphoblastoid cell lines (GM03715 and GM00546) were cultured and treated with and without aphidico-lin at a final concentration of 0.4 μM for 24 h. The cells were then pulse-labeled for 90 min with BrdU at a final concentration of 50 μM. Before sorting, the cells were collected and stained with propidium iodide. The aphidicolin-treated and -untreated BrdU-labeled cells were separated into six different cell cycle phases on a FACS cell sorter. They include G_1, four S phases (S_1, S_2, S_3 and S_4) and G_2/M (30). For each phase, 1×10^5 cells were collected. BrdU-containing DNA from the lymphoblastoid cells and an equal amount of BrdU-labeled DNA from hamster cells were mixed and isolated by co-immunoprecipitation as described previously (27,28,30).

PCR analysis of replicated DNA

A total of 21 PCR-amplifiable sequence-tagged site (STS) markers (see Fig. 4 for the list) were analyzed across the FRA3B region

including 14 STS markers previously described (20) and primers specific for seven *FHIT* exons (exons 3–9) (31). The sequences for the *FHIT* multiplex PCR primer sets were kindly provided by Dr A.F. Gazdar (University of Texas Southwestern Medical Center). The primers for amplifying hamster DNA as a control were designed based on the *HXGPRT* gene (accession no. X53080) and the *TRANA* gene (accession no. X96664). The two hamster-specific primer pairs are: HXGPRT forward, 5′-TTCGGGAAAG-AAAGCTGTGA-3′; HXGPRT reverse, 5′-TCTCAAGTAGA-CAGGAGCCTTCC-3′; TRANA1 forward, 5′-AGCAGTA-GAAGAAATACAGGTG-3′; and TRANA1 reverse, 5′-ACC-TTGTGGTTTGTTGCTC-3′. In addition, internal controls for given replication profiles include assays of several known early and late replicating human sequences. The human *HPRT* gene (30) is an early replication marker. *DXS297* and *DXS7857* are late replication reference markers (28).

For non-polymorphic STS markers, PCR reactions were performed in a volume of 12.5 µl containing 100 µM of each dNTP, 1.5 mM MgCl$_2$, 6.25 pmol of each primer pair, 0.5 U of AmpliGold *Taq* polymerase (Perkin Elmer-Cetus, Branchburg, NJ) and BrdU-labeled DNA corresponding to 1000 flow-sorted cells in 1× reaction buffer II supplied by the manufacturer. For polymorphic STS markers and *FHIT* primers, 5 µCi of [α-^{32}P]dCTP (Amersham) was put into each PCR reaction for direct labeling. All reactions were performed on a Themocycler 480 (Perkin-Elmer Cetus) with 10 min initial denaturation at 95°C to activate the *Taq* polymerase. Amplification was for 25 cycles which included 94°C for 20 s, 58–60°C for 30 s and 72°C for 30 s. Except for *FHIT* primer sets, PCR reactions routinely included a pair of hamster primers as a control.

Replication timing analysis

PCR products from non-polymorphic STS markers were run on 1.5% agarose gels, transferred to nylon membranes and then probed with ^{32}P-labeled PCR products. The membrane was reprobed with α-^{32}P-labeled hamster-specific PCR products. The multiplex PCR products from the *FHIT* exons were run on 5% non-denaturing polyacrylamide gels. PCR products from polymorphic STS markers were analyzed by 6% denaturing polyacrylamide gels with 8 M urea. The films were exposed for 1–48 h before development. All of the experiments analyzing the cell cycle purified fractions were repeated at least twice.

ACKNOWLEDGEMENTS

ABBREVIATIONS

BrdU, 5-bromo-2′-deoxyuridine; *FHIT*, fragile histidine triad; hRCC, hereditary renal cell carcinoma; LR, late replication.

REFERENCES

1. Smeets, D.F.C.M., Scheres, J.M.J.C. and Hustinx, T.W.J. (1986) The most common fragile site in man is 3p14. *Hum. Genet.*, **72**, 215–220.
2. Brauch, H., Johnson, B., Hovis, J., Yano, T., Gazdar, A., Pettengill, O.S., Graziano, S., Sorenson, G.D., Poiesz, B.J., Minna, J. *et al.* (1987) Molecular analysis of the short arm of chromosome 3 in small-cell and non-small-cell carcinoma of the lung. *N. Engl. J. Med.*, **317**, 1109–1113.
3. Zbar, B., Brauch, H., Talmadge, C. and Linehan, M. (1987) Loss of alleles of loci on the short arm of chromosome 3 in renal cell carcinoma. *Nature*, **327**, 721–724.
4. Naylor, S.L., Johnson, B.E., Minna, J.D. and Sakaguchi, A.Y. (1987) Loss of heterozygosity of chromosome 3p markers in small-cell lung cancer. *Nature*, **329**, 451–454.
5. Shridhar, R., Shridhar, V., Wang, X., Paradee, W., Dugan, M., Sarkar, F., Wilke, C., Glover, T.W., Vaitkevicius, V.K. and Smith, D.I. (1996) Frequent breakpoints in the 3p14.2 fragile site, FRA3B, in pancreatic tumors. *Cancer Res.*, **56**, 4347–4350.
6. Shridhar, V., Wang, L., Rosati, R., Paradee, W., Shridhar, R., Mullins, C., Sakr, W., Grignon, D., Miller, O.J., Sun, Q.C., Petros, J. and Smith, D.I. (1997) Frequent breakpoints in the region surrounding FRA3B in sporadic renal cell carcinomas. *Oncogene*, **14**, 1269–1277.
7. Ohta, M., Inoue, H., Cotticelli, M.G., Kastury, K., Baffa, R., Palazzo, J., Siprashvili, Z., Mori, M., McCue, P., Druck, T. *et al.* (1996) The *FHIT* gene, spanning the chromosome 3p14.2 fragile site and renal carcinoma-associated t(3;8) breakpoint, is abnormal in digestive tract cancers. *Cell*, **84**, 587–597.
8. Sozzi, G., Veronese, M.L., Negrini, M., Baffa, R., Cotticelli, M.G., Inoue, H., Tornielli, S., Pilotti, S., De Gregorio, L., Pastorino, U., Pierotti, M.A., Ohta, M., Huebner, K. and Croce, C.M. (1996) The *FHIT* gene 3p14.2 is abnormal in lung cancer. *Cell*, **85**, 17–26.
9. Virgilio, L., Shuster, M., Gollin, S.M., Veronese, M.L., Ohta, M., Huebner, K. and Croce, C.M. (1996) *FHIT* gene alterations in head and neck squamous cell carcinomas. *Proc. Natl Acad. Sci. USA*, **93**, 9770–9775.
10. Barnes, L.D., Garrison, P.N., Siprashvili, Z., Guranowski, A., Robinson, A.K., Ingram, S.W., Croce, C.M., Ohta, M. and Huebner, K. (1996) Fhit, a putative tumor suppressor in humans, is a dinucleoside 5′,5′″-P1,P3-triphosphate hydrolase. *Biochemistry*, **35**, 11529–11535.
11. Paradee, W., Wilke, C.M., Wang, L., Shridhar, R., Mullins, C.M., Hoge, A., Glover, T.W. and Smith, D.I. (1996) A 350-kb cosmid contig in 3p14.2 that crosses the t(3;8) hereditary renal cell carcinoma translocation breakpoint and 17 aphidicolin-induced FRA3B breakpoints. *Genomics*, **35**, 87–93.
12. Boldog, F., Gemmill, R.M., West, J., Robinson, M., Robinson, L., Li, E., Roche, J., Todd, S., Waggoner, B., Lundstrom, R., Jacobson, J., Mullokandov, M.R., Klinger, H. and Drabkin, H.A. (1997) Chromosome 3p14 homozygous deletions and sequence analysis of FRA3B. *Hum. Mol. Genet.*, **6**, 193–203.
13. Laird, C.D., Jaffe, E., Karpen, G., Lamb, M. and Nelson, R. (1987) Fragile sites in human chromosomes as regions of late replicating DNA. *Trends Genet.*, **3**, 274–281.
14. Le Beau, M.M., Rassool, F.V., Neilly, M.E., Espinosa, R. III, Glover, T.W., Smith, D.I. and McKeithan, T.W. (1998) Replication of a common fragile site, FRA3B, occurs late in S phase and is delayed further upon induction: implications for the mechanism of fragile site induction. *Hum. Mol. Genet.*, **7**, 755–761.
15. Glover, T.W., Berger, C. Coyle, J. and Echo, B. (1984) DNA polymerase alpha inhibition by aphidicolin induces gaps and breaks at common fragile sites in human chromosomes. *Hum. Genet.*, **67**, 136–142.
16. Kitsberg, D., Selig, S., Brandeis, M., Simon, I., Keshet, I., Driscoll, D.J., Nicholls, R.D. and Cedar, H. (1993) Allele-specific replication timing of imprinted gene regions. *Nature*, **364**, 459–463.
17. Lin, M.S., Zhang, A. and Fujimoto, A. (1995) Asynchronous DNA replication between 15q11.2q12 homologs: cytogenetic evidence for maternal imprinting and delayed replication. *Hum. Genet.*, **96**, 572–576.
18. Knoll, J.H., Cheng, S.D. and Lalande, M. (1994) Allele specificity of DNA replication timing in the Angelman/Prader–Willi syndrome imprinted chromosomal region. *Nature Genet.*, **6**, 41–46.
19. Reik, W., Brown, K.W., Schneid, H., Le Bouc, Y., Bickmore, W. and Maher, E.R. (1995) Imprinting mutations in the Beckwith–Wiedemann syndrome suggested by altered imprinting pattern in the IGF2–H19 domain. *Hum. Mol. Genet.*, **4**, 2379–2385.
20. Wang, L., Darling, J., Zhang, J.S., Qian, C.P., Hartmann, L., Conover, C., Jenkins, R. and Smith, D.I. (1998) Frequent homozygous deletions in the FRA3B region in tumor cell lines still leave the *FHIT* exons intact. *Oncogene*, **16**, 635–642.

21. Panagopoulos, I., Thelin, S., Mertens, F., Mitelman, F. and Aman, P. (1997) Variable *FHIT* transcripts in non-neoplastic tissues. *Genes Chromosomes Cancer*, **19**, 215–219.
22. Luan, X., Shi, G., Zohouri, M., Paradee, W., Smith, D.I., Decker, H.J. and Cannizzaro, L.A. (1997) The *FHIT* gene is alternatively spliced in normal kidney and renal cell carcinoma. *Oncogene*, **15**, 79–86.
23. Davies, K. (1992) Imprinting and splicing join together. *Nature*, **360**, 492.
24. Dittrich, B., Buiting, K., Korn, B., Rickard, S., Buxton, J., Saitoh, S., Nicholls, R.D., Poustka, A., Winterpacht, A., Zabel, B. and Horsthemke, B. (1996) Imprint switching on human chromosome 15 may involve alternative transcripts of the *SNRPN* gene. *Nature Genet.*, **14**, 163–170.
25. Eichler, E.E., Richards, S., Gibbs, R.A. and Nelson, D.L. (1993) Fine structure of the human *FMR1* gene. *Hum. Mol. Genet.*, **2**, 1147–1153.
26. Gecz, J., Bielby, S., Sutherland, G.R. and Mulley, J.C. (1997) Gene structure and subcellular localization of FMR2, a member of a new family of putative transcription activators. *Genomics*, **44**, 201–213.
27. Hansen, R.S., Canfield, T.K., Lamb, M.M., Gartler, S.M. and Laird, C.D. (1993) Association of fragile X syndrome with delayed replication of the *FMR1* gene. *Cell*, **73**, 1403–1409.
28. Hansen, R.S., Canfield, T.K., Fjeld, A.D., Mumm, S., Laird, C.D. and Gartler SM. (1997) A variable domain of delayed replication in FRAXA fragile X chromosomes: X inactivation-like spread of late replication. *Proc. Natl Acad. Sci. USA*, **94**, 4587–4592.
29. Latos-Bielenska, A., Hameister, H. and Vogel, W. (1987) Detection of BrdUrd incorporation in mammalian chromosomes by a BrdUrd antibody. III. Demonstration of replication patterns in highly resolved chromosomes. *Hum. Genet.*, **76**, 293–295.
30. Hansen, R.S., Canfield, T.K. and Gartler, S.M. (1995) Reverse replication timing for the *XIST* gene in human fibroblasts. *Hum. Mol. Genet.*, **4**, 813–820.
31. Ahmadian, M., Wistuba, I.I., Fong, K.M., Behrens, C., Kodagoda, D.R., Saboorian, M.H., Shay, J., Tomlinson, G.E., Blum, J., Minna, J.D. and Gazdar, A.F. (1997) Analysis of the *FHIT* gene and FRA3B region in sporadic breast cancer, preneoplastic lesions, and familial breast cancer probands. *Cancer Res.*, **57**, 3664–3668.

Keratin 23 (K23), a Novel Acidic Keratin, Is Highly Induced by Histone Deacetylase Inhibitors During Differentiation of Pancreatic Cancer Cells

Jin-San Zhang, Liang Wang, Haojie Huang, Matthew Nelson, and David I. Smith*

Division of Experimental Pathology, Department of Laboratory Medicine and Pathology, Mayo Foundation, Rochester, Minnesota

Sodium butyrate (NaBu) was shown to induce differentiation and apoptosis in the human pancreatic cancer cell line AsPC-1. A suppression subtractive hybridization-based technique was used to identify genes induced by NaBu. A novel cDNA was found to be highly up-regulated in AsPC-1 cells in response to NaBu. The gene expresses a 1.65-kb mRNA encoding a protein with an open reading frame of 422 amino acids. It has an intermediate filament signature sequence and extensive homology to type I keratins. Sequence comparison with known keratins indicated that the gene shares 42–46% amino acid identity and 60–65% similarity within the α-helical rod domain. The gene is named K23 (for human type I Keratin 23, KRT23). K23 mRNA was highly induced by NaBu in different pancreatic cancer cells. Trichostatin A (TSA), a potent and specific inhibitor of histone deacetylase, similarly induced K23 mRNA expression. Treatment with either actinomycin D or cycloheximide efficiently blocked the induction of K23 mRNA by NaBu/TSA. These results indicate that K23 mRNA induction by NaBu or TSA is a downstream event of histone hyperacetylation. We also demonstrated that expression of $p21^{WAF1/CIP1}$ antisense RNA efficiently blocked the induction of K23 mRNA induced by NaBu. Our results suggest that K23 is a novel member of the acidic keratin family that is induced in pancreatic cancer cells undergoing differentiation by a mechanism involving histone hyperacetylation. $p21^{WAF1/CIP1}$ serves as an important mediator during the induction process of K23 by NaBu.
© 2000 Wiley-Liss, Inc.

INTRODUCTION

Pancreatic adenocarcinoma is the fifth leading cause of cancer mortality in the United States, with an extremely dismal prognosis (Silverberg et al., 1990). Only about 10% of patients have resectable tumors at the time of diagnosis, and the 5-year survival rate of these patients is less than 10% (Warshaw et al., 1992). It is therefore imperative to identify new molecular markers for the early diagnosis and to explore novel therapeutic strategies for this lethal disease. One of the therapeutic agents that is potentially important in the treatment of pancreatic adenocarcinoma is sodium butyrate (NaBu). Recently, butyrate and its structural analogs have entered clinical trial as a differentiation therapy for advanced prostate cancer and brain tumors (Samid et al., 1997). NaBu is a short-chain fatty acid generated in the large intestine by bacterial fermentation of dietary fibers. The biological significance of this compound is its ability to regulate cell growth and differentiation. NaBu has been shown to induce growth inhibition, differentiation, and apoptosis in various cell lines derived from primary tumors such as breast cancer (Graham and Buick, 1988), colorectal tumors (Barnard and Warwick, 1993; Hague et al., 1993), prostate cancer

(Halgunset et al., 1988; Huang et al., 1999), hepatoma (Saito et al., 1991), neuroblastomas (Rocchi et al., 1992), as well as pancreatic cancer (Egawa et al., 1996; Mullins et al., 1991). The concentrations of butyrate that cause growth inhibition in vitro are similar to those measured within the mammalian colon.

One of the known functions of NaBu is inhibition of histone deacetylase, that leads to the development of histone hyperacetylation (Riggs et al., 1977). Reversible histone acetylation is now thought to play an important role in the regulation of chromatin structure and in transcriptional activity (Turner, 1993). The discovery of enzymes controlling the acetylation and deacetylation of histones has brought new insights into the understanding of the transcriptional machinery within the cell. Nuclear histone acetylases have been shown to be either transcriptional coactivators

or coactivator-associated proteins, whereas histone deacetylases have been identified as components of nuclear co-repressor complexes providing a direct link between histone acetylation and transcriptional regulation (Armstrong and Emerson, 1998; Davie, 1998). More recent findings have shown that many transcriptional regulatory proteins possess intrinsic histone acetylase activity, including *Gcn5p*, *TAF130/250*, and *p300/CBP* (Kuo et al., 1996; Mizzen et al., 1996; Ogryzko et al., 1996). The *retinoblastoma protein* (*RB1*) inhibits transcription of S-phase specific protein by recruiting *HDAC1* (Luo et al., 1998). The p53 tumor suppressor protein also utilizes histone deacetylases to repress the transcription of specific genes, and its interaction with histone deacetylases is mediated by the transcriptional co-repressor protein mSin3a (Murphy et al., 1999). There is also evidence that histone deacetylation is associated with DNA methylation. The methyl-CpG-binding protein *MECP2* appears to reside in a complex that has histone deacetylase activity (Jones et al., 1998; Nan et al., 1998). DNA methylation and histone deacetylation seem to act in synergy for the silencing of some important genes in cancer, although CpG island methylation is the dominant mechanism for the stable maintenance of the silent state at these loci (Cameron et al., 1999).

It was recently shown that butyrate mediates growth inhibition of colon cancer cells by inducing $p21^{WAF1/CIP1}$ expression through histone deacetylation (Archer et al., 1998). In addition, the products of certain oncogenes have been shown to suppress transcription of their target genes by recruiting histone deacetylase (Ogryzko et al., 1996; Yang et al., 1996), that cleaves acetyl groups from histones and blocks their ability to induce DNA conformational changes. This transcriptional block can be overcome by agents that inhibit histone deacetylase, and clinically, transcription targeting therapy for leukemia has been achieved using butyrate to inhibit histone deacetylase to relieve the transcriptional repression caused by certain oncogenes (Warrell et al., 1998).

We sought to investigate the molecular mechanism by which butyrate mediates growth arrest and differentiation of pancreatic cancer cells, and to identify potential markers for diagnosis and treatment. In the present study, we report on the identification and characterization of a novel intermediate filament protein, designated *K23*, that is highly induced upon NaBu treatment of pancreatic cancer cells. Our data demonstrate that *K23* repre-

sents a novel member of the type I keratin family and is highly induced by agents causing histone hyperacetylation. We have also demonstrated that $p21^{WAF1/CIP1}$ is a critical mediator of *K23* mRNA induction by NaBu.

MATERIALS AND METHODS

Cell Cultures and Treatment

The human pancreatic carcinoma cell line AsPC-1 was obtained from the American Type Culture Collection (Rockville, MD). The cell line was originally derived from pancreatic adenocarcinoma cells that had metastasized to the liver. The cells were maintained as a monolayer in RPMI 1640 (Life Technologies, Gaithersburg, MD) supplemented with 15% fetal calf serum, penicillin (50 IU/ml)/streptomycin (50 mg/ml) (Life Technologies, Gaithersburg, MD), L-glutamine (2 mM), and sodium pyruvate (1 mM; Sigma, St. Louis, MO) and were grown in 5% CO_2, in 95% humidified air at 37°C. Other cell lines including SU.86.86, BxPC-3, Capan-1, MIA, Hs766T, and PANC-1 were also obtained from the American Type Culture Collection (Rockville, MD) and cultured under the conditions recommended for each cell line. Chemical treatments were performed on cells that were 60–80% confluent. All the chemical reagents including NaBu (sodium butyrate), paraquat, 5-AC (5-azacytidine), TSA (trichostatin A), ACD (actinomycin D), and CHX (cycloheximide) were purchased from Sigma. NaBu, paraquat, 5-AC, and TSA were added to cultures at the concentration and for the times indicated in the text. The final concentrations of ACD and CHX used were 4 μM and 35 μM, respectively. In the case of combined treatments, ACD or CHX was added to cultures 30 min before the addition of NaBu or TSA. Images were taken on an inverted Zeiss microscope at 200× magnification using a phase contrast objective. Representative digital images were captured using the Spot digital camera (Diagnostic Instruments Inc., Sterling Height, MI).

Analysis of Apoptotic DNA

To determine whether treatment of cells with NaBu resulted in DNA fragmentation, collected cells and DNA was extracted by the method of Borner et al. (1995), as has been described (Huang et al., 1999). Attached cells were detached from the culture dishes with 5 mM EDTA, spun down, and lysed in 5 mM Tris (pH 7.4), 5 mM EDTA, and 0.5% Triton X-100 for 2 hr on ice. The detached

cells were directly spun down from culture medium and lysed as above. The lysate was centrifuged at 27,000 × g for 20 min. The supernatant was incubated with 200 μg/ml proteinase K for 1 hr at 50°C and extracted with phenol/chloroform; then the DNA was precipitated overnight at 20°C in 2 vol of ethanol and 0.13 M NaCl with 20 μg of glycogen. Nucleic acids were treated with 1 mg/ml boiled bovine pancreatic RNase A for 1 hr at 50°C, then the DNA was resolved on 1.8% (W/V) agarose gels containing 0.3 μg/ml ethidium bromide, and run in 1× TBE buffer at 2.5 V/cm.

Construction of Subtracted cDNA Libraries and Screening With Reverse Northern Hybridization

The SSH-based technique was used to generate subtracted cDNA libraries (Diatchenko et al., 1996). Briefly, total RNA was prepared from control and NaBu-treated cells using Trizol reagent. Polyadenylated RNA was purified using the Oligotex mRNA purification kit (Qiagen, Valencia, CA). SSH was performed between control AsPC-1 cells and AsPC-1 cells treated with 1 mM NaBu for 24 hr using the PCR-Select™ cDNA subtraction kit (Clontech, Palo Alto, CA) following the procedures described by the manufacturer. The subtraction efficiency was determined by PCR analysis of GAPDH expression in subtracted and unsubtracted cDNA libraries. The differentially expressed cDNAs were enriched through a nested PCR approach. The PCR conditions were modified from the original protocol to increase specificity. The thermocycling conditions used for initial suppression PCR were 75°C 5 min, 94.5°C 30 sec, then 5 cycles at 94.5°C 10 sec, 68°C 10 sec, 72°C 1.5 min, followed by 22 cycles of 94.5°C 10 sec, 66°C 10, sec and 72°C 1.5 min using a single primer (5'-CTAATACGACTCACTATAGGGC-3'). The primary PCR products were diluted 50 times, and 1 μl was used as template in 100 μl of nested PCR reaction. The PCR was performed at 94.5 10 sec, 72°C 1.5 min for 15 cycles with primers NP1 (5'-TCGAGCGGCCGCCCGGGCAGGT-3') and NR2 (5'-AGCGTGGTCGCGGCCGAGGT-3').

The PCR products from either forward (control AsPC-1 as driver) or reverse (NaBu-treated cell as driver) subtracted cDNA libraries were subcloned into pGEM-T vector (Promega, Madison, WI). A total of 190 random picked single colonies were used for colony PCR with NP1 and NR2 primers. The PCR products from each individual clone were arrayed onto nylon filters in duplicates for further screening. The adaptor-free nested PCR

products from forward and reverse subtracted cDNA libraries, respectively, were used as probes for Reverse Northern hybridization. The hybridized filters were exposed to autoradiography film at −80°C for from 3 hr to 3 days.

Rapid Amplification of cDNA Ends (RACE) and Sequencing

To obtain the full-length cDNA sequence of *K23*, the 5'-RACE procedure was employed, with Marathon-Ready cDNA from pancreas used as a template and the Advantage cDNA Klentaq DNA polymerase (Clontech, Palo Alto, CA) used following the manufacturer's instructions. Two gene-specific primers (GSP1 and GSP2) were designed based upon the original sequence obtained from the SSH cDNA library. The primer sequences are GSP1: 5'-CACTCACTGGTGTCTGTGCAAG-GACTT-3' and GSP2: 5'-CTCTCCCTCCAG-GAGCCGTCGGTA-3'. A RACE product of 1.2 kb was obtained and cloned into the pGEM-T vector (Promega, Madison, WI). Automatic sequencing was performed in the Mayo Foundation Molecular Biology Core. The Genbank™ database was used for sequence searches.

Northern Blot Hybridization

Total RNA was prepared from control and treated cells using Trizol regent. Aliquots of 15 μg of total RNA were fractionated on 1.2% formaldehyde-agarose gels and blotted in 1× SPC buffer (20 mM Na_2HPO_4, 2 mM CDTA, pH 6.8) onto Hybond N membranes (Amersham, Piscataway. NJ). The probes were labeled using the Random primer labeling system (Life Technologies, Gaithersburg, MD) and purified with a spin column 100TE (Clontech). Filters were hybridized at 68°C with radioactive probes in a microhybridization incubator for 1–2 hr using Express Hybridization Solution (Clontech), and washed according to the manufacturer's instructions.

Construction of p21$^{WAFI/CIPI}$ Sense and Antisense Expression Vectors

Two primers flanking the full open reading frame of *p21$^{WAFI/CIPI}$* were designed to amplify a 530-bp cDNA fragment (from base 66–595, GenBank accession number U03106). A *BamHI* site (underlined) was introduced into the forward primer AGGAGGATCCATGTCAGAA, and a *HindIII* site (underlined) was inserted into the reverse primer GGACTGCAAGCTTCCTGTGG. The PCR product was digested with both *BamHI*

and *HindIII*, and a 517-bp cDNA fragment was isolated and subcloned into the mammalian expression vectors pcDNA3.1(+) and pcDNA3.1(−) (Invitrogen, Carlsbad, CA), respectively, and transformed into *E. coli* DH5α (Life Technologies, Gaithersburg, MD). Mini-preparations of ampicillin-resistant clones were sequenced and analyzed for the orientation and sequence of inserts.

Transient and Stable Transfection of $p21^{WAFI/CIP1}$ Expression Vectors

Transient transfections were performed with the LipofectAminePLUS™ system (Life Technologies, Gaithersburg, MD). Exponentially growing cells were cultured in 10-mm dishes for 24 hr in medium without antibiotics before transfection. A mixture of 5 μg of plasmid, 30 μl of Lipofectamine and 20 μl of PLUS in 6 ml of serum free medium was added. After a 5 hr incubation, complete medium with serum was added. The cells were incubated at 37°C for 24 hr after the start of transfection. Cells were then treated with or without NaBu for 24 hr and harvested, and total RNA was isolated. Northern blot analysis was performed using $p21^{WAFI/CIP1}$ and *K23* cDNA as probes.

To generate stable transfected clones, AsPC-1 cell were subcultured at 48 hr after transfection, and G418 was added to cultured cells at a final concentration of 450 μg/ml. The cells were selected for over 6-8 weeks, and pooled cells of either transfected with $p21^{WAFI/CIP1}$ sense or $p21^{WAFI/CIP1}$ antisense construct were used for analysis. To examine the effects of $p21^{WAFI/CIP1}$ transactivation on *K23* mRNA induction by NaBu, pooled AsPC-1 cells stably transfected with either $p21^{WAFI/CIP1}$ sense or antisense vector were treated with NaBu for 24 hr. For controls, AsPC-1 cells similarly transfected with PcDNA3.1(+) were used.

RESULTS

NaBu Induced Differentiation and Apoptosis in AsPC-1 Cells

Treatment of AsPC-1 cells with NaBu induced differentiation. NaBu at concentrations as low as 0.2 mM produced elongated cells with multiple filamentous protrusions characteristic of cells undergoing differentiation. The morphologic changes were associated with increased expression of alkaline phosphatase, a well-known differentiation marker. The morphology change could be observed at about 24 hr after treatment with 0.2 mM NaBu, and tended to occur earlier

with increasing doses of NaBu. Cell cycle analysis using flow cytometry indicated that there was a G1 as well as G2-M block associated with NaBu treatment. A substantial fraction of the sub-G1 population was detected when treated with concentrations of NaBu of 2 mM or higher for 48 hr, suggesting induction of apoptosis in these cells. Apoptosis induction in the presence of higher concentrations of NaBu (e.g., above 2 mM) was confirmed by detecting the formation of DNA ladders in these cells, and most of the apoptotic cells were found in the detached cell population. (data not shown). The changes in cell morphology and the expression of alkaline phosphatase mRNA expression associated with NaBu treatment are shown in Figure 1. Based on the above observation, we concluded that treatment of AsPC-1 cells with a concentration of 1 mM NaBu resulted in cells undergoing a differentiation phenotype, whereas increased NaBu concentrations resulted in a significant increase in the number of cells undergoing apoptosis.

F1

Identification and Cloning of a Novel Transcript Induced by NaBu

In an attempt to identify genes with altered expression as a result of NaBu treatment, two subtracted cDNA libraries highly enriched for NaBu either up- or down-regulated genes were constructed using the SSH (Suppression Subtraction Hybridization)-based technique (Diatchenko et al., 1996). This previously led to the identification of *CTNNAL1*, a gene with high homology to α-catenin that was down-regulated by NaBu (Zhang et al., 1998). The cells used for the construction of the subtracted cDNA libraries were derived from control cells and cells treated with 1 mM NaBu for 24 hr, a time and dose that induce the differentiation phenotype with limited apoptosis. The clones from the subtracted cDNA libraries were arrayed onto nylon filters and further screened by Reverse Northern hybridization. Figure 2 shows matched parts of duplicated array filters hybridized with forward and reverse subtracted cDNA probes, respectively. There are eight clones (marked with arrows) that were significantly increased in expression upon NaBu treatment.

F2

Sequence analysis indicated that six clones were homologous to known human genes, including *IGFBP-3* (1A, 2B), tissue transglutaminase (1B), Alkaline phosphatase (4B), *GADD45* (5E), and *IGFBP-1* (1G). The remaining two clones (3G, 3F) represent novel transcripts that have no matches in

Figure 2. Screening of arrayed cDNA clones with Reverse Northern hybridization. Colony PCR products of 190 individual clones from the forward-subtracted cDNA libraries were arrayed onto nylon filters in duplicates and used for hybridization as described in Materials and Methods. The cDNA probes from forward subtracted library (enriched for NaBu up-regulated transcripts) is designated as NaBu(+) and that from reverse subtracted cDNA probes as NaBu(−). Shown in the figure is part of the matched duplicated filters hybridized with NaBu(+) and NaBu(−) probes, respectively. The clones marked with arrows correspond the cDNA clones with increased expression upon NaBu treatment.
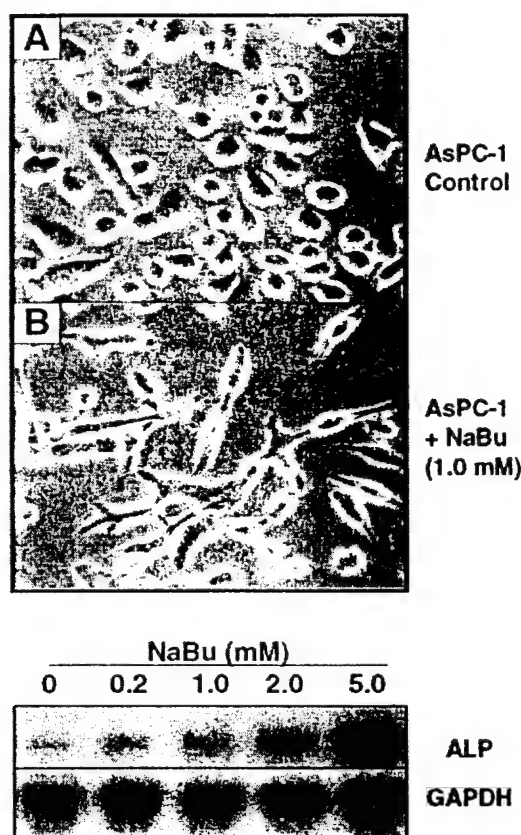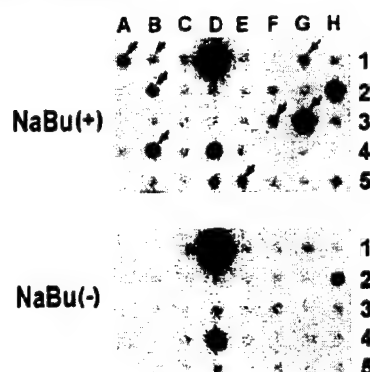
Figure 1. NaBu-induced morphological changes and alkaline phosphatase mRNA expression. AsPC-1 monolayers (50% confluency) were exposed to various concentrations of NaBu for different periods of time, and the cells were then assessed for morphology changes with a phase contrast lens using an inverted microscope. Shown here are the control AsPC-1 cells and those treated with 1 mM NaBu for 24 hr. For analysis of alkaline phosphatase mRNA expression, total RNA from NaBu treated AsPC-1 cells was prepared and used for Northern blot analysis. The probe for alkaline phosphatase was the cDNA fragment derived from the same subtracted cDNA library as *K23* (Clone 4B in Fig. 2). ALP, alkaline phosphatase. The same blot was stripped and rehybridized with a *GAPDH* probe to demonstrate even loading of RNA samples.

the "Nr" database. Clone 3G is of particular interest in that it is the most highly induced. Sequencing revealed that clone 3G had an insert of 473 bp with a short poly-A tail and also a putative poly-A adenylation signal (AATAAA), suggesting that this sequence may have been derived from the 3' end of an mRNA. Searching of the NCBI's nucleotide database revealed no hits in "Nr" by BLASTIN, but several highly matched ESTs from the EST database. We first attempted to assemble the matching ESTs from the database using the Sequencher 3.1 program, but this work did not generate a reasonable open reading frame. We therefore performed 5' RACE using primers based on

the cDNA sequence obtained. A RACE product of 1.2 kb was cloned and fully sequenced.

K23, an Intermediate Filament Protein, is a New Member of Type I Keratin

A 1.62 kb mRNA sequence was obtained based on sequencing of the RACE product as well as the original cDNA. The cDNA and predicted amino-acid sequences are presented in Figure 3. The cDNA contained a 1269 bp open reading frame, that could code for a protein of 422 a.a. that would have a predicted molecular mass of 48 kd and a PI of 6.01. Protein motif analysis using MOTIF finder (http://www.motif.genome.ad.jp) revealed the presence of several domains, most significantly an intermediate filament protein signature sequence, *ITTYRRLLE*. Probability analysis of the conformation of this protein showed long regions with α-helical character. The central rod domain consists of a seven residue heptated repeat capable of forming a coiled-coil conformation. The α-helical rod domain consisting of 309 a.a. is boxed in Figure 3. Sequence comparison with protein sequences in the NCBI database showed significant sequence homology to all the type I keratins within the α-helical rod domain. No significant homology was found between this putative protein and type II keratins (data not shown). Based on the sequence similarity and structural conservation, this protein is named *K23* (for *KRT23, type I keratin 23*). The

```
                                        CAGTCTGGGGCGGCTC   -61
    AGTTCTGCGGTGCCAGGGAGTGGAGCAGAGCTCAGCCCCGTCCCAAACACAGATGGGACC   -1
    ATGAACTCCGGACACAGCTTCAGCCAGACCCCCTCGGCCTCCTTCCATGGCGCCGGAGGT   60
1    M  N  S  G  H  S  F  S  Q  T  P  S  A  S  F  H  G  A  G  G
    GGCTGGGGGCCGGCCCAGGGAGCTTCCCCAGGGGCTCCCACCGTCCATGGCGGTGCGGGGGA  120
21   G  W  G  R  P  R  S  F  P  R  A  P  T  V  H  G  G  A  G  G
    GCCCGCATCTCCCTGTCCTTCACCACGCGGAGCTGCCCACCCCCTGGAGGGTCTTGGGGT  180
41   A  R  I  S  L  S  F  T  T  R  S  C  P  P  P  G  G  S  W  G
    TCTGGAAGAAGCAGCCCCCTACTAGGCGGAAATGGGAAGGCCACCATGCAGAATCTCAAC  240
61   S  G  R  S  S  P  L  L  G  G  N  G  K  A  T  M  Q  N  L  N
    GACCGCCTGGCCTCCTACCTGGAGAAGGTTCGCGCCCTGGAGGAGGCCAACATGAAGCTG  300
81   D  R  L  A  S  Y  L  E  K  V  R  A  L  E  E  A  N  M  K  L
    GAAAGCCGCATCCTGAAATGGCACCAGCAGAGAGATCCTGGCAGTAAGAAAGATTATTCC  360
101  E  S  R  I  L  K  W  H  Q  Q  R  D  P  G  S  K  K  D  Y  S
    CAGTATGAGGAAAACATCACACACCTGCAGGAGCAGATAGTGGATGGTAATATGACCAAT  420
121  Q  Y  E  E  N  I  T  H  L  Q  E  Q  I  V  D  G  N  M  T  N
    GCTCAGATTATTCTTCTCATTGACAATGCCAGGATGGCAGTGGATGACTTCAACCTCAAG  480
141  A  Q  I  I  L  L  I  D  N  A  R  M  A  V  D  D  F  N  L  K
    TATGAAAATGAACACTCCTTTAAGAAAGACTTGGAAATTGAAGTCGAGGGCCTCCGAAGG  540
161  Y  E  N  E  H  S  F  K  K  D  L  E  I  E  V  E  G  L  R  R
    ACCTTAGACAACCTGACCATTGTCACAACAGACCTAGAACAGGAGGTGGAAGGAATGAGG  600
181  T  L  D  N  L  T  I  V  T  T  D  L  E  Q  E  V  E  G  M  R
    AAAGAGCTCATTCTCATGAAGAAGCACCATGAGCAGGAAATGGAGAAGCATCATGTGCCA  660
201  K  E  L  I  L  M  K  K  H  H  E  Q  E  M  E  K  H  H  V  P
    AGTGACTTCAATGTCAATGTGAAGGTGGATACAGGTCCCAGGGAAGATCTGATTAAGGTC  720
221  S  D  F  N  V  N  V  K  V  D  T  G  P  R  E  D  L  I  K  V
    CTGGAGGATATGAGACAAGAATATGAGCTTATAATAAAGAAGAAGCATCGAGACTTGGAC  780
241  L  E  D  M  R  Q  E  Y  E  L  I  I  K  K  K  H  R  D  L  D
    ACTTGGTATAAAGAACAGTCTGCAGCCATGTCCCAGGAGGCAGCCAGTCCAGCCACTGTG  840
261  T  W  Y  K  E  Q  S  A  A  M  S  Q  E  A  A  S  P  A  T  V
    CAGAGCAGACAAGGTGACATCCACGAACTGAAGCGCACATTCCAGGCCCTGGAGATTGAC  900
281  Q  S  R  Q  G  D  I  H  E  L  K  R  T  F  Q  A  L  E  I  D
    CTGCAGACACAGTACAGCACGAAATCTGCTTTGGAAAACATGTTATCCGAGACCCAGTCT  960
301  L  Q  T  Q  Y  S  T  K  S  A  L  E  N  M  L  S  E  T  Q  S
    CGTAACTCCTGCAAGCTCCAGGACATGCAAGAGATCATCTCCCACTATGAGGAGGAACTG  1020
321  R  N  S  C  K  L  Q  D  M  Q  E  I  I  S  H  Y  E  E  L
    ACGCAGCTACGCCACGAACTGGAGCGGCAGAACAATGAATACCAAGTGCTGCTGGGCATC  1080
341  T  Q  L  R  H  E  L  E  R  Q  N  N  E  Y  Q  V  L  L  G  I
    AAAAACCCACCTGGAGAAGGAAATCACCACGTACCGACGGCTCCTGGAGGGGAGAGAGTGAA  1140
361  K  T  H  L  E  K  E  ░░░░░░░░░░░░░░░░░░░  G  E  S  E
    GGGACACGGGAAGAATCAAAGTCGAGCATGAAAGTGTCTGCAACTCCAAAGATCAAGGCC  1200
381  G  T  R  E  E  S  K  S  S  M  K  U  S  A  T  P  K  I  K  A
    ATAACCCAGGAGACCATCAACGGAAGGATTAGTTCTTTGTCAAGTGAATGAAATCCAAAAG  1260
401  I  T  Q  E  T  I  N  G  R  L  U  L  C  Q  U  N  E  I  Q  K
    CACGCATGAGACCAATGAAAGTTTCCGCCTGTTGTAAAATCTATTTTCCCCCAAGGAAAG  1320
421  H  A  *
    TCCTTGCACAGACACCAGTGAGTGAGTTCTAAAAGATACCCTTGGAATTATCAGACTCAG  1380
    AAACTTTTATTTTTTTTTTCTGTAACAGTCTCACCAGACTTCTCATAATGCTCTTAATAT  1440
    ATTGCACTTTTCTAATCAAAGTGCGAGTTTATGAGGGTAAAGCTCTACTTTCCTACTGCA  1500
    GCCTTCAGATTCTCATCATTTTGCATCTATTTTGTAGCCAATAAAACTCCGCACTAGCTG  1560
    AAAAAAAAAAAAA                                                  1620
```

Figure 3. Full nucleotide sequence and deduced amino-acid sequence of human *K23*. The nucleotide sequence is numbered on the right and the amino-acid sequence is numbered on the left. The *K23* cDNA contains a 1269 bp open reading frame encoding a 422 amino-acid protein. The boxed sequence containing 309 amino acid residues corresponds to the predicted α-helical rod domain. A putative leucine zipper motif is underlined. The intermediate filament signature sequence was identified at amino-acid residues 368–376 and is shaded. The poly-A adenylation signal is underlined and shaded.

cDNA sequence for *K23* has been deposited in GenBank (accession number AF102848).

The sequence alignment of *K23* with known human type I keratins *including K20. K19, K18, K17, K16, K15, K14, K13,* and *K12* was performed using the MegAlign program (DNAstar, Inc., Madison, WI) and is shown in Figure 4. *K10* was not included in this figure because of its long tail domain. The tail domain of *K10*, that is rich in glycine and serine residues, would introduce a long gap in the alignment. The sequence conservation was observed mainly in the coiled coil domain, with sequence identity of 41–46% and similarity of 60–66%. The sequence identity among all the previously known type I keratins ranged from 50–97%. As observed in other type I keratins, two short interruptions

were found within the rod domain of *K23* demarcating subcoiled-coil domains 1a, 1b, and 2. The three subcoiled-coil domains are indicated by flanking horizontal arrows. The amino acid residues that are conserved in *K23* as well as in known keratins are shown on the top of each alignment block. The amino-acid residues that are conserved in known keratins, but that are distinct in *K23*, are underlined for each specific residue in *K23*.

Characterization of *K23* mRNA Induction by NaBu

Based on Reverse Northern hybridization, the *K23* mRNA was highly induced in response to NaBu (Fig. 2). This result was confirmed by Northern blot analysis. The data shown in Figure 5 indicates that the untreated AsPC-1 cells express basal levels of *K23* mRNA as a single 1.7 kb transcript. This is in agreement with the size of the cDNA we cloned. Expression of *K23* mRNA was highly induced by treatment with 1.0 mM NaBu. An increase in the level of the *K23* transcript first appeared around 6 hr, reached a maximal level by 24 hr, and remained at an elevated level for up to 48 hr. A quantitative analysis of the *K23* transcript is also shown. A nearly 20-fold increase in *K23* mRNA message was achieved by 24 hr.

Expression of *K23* and Its Induction by NaBu in Pancreatic Cancer Cell Lines

Further analysis of *K23* mRNA expression in AsPC-1 cells treated with various doses of NaBu indicated that significant induction could be detected at concentrations as low as 0.2 mM (Fig. 6A). NaBu has been shown to induce differentiation in a variety of in vitro cultured cell lines, including pancreatic cancer cells. The cellular response to NaBu treatment, however, can be very different in cells of different tissues, or even in different cell lines derived from the same tissue. To examine whether induction of *K23* mRNA by NaBu was limited to this particular cell line, we have compared the expression of *K23* mRNA with and without NaBu treatment in AsPC-1 (Fig. 6A) and 3 additional pancreatic adenocarcinoma cell lines, including BxPC-3 (Fig. 6B), Capan-1 (Fig. 6C) and Su.86.86 (Fig. 6D). The result indicated that all 4 cell lines express basal levels of *K23* mRNA, and that the expression was significantly induced by treatment with NaBu. AsPC-1 cells showed the greatest induction, followed by SU.86.86, BxPC-3, and Capan-1. These data indicate that the induction of *K23* mRNA by NaBu is a general phenomenon, that could involve the same signaling pathway.

Induction of *K23* Expression Is the Result of Histone Hyperacetylation

Consistent induction of *K23* mRNA by NaBu led us to investigate the signaling pathway involved in the induction process. NaBu is a well-known general histone deacetylase inhibitor, that may result in histone hyperacetylation, a process now known to turn on the transcription of specific genes. We decided to test whether the induction of *K23* was due to an effect on histone acetylation. TSA, a chemical that is structurally distinct from NaBu, is a potent and specific histone deacetylase inhibitor. TSA has also been shown to cause growth arrest and differentiation of various cell types. We examined the effect of TSA on *K23* mRNA expression in the AsPC-1 and Su.86.86 cell lines. The result shown in Figure 7 demonstrates that 0.30 μM TSA, a concentration known to cause specific histone hyperacetylation, efficiently induced *K23* mRNA expression in both cell lines tested. The kinetics and extent of induction were comparable to those of NaBu. To investigate whether oxidative stress or DNA demethylation could also result in the induction of *K23*, we examined the effect of paraquat and 5-AC on *K23* mRNA expression. Neither reagent, however, could induce the expression of *K23* mRNA (data not shown). These results suggest that induction of *K23* mRNA by NaBu is due mainly to histone hyperacetylation.

To investigate whether *K23* mRNA induction by either TSA or NaBu was due to an increase in the rate of mRNA synthesis or an enhancement of its stability, the transcriptional inhibitor ACD was used. Although induction of *K23* mRNA was highly induced by either TSA or NaBu, addition of 4 μM ACD completely abolished the induction process, suggesting that NaBu caused an increase in *K23* expression by stimulating the rate of its mRNA transcription (Fig. 8A). Similar results were obtained for CHX, that also efficiently blocked the induction of *K23* mRNA, suggesting that de novo protein synthesis is also necessary for this induction (Fig. 8B).

$p21^{WAF1/CIP1}$ As a Main Mediator in *K23* mRNA Induction by NaBu

The induction of $p21^{WAF1/CIP1}$ is associated with butyrate-mediated growth inhibition in the colorectal cancer cell line HT-29 (Archer et al., 1998). Induction of $p21^{WAF1/CIP1}$ by NaBu and TSA is not

```
                                                                                                 M.
K20   MD···FSRRSFHRSLSSSLQAPVVSTVGMQRLGT············TPSVYGGAGGRGIRISNSRHTVN··········· 55
K19   MTSYSYRQSSATSSF······GGLGGGSVRFGPGVAF···RAPSIHGGSGGRGVSVSSSARFVSSSSSG····· 60
K18   MS··FTTRSTESTNYRSLG·····························SVQAPSYGARPVSSAASVYA 37
K17   MTTSI·RQETSSSSIKGSSGLGGGSSRTSCRLSGGLGAGSCRL············GSAGGLGSTLG 53
K16   MATCS·RQETSSSSMKGSCGIGGGIGGGSRISSVLAGGSCRAPSTYGG···GLSVSS·RFSSGGACGLGGGYG 69
K15   MTT·TFLQ·TSSSTFGGGSTRGGSLLAGGGGFGGG···SLSGGGGSRSISASSARFVSSGS···GGGYG 61
K14   MTTCS·RQFTSSSSMKGSCGIGGGIGAGSSRISSVLAGGSCRAPNTYGG···GLSVSSSRFSSGGAYGLGGGYG 70
K13   MSL·R·LQ·SSSASYGG················GFGGG·······S·CQLGGGRGVSTCSTRFVSGGS···AGGYG 46
K12   MDLS·······NNTMSLSVRTPGLSRRLSSQSVIGRPRGMSASSVGSGYG······GSAFGFGASCG·GGFSA 59
K23   MN·····················SGHSFSQTPSASFHGAGGGWGRPRSFPR············ 31

                                                                           C1a
                                                                              K. MQ. LND
K20   ···················YGSDLTGG················GDLFVGNEKMAMQHERD 79
K19   ···········G·······YGGGYGGVLTAS···············DGLLAGNEKLTMQNLND 89
K18   GA·········GGSGSRISVSRSTSFRGGMGS···GGLATGIAGGLAG····MGGIQ·······NEKETMQSLND 89
K17   GSSYSSCYSFGSG················GGYGSGFGGV··········DGLLAGGEKATMQNLHD 93
K16   GGFSSSSS·FGSG·········FGGGYGGGLGAGFGGGLGAGFGGGFAGG··········DGLLVGSEKVTMQNLHD 128
K15   GGM·RVCGFGGGAGS······VFGGGFGGGVGGGFGGGFGGG············DGGLLSGNEKITMQNLHD 114
K14   GGFSSSSSSFGSG·········FGGGYGGGLGAGLGGG·····FGGGFAGG·········DGLLVGSEKVTMQNLHD 124
K13   GGV··S·CGFGGGADS····GFGGGYGGGLGGGYGGGLGGGFGGGFAGGFVD·FGACDGGLLTGNEKITMQNLHD 113
K12   ASMFGSSSGFGGGSGSSMAGGLGAGYGRALGGGSFGGLGMGFGGSPGGGSLGILSGNDGGLLSGSEKETMQNLHD 134
K23   ·····APTVHGGAGGARISLSFTTRSCPPPGGSWGSGRSSP···········LLGGNGKATMQNLHD 81

      RLASYL. .VR.LE. .N. .LE.I               C1b    D.S.Y. . .I. .L. . .I. . . . .N. . .L.IDNA.
K20   RLASYLEKVRTLEQSNSKLEVQIKQWYETNAPRAG···RDYSAYYRQIEELRSQIKDAQLQNARCVLQIDNAKD 150
K19   RLASYLDKVRALEAANGELEVKIRDWYQKQGPG·PS···RDYSHYYTTIQDLRDKILGATHENSRIVLQIDNARL 160
K18   RLASYLDRVRSLETENRRLESKIREHLEKKGPQV·····RDWSHYFKIIEDLRAQIFANTVDNARIVLQIDNARL 159
K17   RLASYLDKVRALEEANTELEVKIRDWYQRQAPG·PA···RDYSQYYRTIEELQNKILTATVDNANILLQIDNARL 164
K16   RLASYLDKVRALEEANADLEVKIRDWYQRQRPS·EI···KDYSPYFKTIEDLRNKIIAATIENAQPILQIDNARL 197
K15   RLASYLDKVRALEEANADLEVKIHDWYQKQTPASPE···CDYSQYKTIEELRDKIMATTIDNSRVLLEIDNARL 186
K14   RLASYLDKVRALEEANADLEVKIRDWYQRORPA·EI···KDYSPYFKTIEELRDKILTATVDNANVLLQIDNARL 195
K13   RLASYLEKVRALEEANADLEVKIRDWHLKQSPASPE···RDYSPYYKTIEELRDKILTATIENNRVLLEIDNARL 185
K12   RLASYLDKVRALEEANTELENKIREWYETRGTGTADASQSDYSKYYPLIEDLRNKIIISASIGNAQLLEQIDNARL 209
K23   RLASYLEKVRALEEANMKLESRILKWHQQRDPG····SKKDYSQYEENITHLQEQIVDGNMTNAQIFLLIDNARM 152

      A. .DF. .K. .E. . . . . .E. . .GL. . .D. . . . LE. . .E. . . .L. . . .K. .H. . .E
K20   AAEDFRLKYETERGIRLTVEADLQGLNKVFDDLTLHKTDLEIQIEELNKDLALLKKERQEEVDGLHKHLGNT··V 223
K19   AADDFRTKFETEQALRMSVEADINGLRRVLDELTLARTDLEMQIEGLKEELAYLKKNHEEEISTLRGDVGGQ··V 233
K18   AADDFRVKYETELAMRQSVENDIHGLRKVIDDTNITRLQLETEIEALKEELFMKKNHEEEVKGLQADIASS·GL 233
K17   AADDFRTKFETEQALRSVEADINGLRRVLDELTLARADLEMQIENLKEELAYLKKNHEEEMNALRGQVGGE··I 237
K16   AADDFRTKYEHELALRQTVEADVNGLRRVLDELTLARTDLEMQIEGLKEELAYLRKNHEEEMLALRGQTGGD··V 270
K15   AADDFRLKYENELALRQGVEADINGLRRVLDELTLARTDLEMQIEGLNEELAYLKKNHEEEMKEFSSQLAGQ··V 259
K14   AADDFRTKYETELNLRMSVEADINGLRRVLDELTLARADLEMQIESLKEELAYLKKNHEEEMNALRGQVGGD··V 268
K13   AVDDFRLKYENELALRQSVEADINGLRRVLDELTLSKTDLEMQIESLNEELAYMKKNHEEEMKEFSNQVVGQ··V 259
K12   AAEDFRMKYENELALRQNIGLRRVLDELTLTRTDLEMQLESLNEEIAYMKKNHEDELQSFRVGGPGE··V 282
K23   AVDDENLKYENEHSFKKDLEIEVEGLRRTLDNLTIVTTDLEQEVEGMRKELILMKKHHEQEME··KHHVPSDFNV 225

      .V. .D. . . . .     C2         R. .Y. . . . . . . . . .L.R. . .Q.LEI
K20   NVEVDAAPGLNLGVIMNEMRQKYEVMAQKNLQEAKEQFERQTAVLQQQVTVNTEELKGTEVQLTELRRTSQSLEI 298
K19   SVEVDSAPGTDLAKILSDMRSQYEVMAEQNRKDAEAWFTSRTEELNREVAGHTEQLQMSRSEVTDLRRTLQGLEI 308
K18   TVEVDAPKSQDLAKIMADIRAQYDELARKNREELDKYWSQQIEESTTVVTTQSAEVGAAETTLTELRRTVQSLEI 308
K17   NVEMDAAPGVDLSRILNEMRDQYEKMAEKNRKDAEDWFFSKTEELNREVATNSELVQSGKSEISELRRTMQAEEL 312
K16   NVEMDAAPGVDLSRILNEMRDQYEQMAEKNRRDAETWFLSKTEELNKEVASNSELVQSSRSEVTELRRVLQGLEI 346
K15   NVEMDAAPGVDLTRVLAEMREQYEAMAEKNRRDVEAWFKEQTEELNREVASNTEMIQTSKTEITDLRRTMQELEI 334
K14   NVEMDAAPGVDLSRILNEMRDQYEKMAEKNRKDAEEWFFTKTEELNREVATNSELVQSGKSEISELRRTMQNLEI 343
K13   NVEMDATPGIDLTRVLAEMREQYEAMAERNRRDAEEWFHAKSAELNKEVSTNTAMIQTSKTEITELRRRTLQGLEI 333
K12   SVEMDAAPGVDLTRLLNDMRAQYETIAEQNRKDAEAWIEKSGELRKEISTNTEQLQSSKSEVTDLRRAFQNLEI 357
K23   NVKVDTGPREDLIKVLEDMRQEYELIIKKKHRDLDTWYKEQSAAMSQE··AASPATVQSRQGDIHELKRTFQALEI 299

      . .L. . . . . .K. .LE. . . .E. . . . . . . . . . . . . . .E. .L. . .R. . . .Q. . . . .L. . .K. .LE.EI. .TYR. L
K20   ELQSHLSMKESLEHTLEEIKARYSSQLANLQSLLSSLEAQLMQIRSNMERQNNEYHILLDIKTRLEQEIATYRRL 373
K19   ELQSQLSMKAALEDTLAETEARFGAQLAHLQALISGIEAQLADVRADSERQNQEYQRLMDIKSRLEQEIATYRSL 383
K18   DLDSMRNLKASLENSLREVEARYALQMEQLNGILLHLESELAQTRAEGQRQAQEYQRLIKVKLEAEIATYRRE 383
K17   ELQSQLSMKASLEGNLAETENRYCVQLSQIQGLIGSVEEQLAQERCEMEQQNQEYKILLDVKTRLEQEIATYRRE 387
K16   ELQSQLSMKASLENSLEETKGRYCMQLSQIQGLIGSVEEQLAQLRCEMEQQSQEYQILLDVKTRLEQEIATYRRL 420
K15   ELQSQLSMKAGLENSLAETECRYATQLQQIQGLIGGLEAQLSELRCEMEAQNQEYKLLLDIKTRLEQEIATYRSL 409
K14   ELQSQLSMKASLENSLEETKGRYCMQLAQIQEMIGSVEEQLAQLRCEMEAQNQEYKLLLDVKTRLEQEIATYRRL 418
K13   ELQSQLSMKENTVAETECRYALQLQQIQGLISSIEAQLSELRSEMECQNQEYKMLLDIKTRLEQEIATYRSL 408
K12   ELQSQLAMKKSLEDSLAEAEGDYCAQLSQVVQQLISNLEAQLLQVRADAERQNVDHQRLLNVKARLELEIETYRRL 432
K23   DLQTQYSTKSALENMLSETQSRNSCKLQDMQEIISHYEEELTQLRHELERQNNEYQVLLGIKTHLEKEITTYRRL 374

      L.
K20   LEGE····DVKTTEYQLSTLEERDI·······KKTRKIKTVVQEVVDGKVVSSEVKEVEENI 424
K19   LEGQ··EDHYN···············NLSASKVL 400
K18   LE·DGEDFNLGDALDSSNSMQTIC·············KTTTRRIVDGKVVSETNDTKVLRH 430
K17   LEGE·DAHLITQ···········YKKEPVTT·RQVRTIVEEVQDGKVISSREQVHQTTR 432
K16   LEGE·DAHLSSQQASGQSYSSREVFTSSSSSS·SRQTRPILKEQSSSSSFSQGQS······S 473
K15   LEGQ·DAKMAGI····GIREAS···S·GGGGS·SSNFHINVEESVDGQVVSSH···KREL 468
K14   LEGE·DAHLSSSQF8SGSQSSRDV····TSS·SRQIRTKVMDVHDGKVVSTHEQVLRTKN 472
K13   LEGQ·DAKMIGFPSSAGSVSPR···STSVTT·ISSASVTTTSNASGRRTSDV···RRP 458
K12   LDGEAQGDGLEESLFVTDSKSQAQSTDSSKDPTKTRKIKTVVQEMVNGEVVSSDVQEIEELM 464
K23   LEGESEGT···········REESKSSMKVSATPKIKAITQETINGRLVLCQVNEIQKHA 422
```

blocked by the protein synthesis inhibitor cyclo-heximide, indicating that $p21^{WAF1/CIP1}$ was induced by these chemicals as an immediate-early gene. We obtained similar results in each of the pancreatic cancer cell lines tested including AsPC-1, BxPC-3, MIA, Su.86.86, PANC-1 and Capan-1 (data not shown). Although the level of $p21^{WAF1/CIP1}$ mRNA after NaBu treatment was higher in BxPC-3 and Su.86.86, significant induction of $p21^{WAF1/CIP1}$ by NaBu was also observed in all other cell lines, including MIA, in which the basal level of $p21^{WAF1/CIP1}$ mRNA was barely detectable by Northern blot hybridization. These results suggested that $p21^{WAF1/CIP1}$ mRNA induction by NaBu is a common feature in pancreatic cancer cells. Because induction of K23 mRNA by NaBu or TSA is a late event, induction of both $p21^{WAF1/CIP1}$ and K23 is mediated through histone hyperacetylation. We wondered whether transactivation of $p21^{WAF1/CIP1}$ was involved in K23 mRNA induction by NaBu. To test this, an antisense $p21^{WAF1/CIP1}$ expression vector was transiently transfected into AsPC-1 cells, and the cells were treated with NaBu. As shown in Figure 9, transfection of $p21^{WAF1/CIP1}$ antisense was associated with a significant down-regulation of wild-type $p21^{WAF1/CIP1}$ mRNA expression. The induction of K23mRNA was efficiently blocked by expression of $p21^{WAF1/CIP1}$ antisense cDNA, whereas in non-transfected control cells and cells transfected with a control vector, K23 remained highly induced by NaBu. Therefore, $p21^{WAF1/CIP1}$ seems to be a key mediator in the process of K23 mRNA induction by histone deacetylation.

K23 mRNA Expression Is Increased in AsPC-1 Cell Overexpressing $p21^{WAF1/CIP1}$

To examine further the relationship between $p21^{WAF1/CIP1}$ expression and K23 induction by NaBu, we generated AsPC-1 cell lines stably transfected with either $p21^{WAF1/CIP1}$ sense expression

vectors [p21(S)], or a $p21^{WAF1/CIP1}$ antisense expression vector [p21(AS)]. Pooled cells containing about 60 individual clones with p21(S) and more than 100 clones with p21(AS) were used for our analysis. Overexpression of p21(S) is not compatible with cell growth. We observed that the doubling time of p21(S) cells was 65 hr, as compared to that of 35 hr for p21(AS) cells under the same culture conditions. A fraction of cells with a differentiated morphology characterized by the presence of multiple thin filamentous protrusions was constantly observed in p21(S) cells. This morphology was similar to that observed in NaBu treated cells, although the latter showed a more uniform change with longer and bigger membranous protrusions. In addition, a significant number of cells kept detaching from the culture monolayer, and these cells were found to be undergoing apoptosis as determined by the presence of DNA fragmentation. In the p21(AS) cells, we did not observe a significant difference from the parent cells in terms of morphology or growth rate. These results suggested that over-expression of $p21^{WAF1/CIP1}$ is associated with a more differentiated phenotype and increased apoptosis in AsPC-1 cells. These effects overlap to some extent that of NaBu treatment. We then examined K23 expression in p21(S) and p21(AS) cells with and without NaBu treatment. The result presented in Figure 10 indicates that p21(S) cells expressed a much higher basal level of K23 mRNA than did p21(AS) cells. NaBu at 0.2 and 2 mM further induced K23 mRNA expression in p21(S) cells. In p21(AS) cells, however, induction of K23 was observed only at 2-mM, with no obvious increase at 0.2 mM of NaBu, whereas a significant increase(70%) in K23 mRNA was observed after treatment with 0.2 mM NaBu in non-transfected AsPC-1 (Fig.6A). These data suggest an important role of $p21^{WAF1/CIP1}$ in both basal-level expression and induction of K23 mRNA by NaBu.

DISCUSSION

In the present paper, we report on the identification, cloning, and characterization of K23, a novel member of the keratin family, that is highly induced by NaBu during the differentiation process of pancreatic cancer cells.

Keratins are a family of intermediate-filament proteins consisting of two subclasses based on their charges and sequence homologies, the acidic type I keratins and neutral to basic type II keratins (Fuchs and Weber, 1994). An interesting feature of

Figure 4. Comparison of the amino-acid sequence of K23 to those of known keratins The accession numbers for protein sequences used in the analysis are AF102848 (K23), P35900 (K20), P08727 (K19), P05783 (K18), Q04695 (K17), JC4313 (K16), P19012 (K15), P02533 (K14), P13646 (K13), and Q99456 (K12). The amino-acid sequence is numbered on the right, and the name of each gene is shown on the left. Multiple alignment was performed using MegAlign (DNAstar Inc., Hercules, CA) by the CLUSTAL method. The amino-acid residues that are conserved in at least two out of six candidate sequences are shaded. The position of the coiled-coil subdomains are designated C1a, C1b and C2 (arrows). The amino acid residues conserved in all proteins are shown on the top of the alignment. Each amino acid residue that is conserved in known keratins except in K23 is underlined.
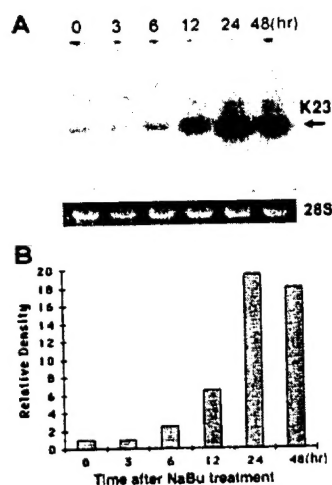
Figure 5. Time-course of K23 mRNA induction by NaBu. AsPC-1 monolayers (60–80%) were exposed to 1.0 mM NaBu for the time period indicated in the figure. RNA was isolated, and Northern blot analysis was performed using K23 cDNA as probe (A) as described in Materials and Methods. Also included in this figure is an ethidium bromide-stained gel of 28S RNA to control for the loading in different samples. The hybridization signals were quantitated using Bio-Rad Image Analysis System (Bio-Rad Corp, Hercules, CA). Values for K23 were normalized to 28S RNA and expressed relative to the control. The relative value of each band was used to construct the histogram (B).

is not surprising to find that, among all the residues fully conserved, most are lipid amino acids (e.g., L = 20 and I = 6) and charged amino acids (e.g., E = 13, D = 6, R = 6, K = 5), because these are important in determining the coiled-coil structure and charge characteristic important for keratin to form a functional fiber network. The above six amino acids account for 70% (56 of 80) of the consensus residues among type I keratins, including K23. The above analysis suggested that these highly conserved residues may be critical in maintaining the functional integrity of keratins.

Despite the high similarity in the rod domain, the head and tail regions showed greater divergence in sequence composition and length. K23 does not have repeats of the tetrapeptide motif XXXZ found in the head domain of most of other keratins. X is one of the two small amino acids, glycine and serine, and Z is an aromatic residue (phenylalanine or tyrosine). K23 also does not have a heptapeptide motif similar to the consensus sequence DGKI/V VST/E that has been identified near the carboxyl termini of K20, K18, K17, K15, and K14. K23 has 5 serine residues in its tail domain as compared to 2 in K17 and K19, 3 in K20, 4 in K18, 7 in K12, 8 in K15, 12 in K13 and K14, and 20 in K15. In contrast, K10 has as many as 40 serine residues in its tail (not shown). The presence of serine-rich residues in the rod tail is typical for simple epithelium-type keratins. K23 is also different from other known keratins in that it has a lower sequence identity (42–46% as compared to 50–97% among all the previously known keratins). Based on the protein sequence similarity, a conserved exon/intron structure, and the fact that all the keratins are located in compact clusters within the human genome, it has been proposed that all

keratins is that they form a 10-nm intermediate filament network of epithelial cells by the obligatory association of equimolar amounts of type I and type II keratins (Coulombe and Fuchs, 1990; Stewart, 1993). Despite the great divergence in the head and tail sequences, the central α-helical rod domain is highly conserved among each group of keratins. The homology to K23 was also identified in this region (Fig. 4). Among the 95 conserved a.a. residues found in known type I keratins, 84% (80 out of 95) are conserved in K23, whereas the remaining 15 amino acid residues represent consensus substitutions (e.g., R by K, E by D, Y by S). It
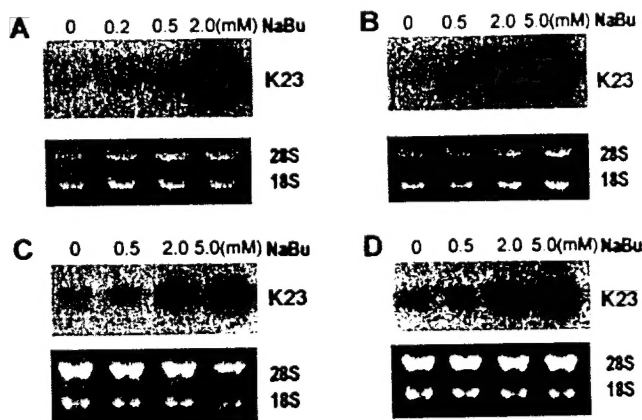

Figure 6. Effect of NaBu on K23 mRNA expression in different cell lines. (A) AsPC-1 cells were treated with 0, 0.2, 0.5 and 2.0 mM NaBu for 24 hr; 15 μg of total RNA was applied for Northern blot analysis and hybridized with the full-length K23 cDNA. (B–D) Correspond to Su.86.86, BxPC-3, and Capan-1 cells treated with 0, 0.5, 2.0, and 5.0 mM NaBu for 24 hr. 15 μg of total RNAs was then applied for Northern blot analysis, and the membranes were hybridized with the K23 cDNA. The ethidium bromide-stained RNA gels are shown to indicate the loading in each lane of the gel.
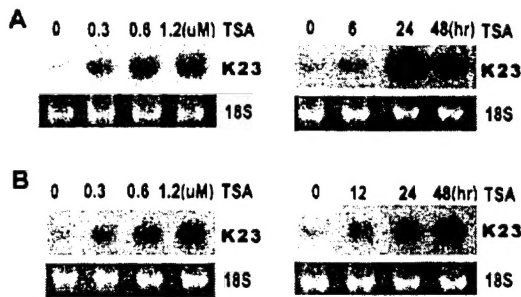
Figure 7. Induction of K23 mRNA expression by TSA. (A, left) Dose response of K23 mRNA induction by TSA. AsPC-1 cells were treated with various concentrations of TSA indicated for 24 hr, and K23 mRNA expression was examined by Northern blot analysis using K23 and GAPDH cDNAs as probes. (A, right): Time course of K23 mRNA induction by TSA. AsPC-1 cells were treated with 0.3 μM TSA for varying lengths of time from 0 to 48 hr, and induction of K23 mRNA expression was examined by Northern blot analysis. (B) Similar dose response and time course of K23 mRNA induction by TSA in Su.86.86 cells. Ethidium bromide stained RNA gel corresponding to 18S RNA is shown for each blot not hybridized with GAPDH to indicate the RNA loading.

Figure 9. Expression of antisense p21$^{WAF1/CIP1}$ RNA inhibits K23 mRNA induction by NaBu. The antisense p21$^{WAF1/CIP1}$ expression vector was constructed and transiently transfected into AsPC-1 cells (see Materials and Methods). Twenty-four hours later, cells were subjected to treatment with 2 mM NaBu for 24 hr. Fifteen μg of total RNA was then loaded onto gels for Northern blot analysis using p21$^{WAF1/CIP1}$, K23, and GAPDH cDNAs as probes. As a control, AsPC-1 cells without transfection and transiently transfected with pcDNA3.1(+) expression vector were treated with 2 mM NaBu for 24 hr, and RNA was isolated for Northern blot analysis. p21(WT): endogenous wild-type p21$^{WAF1/CIP1}$ (2.1 kb); p21(AS): antisense transcript of p21(0.8-kb). Each figure is representative of the results of three independent experiments.

Figure 8. Effect of ACD and CHX on K23 expression. (A) AsPC-1 monolayers (60–80% confluent) were treated with ACD (4 μM), NaBu (2 mM), and TSA (0.3 μM) alone or in combination as indicated in the figure. In the case of combined treatment, ACD was added to cell cultures 30 min before TSA or NaBu. Cells were treated for 24 hr before preparation of RNA. Total RNA was extracted and used for Northern blot analysis and hybridized with K23 cDNA. (B) AsPC-1 monolayers (60–80% confluent) were treated with CHX (35 μM). NaBu (2 mM) and TSA (0.3 μM) alone or in combination as indicated in the figure. In the case of combined treatment, CHX (35 μM) was added to cell cultures 30 min before TSA or NaBu. Cells were treated for 24 hr before the preparation of RNA. Total RNA was extracted for Northern blot analysis and hybridized using the K23 cDNA as probe. The matching ethidium bromide-stained 28S and 18S RNA is shown below to indicate the loading of RNA samples.

Figure 10. Induction of K23 mRNA in cells stably expressing p21$^{WAF1/CIP1}$. p21$^{WAF1/CIP1}$ sense and antisense expression vectors were transfected into AsPC-1 cells and stable clones were selected (see Material, and Methods). Pooled p21(S) and p21(AS) cells were treated with 0, 0.2, and 2 mM NaBu for 24 hr, and RNA was isolated for Northern blot hybridization using p21$^{WAF1/CIP1}$, K23 and GAPDH cDNA as probes. As a control, AsPC-1 cells were transfected with pcDNA3.1(+) vector.

the type I keratins are derived from a common ancestral gene. Evolutionary tree analysis has shown that K18 is the first to diverge in the acidic keratin family (Blumenberg, 1988). K20 and K23, however, were not included in that analysis. Our evolutionary analysis using the MegAlign program (DNAstar, Inc., Madison, WI) suggests that K23 is most closely related to K18 and K20 (data not shown).
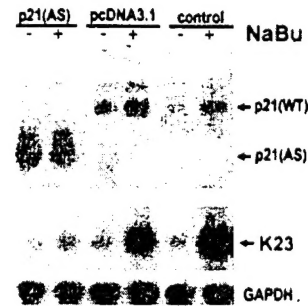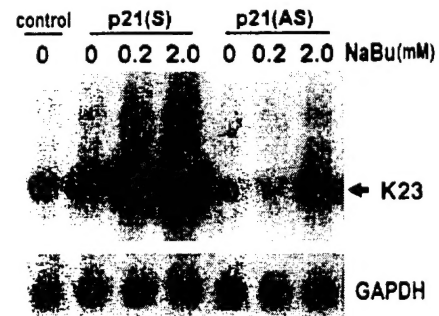
NaBu is known to induce general histone acetylation, but, more specifically, hyperacetylation of the H3 and H4 species through noncompetitive inhibition of the histone deacetylate enzyme. Hyperacetylation of histones at lysine residues neutralizes their positive charge, thereby disrupting their ionic interaction with DNA, that allows transcription factors to access and activate specific genes. Thus, it seems that specific genes are targeted for activation or repression by the histone-acetylating or histone-deacetylating activities of specific transcription factors or cofactors. Our results demonstrated that K23 can be induced by

NaBu and also by TSA, a specific deacetylase inhibitor, but not by oxidative stress or a demethylation agent, suggesting that *K23* mRNA induction is a downstream event of histone hyperacetylation. A protein synthesis inhibitor abolished the induction process, suggesting that this induction is a late event that requires transactivation by other genes.

It has been reported that $p21^{WAF1/CIP1}$ plays an important role in mediating NaBu effects on growth arrest and differentiation. In colon cancer cells, $p21^{WAF1/CIP1}$ is absolutely required for growth arrest caused by NaBu, and the induction is mainly due to the effect on histone acetylation, because overexpression of *HDAC1* largely blocks the induction of $p21^{WAF1/CIP1}$ in reporter constructs by both NaBu and TSA (Archer et al., 1998). In addition, induction of $p21^{WAF1/CIP1}$ by NaBu and TSA cannot be blocked by the protein synthesis inhibitor cycloheximide, indicating that $p21^{WAF1/CIP1}$ was induced by these chemicals as an immediate-early gene.

We have found that NaBu induced $p21^{WAF1/CIP1}$ expression as an immediate early response independent of the *p53* status in a panel of pancreatic cancer cell lines. This consistent induction pattern supports a role of $p21^{WAF1/CIP1}$ in mediating NaBu-induced growth arrest and differentiation in pancreatic cancer cells. To directly demonstrate a link between $p21^{WAF1/CIP1}$ expression and *K23* induction by NaBu, we constructed mammalian expression vectors to direct the expression of either p21(S) or p21(AS) in AsPC-1 cells. Interestingly, overexpression of p21(S) alone resulted in changes in cell morphology and growth characteristics that resembled those induced by NaBu. This result further supports a crucial role of $p21^{WAF1/CIP1}$ in NaBu induced growth arrest and differentiation in pancreatic cancer cells. At present, however, it is not known whether transactivation of *K23* mRNA is the result of direct interaction with $p21^{WAF1/CIP1}$ or is the secondary effect of induction of differentiation. We propose that *K23*, like most of its family members, may be a potential marker of cell differentiation.

In summary, we report here the cDNA and peptide sequences of *K23*, a novel and distinct member of type I keratin gene family. *K23* mRNA is highly induced in response to NaBu, that has been shown to induce differentiation in AsPC-1 cells. Induction of *K23* is a downstream event of histone hyperacetylation. We also demonstrated that the cyclin-dependent kinase inhibitor $p21^{WAF1/CIP1}$ plays a critical role in mediating NaBu-induced

growth arrest and differentiation in pancreatic cancer cells. Its expression is also necessary for efficient induction of *K23* mRNA by histone deacetylase inhibitors.

ACKNOWLEDGMENT

REFERENCES

Archer SY, Meng S, Shei A, Hodin RA. 1998. p21(WAF1) is required for butyrate-mediated growth inhibition of human colon cancer cells. Proc Natl Acad Sci USA 95:6791–6796.

Armstrong JA, Emerson BM. 1998. Transcription of chromatin: these are complex times. Curr Opin Genet Dev 8:165–172.

Barnard JA, Warwick G. 1993. Butyrate rapidly induces growth inhibition and differentiation in HT-29 cells. Cell Growth Differ 4:495–501.

Blumenberg M. 1988. Concerted gene duplications in the two keratin gene families. J Mol Evol 27:203–211.

Bomer MM, Myers CE, Sartor O, Sei Y, Toko T, Trepel JB, Schneider E. 1995. Cancer Res 55:2122–2128.

Cameron EE, Bachman KE, Myohanen S, Herman JG, Baylin SB. 1999. Synergy of demethylation and histone deacetylase inhibition in the re-expression of genes silenced in cancer. Nat Genet 21:103–107.

Coulombe PA, Fuchs E. 1990. Elucidating the early stages of keratin filament assembly. J Cell Biol 111:153–169.

Davie JR. 1998. Covalent modifications of histones: expression from chromatin templates. Curr Opin Genet Dev 8:173–178.

Diatchenko L, Lau YF, Campbell AP, Chenchik A, Moqadam F, Huang B, Lukyanov S, Lukyanov K, Gurskaya N, Sverdlov ED, Siebert PD. 1996. Suppression subtractive hybridization: a method for generating differentially regulated or tissue-specific cDNA probes and libraries. Proc Natl Acad Sci USA 93:6025–6030.

Egawa N, Maillet B, VanDamme B, De Greve J, Kloppel G. 1996. Differentiation of pancreatic carcinoma induced by retinoic acid or sodium butyrate: a morphological and molecular analysis of four cell lines. Virchows Arch 429:59–68.

Fuchs E, Weber K. 1994. Intermediate filaments: structure, dynamics, function, and disease. Annu Rev Biochem 63:345–382.

Graham KA, Buick RN. 1988. Sodium butyrate induces differentiation in breast cancer cell lines expressing the estrogen receptor. J Cell Physiol 136:63–71.

Hague A, Manning AM, Hanlon KA, Huschtscha LI, Hart D, Paraskeva C. 1993. Sodium butyrate induces apoptosis in human colonic tumour cell lines in a p53-independent pathway: implications for the possible role of dietary fibre in the prevention of large-bowel cancer. Int J Cancer 55:498–505.

Halgunset J, Lamvik T, Espevik T. 1988. Butyrate effects on growth, morphology, and fibronectin production in PC-3 prostatic carcinoma cells. Prostate 12:65–77.

Huang H, Reed CP, Zhang JS, Shridhar V, Wang L, Smith DI. 1999. Carboxypeptidase A3 (CPA3): a novel gene highly induced by histone deacetylase inhibitors during differentiation of prostate epithelial cancer cells. Cancer Res 59: 2981–2988.

Jones PL, Veenstra GJ, Wade PA, Vermaak D, Kass SU, Landsberger N, Strouboulis J, Wolffe AP. 1998. Methylated DNA and MeCP2 recruit histone deacetylase to repress transcription. Nat Genet 19:187–191.

Kuo MH, Brownell JE, Sobel RE, Ranalli TA, Cook RG, Edmondson DG, Roth, SY, Allis CD, 1996. Transcription-linked acetylation by Gcn5p of histones H3 and H4 at specific lysines. Nature 383:269–272.

Luo RX, Postigo AA, Dean DC. 1998. Rb interacts with histone deacetylase to repress transcription. Cell 92:463–473.

Mizzen CA, Yang XJ, Kokubo T, Brownell JE, Bannister AJ, Owen-Hughes T, Workman J, Wang L, Berger SL, Kouzarides T, Nakatani Y, Allis CD. 1996. The TAF(II)250 subunit of TFIID has histone acetyltransferase activity. Cell 87:1261–1270.

Mullins TD, Kern HF, Metzgar RS. 1991. Ultrastructural differentiation of sodium butyrate-treated human pancreatic adenocarcinoma cell lines. Pancreas 6:578–587.